Nonlinear Inelastic Analysis of Concrete-Filled Steel Tubular Slender Beam-Columns

by

Vipulkumar Ishvarbhai Patel, ME

VICTORIA UNIVERSITY
MELBOURNE AUSTRALIA

Thesis submitted in fulfillment of the requirement for the degree of

Doctor of Philosophy

College of Engineering and Science, Victoria University, Australia

January 2013

ABSTRACT

High strength thin-walled concrete-filled steel tubular (CFST) slender beam-columns may undergo local and global buckling when subjected to biaxial loads, preloads or cyclic loading. The local buckling effects of steel tube walls under stress gradients have not been considered in existing numerical models for CFST slender beam-columns. This thesis presents a systematic development of new numerical models for the nonlinear inelastic analysis of thin-walled rectangular and circular CFST slender beam-columns incorporating the effects of local buckling, concrete confinement, geometric imperfections, preloads, high strength materials, second order and cyclic behavior.

In the proposed numerical models, the inelastic behavior of column cross-sections is simulated using the accurate fiber element method. Accurate constitutive laws for confined concrete are implemented in the models. The effects of progressive local buckling are taken into account in the models by using effective width formulas. Axial load-moment-curvature relationships computed from the fiber analysis of sections are used in the column stability analysis to determine equilibrium states. Deflections caused by preloads on the steel tubes arising from the construction of upper floors are included in the analysis of CFST slender columns. Efficient computational algorithms based on the Müller's method are developed to obtain nonlinear solutions. Analysis procedures are proposed for predicting load-deflection and axial load-moment interaction curves for CFST slender columns under axial load and uniaxial bending, biaxial loads, preloads or axial load and cyclic lateral loading.

The numerical models developed are verified by comparisons of computer solutions with existing experimental results and then utilized to undertake extensive parametric studies on the fundamental behavior of CFST slender columns covering a wide range of parameters. The numerical models are shown to be efficient computer simulation tools for designing safe and economical thin-walled CFST slender beam-columns with any steel and concrete strength grades. The thesis presents benchmark numerical results on the behavior of high strength thin-walled CFST slender beam-columns accounting for progressive local buckling effects. These results provide a better understanding of the fundamental behavior of CFST columns and are valuable to structural designers and composite code writers.

DECLARATION

"I, Vipulkumar Ishvarbhai Patel, declare that the PhD thesis entitled 'Nonlinear inelastic analysis of concrete-filled steel tubular slender beam-columns' is no more than 100,000 words in length including quotes and exclusive of tables, figures, appendices, bibliography, references and footnotes. This thesis contains no material that has been submitted previously, in whole or in part, for the award of any other academic degree or diploma. Except where otherwise indicated, this thesis is my own work".

Signature   Date:

ACKNOWLEDGMENTS

The author would like to thank his principal supervisor A/Prof. Qing Quan Liang for his close supervision, productive discussions and invaluable suggestions throughout the period of the research project. The author would also like to thank his associate supervisor A/Prof. Muhammad N.S. Hadi of the University of Wollongong for his discussions, invaluable suggestions, encouragement and support.

The research presented in this thesis was carried out in the College of Engineering and Science at Victoria University (2010-2013). The author was supported by an Australian Postgraduate Award and a Faculty of Health, Engineering and Science scholarship. The financial support is gratefully acknowledged.

The author would also like to thank all staff in the College of Engineering and Science and Postgraduate Research Office for their kind assistance. I am grateful to the staff of the Victoria University library for their strong support of my enthusiasm to find the research articles and reports.

The author wishes to express his appreciation to his friends and colleagues for their help and support.

Last, but certainly not the least, the author would like to thank his family for their support and understanding during three years study.

LIST OF PUBLICATIONS

Based on this research work, the candidate has written the following papers, which have been published or submitted for publication in international journals and conference proceedings.

Journal Articles

1. **Patel, V. I.,** Liang, Q. Q. and Hadi, M. N. S., "High strength thin-walled rectangular concrete-filled steel tubular slender beam-columns, Part I: Modeling," *Journal of Constructional Steel Research*, 2012, 70, 377-384.

2. **Patel, V. I.,** Liang, Q. Q. and Hadi, M. N. S., "High strength thin-walled rectangular concrete-filled steel tubular slender beam-columns, Part II: Behavior," *Journal of Constructional Steel Research*, 2012, 70, 368-376.

3. **Patel, V. I.,** Liang, Q. Q. and Hadi, M. N. S., "Inelastic stability analysis of high strength rectangular concrete-filled steel tubular slender beam-columns," *Interaction and Multiscale Mechanics, An International Journal*, 2012, 5(2), 91-104.

4. Liang, Q. Q., **Patel, V. I.** and Hadi, M. N. S., "Biaxially loaded high-strength concrete-filled steel tubular slender beam-columns, Part I: Multiscale simulation," *Journal of Constructional Steel Research*, 2012, 75, 64-71.

5. **Patel, V. I.,** Liang, Q. Q. and Hadi, M. N. S., "Biaxially loaded high-strength concrete-filled steel tubular slender beam-columns, Part II: Parametric study," *Journal of Constructional Steel Research* (currently under review).

6. **Patel, V. I.**, Liang, Q. Q. and Hadi, M. N. S., "Numerical analysis of circular concrete-filled steel tubular slender beam-columns with preload effects," *International Journal of Structural Stability and Dynamics*, 2013, 13(3), 1250065 (23 pages).

7. **Patel, V. I.**, Liang, Q. Q. and Hadi, M. N. S., "Nonlinear analysis of rectangular concrete-filled steel tubular slender beam-columns with preload effects," *Journal of Constructional Steel Research* (currently under review).

8. **Patel, V. I.**, Liang, Q. Q. and Hadi, M. N. S., "Numerical analysis of high-strength concrete-filled steel tubular slender beam-columns under cyclic loading," *Journal of Constructional Steel Research* (currently under review).

Refereed Conference Papers

9. Liang, Q. Q., **Patel, V. I.** and Hadi, M. N. S., "Nonlinear analysis of biaxially loaded high strength rectangular concrete-filled steel tubular slender beam-columns, Part I: Theory," *Proceedings of the 10th International Conference on Advances in Steel Concrete Composite and Hybrid Structures*, Singapore, July 2012, 403-410.

10. **Patel, V. I.**, Liang, Q. Q. and Hadi, M. N. S., "Nonlinear analysis of biaxially loaded high strength rectangular concrete-filled steel tubular slender beam-columns, Part II: Applications," *Proceedings of the 10th International Conference on Advances in Steel Concrete Composite and Hybrid Structures*, Singapore, July 2012, 411-418.

11. **Patel, V. I.**, Liang, Q. Q. and Hadi, M. N. S., "Nonlinear inelastic behavior of circular concrete-filled steel tubular slender beam-columns with preload effects," *Proceedings of the 10th International Conference on Advances in Steel Concrete Composite and Hybrid Structures*, Singapore, July 2012, 395-402.

PART A:

DETAILS OF INCLUDED PAPERS: THESIS BY PUBLICATION

Please list details of each Paper included in the thesis submission. Copies of published papers and submitted and/or final draft Paper manuscripts should also be included in the thesis submission.

Item/ Chapter No.	Paper Title	Publication Status (e.g. published, accepted for publication, to be revised and resubmitted, currently under review, unsubmitted but proposed to be submitted)	Publication Title and Details (e.g. date published, impact factor etc.)
3	High strength thin-walled rectangular concrete-filled steel tubular slender beam-columns, Part I: Modeling	Published.	*Journal of Constructional Steel Research*, 2012, 70, 377-384. ERA Rank: A*. Impact Factor: 1.251.
	High strength thin-walled rectangular concrete-filled steel tubular slender beam-columns, Part II: Behavior	Published.	*Journal of Constructional Steel Research*, 2012, 70, 368-376. ERA Rank: A*. Impact Factor: 1.251.
	Inelastic stability analysis of high strength rectangular concrete-filled steel tubular slender beam-columns	Published.	*Interaction and Multiscale Mechanics, An International Journal*, 2012, 5(2), 91-104.
4	Biaxially loaded high-strength concrete-filled steel tubular slender beam-columns, Part I: Multiscale simulation	Published.	*Journal of Constructional Steel Research*, 2012, 75, 64-71. ERA Rank: A*. Impact Factor: 1.251.
	Biaxially loaded high-strength concrete-filled steel tubular slender beam-columns, Part II: Parametric study	Revised and resubmitted.	*Journal of Constructional Steel Research*. Revised and resubmitted in January 2012. ERA Rank: A*. Impact Factor: 1.251.

5	Numerical analysis of circular concrete-filled steel tubular slender beam-columns with preload effects	Published.	*International Journal of Structural Stability and Dynamics,*2013,13(3), 1250065 (23 pages). ERA Rank: B. Impact Factor: 0.455.
	Nonlinear analysis of rectangular concrete-filled steel tubular slender beam-columns with preload effects	Currently under review.	*Journal of Constructional Steel Research.* Submitted in August 2012. ERA Rank: A*. Impact factor: 1.251.
6	Numerical analysis of high-strength concrete-filled steel tubular slender beam-columns under cyclic loading	Currently under review.	*Journal of Constructional Steel Research.* Submitted on 10 January 2013. ERA Rank: A*. Impact factor: 1.251.

Declare by: [Candidate name]　　　　　**Signature**:　　　　　**Date**:

Vipulkumar Ishvarbhai Patel

CONTENTS

Chapter 1

INTRODUCTION

1.1 CONCRETE-FILLED STEEL TUBULAR BEAM-COLUMNS

Concrete-filled steel tubular (CFST) slender beam-columns have been widely used in high rise composite buildings, bridges and offshore structures owing to their excellent performance, such as high strength, high ductility, large energy absorption capacity and low costs. A CFST beam-column is constructed by filling either normal or high strength concrete into a normal or high strength hollow steel tube. Concrete with compressive strength above 50 MPa is considered as high strength concrete while structural steels with yield strength above 460 MPa are treated as high strength steels. The most common CFST beam-column sections are shown in Fig. 1.1.
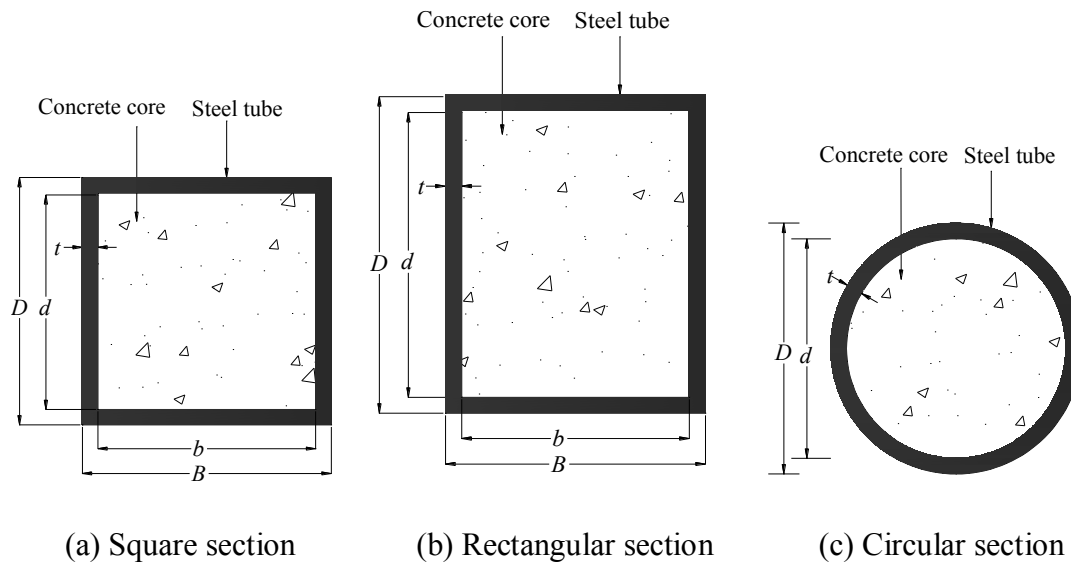
Fig. 1.1 Cross-sections of concrete-filled steel tubular beam-columns.

CFST columns have several advantages over the conventional reinforced concrete and structural steel columns. Firstly, the concrete infill is confined by the steel tube. This confinement effect increases the strength and ductility of the concrete core in rectangular steel tubes. Secondly, the concrete infill delays local buckling of the steel tube. Thirdly, the combined capacity of the steel and concrete significantly increases the stiffness and ultimate strength of CFST columns which makes them very suitable for columns and other compressive members. Finally, the steel tube serves as longitudinal reinforcement and permanent formwork for the concrete core, which results in rapid construction and significant saving in materials. The steel tube can also support a considerable amount of construction and permanent loads prior to the pumping of wet concrete.

The in-filled concrete effectively prevents the inward local buckling of the steel tube so that the steel tube walls can only buckle locally outward. The local buckling modes of hollow columns and CFST box columns are depicted in Fig. 1.2. The steel tube walls of a CFST column under axial load and bending may be subjected to compressive stress gradients. No bifurcation point can be observed on the load-deflection curves of real steel plates under compressive stresses (Liang and Uy 2000). This is caused by the presence of initial geometric imperfections in real thin steel plates. This also leads to difficulty in determining the initial local buckling loads of thin steel plates with imperfections. The classical elastic local buckling theory cannot be used to determine the initial local buckling stress of real steel plates with imperfections. The local buckling of the steel tube walls with initial geometric imperfections and residual stresses reduces the strength and ductility of thin-walled CFST slender beam-columns. The local and overall stability problem is encountered in high strength thin-walled rectangular CFST slender beam-columns with large depth-to-thickness ratios. As a result, the effects of local buckling must be taken into account in the nonlinear analysis and design of CFST slender beam-columns.

When a CFST beam-column is used in the corner of a composite building, the beam-column may be subjected to axial load and biaxial bending. Columns resisting earthquake or wind loads are also subjected to axial load and bending. In practice, all CFST columns should be designed to resist the combined actions of axial load and bending moments. This implies that all columns should be treated as beam-columns. The design of CFST beam-columns under axial load and bending for strength and ductility is complex because of the interaction behavior between the axial load and

bending and the interaction between local and global buckling. In addition, current design codes do not provide adequate specifications for the design of high-strength CFST beam-columns under axial load and bending.

(a) Hollow section   (b) Concrete-filled section
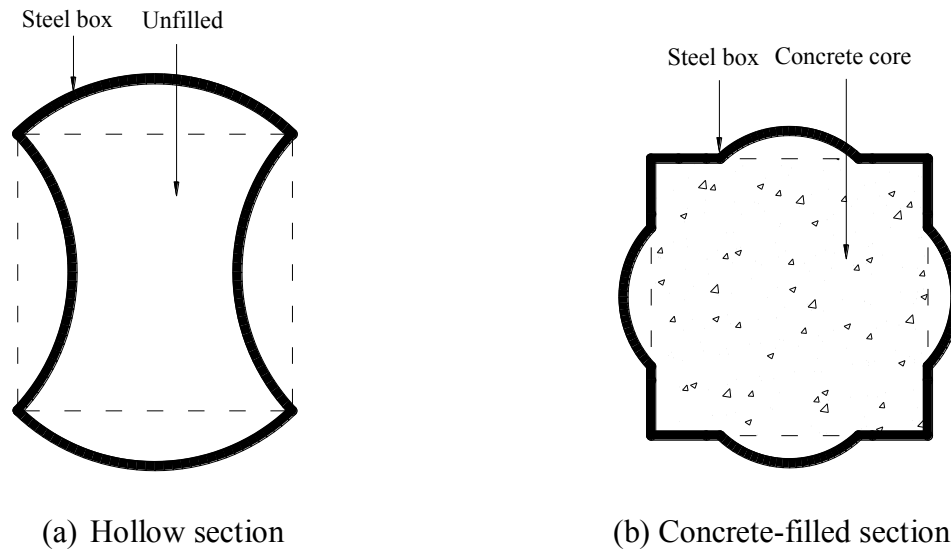
Fig. 1.2 Local buckling modes of steel box columns.

The common construction practice of a high rise composite building is to erect the hollow steel columns several storeys ahead before filling the wet concrete. The hollow steel tubular columns support a considerable amount of construction and permanent loads. This construction method induces preloads on the steel tubes. These preloads on the hollow steel columns cause initial stresses and deformations which may significantly reduce the stiffness and ultimate strength of CFST slender beam-columns. Therefore, the effects of preloads must be considered in the analysis and design of CFST slender beam-columns.

CFST slender beam-columns may be subjected to a constant axial load and cyclic lateral loads in seismic regions. The steel tube walls of a cyclically loaded thin-walled rectangular CFST slender beam-column may undergo cyclic local and overall buckling. The nonlinear inelastic analysis of thin-walled CFST slender beam-columns is complicated because it must account for not only material and initial geometric imperfections as well as second order effects but also the interaction between cyclic local and overall buckling. Cyclic local buckling of steel tube walls reduces the strength and ductility of thin-walled CFST slender beam-columns.

The behavior of CFST slender beam-columns depends on many parameters such as the depth-to-thickness ratio, loading eccentricity ratio, column slenderness ratio, concrete compressive strengths and steel yield strengths. It is highly expensive and time consuming to conduct tests to study the effects of every parameter on the behavior of CFST slender beam-columns. Additionally, the dimensions of the slender column are usually very large, hence it is impractical to experimentally investigate the effects of every parameter on the behavior of CFST slender beam-columns under various loading conditions. In such cases, verified nonlinear inelastic analysis techniques may be the cost-effective methods for determination of the behavior of full scale CFST slender beam-columns.

1.2 RESEARCH SIGNIFICANCE

Even though thin-walled high strength CFST slender beam-columns are frequently used in high rise composite buildings, the understanding of their fundamental behavior is still

not sufficient and efficient analysis and design methods have not been developed owing to the lack of experimental and numerical research on this type of composite columns. The use of high strength concrete in CFST slender columns increases the ultimate strengths of the composite beam-columns but reduces the ductility of the columns because of the brittle nature of high strength concrete. On the other hand, the use of the high strength thin-walled steel tubes leads to economical designs but may cause local buckling. Local bucking of the steel tubes reduces the ultimate loads of concrete-filled thin-walled steel box columns. After the onset of initial local buckling, a thin steel plate can still carry increasing loads without failure. The plate progressively buckles locally with gradually increasing the load. This behavior of thin steel plates is called post-local buckling (Liang et al. 2007). The effects of progressive local bucking have not been considered in existing nonlinear inelastic methods of analysis for CFST slender beam-columns under static uniaxial loads, biaxial loads, preloads and cyclic loads. The inelastic analysis methods that do not consider local buckling effects, may overestimate the ultimate loads of composite columns and frames. The current design codes such as Eurocode 4 (2004), LRFD (1999) and ACI 318 (2002) do not provide specifications for the design of high strength CFST slender beam-columns.

The proposed research aims to develop new numerical models for simulating the nonlinear inelastic behavior of thin-walled high strength CFST slender beam-columns under various loading conditions. The research findings from this project make significant contributions to the analysis and design of CFST slender beam-columns under static uniaxial loads, biaxial loads, preloads and cyclic loads. The numerical models developed provide structural designers with advanced analysis and design tools

that can be used to design safe and economical composite buildings. Furthermore, the proposed numerical models allow the designer to analyse and design CFST beam-columns made of compact, non-compact or slender steel tubes with any strength grades and high strength concrete.

1.3 AIMS OF THIS RESEARCH WORK

The main aim of this research work is to develop new efficient numerical models for predicting the strength and ductility of thin-walled CFST slender beam-columns under static uniaxial loads, biaxial loads, preloads and cyclic loads. The effects of local buckling, concrete confinement and high strength materials are taken into account in the numerical models. Specific aims are given as follows:

- Develop a numerical model for high strength rectangular CFST slender beam-columns under axial load and uniaxial bending with local buckling effects.

- Develop a numerical model for biaxially loaded high strength rectangular CFST slender beam-columns with local buckling effects.

- Develop a numerical model for circular high strength CFST slender beam-columns with preload effects.

- Develop a numerical model for high strength thin-walled rectangular CFST slender beam-columns with preload and local buckling effects.

- Develop a numerical model for high strength rectangular CFST slender beam-columns under cyclic loads.

- Verify numerical models developed by comparisons with existing experimental results.

- Undertake extensive parametric studies to examine the effects of important parameters on the fundamental behavior of CFST slender beam-columns under various loading conditions.

1.4 LAYOUT OF THIS THESIS

The contents of this thesis are divided into 7 chapters. *Chapter 2* presents an extensive literature review on the nonlinear analysis and behavior of CFST columns. Published work on the nonlinear analysis and behavior of CFST beam-columns under axial load and uniaxial bending is firstly reviewed. Research work on the experimental investigation and nonlinear analysis of biaxially loaded rectangular CFST beam-columns is also reviewed. Extensive reviews are then devoted to the preloaded circular and rectangular CFST beam-columns. Finally, the studies on the CFST beam-columns subjected to axial load and cyclic loading are highlighted.

A numerical model based on the fiber element analysis method for determining the axial load-deflection curves and axial load-moment interaction diagrams of rectangular CFST columns under axial load and uniaxial bending is developed and presented in *Chapter 3*. The effects of local buckling, concrete confinement and initial geometric imperfections are considered in the fiber element analysis program. Computational algorithms based on the Müller's method are developed to iterate the neutral axis depth and to adjust the curvature at the column ends to satisfy equilibrium conditions. Performance indices are

proposed to quantify the contributions of the concrete core and steel tube to the ultimate strengths of CFST slender beam-columns. The numerical model developed is employed to study the effects of key parameters on the ultimate strengths and performance indices of CFST columns.

Chapter 4 describes a multiscale numerical model for simulating the local and global buckling behavior of biaxially loaded high strength thin-walled rectangular CFST slender beam-columns. Mesoscale models based on the fiber element method are developed for analysing the column cross-section while macroscale models are proposed to model the axial load-deflection and axial load-moment interaction responses of slender beam-columns. Müller's method algorithms are developed and implemented in the numerical model to iterate the neutral axis depth of the composite section and the curvature at the column ends until nonlinear solutions are obtained. The axial load-deflection curves and ultimate strengths of high strength thin-walled rectangular CFST slender beam-columns obtained from the multiscale numerical model are compared with the experimental results available in the published literature. Steel and concrete contribution ratios and strength reduction factor are proposed to quantify the performance of rectangular CFST beam-columns. The multiscale numerical model is utilized to investigate the effects of concrete compressive strength, depth-to-thickness ratio, loading eccentricity ratio and column slenderness ratio on the performance indices.

In *Chapter 5*, a numerical model is developed for the nonlinear inelastic analysis of high strength circular and rectangular CFST slender beam-columns with preload effects. The

numerical model accounts for the effects of local buckling of steel tubes under stress gradients, initial geometric imperfections, deflection caused by preloads and concrete confinement. Müller's method based on computational algorithms is developed to solve nonlinear equilibrium equations. The accuracy of the numerical model developed is verified by comparisons of numerical results with existing experimental data. The numerical model is utilized to investigate the effects of the preloads, columns slenderness ratios, diameter-to-thickness ratios, loading eccentricity ratios, steel yield strengths and concrete confinement on the behavior of normal and high strength circular and rectangular CFST slender beam-columns under eccentric loading.

Chapter 6 presents a numerical model for simulating the behavior of cyclically loaded high strength thin-walled rectangular CFST slender beam-columns. The numerical model considers the effects of cyclic local buckling of the steel tube walls under stress gradients. The initial geometric imperfections of the slender beam-columns are also included in the fiber element model. The numerical model is developed using the fiber element analysis method and is validated against the experimental results. Parametric studies are performed to investigate the effects of different concrete compressive strengths, steel yield strengths, depth-to-thickness ratios and column slenderness ratios on the cyclic load-deflection curves of rectangular CFST beam-columns.

Important conclusions drawn from this research work are given in *Chapter 7*. Significant achievements in this research work are summarized. Further research in this field is also recommended.

Chapter 2

LITERATURE REVIEW

2.1 INTRODUCTION

The nonlinear analysis and behavior of CFST beam-columns have been an active research area for many years. Extensive research and development work has been undertaken in this area during the last five decades. Several survey papers have appeared in the literature (Shams and Saadeghvaziri 1997; Shanmugam and Lakshmi 2001; Spacone and El-Tawil 2004). This chapter reviews extensive experimental studies and the nonlinear analysis of CFST beam-columns.

The nonlinear inelastic analysis of thin-walled CFST beam-columns is a challenging task as it involves an interaction between local and global buckling of the steel tube. The fundamental behavior of high strength thin-walled CFST beam-columns is influenced by many parameters such as the diameter-to-thickness ratios, column

slenderness ratios, loading eccentricity ratios, concrete compressive strengths and steel yield strengths. Experiments can be conducted to investigate the behavior of CFST beam-columns. However, experimental investigations on CFST beam-columns under various loading conditions are very expensive and time consuming. In addition, it is not rational to derive a theory for the design of CFST beam-columns from limited test data. Experiments should be used to verify a theory for the design of CFST beam-columns rather than to derive the theory (Liang 2009a). On the other hand, the numerical modeling can compensate the drawbacks of experiments and can be used to investigate the behavior of full-scale high strength CFST beam-columns.

There is a wealth of literature in dealing with CFST beam-columns. The literature review given in the following sections concentrates on experimental works and nonlinear techniques developed by various researchers to investigate the behavior of CFST short and slender beam-columns under uniaxial bending, biaxial bending, preloads and cyclic loading.

2.2 CFST COLUMNS UNDER AXIAL LOAD AND UNIAXIAL BENDING

CFST columns are often subjected to combined axial load and uniaxial bending in composite frame structures. CFST columns under axial load and bending are generally called "beam-columns". Extensive research has been conducted on the behavior of CFST beam-columns subjected to axial load and bending. The experimental work on uniaxially loaded CFST beam-columns is reviewed in the following section. Review on

the nonlinear analyses of CFST beam-columns under axial load and uniaxial bending is given in Section 2.2.2.

2.2.1 Experimental Studies

The first experiment on the ultimate strengths of CFST beam-columns was undertaken by Klöppel and Goder (1957). Further tests on CFST short beam-columns were conducted by Furlong (1967) who tested eight circular CFST columns and five square CFST columns under axial and eccentric loads. The depth-to-thickness ratio of these tested CFST beam-columns ranged from 29 to 98. He found that the steel and concrete components independently resisted the axial load applied to the CFST beam-column. The influences of the steel tube thickness on the ultimate axial strengths of CFST beam-columns were examined. Experimental results indicated that the thick-walled steel tube offered confinement to the concrete core in a CFST beam-column. This confinement effect increased the concrete strength in circular CFST beam-columns. A rectangular steel tube provided less confinement to the concrete core than a circular steel tube. The thin-walled steel tubes of CFST beam-columns locally buckled outward due to the restrains provided by the infilled concrete. It was suggested that a CFST beam-column cross-section could be treated as a reinforced concrete section for determining the axial load-moment interaction diagrams.

Tests were carried out by Knowles and Park (1969) to examine the effects of concrete confinement on the behavior of circular and square CFST beam-columns with various column slenderness ratios and depth-to-thickness ratios. They studied 12 circular and 7

square CFST columns with depth-to-thickness ratios of 15, 22 and 59. Test results indicated that the confinement of the concrete core provided by the steel tube in a square CFST column increased only the ductility of the concrete core but not its ultimate strength. On the other hand, confinement provided by the steel tube increased both the compressive strength and ductility of the concrete core in a circular CFST beam-column. However, this confinement effect was shown to decrease with increasing column slenderness. This has contributed to the fact that the column failed by buckling before the strain caused an increase in the concrete compressive strength. All CFST columns tested under axial load failed by column buckling. Local buckling was not observed in all tested CFST columns. The concrete failure appeared after the maximum load was reached. The straight line interaction formula for eccentrically loaded CFST columns was shown to be conservative for short columns and to be unsafe for slender columns. It was concluded that the tangent modulus method gave good prediction of the strengths of columns with L/D ratios greater than 11 but conservative prediction for columns with L/D ratios less than 11.

The experimental behavior of pin-ended normal strength square CFST slender beam-columns under axial load and uniaxial bending was investigated by Bridge (1976). A series of slender column tests was performed to examine the effects of loading eccentricity, steel tube thickness, column slenderness ratios and uniaxial bending on the behavior of the slender beam-columns. The test specimens were made of normal strength steel tubes and concrete. Initial geometric imperfections at the mid-height of the specimens were measured. Test results indicated that the ultimate axial strengths of CFST beam-columns increased with increasing the steel tube thickness. Increasing the

loading eccentricity ratio decreased the ultimate axial strengths of CFST beam-columns. In addition, increasing column slenderness ratio reduced the ultimate axial strengths of CFST beam-columns. The ultimate axial strengths and axial load-deflection curves measured from the tests were compared with those predicted by an inelastic stability analysis technique developed by Roderick and Rogers (1969). The local buckling of the steel tube walls for CFST slender beam-columns was not identified in his tests.

Shakir-Khalil and Zeghiche (1989) tested rectangular CFST slender beam-columns in single curvature bending. These CFST beam-columns were subjected to axial load and uniaxial bending. The axial load was applied at an eccentricity about the major or minor axis. Seven CFST slender beam-columns were tested to failure. One of these columns was tested under a concentric axial load. The slender beam-columns were constructed from cold-formed steel tubes and normal strength concrete. The steel yield strengths varied from 343 MPa to 386 MPa while the concrete compressive strength varied from 40 MPa to 45 MPa. Specimens were fabricated from 5 mm thick steel tubes so that their depth-to-thickness ratio was 24. Although the initial geometric imperfection was not measured in the study, the effects of initial geometric imperfection on the ultimate axial strengths of CFST beam-columns were recognized. Experimental results were compared with the design loads calculated by BS5400 (1979) and finite element analysis. The experimental ultimate axial loads, axial load-deflection curves and failure modes of rectangular CFST beam-columns were reported. It was observed that all tested CFST columns failed by overall column buckling. The local buckling of the steel tube walls was not observed in all tested columns. Further tests on normal strength rectangular CFST slender beam-columns under uniaxial bending were conducted by Shakir-Khalil

and Mouli (1990). Three different rectangular CFST column cross-sections were used in their study such as 120 × 80 × 5 mm, 150 × 100 × 5 mm and 250 × 150 × 6.3 mm. The yield strength of the steel section varied from 340 MPa to 363 MPa while the concrete compressive strength ranged from 35 MPa to 40 MPa. The test results showed that the ultimate axial strength of the CFST slender beam-columns significantly increased when a larger steel section was used. It was found that the steel tube walls were pushed out by the crushed concrete which took the shape of the deformed steel section.

The behavior of circular and square CFST columns under axial and uniaxial bending was investigated experimentally by Matsui et al. (1995). These columns were made of steel tubes with a yield strength of 445 MPa filled with 32 MPa concrete. The steel tube had a depth-to-thickness ratio of 33. Test parameters included concrete compressive strengths, buckling length, depth-to-thickness ratio and loading eccentricity. A total of sixty columns were tested including twelve hollow steel tubular columns under axial load. The columns were loaded through hemispherical oil film bearing so that they were pin-ended in the plane of bending. The design strengths calculated from AIJ (Architectural Institutive of Japan 1997), modified AIJ and CIDECT (International committee for the Development and Study of Tubular Structures) design methods were compared with experimental ultimate axial strengths. It was found that AIJ design method yielded conservative predictions of the ultimate strengths of slender beam-columns. Test results indicated that increasing the loading eccentricity reduced the ultimate axial strengths of the beam-columns. The effects of the loading eccentricity on the ultimate axial strengths of CFST beam-columns were shown to reduce with an increase in the column slenderness ratio. The mid-height deflection at the ultimate axial

strength of the slender beam-column increased with an increase in the loading eccentricity. The axial load-moment-interaction diagrams obtained from tests were compared with those predicted by AIJ and CIDECT for circular and square CFST beam-columns. The beam-columns with a length-to-depth ratio greater than 18 could not attain the full plastic moment at the maximum load due to the overall column buckling.

Shams and Saadeghvaziri (1997) presented a state-of-the art review on CFST columns. They highlighted the experimental and analytical studies on the design and behavior of CFST columns. The behavior of circular and rectangular CFST beam-columns under various loading conditions was discussed in their study. The effects of the cross-section shape, width-to-thickness ratios and column slenderness ratios on the performance of CFST beam-columns were summarized. It was found that the confinement of the concrete core provided by the steel tube increased the strain in the concrete. It was observed that steel plates buckled outward in one of the sides of a column before the ultimate axial strength was reached. The remaining sides of a column cross-section were buckled after the ultimate load was attained. The steel plates were buckled outward in four sides of a column with large width-to-thickness ratios. In addition, local buckling of the steel tube occurred after crushing of the concrete core.

The experimental study of axially loaded short CFST columns with depth-to-thickness ratio ranging from 17 to 50 was undertaken by Schneider (1998). He tested fourteen specimens to examine the effects of steel tube shape and tube wall thickness on the ultimate axial strengths of CFST columns. All steel boxes of the specimens were cold-

formed carbon steel and were seam welded and annealed to relieve residual stresses. The yield strength of the steel section varied from 322 MPa to 430 MPa and the compressive concrete strength ranged from 23 MPa to 30 MPa. Test results indicated that the post-yield strength and stiffness of circular CFST columns were higher than those of square or rectangular CFST beam-columns. Local buckling of circular steel tubes occurred at an axial ductility of 10 or more while square and rectangular tubes buckled locally at a ductility ranged from 2 to 8. Circular steel tubes possessed higher post-yield axial ductility and strength than square or rectangular concrete-filled tube sections. All circular CFST columns displayed the strain hardening which occurred in rectangular CFST columns with $D/t < 20$. The confinement provided by the steel tube only occurred after the axial load reached about 92% of the column yield strength. The yield load of a CFST column was found to increase significantly with decreasing the depth-to-thickness ratio.

Bridge and O'Shea (1998) studied experimentally the behavior of axially loaded thin-walled steel box sections with or without concrete infill. The width-to-thickness ratios of these sections ranged from 37 to 131 while the length-to-width ratios of the columns ranged from 0.8 to 3. The performance of thin-walled CFST short columns was compared with that of hollow steel tubular columns. The buckling modes for a wide range of width-to-thickness ratios were examined. It was observed that the concrete core prevented the inward buckling of the steel tube. This buckling mode significantly increased the strength of the steel tubes. They suggested that the effective width formula for clamped steel plates could be used to calculate the strength of thin-walled steel tubes

with concrete infill. Local buckling of the steel tubes was found to reduce the ultimate strength of thin-walled CFST short beam-columns under axial compression.

Experimental studies on the ultimate strengths of high strength thin-walled square CFST slender beam-columns under axial load and uniaxial bending have been conducted by Chung et al. (1999). These beam-columns were made of steel tubes with a yield strength of 445 MPa filled with 88 MPa high strength concrete. The width-to-thickness ratio of CFST slender beam-columns was 39 while the length of the beam-column ranged from 2250 mm to 3000 mm. The effects of the buckling length-depth ratio and eccentricity of the applied axial load on the behavior of CFST beam-columns were studied. They found that local buckling of slender columns under concentric or eccentric loading occurred after the ultimate axial strength was attained while local buckling of short columns under concentric load occurred at the ultimate axial strength. The column with a smaller slenderness ratio had a higher ultimate strength.

O'Shea and Bridge (2000) conducted experiments to study the behavior of circular CFST short columns. These columns were tested under axial compression which was applied on either steel tube or both steel tube and concrete core at small eccentricities. The specimens had a length-to-diameter ratio of 3.5 and diameter-to-thickness ratios ranging from 60 to 220. The steel tubes were filled with high strength concrete. The compressive strengths of the concrete cylinders were measured as 50 MPa, 80 MPa and 120 MPa. Test results demonstrated that local buckling remarkably influenced the strength of hollow steel tubular columns. The bond between the steel tube and concrete was shown to be critical in determining the mode of local buckling. The sufficient bond

between the steel tube and concrete core prevents the buckling of the steel tube. In addition, the confinement of the concrete core provided by the circular steel tube was affected by the loading conditions. The effect of the confinement increased with increasing the axial load applied on the concrete core. Design methods were suggested for determining the strength of circular CFST columns subjected to various loading conditions. The strengths obtained from these design methods were compared with experimental strengths. The comparison was also conducted between the design method and Eurocode 4. They reported that Eurocode 4 provided conservative strength predictions for circular steel tubes filled with concrete strength up to 50 MPa and subjected to axial load and bending.

Han (2002) investigated experimentally the influences of constraining factors and the depth-to-width ratios on the ultimate strength and ductility of axially loaded rectangular CFST columns. A total of 24 CFST columns were tested. The main variables examined in the test program were the constraining factor and depth-to-width ratio. The width of the steel tubes varied from 70 mm to 160 mm while the depth of the steel tubes ranged from 90 mm to 160 mm. The short columns were constructed by steel tubes filled with high strength concrete of 60 MPa. The steel yield strength varied from 194 MPa to 228 MPa. He reported that the axial strength and ductility of CFST columns decreased with an increase in the depth-to-width ratio but increased with an increase in the constraining factor. A confinement factor was proposed for determining the section performance of composite columns but it did not take into account the effects of b/t ratios on the behavior of composite sections.

Zhang et al. (2003) presented test results of 8 high strength CFST beam-columns subjected to axial load and uniaxial bending. A 150 × 150 mm cross-section was used in the tests. Test parameters included column slenderness ratios, steel ratios and loading eccentricity. Test specimens were made of high strength concrete with the compressive strength of 94 MPa and steel tubes with yield strengths of 316 MPa or 319 MPa. Their test results indicated that increasing the column slenderness ratio and loading eccentricity reduced the ultimate axial strengths of CFST beam-columns. The ultimate axial strengths of CFST beam-columns were shown to decrease with increasing the steel ratio.

Han and Yang (2003) carried out several tests to study the behavior of rectangular CFST short columns under long-term sustained loading. They investigated the effects of steel ratios, long-term sustained load level, slenderness ratio, strength of the materials and depth-to-thickness ratio on the ultimate strengths of CFST columns. A theoretical model given in ACI codes (ACI 1992) was used to compare the predicted behavior of CFST columns under long-term loading. It was found that the axial strain due to long-term sustained loading affected the results and tended to stabilize after about 100 days of loading. The strength index decreased as the slenderness ratio and the concrete strength increased, when the slenderness ratio was less than 10. The maximum strength reduction due to long-term loading effects was approximately 20% of the strength under short-term loading. A set of formulas was developed by Han and Yang (2003) for predicting the ultimate strengths of rectangular CFST short columns with long-term sustained loading effects.

Fujimoto et al. (2004) examined experimentally the effects of high strength materials on the behavior of circular and square CFST short columns under eccentric loading. They tested CFST short columns with a wide range of parameters including the tubes' diameter-to-thickness ratio, normal and high strength concrete, and normal and high strength steels. Circular steel tubes used to construct these CFST columns were cold formed from a flat plate by press welding and seam welding. The length-to-diameter ratio of the specimens was 3.0. The depth-to-thickness ratios of these specimens ranged from 27 to 101. The yield strengths of the steel tubes were 283, 579 and 834 MPa and the concrete cylinder compressive strengths were 25, 41 and 78 MPa. The applied axial load ranged from 13% to 59% of the ultimate axial load of corresponding column obtained by the theoretical model. They reported that the use of high strength concrete reduced the ductility of circular CFST beam-columns. Also, the use of high strength steel tubes or steel tubes with a smaller diameter-to-thickness ratio increased the ductility of circular CFST columns. It was concluded that the confinement effect did not increase the moment capacity of square CFST beam-columns and local buckling must be taken into account in evaluating the strengths of square CFST beam-columns with large width-to-thickness ratios.

Sakino et al. (2004) have investigated experimentally the ultimate loads and behavior of circular CFST short columns under axial load. They tested 114 CFST columns to study the effects of the tube shape, steel yield strengths, diameter-to-thickness ratio and concrete strengths on the behavior of axially loaded CFST columns. The circular steel tubes used in these CFST columns were cold formed from a flat plate by press bending and seam welding. The depth-to-thickness ratios of these columns ranged from 17 to

102. The yield strengths of steel tubes ranged from 279 MPa to 853 MPa. The concrete cylinder compressive strengths ranged from 25 MPa to 85 MPa. The test data was used to develop design methods for CFST columns. A new design formula based on the test results was also proposed for circular and square CFST columns.

The behavior of axially loaded circular CFST short columns with various concrete strengths was presented by Giakoumelis and Lam (2004). The effects of the steel tube thickness, the bond strength between the concrete and the steel tube and concrete confinement on the behavior of circular CFST short columns were examined. They tested 15 circular CFST short columns with concrete compressive strengths of 30, 60 and 100 MPa and depth-to-thickness ratios varied from 23 to 31. The yield strength of the steel tube was either 343 MPa or 365 MPa. The diameter of the circular CFST short columns was 114 mm. The length of the beam-columns was 300 mm. They compared various design codes for circular CFST columns. They reported that Eurocode 4 provided accurate strength predictions for circular CFST beam-columns with normal and high strength concrete. Their results indicated that the concrete strength had a considerable effect on the bond between the steel tube and concrete core.

Liu (2006) undertook experimental studies on the structural behavior of high strength rectangular CFST beam-columns subjected to axial load and uniaxial bending. He tested four slender and sixteen stub rectangular high strength steel tubes with yield strength of 495 MPa filled with high strength concrete of 60 MPa. The ultimate axial strengths of CFST columns measured from the tests were compared with the design ultimate loads calculated using Eurocode 4. It was shown that EC4 accurately predicted the ultimate

axial strengths of axially loaded CFST columns, but was quite conservative for predicting the ultimate axial strengths of eccentrically loaded CFST columns. The conservatism of the EC4 predictions increased as the eccentricity increased. Moreover, the ultimate capacities of CFST slender beam-columns were significantly reduced by increasing the load eccentricity ratio.

Lue et al. (2007) tested twenty-four rectangular CFST slender beam-columns with a depth-to-thickness ratio of 33 and concrete compressive strengths varying from 29 to 84 MPa. These beam-columns with a cross-section of 100 × 150 mm were constructed by cold-formed steel tubes. Specimens were fabricated from 4.5 mm thick steel tube so that their depth-to-thickness ratio was 33. The length of the column was 1855 mm. The yield strength of the steel tube was 379 MPa. It was observed that CFST columns with normal strength concrete failed by the global buckling while local buckling failure mode was found in the specimens with high strength concrete. Test results were compared with various composite design codes to examine the validity of the design codes. It was concluded that the AISC-LRFD (2005) generally gave a good estimate of the ultimate loads of high strength CFST columns while the AISC-LRFD (1999) overestimated the ultimate loads of high strength CFST columns.

Experiments on high strength circular CFST slender beam-columns under axial load and bending were undertaken by Lee et al. (2011). They studied the effects of the diameter-to-thickness ratios and loading eccentricity ratios on the axial load-deflection responses and axial load-moment interaction diagrams of CFST beam-columns. Their studies indicated that the confinement effect on the ultimate bending strength was insignificant

for the beam-column with diameter-to-thickness ratios ranging from 40 to 100 and loading eccentricity ratios ranging from 0.2 to 0.5. In addition, the axial stiffness and flexural rigidity of a circular CFST column decreased with an increase in the diameter-to-thickness ratio. The ductility of normal strength circular CFST beam-columns was higher than that of high strength circular CFST beam-columns.

Portolés et al. (2011) described results obtained from a series of 37 tests on normal and high strength circular CFST slender beam-columns under eccentric loading. The specimens were tested under eccentric compression to investigate the effects of the concrete compressive strengths, diameter-to-thickness ratio, loading eccentricity ratio and column slenderness ratio. The ultimate axial strengths obtained from the experiments were compared with the design ultimate loads calculated using the design rules specified in Eurocode 4. They used performance indices to quantify the effects of the primary variables on the ultimate axial strength and ductility of circular CFST slender beam-columns. Design recommendations based on the test results were proposed for high strength circular CFST beam-columns. It was concluded that the ultimate axial strength of eccentrically loaded circular CFST beam-columns decreased with increasing either the column slenderness ratio or loading eccentricity ratio but increased due to the use of either high strength concrete or small depth-to-thickness ratio of the steel tube.

Uy et al. (2011) carried out an experimental investigation on concrete-filled stainless steel tubular short and slender columns with circular, square and rectangular cross-sections. The ultimate axial strengths, failure modes, axial load-strain relationships,

axial load-shorting curves and axial load-deflection responses were measured in the tests. The experimental ultimate axial strengths of CFST columns were compared with the design strengths calculated using AS 5100 (2004), AISC (2005), Chinese code DBJ/T (2010) and Eurocode 4 (2004) for CFST columns. The authors concluded that AS 5100, AISC, DBJ/T and EC4 underestimated the ultimate axial strengths of concrete-filled stainless steel tubular columns under axial compression.

Ellobody and Ghazy (2012a, 2012b) studied the experimental behavior of pin-ended fiber reinforced concrete-filled stainless steel tubular columns under axial and eccentric loads. The length of composite columns varied from short to slender. The circular stainless steel tubes used in the tests were cold-rolled from flat strips of austenitic stainless steel. The tubes had an outer diameter of 100 mm and a plate thickness of 2 mm so that the tubes had diameter-to-thickness ratio of 50. The stainless steel tubes were filled with plain and polypropylene fiber reinforced concrete having a nominal cub strength of 40 MPa. The ultimate axial strengths, axial load-strain curves, axial load-shortening relationships and axial load-deflection responses of circular concrete-filled stainless steel tubular columns were measured. Four failure modes such as the stainless steel yielding, local buckling, concrete crushing and flexural buckling were observed. Test results indicated that fiber reinforced CFST columns had improved ductility compared with plain CFST columns. It was concluded that the EC4 accurately predicted the ultimate loads of axially loaded concrete-filled stainless steel circular tubular columns, but was quite conservative for predicting the ultimate loads of the eccentrically loaded columns. The conservatism of the EC4 predictions increased as the eccentricity increased.

A test was undertaken by Liew and Xiong (2012) to investigate the behavior of 27 axially loaded CFST columns. Steel fibers were added into the ultra-high strength concrete. The effects of ultra-high strength concrete on the strength and ductility of CFST column were studied. Test results demonstrated that the ultra-high strength concrete increased the ultimate strengths of CFST columns but reduced the ductility of the columns because of the brittle nature of the ultra-high strength concrete. However, the ductility and strength of CFST columns with ultra-high strength concrete increased with an increase in the steel contribution ratio. The use of fiber reinforced concrete in CFST beam-columns resulted in the similar behavior. The experimental ultimate axial strengths were compared with the design strengths calculated by Eurocode 4. It was shown that the EC4 accurately predicted the ultimate strengths of axially loaded ultra-high strength concrete columns.

Abed et al. (2013) carried out tests on 16 CFST short columns under axial load. The steel tubes were filled with normal and high strength concrete having a compressive strength of 44 MPa or 60 MPa. The diameter-to-thickness ratios of 20, 32 and 54 were considered in the experimental investigation. The main variable parameters in the tests were the concrete compressive strength and diameter-to-thickness ratio. Test results indicated that the ultimate axial strength of circular CFST columns increased with an increase in the concrete compressive strength. The ductility of circular CFST columns decreased with an increase in the concrete compressive strength for larger diameter-to-thickness ratios. Increasing in the diameter-to-thickness ratio reduced the stiffness and ultimate axial strength of axially loaded circular CFST short columns. The ultimate axial strengths measured from the tests were compared with the design strengths

calculated by the theoretical equation, AISC code (2010), American Concrete Institute (ACI 2011) and Australian Standard (AS 2009) codes, Giakoumelis and Lam (2004) equations, Mander et al. (1988) equations and Eurocode 4 (2005). They concluded that the equations given by Mander et al. (1988) gave a good estimate of the ultimate loads of CFST columns while AISC, ACI and AS and Eurocode 4 underestimated the ultimate loads of CFST columns up to 43%. These design codes except Eurocode 4 for CFST beam-columns have not considered the effects of concrete confinement that significantly increase the strength and ductility of the concrete core. As a result, the ultimate loads calculated by these codes deviate considerably from experimental results.

It can be seen from the past experimental investigations that the behavior of uniaxially loaded high strength thin-walled rectangular CFST slender beam-columns has not been adequately investigated. Literature review on nonlinear analysis techniques for predicting the behavior of CFST columns under axial load and uniaxial bending is provided in the following section.

2.2.2 Nonlinear Analysis

Neogi et al. (1969) proposed a numerical model for predicting the elasto-plastic behavior of pin-ended circular CFST slender beam-columns under eccentric loading. In the numerical model, the tangent modulus method was used to analyze axially loaded columns while eccentrically loaded beam-columns were analyzed by assuming a displacement function. However, the effects of the concrete tensile strength and concrete confinement were not taken into account in their numerical model. As a result

of this, their numerical model was found to underestimate the ultimate strengths of circular CFST slender beam-columns. The load-deflection analysis procedure presented by Neogi et al. (1969) can be used to develop strength envelopes by varying the loading eccentricity. However, it is not efficient when the loading eccentricity is large. Despite of this, the axial load-moment interaction diagrams of circular CFST slender beam-columns have not been studied by Neogi et al. (1969).

Tang et al. (1996) proposed a confining pressure model for concrete in circular CFST columns. The model accounts for the effects of material and geometric properties of the column on the strength enhancement and the post-peak behavior. It was found that their model generally overestimated the lateral confining pressure in circular CFST columns (Liang and Fragomeni 2009). Susantha et al. (2001) proposed uniaxial stress-strain relationships for concrete confined by various shaped steel tubes. Susantha et al. (2001) used the confining pressure model proposed by Tang et al. (1996) for circular CFST columns.

The nonlinear behavior of CFST short columns was discussed by Schneider (1998) who developed a nonlinear three-dimensional finite element model for the analysis of CFST columns. The model was developed using the finite element program ABAQUS. An eight-node shell element was employed to model the steel tube while the concrete core was modeled using 20-node brick elements. The model considered the inelastic behavior of structural steels and concrete. The Prandtl-Reuss flow rule was used to determine the inelastic deformation of steel plates while von Mises yield criteria were employed to define the yield surfaces. The results obtained from the finite element

analysis were compared with experimental results. It was shown that the elastic and plastic behavior of CFST beam-column specimens could be predicted by the finite element model. However, the ultimate axial strengths predicted by the finite element model were slightly higher than the test results.

Vrcelj and Uy (2002) presented a numerical model for simulating the load-deflection responses of high strength square CFST slender beam-columns under axial load and uniaxial bending. They investigated the effects of compressive strengths, steel yield strengths and column slenderness ratios on the ultimate axial strengths of high strength square CFST slender beam-columns. However, their model did not account for the effects of confinement provided by the steel box on the ductility of the concrete core and progressive local buckling of thin steel plates under stress gradients. The axial load-moment interaction diagrams of high strength rectangular CFST slender beam-columns have not been studied by Vrcelj and Uy (2002).

Hu et al. (2003) developed a finite element model for the nonlinear analysis of axially loaded CFST short beam-columns with confinement effect. They employed the general purpose finite element analysis program ABAQUS to study the inelastic behavior of CFST beam-columns. Square and circular concrete-filled sections with stiffened reinforcing ties were used in the nonlinear analysis. The steel tubes were simulated using an elastic-perfectly-plastic model with associated flow theory while an elastic-plastic theory with associated flow and isotropic hardening rule was used to model the concrete. The von Mises yield criterion was employed to define the elastic limit of the steel tubes when it was subjected to multiple stresses. On the other hand, a linear

Drucker-Prager yield criterion was used to model the yield surfaces of the concrete because the concrete is usually subjected to triaxial compressive stress and failure of the concrete is dominated by increasing in the hydrostatic pressure. The interaction between the concrete core and steel tube was modeled by special nine-node interface elements. The finite element model was verified by experimental results. They concluded that circular steel tube provided a good confining effect on concrete core especially when the width-to-thickness ratio of the steel tube was small and local buckling of the steel tube was not occurred. However, square CFST beam-columns did not provide a good confining effect on the concrete core especially when the width-to-thickness ratio of the steel tube was larger and the steel tube was buckled locally outward. They proposed a confining pressure model for concrete in circular CFST beam-columns made of normal strength steel and concrete. However, their confining pressure model was found to overestimate the confining pressure in high strength circular CFST columns with depth-to-thickness ratio less than 47 (Liang and Fragomeni 2009).

Liang and Uy (2000) investigated the post-local buckling behavior and ultimate strength of thin steel plates in rectangular CFST columns using the nonlinear finite element analysis method. In their investigation, an eight-node quadratic plate element based on the Mindlin plate theory was used to describe the local buckling displacement of the plate in the finite element analysis. The plate was divided into 10 layers in order to treat the plasticity of the plate by using the von Mises yield criterion with volume approach. The effects of geometric imperfection, slenderness ratio and residual stress on the post-local buckling strengths of clamped steel plates were studied. Well-known Ramberg-Osgood formula was employed to model steel plates with residual stresses. They found

that the residual stresses had considerable effects on the load-deflection behavior of clamped plates, and the stiffness and ultimate strength of plates decreased by increasing the residual stresses. It is worth mentioning that the method developed by Liang and Uy (2000) is an efficient theoretical method for determining the initial local buckling loads and the post-local buckling reserve strengths of plates with imperfections.

Ellobody et al. (2006) presented the design and behavior of circular CFST short columns under axial compression. They employed the finite element program ABAQUS to study the inelastic behavior of normal and high strength circular CFST short columns under axial compression. The compressive strength of concrete ranged from 30 MPa to 110 MPa covering normal and high strength concrete. The finite element analysis was conducted on columns with a wide range of diameter-to-thickness ratios ranging from 15 to 80 which covers non-compact and compact steel tube sections. The concrete confinement model proposed by Hu et al. (2003) was used in the finite element analysis. The ultimate axial strengths and axial load-shortening curves for circular CFST columns were evaluated. The finite element results were compared with the test results provided by Giakoumelis and Lam (2004) and Sakino et al. (2004). Parametric studies were conducted to examine the effects of concrete compressive strengths, steel yield strengths and diameter-to-thickness ratios. The ultimate axial strengths obtained from the finite element analyses were compared with the design strengths calculated using Australian, American and European specifications. They reported that the design strengths obtained by Australian and American specifications were conservative.

Liang et al. (2007) investigated the local and post-local buckling behavior of thin steel plates in CFST beam–columns using the nonlinear finite element method. Clamped steel plates with various width-to-thickness ratios and restrained by the concrete core were studied. Geometric and material nonlinear effects were considered in their study. A 10 ×10 mesh was used in the analyses in order to obtain accurate results. The material plasticity was defined by the von Mises yield criterion. They found that increasing the width-to-thickness ratio of a steel plate under the predefined stress gradients reduced its lateral stiffness, initial local buckling stress and ultimate strength. They proposed formulas for predicting the initial local buckling stresses of thin steel plates in CFST beam-columns with initial geometric imperfections and residual stresses. They also proposed effective strength and width formulas for determining the post local buckling strengths of steel plates in thin-walled CFST beam-columns. It is worth mentioning that the formulas proposed by Liang et al. (2007) can be used directly in the design of thin-walled CFST beam-columns. In addition, they can be incorporated in numerical models to account for local buckling effects on the behavior of CFST beam-columns under various loading conditions.

Numerical models for the nonlinear inelastic analysis of circular CFST short columns under axial and eccentric loading were developed by Liang and Fragomeni (2009, 2010). They proposed constitutive material models for confined concrete. The numerical models incorporated accurate constitutive models for normal and high strength concrete confined by either normal or high strength circular steel tubes. In their study, a circular CFST section was divided into fine fiber elements which were assigned with either steel or concrete material properties. The coordinates and cross-section area

of each element were automatically calculated based on the geometry of the cross-section. Fiber stresses were calculated from fiber strains. Secant method algorithms developed by Liang (2009b) were incorporated in the numerical models to iterate the neutral axis depth in a circular CFST beam-column section until the force equilibrium conditions were satisfied. The accuracy of the numerical models was examined by comparing the ultimate axial strengths, ultimate bending strengths, axial load-strain curves and moment-curvature responses with corresponding experimental results. The accuracy and reliability of various confining pressure models proposed by Tang et al. (1996), Hu et al. (2003) and the authors were evaluated. It was found that the confining pressure models given by Tang et al. (1996) and Hu et al. (2003) overestimated the ultimate axial strengths of high strength circular CFST columns. The comparison demonstrated that the confining pressure models proposed by Liang and Fragomeni (2009) provided reliable results for both normal and high strength circular CFST columns under axial and eccentric loading. The verified numerical models were then utilized to investigate the fundamental behavior of circular CFST columns with various diameter-to-thickness ratios, concrete compressive strengths, steel yield strengths, axial load levels and section shapes. They proposed new design models based on the numerical results for determining the ultimate axial and ultimate pure bending strengths of circular CFST beam-columns. They highlighted that the numerical models and formulas were shown to be effective simulation and design tools for circular CFST beam-columns under axial and eccentric loading.

An analytical model for determining the behavior of axially loaded circular CFST short columns was described by Choi and Xiao (2010). An analytical procedure for predicting

the axial load-strain curves of circular CFST short beam-columns was presented. Various modes of the interaction between the steel tube and infill concrete under axial compression were discussed. The axial load-strain curves for circular CFST short columns under axial compression predicted by the analytical model were compared with experimental data. They found that the behavior of circular CFST short columns depended on the concrete strength and confinement of the concrete provided by the steel tube. The drawbacks of the analytical procedure are that the strain hardening of materials was not taken into account. Consequently, the procedure produced solutions that deviated considerably from the corresponding experimental results in the post-peak range of the axial load-strain curves.

The nonlinear inelastic behavior of high strength circular CFST slender beam-columns was investigated by Liang (2011a, 2011b). He developed a numerical model based on the accurate fiber element method. Material constitutive material model proposed by Liang and Fragomeni (2009) for confined concrete was incorporated in the numerical model. The numerical model accounted for the effects of concrete confinement, initial geometric imperfection and second order. The cross-section analysis of circular CFST beam-columns was discussed. In his numerical model, the deflected shape of circular CFST beam-columns was assumed to be a part of sine curve. Computational algorithms based on the secant method were developed to adjust the neutral axis depth of the composite section. In the axial load-deflection analysis, the deflection at the mid-height of a slender beam-column was gradually increased. The equilibrium of internal and external bending moments was maintained at the mid-height of the beam-column. In axial load-moment interaction strength analysis, the curvature at the mid-height of the

beam-column was gradually increased. The curvature at the column end was iteratively adjusted by the secant method to satisfy the moment equilibrium at the mid-height of the beam-column. The ultimate axial strengths, ultimate bending strengths and axial load-deflection responses of circular CFST slender beam-columns under eccentric loading obtained from numerical model were compared with experimental results available in the published literature. The numerical model was then utilized to investigate the effects of column slenderness ratio, loading eccentricity ratio, concrete compressive strengths, steel yield strengths, steel ratio and concrete confinement on the behavior of high strength circular CFST slender beam-columns in terms of axial load-deflection responses, ultimate strengths, axial load-moment interaction diagrams and strength increase due to confinement effects. It was concluded that increasing column slenderness ratio and eccentricity ratio significantly reduced the flexural stiffness and ultimate axial strength of eccentrically loaded circular CFST beam-columns. The deflections and displacement ductility of the beam-columns increased with an increase in the column slenderness ratio. In addition, the stiffness and strength of circular CFST slender beam-columns increased with increasing the concrete compressive strength. It was noted that the steel yield strength did not have an effect on the initial flexural stiffness of slender beam-columns. However, the ultimate axial strengths of slender beam-columns increased significantly with increasing the steel yield strength. Moreover, the flexural stiffness and ultimate strength were shown to increase significantly with increasing the steel ratio. The confinement effect was shown to decrease with increasing the eccentricity ratio and the column slenderness ratio.

Portolés et al. (2011) proposed numerical procedures for predicting the axial load-deflection responses of high strength circular CFST slender beam-columns under eccentric loading. The effects of initial geometric imperfection on the performance of circular CFST slender beam-columns were incorporated in the numerical model. The confinement provided by the circular steel tube was also considered. The ultimate axial strengths and axial load-deflection curves obtained from the numerical model were compared with experimental data to examine the accuracy of the numerical model. It was found that the numerical model predicted well the behavior of normal and high strength circular CFST slender beam-columns. A parametric study was conducted to investigate the effects of confinement index, column slenderness ratio and concrete compressive strengths on the ultimate axial strengths, concrete contribution ratio and strength index of CFST beam-columns. Recommendations for the design of CFST slender beam-columns were given based on the parametric study.

El-Heweity (2012) employed the finite element program ANSYS to study the inelastic behavior of axially loaded high strength circular CFST short columns. The finite element model incorporated the constitutive models for steels and concrete. The finite element model was verified by comparisons with experimental results. The fundamental behavior of circular CFST beam-columns with various column diameters and steel yield strengths was studied. Strength enhancement factor and ductility index were proposed to quantify the performance of the CFST beam-columns. They reported that the steel yield strength did not have a significant influence on the concrete ductility in circular CFST columns. However, the steel yield strength had considerable effect on the concrete strength of circular CFST beam-columns.

Ellobody (2013) discussed the nonlinear behavior of fiber reinforced concrete-filled stainless steel tubular (CFSST) columns. A three-dimensional finite element model was developed using ABAQUS for the analysis of CFSST columns. The pin-ended axially loaded CFSST columns were considered in the finite element model. The length of CFSST columns varied from short to slender. The effects of fiber reinforced concrete confinement provided by stainless steel tube and interface between the stainless steel tube and fiber reinforced concrete were also considered in the analysis. In addition, the initial geometric imperfection was incorporated in the finite element model. The finite element model had been validated against tests conducted by Ellobody and Ghazy (2012a) and Ellobody and Ghazy (2012b) on fiber reinforced concrete-filled stainless steel tubular columns. The ultimate axial strengths, axial load-strain curves and failure modes obtained from the finite element model were compared with experimental results. The finite element model was shown to be accurate for predicting the nonlinear behavior of fiber reinforced concrete-filled stainless steel tubular columns. A parametric study was conducted to investigate the influence of the depth-to-thickness ratios, fiber reinforced concrete compressive strengths and column slenderness ratio on the behavior of fiber reinforced concrete-filled stainless steel tubular columns. The parametric study indicated that increasing the concrete compressive strength significantly increased the ultimate axial strength for the columns with L/D ratio less than 6 and depth-to-thickness ratio less than 50. The ultimate axial strengths obtained from the finite element model were compared with the design strengths calculated using Eurocode 4 for composite columns. It was shown that the EC4 predicted well the design strengths of axially loaded fiber reinforced CFST columns.

It is evident from the above literature review that there is a lack of numerical studies on high strength thin-walled rectangular CFST slender beam-columns. It is also shown that existing numerical models do not consider the effects of progressive local and post-local buckling of steel tube walls under stress gradients on the behavior of CFST slender beam-columns. In addition, the effects of high strength materials on the behavior of rectangular CFST slender beam-columns under uniaxial bending have not been studied adequately. Furthermore, the axial load-moment interaction diagrams of uniaxially loaded high strength thin-walled rectangular CFST slender beam-columns have not been investigated.

2.3 CFST COLUMNS UNDER AXIAL LOAD AND BIAXIAL BENDING

In practice, CFST columns in composite buildings are often subjected to axial load and biaxial bending. Experimental and numerical studies have been carried out on the behavior of CFST beam-columns under axial load and biaxial bending. Reviews on experimental investigations and nonlinear analysis of biaxially loaded CFST beam-columns are given in this section.

2.3.1 Experimental Studies

Bridge (1976) presented an experimental study on the behavior of biaxially loaded square CFST slender beam-columns with a depth-to-thickness ratio of 20. The angle of

applied load was fixed at 0°, 45° or 60°. The square CFST column section of 200 × 200 mm was considered in his study. Test parameters included the loading eccentricity, column slenderness ratio and biaxial bending. Experimental results demonstrated that the ultimate axial strength of slender square columns was shown to decrease with increasing the loading eccentricity. Increasing the column slenderness ratio significantly reduced the ultimate axial strengths of eccentrically loaded square CFST slender beam-columns. It was observed that all tested columns with compact sections failed by overall buckling with no sign of local buckling.

Shakir-Khalil and Zeghiche (1989) conducted tests on 7 full-scale rectangular CFST slender beam-columns. One column was tested under axial load, four columns were subjected to axial load and uniaxial bending and two columns were tested under axial load and biaxial bending. The bond between the steel tube and concrete core were studied. The effects of loading eccentricity on the behavior of slender beam-columns were examined. They found that the primary moment caused by the loading eccentricity had a pronounce effect on the ultimate axial strengths of CFST slender beam-columns with a small eccentricity. On the other hand, the secondary moment induced from the second order effect had a significant effect on the behavior of CFST slender beam-column with a large loading eccentricity ratio. The effect of initial geometric imperfection was recognized, although it was not measured for the tested columns. A linear distribution of strains through the cross-section was observed for all tested columns. All tested columns were failed by overall flexural buckling. Local buckling was not observed in the tested columns. The experimental results were compared with the results obtained from a finite element analysis and BS5400 (1979). The prediction

of BS5400 (1979) for eccentrically loaded CFST columns was shown to unsafe for columns subjected to minor axis bending.

Shakir-Khalil and Mouli (1990) carried out further study on rectangular CFST slender beam-columns. The steel section of $150 \times 100 \times 5$ mm was used in the tests. Tests on nine rectangular CFST slender beam-columns were conducted. Some of the columns were subjected to axial load and uniaxial bending, but most of the columns were tested under axial load and biaxial bending. Test parameters included the column cross-section size, steel yield strengths, concrete compressive strengths and column length. Test results demonstrated that the ultimate axial strength of rectangular CFST slender beam-columns increased with an increase in the size of the steel section. Increasing the concrete compressive strength increased the ultimate axial strength of CFST beam-columns. In addition, increasing the column length reduced the ultimate axial strength of CFST beam-columns.

Mursi and Uy (2006a) studied the experimental behavior of biaxially loaded square CFST short and slender beam-columns which were constructed from high strength structural steel tubes with yield strength of 690 MPa. In the experiment, special test procedure and orthogonal knife edge end supports were designed to prevent the friction at the column ends and ensure the free rotations in the two orthogonal planes of bending. The composite columns were pin-ended and subjected to single curvature bending. Test parameters included the slenderness of the steel plates in CFST beam-columns. The depth-to-thickness ratio of the steel tube section was varied from 24 of compact sections to 54 of relatively slender sections. The composite columns had a

length of 2800 mm. Their study indicated that the concrete core delayed the local buckling of thin steel walls. Local buckling occurred at the maximum load and steel plates buckled outward on all faces of a slender column. The results indicated that the ultimate axial strength of hollow steel short beam-columns under axial load and biaxial bending was significantly increased by the infill concrete which delayed the local buckling of the steel plates in compression.

Guo et al. (2011) investigated the experimental behavior of rectangular CFST beam-columns with large depth-to-thickness ratio. Four large thin-walled rib-stiffened rectangular CFST beam-columns were tested under axial load and biaxial bending. These specimens were fabricated from the steel tube with depth-to-thickness ratio of 175. These specimens were loaded through spherical hinges with ball bulb and groove so that they were pin-ended in the plane of bending. Test results indicated that local buckling of steel plate occurred after the maximum load was attained. The design strengths calculated by EC4 (1992), LRFD (1999), CECS (2004) and DBJ (2003) were compared with experimental ultimate axial strengths. It was shown that DBJ (2003) gave good estimate of the ultimate loads of CFST columns while EC4 (1992), LRFD (1999) and CECS (2004) overestimated the ultimate loads of CFST beam-columns by about 20%.

Although a limited number of experiments have been conducted on CFST columns under biaxial loads, there is still lack of adequate experimental data on square or rectangular high strength thin-walled CFST slender beam-columns under axial load and

biaxial bending particularly with yield strength of 690 MPa and concrete compressive strength of 110 MPa.

2.3.2 Nonlinear Analysis

El-Tawil et al. (1995) developed a nonlinear fiber element analysis technique for modeling the inelastic behavior of biaxially loaded concrete-encased composite columns. The composite cross-section was divided into small fiber elements. Each element was assigned with either steel or concrete material properties. The confinement of the concrete core provided by the steel sections was modeled using the stress-strain relationships for the confined concrete. In the fiber element analysis of composite beam-columns under axial load and biaxial bending, moment-curvature responses were obtained by incrementally increasing the curvature and solving for the corresponding moment value for an axial load applied at a fixed load angle. The results of the fiber analyses were used to evaluate nominal uni- and biaxial bending strengths of composite columns determined based on ACI-318 (2002), AISC-LRFD (1999) specifications. The fiber element model was used to investigate the effects of steel ratios, concrete compressive strengths and concrete confinement on the strength and ductility of concrete-encased composite beam–columns.

A polynomial equation was developed by Hajjar and Gourley (1996) to represent the three-dimensional cross-section strengths of square or rectangular CFST beam-columns with a wide range of material strengths and cross-section dimensions. They employed a fiber element analysis program to generate axial load-moment interaction diagrams for

CFST beam-columns and proposed strength interaction equations. In fiber element model, the CFST beam-column cross-section was divided into five regions. Each region was then discretized into a grid of fibers. The concrete confinement effects on the ductility and tension stiffening were simulated based on the constitutive material model for concrete in CFST columns suggested by Tomii and Sakino (1979). The fiber element analysis program developed by Sanz-Picón (1992) and El-Tawil et al. (1995) was used to determine the cross-section strength of steel, reinforced concrete and steel-reinforced cross-sections. The results obtained from the fiber element analysis were compared with experimental results. The empirical polynomial equations were developed to represent the strength of a rectangular CFST beam-column. The accuracy of the polynomial expressions was verified by comparisons with a detailed fiber element analysis and experimental results. The limitation of their model is that it did not account for the effects of concrete confinement provided by the circular steel tubes.

A general iterative computer method for biaxially loaded short concrete-encased composite columns was presented by Chen et al. (2001). The fiber element analysis method was used to obtain the stress resultants of the arbitrary shaped short columns. The composite section was discretized into small fibers. The steel section and the longitudinal reinforcing bars used in the composite section were assumed to be elastic-perfectly plastic. The stress resultants of the concrete were evaluated by integrating the stress-strain curve over the compression zone while those of structural steel and reinforcement were obtained using the fiber element method. An iterative quasi-Newton procedure with the Regula-Falsi numerical method was used to obtain the solution of equilibrium equations. Numerical results closely agreed with the test results and the

proposed method was shown to be effective and accurate. They concluded that the proposed method can be used directly in the practical design of composite as well as reinforced concrete columns of arbitrary sections.

An efficient semi-analytical model for the nonlinear inelastic analysis of square and rectangular CFST slender beam-columns under axial load and biaxial bending was formulated by Lakshmi and Shanmugam (2002). The semi-analytical model was utilized to determine the axial load-moment-curvature relationship for CFST beam-column sections. Incremental and iterative numerical schemes were used to predict the axial load-deflection curves for CFST beam-columns. The semi-analytical model can generate axial load-moment interaction diagrams for CFST short beam-columns. They examined the accuracy of their semi-analytical model by comparisons of computational and experimental ultimate axial strengths of rectangular CFST slender beam-columns under biaxial bending. The limitations of their model are that it did not account for the effects of local buckling, concrete confinement, steel strain hardening and concrete tensile strength on the ultimate axial strengths of rectangular CFST beam-columns. Although the load-deflection analysis procedure can be used to develop strength envelopes by varying the loading eccentricity, it is not efficient when the loading eccentricity is large. Despite of this, the axial load-moment interaction diagrams of CFST slender beam-columns under biaxial loads have not been studied.

Shanmugam et al. (2002) developed an analytical model for the nonlinear inelastic analysis of thin-walled CFST columns under axial load and biaxial bending. Nonlinear constitutive laws for concrete and structural steel were taken into account in the

analytical model. The effective width formulas for steel plates were incorporated in the analytical model to account for local buckling effects on the ultimate strengths of thin-walled CFST beam-columns. The analysis procedure for thin-walled CFST beam-columns under axial load and biaxial bending was described. The accuracy of the analytical model was verified by comparisons of analysis results with experimental data. The limitation of their model is that it did not account for the effects of the progressive post-local buckling of the steel tube walls under stress gradients. The axial load–moment interaction diagrams of high strength rectangular CFST slender beam-columns have not been studied.

Mursi and Uy (2006b) compared the plate slenderness limit based on international code standards AS4100 (1998), Eurocode 3 (1992), Eurocode 4 (1994), and AISC-LRFD (1993). They presented a numerical model for the nonlinear inelastic analysis of rectangular CFST short and slender beam-columns under axial load and biaxial bending. Material constitutive relationships for normal and high strength concrete were incorporated in the numerical model. The predicted axial load-deflection curves of rectangular CFST slender beam-columns under axial load and biaxial bending were compared with experimental results to examine the accuracy of the numerical model. The axial load-moment interaction diagrams for rectangular CFST slender beam-columns have not been studied. The local buckling of steel plates under uniform edge compression was considered. However, the effects of local and post-local buckling of steel tube walls under non-uniform compression have not been considered in the numerical model. The ultimate axial strengths measured from the tests conducted by authors in the companion paper (Mursi and Uy 2006a) were compared with the design

strengths calculated by the international codes AS4100 (1998), Eurocode 4 (1994), and AISC-LRFD (1993). They concluded that AS4100 (1998), Eurocode 4 (1994), and AISC-LRFD (1993) overestimated the ultimate loads of high strength CFST beam-columns by about 19%, 15% and 10% respectively.

A performance-based analysis (PBA) technique was developed by Liang (2009a, 2009b, 2009c) for predicting the ultimate strength and ductility of high strength thin-walled rectangular CFST short beam-columns under axial load and biaxial bending. Nonlinear constitutive laws for confined concrete and structural steels were considered in the PBA program. Initial local buckling and effective width formulas for steel plates under stress gradients were incorporated in the PBA technique to account for the effects of local and post-local buckling on the axial load-strain responses, moment-curvature curves and axial load-moment interaction diagrams of thin-walled CFST short beam-columns. The progressive local and post-local buckling of a thin-walled steel tube was simulated by gradually redistributing the normal stresses within the steel tube walls. The effects of concrete confinement, residual stresses, geometric imperfections and inelastic material behavior were also incorporated in the PBA program. Computational algorithms based on the secant method were developed and implemented in the PBA technique to iterate the depth and orientation of the neutral axis in a column cross-section to satisfy equilibrium conditions. The detailed analysis procedures for thin-walled CFST short beam-columns under axial load and biaxial bending were described. The axial load-strain curves, ultimate axial strengths and moment-curvature curves obtained from the PBA program were compared with experimental results to examine the accuracy of the PBA program. The PBA program was further employed to study the effects of local

buckling, depth-to-thickness ratios, concrete compressive strengths, steel yield strengths and axial load levels. He concluded that the PBA technique developed can efficiently generate complete axial load-moment interaction diagrams for thin-walled CFST short beam-columns under uni- and biaxial bending. The results obtained from the PBA program indicated that increasing the depth-to-thickness ratio and axial load levels significantly reduced the stiffness, strength and ductility of CFST beam-columns. Increasing concrete compressive strengths increased the stiffness and strength, but reduced the axial ductility and section performance of CFST beam-columns. Moreover, the steel yield strength had a significant effect on the section and strength performance of CFST beam-columns but did not have a significant effect on their axial and curvature ductility.

Thai and Kim (2011) presented a numerical procedure for the nonlinear inelastic analysis of CFST columns in frames. Geometric nonlinearities were considered in the numerical model using the stability functions. The stability solution of a CFST beam-column under axial load and bending was used to derive the stability functions. Incremental and iterative computational algorithms were developed to solve nonlinear equilibrium equations of a slender beam-column. To verify the fiber element program, the ultimate axial loads and axial load-deflection curves of CFST beam-columns predicted by the computer program were compared with corresponding experimental results presented by Bridge (1976), Rangan and Joyce (1992), O'Brien and Rangan (1993) and Matsui et al. (1995). The limitation of their model is that it did not account for the effects of the progressive post-local buckling of the steel tube walls under stress

gradients. The axial load–moment interaction diagrams of high strength rectangular CFST slender beam-columns have not been studied by Thai and Kim (2011).

Guo et al. (2011) developed a fiber element model for thin-walled rid-stiffened rectangular CFST slender beam-columns under axial load and biaxial bending. The deflected shape of the column was assumed to be part of a sine wave. Material laws proposed by Zhang et al. (2005) for structural steel and concrete were implemented in the fiber element model. Initial geometric imperfection at the mid-height of the slender beam-column was considered in the numerical model. To predict the axial load-deflection responses of a slender beam-column, the deflection control method was employed in the numerical model. In the analysis, the deflection at the mid-height of a slender beam-column was gradually increased. The force equilibrium was maintained at the mid-height of the beam-column. The effects of local buckling of thin-walled steel tube and high strength materials were not considered in the numerical model. In addition, the axial load-moment interaction diagrams of rectangular CFST slender beam-columns have not been studied.

Only a few numerical models have been reported in the literatures that predict the behavior of high strength thin-walled CFST slender beam-columns subjected to axial load and biaxial bending. However, existing numerical models for thin-walled rectangular CFST slender beam-columns have not accounted for the effects of progressive local buckling of the steel tube walls under stress gradients.

2.4 CFST COLUMNS WITH PRELOAD EFFECTS

The hollow steel tubes are firstly erected in the construction of a high-rise composite building. The horizontal floors with six to eight storeys are constructed before pouring the wet concrete. The hollow steel tubular columns are subjected to preloads from the upper floors and wet infilled concrete. Initial stresses and deflection caused by these preloads may reduce the ultimate axial strengths of CFST beam-columns. Experiments and numerical studies on the behavior of CFST columns with preload effects have been conducted by researchers.

2.4.1 Experimental Studies

Zha (1996) performed tests on twenty-three circular CFST beam-columns under eccentric loading. The effects of preload on the ultimate axial strengths were examined. Column slenderness ratios ranging from 14 to 82 were considered in his study. CFST slender columns were tested with or without preloads on the steel tubes. The preload on the steel tubes induced initial deflections in the CFST beam-columns. Test results indicated that the presence of preload on the hollow steel tubular column reduced the ultimate axial strengths of CFST beam-columns. When the preload ratio was greater than 0.4, the strength reduction could be more than 5%. The behavior of CFST columns with or without preloads on the hollow steel tubes was different. The behavior of eccentrically loaded circular CFST slender beam-columns with preload effects was discussed by Zhang et al. (1997). The composite columns were pin-ended and subjected to eccentric loading. The composite columns had different lengths varied from 1670

mm to 2730 mm. A series of tests were conducted to investigate the effects of the preload ratio, column slenderness and loading eccentricity.

Han and Yao (2003) investigated the experimental behavior of square CFST columns with preloads on the steel tubes. They tested 19 CFST columns to examine the effects of preloads on the ultimate axial strengths of square CFST columns. Test parameters were the preload ratios, column slenderness ratios, number of braces between the floor levels, steel and concrete ratios, steel yield strengths and concrete compressive strengths. Test specimens were loaded eccentrically or concentrically. Preload ratios varied from 0 to 0.7 while the eccentricity varied from 0 to 31 mm and the column slenderness ratios varied from 10 to 40. The test results showed that the preload on the steel tube increased the deflection and decreased the strength of the CFST beam-column. The maximum strength reduction was 5% due to preload on the steel tube. The preload ratio, slenderness ratio and load eccentricity ratio had a significant influence on the strength. On the other hand, the steel ratio, concrete compressive strengths and steel yield strengths had influence on the ultimate axial strength of the CFST beam-columns. They developed formulas for calculating the ultimate strength of CFST beam-columns with the steel tubes subjected to preloads.

An experimental study was conducted by Liew and Xiong (2009) to investigate the effects of the preloads on the ultimate axial strengths of circular CFST slender beam-columns. Eight full-scale circular CFST columns were tested under axial compression. All CFST columns were fabricated from circular hot-rolled steel tubes of 219 mm diameter and 6.3 mm thick. Test parameters included the concrete compressive

strengths, column slenderness ratios and the preload applied on the steel tube. The preload was applied to the hollow steel tube by prestressing strands before filling the wet concrete. The preload applied on circular CFST beam-columns was 40% of the composite section's strength. The prestress strands were gradually released to zero during the test. These columns exhibited a more than 15% reduction in its ultimate axial strength compared to the corresponding non-preloaded columns. It was observed that the column buckling resistance of CFST beam-columns reduced with increasing the preload ratio. When the preload was applied to intermediate and slender columns, the effects of preload on the ultimate axial strengths of CFST beam-columns were most pronounced. The effects decreased for short CFST beam-columns. In addition, a design method for evaluating the ultimate axial strengths of circular CFST columns with preload effects was proposed based on the rules specified in the Eurocode 4.

The above literature review demonstrates that there is relatively little experimental research on CFST slender beam-columns with preload effects. In addition, the effects of preloads on the ultimate axial strengths of CFST slender beam-columns under axial load and biaxial bending have not been experimentally investigated.

2.4.2 Nonlinear Analysis

Xiong and Zha (2007) studied the behavior of circular and square CFST beam-columns under axial compression using the finite element program ABAQUS. They investigated the effects of preload on the ultimate axial strengths of CFST beam-columns. The solid element, conventional shell element and continuum shell element were used to model

the concrete core, square steel tube and circular steel tube respectively. The ultimate axial strengths and axial load-deflection curves of preloaded square CFST columns obtained from the finite element analyses were compared with experimental results to examine the accuracy of the finite element model. Parametric studies were conducted to study the effects of the column slenderness ratios, loading eccentricity ratios and initial stress ratio on the ultimate axial strength of CFST short and slender beam-columns. It was observed that the initial stresses did not have a significant effect on the composite section's strength. The contribution of concrete in CFST columns decreased with increasing the initial stresses. As a result, the ultimate axial strength of CFST slender beam-columns decreased with increasing the initial stresses. The effects of initial stresses on the ultimate axial strength of the CFST beam-columns increased with increasing the column slenderness ratio and initial stress ratio. These effects were shown to reduce with increasing the loading eccentricity ratio. Finally, a set of design formulas incorporating initial stress effects was proposed for determining the ultimate axial loads of CFST beam-columns.

Liew and Xiong (2007) employed the finite element program ABAQUS to study the inelastic behavior of axially loaded CFST beam-columns considering preload effects. The results obtained from the finite element model were compared with experimental data. The finite element model was then utilized to investigate the effects of loading eccentricity ratios, column slenderness ratios and initial stress ratio on the ultimate axial strength of CFST short and slender beam-columns. It was observed that the ultimate axial strengths of CFST columns decreased with increasing the preloads on the steel tubes. Their study indicated that the preload on the steel tubes had a little effect on short

columns. They proposed a design method for determining the strength of axially loaded circular CFST slender columns incorporating preload effects.

Wei et al. (2012) analyzed axially loaded concrete-filled double skin steel tubular (CFDST) columns with preload effects using ABAQUS. Shell elements were employed to model the steel tube while concrete core was modeled by solid elements. The von Mises yield surface was adopted in the nonlinear analysis to treat the isotropic yielding. Nonlinear constitutive models for confined concrete and structural steel were considered in the finite element analysis. Experimental results of CFDST columns without the preload effects were used to verify the accuracy of the finite element model. Parametric studies were conducted to examine the effects of preload ratio, slenderness ratio, hollow ratio and material strengths on the ultimate axial strength of CFDST columns. It was found that the column slenderness ratio is one of the important factors which influence the ultimate axial strength of CFDST columns. A design formula accounting for preload effects was also proposed for CFDST columns.

It appears that there are very few numerical studies on the behavior of CFST slender beam-columns with preload effects. Existing nonlinear inelastic methods of analysis do not consider the effects of progressive local and post local buckling of steel plates under stress gradients and high strength materials on the behavior of CFST slender beam-columns. In addition, no numerical models have been developed for predicting the behavior of high strength thin-walled rectangular CFST slender beam-columns under axial load and biaxial bending with preload effects.

2.5 CFST COLUMNS UNDER CYCLIC LOADING

Experimental investigations were carried out on CFST beam-columns subjected to cyclic loading. Two types of loading conditions were adopted by researchers. The first is that the lateral cyclic loading was applied at the mid-height of the beam-columns and the second is that the lateral cyclic loading was applied at the tip of the beam-columns. A constant axial load was also applied to the CFST beam-columns. Experimental and numerical research on CFST beam-columns subjected to cyclic loading is reviewed in the following sections.

2.5.1 Experimental Studies

Ge and Usami (1992) described an experimental investigation on concrete-filled thin-walled box columns subjected to cyclic axial compression. A total of six concrete-filled steel box columns including four hollow steel box columns were tested. The buckling modes of hollow steel box columns were compared with concrete-filled steel box columns. Concrete-filled thin-walled steel box columns offered higher strength and ductility performance than the hollow steel box columns. It was observed that the steel tube walls buckled at the mid-height of the columns. The steel tube buckled locally inward in the two opposite walls and outward in the remaining two walls. However, the steel tube walls buckled locally outward in concrete-filled thin-walled box columns owing to the restraint provided by the concrete core. Local buckling of the steel tube walls occurred after concrete was damaged.

Experiments on high strength CFST beam-columns under monotonic and cyclic loads were conducted by Varma et al. (2002, 2004). They investigated the effects of width-to-thickness ratios, yield strengths of steel tubes and the axial load level on the stiffness, strength and ductility of high strength CFST beam-columns. The specimens were tested under axial loading, combined constant axial loading with monotonically increased flexural loading and combined constant axial loading with cyclic flexural loading. Test results indicated that the monotonic curvature ductility of high-strength square CFST beam-columns significantly decreased with an increase in the axial load level or the width-to-thickness ratio of the steel tube. However, the yield strength of the steel tube did not have a significant effect on the curvature ductility. They reported that the ultimate bending strength of high strength square CFST beam-columns could be well predicted by the design formulas given in ACI. Their test results indicated that cyclic loading did not have a significant influence on the stiffness and strength of CFST beam-columns, but induced a more rapid decrease in the post-peak moment capacity.

Han et al. (2003) conducted tests on thin-walled square and rectangular CFST beam-columns under axial load and cyclic lateral loading. The effects of depth-to-thickness ratio, concrete compressive strength and axial load level on the cyclic behavior of CFST beam-columns were investigated. It was found that local buckling of CFST beam-columns occurred after the steel yielded. An analytical model was developed for CFST beam-columns subjected to axial load and cyclic loading. A multi-linear model was employed in the analytical model. However, the limitation of their model is that it did not account for the local buckling of the steel tube walls. Design formulas for determining the ductility coefficient of rectangular CFST beam-columns were proposed.

Fam et al. (2004) undertook an experimental investigation into the performance of CFST columns under axial load and combination of axial load and lateral cyclic loading. The main variable parameters in the tests were bond, end-loading conditions and axial load levels. Test results illustrated that the ultimate axial strengths of CFST columns obtained by loading both the concrete core and steel tubes were lower than those of CFST columns measured from loading the steel tubes alone. The bond and end loading conditions of CFST columns had little influence on the flexural strength of beam-columns. However the ultimate axial strength of unbounded CFST columns was slightly increased. For unbounded CFST columns, the stiffness was slightly reduced. The ultimate axial strengths measured from the tests were compared with the design strengths calculated from the design specification. They found that the ultimate axial strengths predicted from the design specification were conservative. The limitations of their study were that the research findings were restricted to CFST beam-columns fabricated from the small diameter tubes.

The behavior of circular CFST beam-columns under axial load and cyclic loading was reported by Gajalakshmi and Helena (2012). Test specimens were constructed by normal strength steel tubes and concrete. The effects of amplitude and number of cycles on damage accumulation were studied. The parameters studied were diameter-to-thickness ratios, plain concrete and steel fiber reinforced concrete. A simplified equation for determining the cumulative damage of CFST beam-columns was proposed. They concluded that the high amplitude caused serious damage in the structures. The ductility and energy absorption capacity of CFST beam-columns were found to increase by filling the steel fiber reinforced concrete. However, the damage index tended to

decrease for this type of beam-columns. The depth-to-thickness ratio of the steel tubes was found to control the failure modes of CFST beam-columns regardless of the type of in-filled concrete and loading patterns.

Wu et al. (2012) studied the cyclic behavior of normal strength CFST beam-columns. The strength and ductility of thin-walled square CFST beam-columns with demolished concrete lumps (DCLs) and fresh concrete (FC) were investigated. Ten columns with DCLs and FC and 5 columns filled with FC alone were tested under constant axial compression and cyclic lateral loading. The yield strength of the steel tubes ranged from 256 MPa to 270 MPa while the average cube strength of concrete was 48 MPa. Test parameters included replacement ratio of DCLs, steel tube thickness and axial load ratio. The authors concluded from the test results that the cyclic behavior of thin-walled square CFST beam-columns was not affected by the DCLs and FC. The cyclic behavior of the beam-columns filled with DCLs and FC was similar to that of the columns filled with FC alone. The ultimate lateral load of the beam-column filled with DCLs and FC was lower than that of the column filled with FC alone. The typical failure modes of the tested specimens involved buckling of the steel tube in compression and cracking of the concrete. It was shown that increasing the steel tube thickness of the beam-columns slightly increased their ductility. The ultimate cyclic lateral load of square CFST beam-columns was found to decrease with an increase in the axial load ratio.

2.5.2 Nonlinear Analysis

Lee and Pan (2001) modified the traditional fiber element model with proper failure algorithms in order to predict the behavior of concrete encased composite beam-columns under lateral cyclic loading. The proposed composite beam-column model was incorporated into DRAIN-2DX program with new algorithm to improve the traditional fiber element model. The cross-section was discretized into small fibers of concrete and steel so that the section force-deformation relation was derived by integrating the stress-strain of the concrete and steel in the finer element program. The limitations of the traditional fiber element model were that it did not account for buckling of the longitudinal bars used in the composite encased composite beam-columns and the effects of de-bonding between the steel plates and the concrete. It was found that the failure of composite beam-columns started when the flexural cracks in the concrete cover, spalling of concrete cover, longitudinal steel tube buckling occurred. The accuracy of the model was demonstrated by comparing the experimental and analytical results.

Fiber based models were used by Varma et al. (2002) to investigate the behavior of high strength square CFST beam-columns. A fiber based beam-column element was implemented in the nonlinear structural analysis program DRAIN-2DX. The uniaxial stress-strain curves were derived from the results of three dimensional nonlinear finite element analyses on CFST beam-columns. The CFST beam-column was divided into segments with a slice at the mid-height of the segment. The slice was further divided into small fibers. Uniaxial stress-strain curves were integrated over the cross-section to obtain the axial force, axial strain, bending moment and curvature of each fiber corresponding to segments. They found that the reliable prediction using fiber element

analysis method for CFST columns relies on the use of accurate models for concrete and steels. It also depends on the discretization of the composite cross-section. The accuracy of the fiber element model was established by comparisons of numerical results with experimental data. Although the numerical model incorporated the local buckling of the steel tube walls using the modified stress-strain relationship for steel tube in compression, it cannot model the progressive cyclic local buckling of the steel tube walls under stress gradients.

Gayathri et al. (2004a, 2004b) presented a fiber element analysis technique for the nonlinear analysis and design of circular and rectangular CFST short and slender beam-columns under monotonic and cyclic loading. Uniaxial cyclic constitutive laws for the concrete and structural steel were considered in the fiber element model. The analysis algorithms for CFST beam-columns under cyclic loading were presented. The cyclic load-deflection curves for CFST columns predicted by the fiber element model were verified by experimental data. The effects of local buckling and high strength materials on the cyclic behavior were not taken into account in the fiber element model.

Spacon and El-Tawil (2004) reviewed the nonlinear analysis techniques for the design and analysis of composite structures. Resultant and fiber models, frame element flow models, lump and distributed models and perfect and partial models were discussed in the study. The analyses of composite sections, members, joints and structural systems including moment frames and wall systems were reviewed. Local buckling of the steel plates has not been incorporated in the fiber element analysis. They discussed the advantages and drawbacks of the fiber element analysis method. The advantages of

fiber element analysis are that it can easily model the behavior of steel and concrete as compared to the other methods.

Chung et al. (2007) and Chung (2010) employed the nonlinear fiber element analysis technique to investigate the pre- and post-peak behavior of square and circular CFST slender columns subjected to a constant axial load and cyclically increasing lateral loading. The modified stress-strain curves for steel in compression were used to approximately consider the local buckling effects in the numerical model. The pre- and post-peak cyclic load-deflection responses and cumulative plastic strain energy of square and cylinder CFST beam-columns obtained from the numerical model were compared with experimental results. The tensile stress of concrete fibers was neglected in the fiber element models. Their model did not consider the effects of high strength materials on the cyclic behavior of CFST beam-columns. In addition, the method cannot simulate the progressive local buckling of steel tube walls under stress gradients.

Han et al. (2008) studied the behavior of CFST columns under shear and constant axial compression using the nonlinear finite element analysis program ABAQUS. Circular and square sections were considered in their study. The numerical results obtained by the finite element model were used to develop a design formula for determining the ultimate shear strengths of CFST beam-columns. The ultimate shear strengths and shear load-deflection curves of CFST columns under axial and shear loads were compared with experimental results to examine the accuracy of the finite element model. The behavior of square CFST beam-columns with various concrete compressive strengths,

steel yield strengths, steel ratios and axial load level was studied using the verified model.

Zubydan and ElSabbagh (2011) presented a mathematical model for studying the monotonic and cyclic behavior of rectangular CFST beam-columns. The mathematical model considered the effects of the local buckling of the steel tube walls by modifying the stress-strain curve for steel in compression. The degradations in unloading and reloading stiffness of steel tube due to local buckling were also considered in the mathematical model. The fiber element method was used to model the inelastic behavior of composite cross-sections. The accuracy of the fiber element analysis program was verified by comparisons of fiber analysis results with experimental data. It was shown that the fiber element method overestimated the ultimate loads of the composite columns when local buckling effects were not considered.

A fiber element model, which incorporated the constitutive models of confined concrete and structural steels for simulating the hysteretic behavior of high strength square CFST beam-columns under eccentric and cyclic loading, was presented by Chung et al. (2012). The fiber element was verified by comparisons of computational results with experimental data. The fiber element model was employed to examine the reliability of various concrete material models on the strength and ductility of square CFST columns. Material models proposed by Nakahara et al. (1998), Chung et al. (2007), Liang et al. (2006), and Liu (2006) were investigated. It was observed that the material model given by Liu (2006) generally overestimated the Bauschinger effect after local buckling. The

local buckling of the steel tube walls under stress gradients was not considered in the analytical study.

Wu et al. (2012) presented finite element models for simulating the nonlinear inelastic behavior of cyclically loaded square CFST slender beam-columns. They employed the finite element analysis program ABAQUS to investigate the cyclic lateral load-deflection responses of square CFST slender beam-columns. A force-based Timoshenko beam element B31 was used to develop the finite element model. The effects of local buckling of the steel tube were taken into account in the fiber element models by modifying the uniaxial stress-strain relationships for steel in compression. The monotonic envelope curve for concrete in compression follows the monotonic stress–strain model proposed by Han (2007). The hysteretic unloading and reloading rules for concrete in compression proposed by Chung et al. (2007) were used. The experimental results were compared with the ultimate lateral loads computed using design codes and finite element model.

The above literature review demonstrates that there is relatively little numerical study on the behavior of cyclically loaded high strength rectangular CFST slender beam-columns with large depth-to-thickness ratios.

2.6 CONCLUDING REMARKS

This chapter has presented the literature review on CFST beam-columns under uniaxial loads, biaxial loads, preloads and cyclic loading. Existing experimental works and

nonlinear analysis of CFST beam-columns have been highlighted. The literature review shows that there are not sufficient experimental and numerical studies on high strength CFST slender beam-columns under axial load and uniaxial bending, biaxial loads, preloads or axial load and cyclic lateral loading. Researches on nonlinear analysis techniques for high strength CFST slender beam-columns have been very limited. In addition, the effect of the progressive local buckling of steel tubes and high strength materials on the strength and ductility of thin-walled CFST slender beam-columns were not taken into account in most of the nonlinear inelastic methods. Moreover, the nonlinear analysis and behavior of biaxially loaded thin-walled CFST slender beam-columns with local buckling and preload effects have not been reported in the literature.

Chapter 3

RECTANGULAR CFST SLENDER BEAM-COLUMNS UNDER AXIAL LOAD AND UNIAXIAL BENDING

3.1 INTRODUCTION

In this chapter a numerical model based on the fiber element analysis method is developed for simulating the local and global interaction buckling behavior of high strength thin-walled rectangular concrete-filled steel tubular (CFST) slender beam-columns under axial load and uniaxial bending. The numerical model accounts for the effects of progressive local buckling, initial geometric imperfections, high strength materials and second order. New Müller's method algorithms are developed to iterate the depth of the neutral axis and the curvature at the columns ends to obtain the load-deflection responses and strength envelopes of thin-walled rectangular CFST slender

beam-columns. Performance indices are proposed to quantify the behavior of uniaxially loaded CFST beam-columns with local buckling effects. The accuracy of the numerical model is examined by comparisons of the computer solutions with existing experimental results. The numerical model is employed to investigate the effects of various parameters on the behavior of CFST slender beam-column under uniaxial bending.

This chapter includes the following papers:

[1] Patel, V. I., Liang, Q. Q. and Hadi, M. N. S., "High strength thin-walled rectangular concrete-filled steel tubular slender beam-columns, Part I: Modeling", *Journal of Constructional Steel Research*, 2012, 70, 377-384.

[2] Patel, V. I., Liang, Q. Q. and Hadi, M. N. S., "High strength thin-walled rectangular concrete-filled steel tubular slender beam-columns, Part II: Behavior", *Journal of Constructional Steel Research*, 2012, 70, 368-376.

[3] Patel, V. I., Liang, Q. Q. and Hadi, M. N. S., "Inelastic stability analysis of high strength rectangular concrete-filled steel tubular slender beam-columns", *Interaction and Multiscale Mechanics, An International Journal*, 2012, 5(2), 91-104.

VICTORIA UNIVERSITY
MELBOURNE AUSTRALIA

PART B:

DECLARATION OF CO-AUTHORSHIP AND CO-CONTRIBUTION: PAPERS INCORPORATED IN THESIS BY PUBLICATION

This declaration is to be completed for each conjointly authored publication and placed at the beginning of the thesis chapter in which the publication appears.

Declaration by [candidate name]:   **Signature:**   **Date:**

VIPULKUMAR ISHVARBHAI PATEL   11|01|2013

Paper Title:

High strength thin-walled rectangular concrete-filled steel tubular slender beam-columns, Part I: Modeling

In the case of the above publication, the following authors contributed to the work as follows:

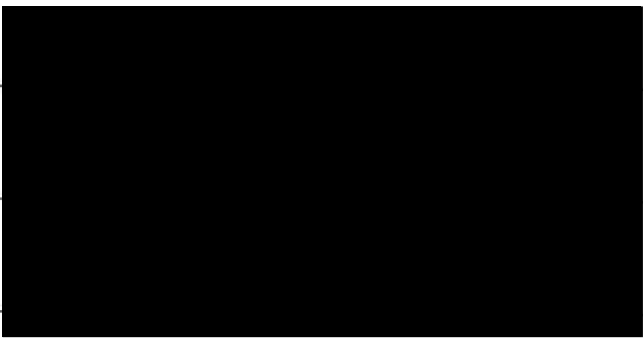| Name	Contribution%	Nature of contribution
Vipulkumar Ishvarbhai Patel	60	Literature review Developed the numerical model Writing of the manuscript
Qing Quan Liang	30	Initial concept Provided critical revision of the article Final approval of the manuscript Manuscript submission
Muhammad N.S.Hadi	10	Provided critical revision of the article Final approval of the manuscript

VICTORIA UNIVERSITY
MELBOURNE AUSTRALIA

DECLARATION BY CO-AUTHORS

The undersigned certify that:

1. They meet criteria for authorship in that they have participated in the conception, execution or interpretation of at least that part of the publication in their field of expertise;

2. They take public responsibility for their part of the publication, except for the responsible author who accepts overall responsibility for the publication;

3. There are no other authors of the publication according to these criteria;

4. Potential conflicts of interest have been disclosed to **a)** granting bodies, **b)** the editor or publisher of journals or other publications, and **c)** the head of the responsible academic unit; and

5. The original data is stored at the following location(s):

Location(s): College of Engineering and Science, Victoria University, Melbourne, Victoria, Australia.

and will be held for at least five years from the date indicated below:

		Date
Signature 1		11|01|2013
Signature 2		11/0/2013
Signature 3		11/01/201
Signature 4		

VICTORIA UNIVERSITY
MELBOURNE AUSTRALIA

PART B:

DECLARATION OF CO-AUTHORSHIP AND CO-CONTRIBUTION: PAPERS INCORPORATED IN THESIS BY PUBLICATION

This declaration is to be completed for each conjointly authored publication and placed at the beginning of the thesis chapter in which the publication appears.

Declaration by [candidate name]:	Signature:	Date:
VIPULKUMAR ISHVARBHAI PATEL		11/01/2013

Paper Title:

High strength thin-walled rectangular concrete-filled steel tubular slender beam-columns, Part II: Behavior

In the case of the above publication, the following authors contributed to the work as follows:

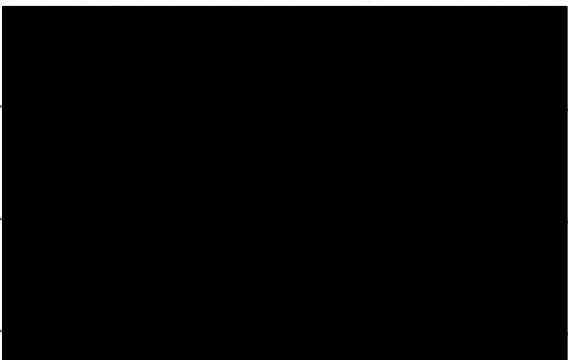| Name	Contribution%	Nature of contribution
Vipulkumar Ishvarbhai Patel	60	Literature review Conducted the verification Carried out the parametric study Writing of the manuscript
Qing Quan Liang	30	Initial concept Provided critical revision of the article Final approval of the manuscript Manuscript submission
Muhammad N.S.Hadi	10	Provided critical revision of the article Final approval of the manuscript

VICTORIA UNIVERSITY
MELBOURNE AUSTRALIA

DECLARATION BY CO-AUTHORS

The undersigned certify that:

1. They meet criteria for authorship in that they have participated in the conception, execution or interpretation of at least that part of the publication in their field of expertise;

2. They take public responsibility for their part of the publication, except for the responsible author who accepts overall responsibility for the publication;

3. There are no other authors of the publication according to these criteria;

4. Potential conflicts of interest have been disclosed to **a)** granting bodies, **b)** the editor or publisher of journals or other publications, and **c)** the head of the responsible academic unit; and

5. The original data is stored at the following location(s):

Location(s): College of Engineering and Science, Victoria University, Melbourne, Victoria, Australia.

and will be held for at least five years from the date indicated below:

		Date
Signature 1		11/01/2013
Signature 2		11/01/2013
Signature 3		11/01/2013
Signature 4		

VICTORIA UNIVERSITY
MELBOURNE AUSTRALIA

PART B:

DECLARATION OF CO-AUTHORSHIP AND CO-CONTRIBUTION: PAPERS INCORPORATED IN THESIS BY PUBLICATION

This declaration is to be completed for each conjointly authored publication and placed at the beginning of the thesis chapter in which the publication appears.

Declaration by [candidate name]:	Signature:	Date:
VIPULKUMARISHVARBHAI PATEL	███████	11/01/2013

Paper Title:

Inelastic stability analysis of high strength rectangular concrete-filled steel tubular slender beam-columns

In the case of the above publication, the following authors contributed to the work as follows:

Name	Contribution%	Nature of contribution
Vipulkumar Ishvarbhai Patel	60	Literature review Develop a numerical model Writing of the manuscript Drafting the manuscript
Qing Quan Liang	30	Initial concept Provided critical revision of the article Final approval of the manuscript Manuscript submission
Muhammad N.S.Hadi	10	Provided critical revision of the article Final approval of the manuscript

VICTORIA UNIVERSITY
MELBOURNE AUSTRALIA

DECLARATION BY CO-AUTHORS

The undersigned certify that:

1. They meet criteria for authorship in that they have participated in the conception, execution or interpretation of at least that part of the publication in their field of expertise;

2. They take public responsibility for their part of the publication, except for the responsible author who accepts overall responsibility for the publication;

3. There are no other authors of the publication according to these criteria;

4. Potential conflicts of interest have been disclosed to **a)** granting bodies, **b)** the editor or publisher of journals or other publications, and **c)** the head of the responsible academic unit; and

5. The original data is stored at the following location(s):

Location(s): College of Engineering and Science, Victoria University, Melbourne, Victoria, Australia.

---

and will be held for at least five years from the date indicated below:

		Date
Signature 1		11/01/2013
Signature 2		11/0/2013
Signature 3		11/01/2013
Signature 4		

High strength thin-walled rectangular concrete-filled steel tubular slender beam-columns, Part I: Modeling

Vipulkumar Ishvarbhai Patel [a], Qing Quan Liang [a,*], Muhammad N.S. Hadi [b]

[a] School of Engineering and Science, Victoria University, PO Box 14428, Melbourne, VIC 8001, Australia
[b] School of Civil, Mining and Environmental Engineering, University of Wollongong, Wollongong, NSW 2522, Australia

ARTICLE INFO

ABSTRACT

High strength thin-walled rectangular concrete-filled steel tubular (CFST) slender beam-columns under eccentric loading may undergo local and overall buckling. The modeling of the interaction between local and overall buckling is highly complicated. There is relatively little numerical study on the interaction buckling of high strength thin-walled rectangular CFST slender beam-columns. This paper presents a new numerical model for simulating the nonlinear inelastic behavior of uniaxially loaded high strength thin-walled rectangular CFST slender beam-columns with local buckling effects. The cross-section strengths of CFST beam-columns are modeled using the fiber element method. The progressive local and post-local buckling of thin steel tube walls under stress gradients is simulated by gradually redistributing normal stresses within the steel tube walls. New efficient Müller's method algorithms are developed to iterate the neutral axis depth in the cross-sectional analysis and to adjust the curvature at the columns ends in the axial load–moment interaction strength analysis of a slender beam-column to satisfy equilibrium conditions. Analysis procedures for determining the load–deflection and axial load–moment interaction curves for high strength thin-walled rectangular CFST slender beam-columns incorporating progressive local bucking and initial geometric imperfections are presented. The new numerical model developed is shown to be efficient for predicting axial load–deflection and axial load–moment interaction curves for high strength thin-walled rectangular CFST slender beam-columns. The verification of the numerical model and parametric studies is given in a companion paper.

© 2011 Elsevier Ltd. All rights reserved.

1. Introduction

The local and overall instability problem is encountered in eccentrically loaded high strength thin-walled rectangular concrete-filled steel tubular (CFST) slender beam-columns with large depth-to-thickness ratios. The inelastic modeling of thin-walled CFST slender beam-columns under axial load and bending is complicated because it must account for not only material and geometric nonlinearities as well as associated second order effects but also the interaction between progressive local and overall buckling. Although these composite beam-columns are increasingly used in high rise composite buildings, their structural performance cannot be accurately predicted without an accurate and efficient computer modeling tool. Currently, there is a lack of such a modeling technique for thin-walled CFST slender beam-columns. This paper describes the important development of a new numerical model that simulates the behavior of high strength thin-walled CFST slender beam-columns incorporating the local buckling effects of the steel tube walls under stress gradients.

Experiments have been undertaken by many researchers to study the behavior of normal strength CFST beam-columns. Early experiments on slender steel tubular columns filled with normal strength concrete included those conducted by Bridge [1], Shakir-Khalil and Zeghiche [2] and Matsui et al. [3]. More recently, Schneider [4] performed tests to study the effects of the steel tube shape and the wall thickness on the ultimate strength and ductility of CFST short columns. He reported that circular CFST columns possessed higher strength and ductility than square and rectangular ones. Experimental results presented by Han [5] illustrated that the ultimate axial strength and ductility of axially loaded CFST columns increased with increasing the constraining factor but decreased with an increase in the depth-to-thickness ratio. Ellobody et al. [6] studied the behavior of normal and high strength circular CFST short columns under axial loading.

The local buckling behavior of thin-walled rectangular CFST short columns under axial compression was studied experimentally by Ge and Usami [7], Bridge and O'Shea [8] and Uy [9]. Tests results demonstrated that the concrete core delayed the occurring of the steel tube local buckling and forced the steel tube walls to buckle outward. In addition, it was found that local buckling remarkably reduced the ultimate strengths of thin-walled CFST columns. Liang and Uy [10] and Liang et al. [11] employed the finite element method to investigate the local and post-local buckling behavior of steel plates in thin-walled CFST

columns under axial load and biaxial bending. They proposed a set of formulas for determining the initial local buckling stresses and post-local buckling strengths of steel plates under stress gradients.

Recently, experimental research has focused on high strength CFST beam-columns as they are increasingly used in high rise composite buildings. An experimental study on CFST beam-columns under eccentric loading was carried out by Chung et al. [12]. These columns were made of steel tubes with a yield strength of 445 MPa filled with 88 MPa high strength concrete. In addition, Liu [13] undertook tests on eccentrically loaded high strength rectangular CFST beam-columns with steel yield strength of 495 MPa and high strength concrete of 60 MPa. His test results demonstrated that the ultimate loads of CFST slender beam-columns were significantly reduced by increasing the load eccentricity ratio. Moreover, Lue et al. [14] reported experimental results on rectangular CFST slender beam-columns with concrete compressive strengths varying between 29 and 84 MPa.

Nonlinear analysis techniques are efficient and cost-effective performance simulation and design tools for CFST columns [2]. Lakshmi and Shanmugam [15] proposed a semi-analytical model for determining the behavior of CFST slender beam-columns under biaxial bending. The limitation of their model is that it did not account for the effects of local buckling, concrete confinement and concrete tensile strength. The load–deflection analysis procedure presented by Vrcelj and Uy [16] could be used to analyze axially loaded high strength square CFST slender beam-columns, but it has not considered the progressive local buckling of the steel tube walls under stress gradients. Liang [17,18] developed a performance-based analysis (PBA) technique for predicting the ultimate strength and ductility of thin-walled CFST short beam-columns under axial load and biaxial bending, incorporating effective width formulas proposed by Liang et al. [11] to account for the effects of progressive local buckling. Moreover, an efficient numerical model was created by Liang [19,20] that simulates the load–deflection responses and strength envelopes of high strength circular CFST slender beam-columns.

This paper extends the numerical models developed by Liang [17,19] to the nonlinear analysis of high strength thin-walled rectangular CFST slender beam-columns under axial load and uniaxial bending. Material constitutive models for concrete in CFST columns and for structural steels are presented. The modeling of cross-sectional strengths accounting for the local buckling effects of the steel tube walls under stress gradients is formulated by the fiber element method. New efficient computational algorithms based on the Müller's method are developed to obtain nonlinear solutions. Computational procedures for simulating the load–deflection and axial load–moment interaction curves for high strength CFST slender beam-columns are described in detail. The verification of the numerical model developed and its applications are given in a companion paper [21].

2. Material stress–strain relationships

2.1. Stress–strain relationships for concrete

The rectangular steel tube provides confinement to the four corners of the concrete core in a rectangular CFST column. This confinement does not have a significant effect on the compressive strength of the concrete core so that it can be ignored in the analysis and design of rectangular CFST columns. However, the ductility of the concrete core in rectangular CFST columns is improved and is included in the concrete model. The stress–strain relationship for concrete in rectangular CFST columns is shown in Fig. 1. The concrete stress from O to A is calculated based on the equations given by Mander et al. [22] as:

$$\sigma_c = \frac{f'_{cc}\lambda\left(\frac{\varepsilon_c}{\varepsilon_{cc}}\right)}{\lambda - 1 + \left(\frac{\varepsilon_c}{\varepsilon_{cc}}\right)^\lambda} \quad (1)$$

$$\lambda = \frac{E_c}{E_c - \left(\frac{f'_{cc}}{\varepsilon_{cc}}\right)} \quad (2)$$

where σ_c stands for the compressive concrete stress, f_{cc}' is the effective compressive strength of concrete, ε_c is the compressive concrete strain, ε_{cc}' is the strain at f_{cc}' and E_c is the Young's modulus of concrete which is given by ACI [23] as

$$E_c = 3320\sqrt{f'_{cc}} + 6900 (MPa). \quad (3)$$

The effective compressive strengths of concrete (f_{cc}') is taken as $\gamma_c f_c'$, where γ_c is the strength reduction factor proposed by Liang [17] to account for the column size effect and is expressed as

$$\gamma_c = 1.85 D_c^{-0.135} (0.85 \le \gamma_c \le 1.0) \quad (4)$$

where D_c is taken as the larger of $(B - 2t)$ and $(D - 2t)$ for a rectangular cross section, B is the width of the cross-section, D is the depth of the cross-section, and t is the thickness of the steel tube wall.

High strength concrete becomes more brittle after reaching the maximum compressive strength. The strain corresponding to the maximum compressive strength of high strength concrete is greater than that of the normal strength concrete. In the numerical model, the strain ε_{cc}' corresponding to f_{cc}' is taken as 0.002 for the effective compressive strength less than or equal to 28 MPa and 0.003 for $f_{cc}' > 82$ MPa. For the effective compressive strength between 28 and 82 MPa, the strain ε_{cc}' is determined by linear interpolation.

The parts AB, BC and CD of the stress–strain curve for concrete in CFST columns as shown in Fig. 1 are defined by the following equations given by Liang [17]:

$$\sigma_c = \begin{cases} f'_{cc} & \text{for } \varepsilon'_{cc} < \varepsilon_c \le 0.005 \\ \beta_c f'_{cc} + 100(0.015 - \varepsilon_c)\left(f'_{cc} - \beta_c f'_{cc}\right) & \text{for } 0.005 < \varepsilon_c \le 0.015 \\ \beta_c f'_{cc} & \text{for } \varepsilon_c > 0.015 \end{cases} \quad (5)$$

where β_c was proposed by Liang [17] based on experimental results presented by Tomii and Sakino [24] and is given by

$$\beta_c = \begin{cases} 1.0 & \text{for } \frac{B_s}{t} \le 24 \\ 1.5 - \frac{1}{48}\frac{B_s}{t} & \text{for } 24 < \frac{B_s}{t} \le 48 \\ 0.5 & \text{for } \frac{B_s}{t} > 48 \end{cases} \quad (6)$$

where B_s is taken as the larger of B and D for a rectangular cross-section.

The tensile strength of concrete is taken as $0.6\sqrt{f'_{cc}}$, which is much lower than its ultimate compressive strength. The stress–strain relationship for concrete in tension is shown in Fig. 1. The concrete
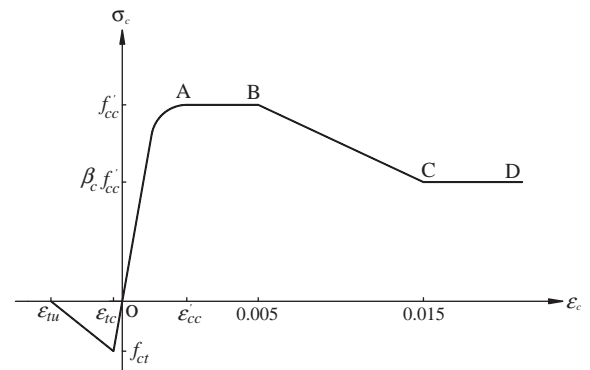

Fig. 1. Stress–strain curve for concrete in rectangular CFST columns.

tensile stress is considered zero at the ultimate tensile strain. The concrete tensile stress is directly proportional to the tensile strain of concrete up to concrete cracking. After concrete carking, the tensile stress of concrete is inversely proportional to the tensile strain of concrete up to the ultimate tensile strain due to concrete cracking. The ultimate tensile strain is taken as 10 times of the strain at cracking.

2.2. Stress–strain relationships for steels

Three types of the structural steels such as high strength structural steels, cold-formed steels and mild structural steels are considered in the numerical model. The steel generally follows the same stress–strain relationship under the tension and compression. The stress–strain relationship for steel under uniaxial compression is shown in Fig. 2. The mild structural steels have a linear stress–strain relationship up to the yield stress, however, it is assumed that high strength steels and cold-formed steels have a linear stress–strain relationship up to $0.9f_{sy}$, where f_{sy} is the steel yield strength. The rounded curve of the cold-formed structural steel can be defined by the equation proposed by Liang [17]. The hardening strain ε_{st} is assumed to be 0.005 for high strength and cold-formed steels and $10\varepsilon_{sy}$ for mild structural steels in the numerical model. The ultimate strain of steels is assumed to be 0.2.

3. Modeling of cross-sectional strengths

3.1. Strain calculations

In the fiber element method, the rectangular cross-section of a slender beam-column is divided into small concrete fiber elements and steel fiber elements for the purpose of the fiber element integration. The typical cross-section discretization is shown in Fig. 3. The strain of each fiber element is calculated by multiplication of the curvature and the orthogonal distance of each fiber element from the neutral axis. In the numerical model, the compressive strain is taken as positive and the tensile strain is taken as negative. The strain ε_t at the top fiber of the section in the composite cross-section can be determined by multiplication of the curvature ϕ and the neutral axis depth d_n.

For bending about the x-axis, the strains in concrete and steel fibers can be calculated by the following equations given by Liang [17]:

$$y_{n,i} = \frac{D}{2} - d_n \tag{7}$$

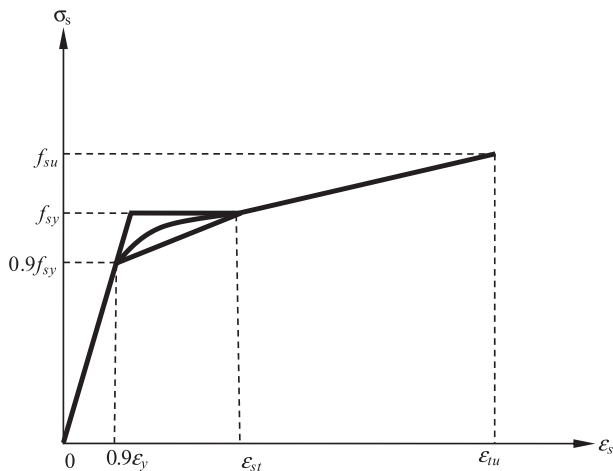$$d_{e,i} = |y_i - y_{n,i}| \tag{8}$$
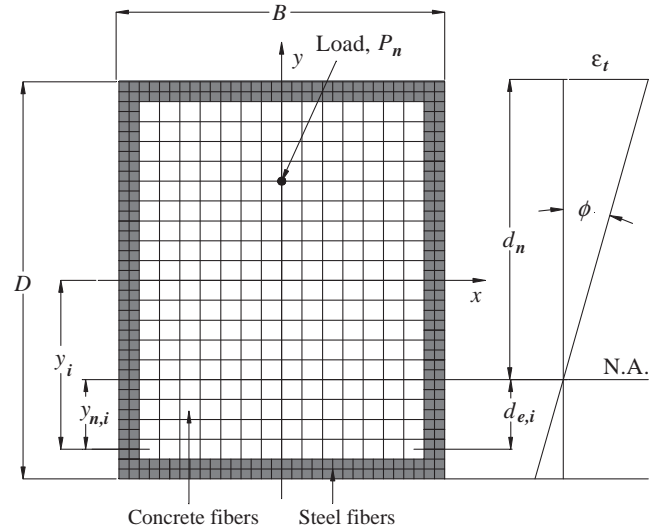

Fig. 2. Stress–strain curves for structural steels.

Fig. 3. Fiber element discretization of CFST beam-column section.

$$\varepsilon_i = \begin{cases} \phi d_{e,i} & \text{for } y_i \geq y_{n,i} \\ -\phi d_{e,i} & \text{for } y_i < y_{n,i} \end{cases} \tag{9}$$

where d_n is the neutral axis depth, $d_{e,i}$ is the orthogonal distance from the centroid of each fiber element to the neutral axis, y_i is the coordinates of the fiber i and ε_i is the strain at the ith fiber element and $y_{n,i}$ is the distance from the centroid of each fiber element to the neutral axis.

For bending about the y-axis, the strain in concrete and steel fibers can be calculated by the following equations given by Liang [17]

$$x_{n,i} = \frac{B}{2} - d_n \tag{10}$$

$$d_{e,i} = |x_i - x_{n,i}| \tag{11}$$

$$\varepsilon_i = \begin{cases} \phi d_{e,i} & \text{for } x_i \geq x_{n,i} \\ -\phi d_{e,i} & \text{for } x_i < x_{n,i} \end{cases} \tag{12}$$

where x_i is coordinates of the fiber i and $x_{n,i}$ is the distance from the centroid of each fiber element to the neutral axis.

3.2. Initial local buckling

Steel plates in thin-walled CFST columns with a large width-to-thickness ratio may buckle locally outward, which reduces the strength and ductility of the beam-columns. The initial local buckling stresses of steel plates depend on the width-to-thickness ratio, residual stresses, geometric imperfections, the yield strength of steel plates, and the applied edge stress gradients. Liang and Uy [10] reported that local buckling of a thin steel plate may occur when its width-to-thickness (b/t) ratio is greater than 30. Steel tube walls of a thin-walled CFST column under axial load and bending are subjected to uniform or non-uniform stresses. Therefore, steel tube walls under both uniform and non-uniform compressive stresses must be taken into account in the interaction buckling analysis of a thin-walled CFST beam-column under axial load and uniaxial bending. Liang et al. [11] proposed formulas for determining the initial local buckling stresses of thin steel plates under stress gradients. These formulas are incorporated in the numerical model to account for initial local buckling effects on the behavior of high strength thin-walled rectangular CFST slender beam-columns.

3.3. Post-local buckling

The post-local buckling strengths of thin steel plates can be determined using the effective strength and width concept. Liang et al. [11] proposed effective strength and width formulas for determining the post-local buckling strengths of steel plates in thin-walled CFST beam-columns under axial load and biaxial bending. Their formulas are incorporated in the numerical model to determine the ultimate strengths of thin steel plates under stress gradients. Fig. 4 shows the effective and ineffective areas of a rectangular thin-walled CFST beam-column cross-section under axial compression and uniaxial bending. The effective widths b_{e1} and b_{e2} shown in Fig. 4 are given by Liang et al. [11] as

$$\frac{b_{e1}}{b} = \begin{cases} 0.2777 + 0.01019\left(\frac{b}{t}\right) - 1.972 \times 10^{-4}\left(\frac{b}{t}\right)^2 + 9.605 \times 10^{-7}\left(\frac{b}{t}\right)^3 & \text{for } \alpha_s > 0.0 \\ 0.4186 - 0.002047\left(\frac{b}{t}\right) + 5.355 \times 10^{-5}\left(\frac{b}{t}\right)^2 - 4.685 \times 10^{-7}\left(\frac{b}{t}\right)^3 & \text{for } \alpha_s = 0.0 \end{cases}$$

$$\tag{13}$$

$$\frac{b_{e2}}{b} = (2 - \alpha_s)\frac{b_{e1}}{b} \tag{14}$$

where b is the clear width of a steel flange or web in a CFST column section, and $\alpha_s = \sigma_2/\sigma_1$, where σ_2 is the minimum edge stress applied to the plate and σ_1 is the maximum edge stress applied to the plate.

3.4. Simulation of progressive post-local buckling

The behavior of a thin steel plate under increasing loads is characterized by the progressive post-local buckling. In the post-local buckling regime, stresses in the steel plate are gradually redistributed from the heavily buckled region to the unloaded edges. This implies that the heavily buckled central region in the plate carries lower stresses while the unloaded edges withstand higher stresses. The effective width concept assumes that a steel plate attains its ultimate strength when the maximum stress in the plate reaches its yield strength. The ineffective width of a thin steel plate increases from zero to maximum value when the applied load is increased from the initial local buckling load to the ultimate load. The maximum ineffective width of each thin steel plate in a CFST beam-column at the ultimate load is determined by

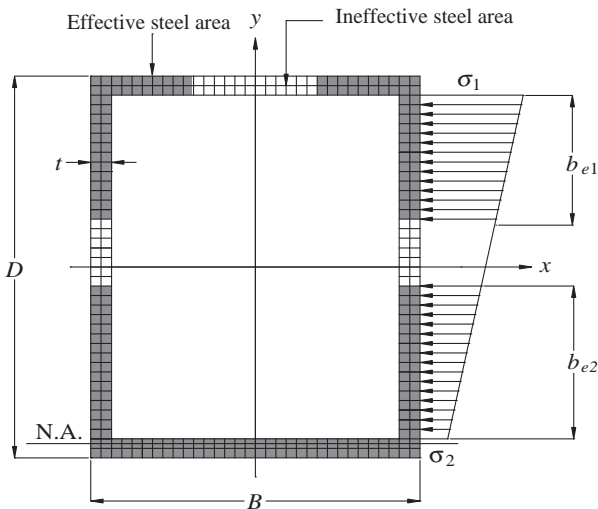$$b_{ne,\max} = b - (b_{e1} + b_{e2}). \tag{15}$$

Fig. 4. Effective area of steel tubular cross-section under axial load and bending.

As suggested by Liang [17], the ineffective width between zero and $b_{ne,\max}$ can be approximately calculated using linear interpolation based on the maximum stress level in the steel plate, and it is given by

$$b_{ne} = \left(\frac{\sigma_1 - \sigma_{1c}}{f_{sy} - \sigma_{1c}}\right) b_{ne,\max} \tag{16}$$

where σ_{1c} is the maximum edge stress in a steel tube wall when initial local buckling occurs.

If the maximum edge stress σ_1 in a steel plate with a b/t ratio greater than 30 is larger than the initial local buckling stress σ_{1c}, it is assumed that steel fiber elements within the ineffective area do not carry any loads. Therefore, the normal stresses in those fibers are assigned to zero. However, if the maximum edge stress σ_1 is greater than the yield strength of the steel plate, stresses within the steel tube wall need to be reduced by a factor of σ_1/f_{sy} to make sure that the effective width concept is valid. The effective strength formulas proposed by Liang et al. [11] are employed to determine the ultimate strength of the thin steel plate, when the total effective width of the plate $(b_{e1} + b_{e2})$ is greater than its width (b). If the maximum edge stress of the thin steel plate is greater than the ultimate edge stress σ_{1u} of the steel plate, the stresses within the steel plate are reduced by a factor of σ_1/σ_{1u}.

3.5. Stress resultants

The axial force and bending moments carried by a rectangular CFST beam-column cross-section are determined as stress resultants in the cross-section as follows:

$$P = \sum_{i=1}^{ns} \sigma_{s,i} A_{s,i} + \sum_{j=1}^{nc} \sigma_{c,j} A_{c,j} \tag{17}$$

$$M_x = \sum_{i=1}^{ns} \sigma_{s,i} A_{s,i} y_i + \sum_{j=1}^{nc} \sigma_{c,j} A_{c,j} y_j \tag{18}$$

$$M_y = \sum_{i=1}^{ns} \sigma_{s,i} A_{s,i} x_i + \sum_{j=1}^{nc} \sigma_{c,j} A_{c,j} x_j \tag{19}$$

where P is the axial force, $\sigma_{s,i}$ is the stress of steel fiber i, $A_{s,i}$ is the area of steel fiber i, $\sigma_{c,j}$ is the stress of concrete fiber j, $A_{c,j}$ is the area of concrete fiber j, x_i and y_i are the coordinates of steel element i, x_j and y_j are the coordinates of concrete element j, ns is the total number of steel fiber elements and nc is the total number of concrete fiber elements.

4. Müller's method algorithms

4.1. Determining the neutral axis depth

Computational algorithms based on the Müller's method [25] are developed to iterate the neutral axis depth in a composite cross-section with local bucking effects. The neutral axis depth d_n of the composite cross-section is iteratively adjusted to maintain the force equilibrium in order to determine the internal moment carried by the section. The Müller's method algorithm requires three initial values of the neutral axis depth $d_{n,1}$, $d_{n,2}$ and $d_{n,3}$ to start the iterative process. The neutral axis depth d_n is adjusted by using the following proposed equations:

$$d_{n,4} = d_{n,3} + \frac{-2c_1}{b_1 \pm \sqrt{b_1^2 - 4a_1 c_1}} \tag{20}$$

$$a_1 = \frac{\left(d_{n,2}-d_{n,3}\right)\left(r_{pu,1}-r_{pu,3}\right)-\left(d_{n,1}-d_{n,3}\right)\left(r_{pu,2}-r_{pu,3}\right)}{\left(d_{n,1}-d_{n,2}\right)\left(d_{n,1}-d_{n,3}\right)\left(d_{n,2}-d_{n,3}\right)} \tag{21}$$

$$b_1 = \frac{\left(d_{n,1}-d_{n,3}\right)^2\left(r_{pu,2}-r_{pu,3}\right)-\left(d_{n,2}-d_{n,3}\right)^2\left(r_{pu,1}-r_{pu,3}\right)}{\left(d_{n,1}-d_{n,2}\right)\left(d_{n,1}-d_{n,3}\right)\left(d_{n,2}-d_{n,3}\right)} \tag{22}$$

$$c_1 = r_{pu,3} \tag{23}$$

where r_{pu} is the residual moment at the mid-height of the column that is given by

$$r_{pu} = P(e+u_m+u_o)-M_{mi} \tag{24}$$

where u_o is the initial geometric imperfection at the mid-height of the beam-column, u_m is the deflection at the mid-height of the beam-column, e is the eccentricity of the applied load as shown in Fig. 5 and M_{mi} is the internal moment carried by the section.

The sign ($+$ or $-$) of the square root term in the denominator of Eq. (20) is chosen to be the same as the sign of b_1 to keep $d_{n,4}$ close to $d_{n,3}$. In order to obtain converged solutions, the values of $d_{n,1}$, $d_{n,2}$ and $d_{n,3}$ and corresponding residual moments $r_{pu,1}$, $r_{pu,2}$ and $r_{pu,3}$ need to be exchanged. The values of $d_{n,1}$, $d_{n,2}$ and $d_{n,3}$ are temporarily stored in $d_{n,1}^T$, $d_{n,2}^T$ and $d_{n,3}^T$ respectively while the values of $r_{pu,1}$, $r_{pu,2}$ and $r_{pu,3}$ are temporarily stored in $r_{pu,1}^T$, $r_{pu,2}^T$ and $r_{pu,3}^T$ respectively. The following computer codes are executed:

IF$\left[\text{Abs}\left(d_{n,4}-d_{n,2}^T\right)<\text{Abs}\left(d_{n,4}-d_{n,1}^T\right), d_{n,1}=d_{n,2}^T; d_{n,2}=d_{n,1}^T; r_{pu,1}=r_{pu,2}^T; r_{pu,2}=r_{pu,1}^T;\right]$;
IF$\left[\text{Abs}\left(d_{n,4}-d_{n,3}^T\right)<\text{Abs}\left(d_{n,4}-d_{n,2}^T\right), d_{n,2}=d_{n,3}^T; d_{n,3}=d_{n,2}^T; r_{pu,2}=r_{pu,3}^T; r_{pu,3}=r_{pu,2}^T;\right]$;
$$d_{n,3}=d_{n,4}; \; r_{pu,3}=r_{pu,4}.$$

Eq. (20) and the above codes are executed repetitively until the convergence criterion of $|r_{pu}|<\varepsilon_k$ is satisfied, where ε_k is the convergence tolerance that is taken as 10^{-4}.

4.2. Determining the curvature at column ends

The maximum moment $M_{e\,\text{max}}$ at the column ends for a given axial load P_n needs to be determined in order to generate the axial load–moment interaction diagram for the slender beam-column. The curvature at the mid-height ϕ_m of the beam-column under axial
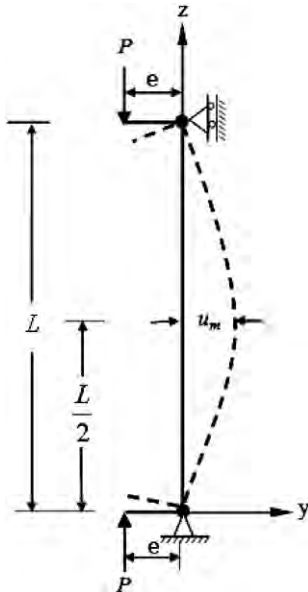

Fig. 5. Pin-ended beam-column model.

load and uniaxial bending is initialized and gradually increased. For each curvature increment at the mid-height of the beam-column, the curvature at the column ends ϕ_e is iteratively adjusted by the Müller's method algorithm to maintain equilibrium between the internal moment M_{mi} and the external moment M_{me} at the mid-height of the beam-column. The Müller's method algorithm requires three initial values of the curvature at the column ends $\phi_{e,1}$, $\phi_{e,2}$ and $\phi_{e,3}$ to start the iterative process. The curvature ϕ_e at the column ends is adjusted by using the following proposed equations:

$$\phi_{e,4} = \phi_{e,3} + \frac{-2c_2}{b_2+\sqrt{b_2^2-4a_2c_2}} \tag{25}$$

$$a_2 = \frac{\left(\phi_{e,2}-\phi_{e,3}\right)\left(r_{pm,1}-r_{pm,3}\right)-\left(\phi_{e,1}-\phi_{e,3}\right)\left(r_{pm,2}-r_{pm,3}\right)}{\left(\phi_{e,1}-\phi_{e,2}\right)\left(\phi_{e,1}-\phi_{e,3}\right)\left(\phi_{e,2}-\phi_{e,3}\right)} \tag{26}$$

$$b_2 = \frac{\left(\phi_{e,1}-\phi_{e,3}\right)^2\left(r_{pm,2}-r_{pm,3}\right)-\left(\phi_{e,2}-\phi_{e,3}\right)^2\left(r_{pm,1}-r_{pm,3}\right)}{\left(\phi_{e,1}-\phi_{e,2}\right)\left(\phi_{e,1}-\phi_{e,3}\right)\left(\phi_{e,2}-\phi_{e,3}\right)} \tag{27}$$

$$c_2 = r_{pm,3} \tag{28}$$

where r_{pm} is the residual moment at the mid-height of the column which is given by

$$r_{pm} = M_e + P_n(u_m+u_o)-M_{mi}. \tag{29}$$

The sign of the square root term in the denominator of Eq. (25) is taken as positive in order to obtain converged solutions. Similar to the determination of d_n, the values of $\phi_{e,1}$, $\phi_{e,2}$ and $\phi_{e,3}$ and corresponding $r_{pm,1}$, $r_{pm,2}$ and $r_{pm,3}$ need to be exchanged in order to obtain the true ϕ_e. The values of $\phi_{e,1}$, $\phi_{e,2}$ and $\phi_{e,3}$ are temporarily stored in $\phi_{e,1}^T$, $\phi_{e,2}^T$ and $\phi_{e,3}^T$ respectively and the values of $r_{pm,1}$, $r_{pm,2}$ and $r_{pm,3}$ are temporarily stored in $r_{pm,1}^T$, $r_{pm,2}^T$ and $r_{pm,3}^T$ respectively. The following computer codes are executed:

IF$\left[\text{Abs}\left(\phi_{e,4}-\phi_{e,2}^T\right)<\text{Abs}\left(\phi_{e,4}-\phi_{e,1}^T\right), \phi_{e,1}=\phi_{e,2}^T; \phi_{e,2}=\phi_{e,1}^T; r_{pm,1}=r_{pm,2}^T; r_{pm,2}=r_{pm,1}^T;\right]$;

IF$\left[\text{Abs}\left(\phi_{e,4}-\phi_{e,3}^T\right)<\text{Abs}\left(\phi_{e,4}-\phi_{e,2}^T\right), \phi_{e,2}=\phi_{e,3}^T; \phi_{e,3}=\phi_{e,2}^T; r_{pm,2}=r_{pm,3}^T; r_{pm,3}=r_{pm,2}^T;\right]$;

$$\phi_{e,3}=\phi_{e,4}; \; r_{pm,3}=r_{pm,4}.$$

The curvature at the column ends is iteratively adjusted until convergence criterion of $|r_{pm}|<\varepsilon_k$ is satisfied.

5. Modeling of load–deflection responses

5.1. Formulation

A new efficient numerical model has been developed to generate axial load–deflection curves for high strength thin-walled rectangular CFST slender beam-columns under axial load and uniaxial bending with local buckling effects. The deflected shape of the column is assumed to be part of a sine wave as suggested by Shakir–Khalil and Zeghiche [2]. The deflection at any point (y, z) along the column length is given by

$$u = u_m \sin\left(\frac{\pi z}{L}\right) \tag{30}$$

where L is the effective length of the beam-column.

77

The curvature (ϕ) along the length of the beam-column can be derived from Eq. (30) as

$$\phi = \frac{\partial^2 u}{\partial z^2} = \left(\frac{\pi}{L}\right)^2 u_m \sin\left(\frac{\pi z}{L}\right). \tag{31}$$

The curvature at the mid-height of the beam-column is given by

$$\phi_m = \left(\frac{\pi}{L}\right)^2 u_m \tag{32}$$

The external bending moment at the mid-height of the beam-column with an initial geometric imperfection u_o and under eccentric loading can be calculated by

$$M_{me} = P(e + u_m + u_o) \tag{33}$$

5.2. Analysis procedure

The axial load–deflection analysis procedure is started by first assuming a small value of the mid-height deflection u_m in the slender beam-column under axial load with an eccentricity. The curvature ϕ_m at the mid-height of the slender beam-column is calculated for the given mid-height deflection using Eq. (32). The proposed Müller's method algorithms are used to adjust the neutral axis depth in the composite cross-section to maintain the force equilibrium. The internal bending moment M_{mi} is determined using the moment-curvature response of the composite cross-section with local buckling effects. The mid-height deflection of the slender beam-column is gradually increased and the process is repeated. A pair of applied axial load and deflection is used to plot the axial load–deflection diagram. The flowchart of the axial load–deflection analysis procedure is shown in Fig. 6. The key steps of the axial load–deflection diagram are given as follows:

(1) Input the dimensions of the beam-column, material properties of the steel and concrete, the loading eccentricity e and initial geometric imperfection u_o.
(2) Divide the concrete core and steel tube into fiber elements.
(3) Initialize the mid-height deflection: $u_m = \Delta u_m$.
(4) Compute the curvature ϕ_m at the mid-height of the beam-column from the given mid-height deflection u_m by using Eq. (32).
(5) Initialize three values of the neutral axis depth of the composite cross-section: $d_{n,1} = D/4$, $d_{n,2} = D/2$ and $d_{n,3} = D$.
(6) Compute the stresses of steel and concrete using the stress–strain relationships.
(7) Check local buckling and redistribute stresses in steel fibers if local buckling occurs.
(8) Calculate the internal bending moment M_{mi} and the external bending moment M_{me} corresponding to $d_{n,1} = D/4$, $d_{n,2} = D/2$ and $d_{n,3} = D$ respectively.
(9) Compute the residual moments $r_{pu,1}$, $r_{pu,2}$ and $r_{pu,3}$ corresponding to $d_{n,1} = D/4$, $d_{n,2} = D/2$ and $d_{n,3} = D$ respectively.
(10) Calculate a_1, b_1 and c_1 and adjust the neutral axis depth d_n using Eq. (20).
(11) Compute fiber element stresses and redistribute normal stresses in steel fibers if local buckling occurs.
(12) Calculate the internal bending moment M_{mi} and external bending moment M_{me} corresponding to the neutral axis depth d_n.
(13) Compute r_{pu} using Eq. (24) and repeat Steps (10)–(12) until the convergence condition $|r_{pu}| < \varepsilon_k$ is satisfied.
(14) Increase the deflection u_m at the mid-height of the beam-column and repeat steps (4)–(13) until the ultimate load P_n is obtained or the deflection limit is reached.
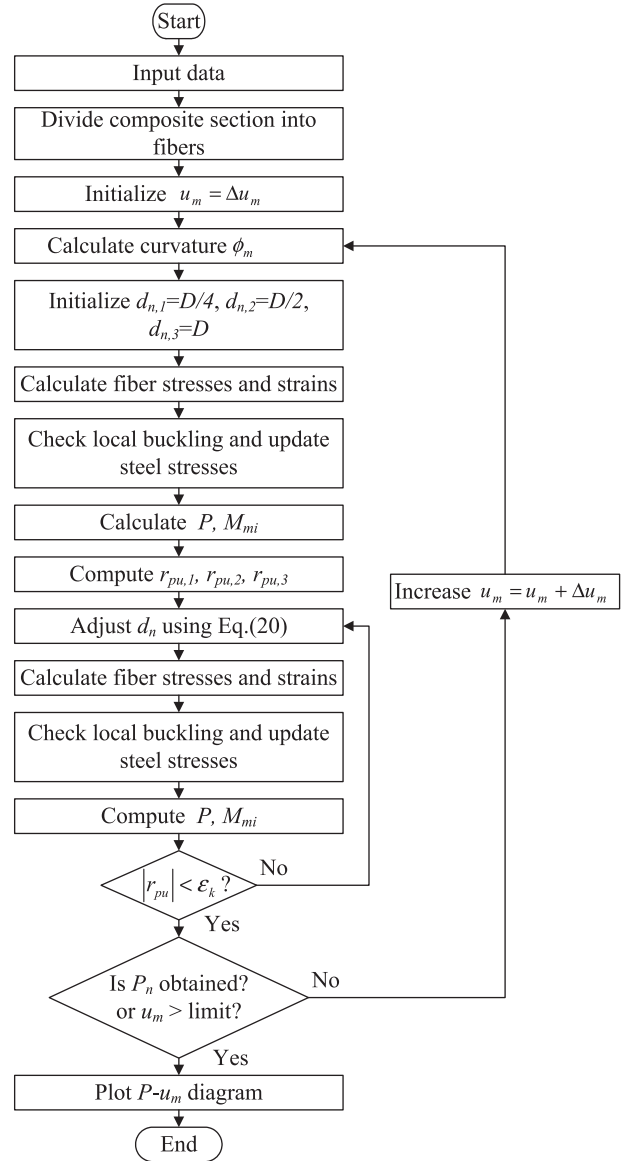(15) Plot the load–deflection curve.

Fig. 6. Flowchart for determining the axial load–deflection curve for rectangular thin-walled CFST slender columns.

The convergence tolerance ε_k is set to 10^{-4} in the analysis. The computational procedure proposed can predict the complete axial load–deflection responses of uniaxially loaded rectangular CFST slender beam-columns with local buckling effects.

6. Modeling of axial load–moment interaction diagrams

6.1. Formulation

The ultimate bending moment M_n is calculated as the maximum applied moment $M_{e\,max}$ at the column ends for a given axial load P_n to generate the axial load–moment interaction diagram. The maximum moment $M_{e\,max}$ is obtained when the external moment M_{me} attains the ultimate bending strength of the beam-column cross-section for the given axial load P_n. The curvature at the column ends is adjusted using the Müller's method algorithms and the corresponding moment M_e at the column ends is calculated. The external

moment at the mid-height of the slender beam-column is calculated by

$$M_{me} = M_e + P_n(u_m + u_o). \tag{34}$$

The curvature at the mid-height of the slender beam-column is gradually increased to calculate the maximum bending moment $M_{e\,max}$ for a given axial load. For each curvature increment at the mid-height of the beam-column, the mid-height deflection is calculated by the following equation:

$$u_m = \left(\frac{L}{\pi}\right)^2 \phi_m. \tag{35}$$

6.2. Analysis procedure

The axial load–moment interaction diagram for high strength thin-walled rectangular CFST slender beam-column is determined by the numerical model developed. The axial load–deflection analysis procedure incorporating local buckling effects is used to determine the ultimate axial load P_{oa} of the slender column under axial load alone. The applied axial load P_n is gradually increased. The curvature ϕ_m at the mid-height is initialized and gradually increased. The load–moment–curvature relationship incorporating local buckling effects is used to determine the corresponding internal moment M_{mi} at the mid-height of the beam-column. The proposed Müller's method algorithms are used to adjust the curvature ϕ_e at the column ends to produce the moment M_e that satisfies equilibrium at the mid-height of the beam-column. The maximum moment $M_{e\,max}$ at the column ends is obtained for each increment of the applied axial load P_n. A pair of the maximum moment $M_{e\,max}$ at the column ends and the given applied axial load P_n is used to plot the axial load–moment interaction diagram. Fig. 7 shows the flowchart for determining axial load–moment interaction diagrams for rectangular CFST slender beam-column. The main steps of the analysis procedure are given as follows:

(1) Input the geometry of the beam-column, material properties of the steel and concrete and the initial geometric imperfection u_o.
(2) Divide composite section into concrete and steel fiber elements.
(3) Compute the ultimate axial load P_{oa} of the axially loaded slender beam-column using the load–deflection analysis procedure accounting for local buckling effects.
(4) Initialize the applied axial load: $P_n = 0$.
(5) Initialize the curvature at the mid-height of the beam-column: $\phi_m = \Delta\phi_m$.
(6) Calculate the mid-height deflection u_m using Eq. (35) from the mid-height curvature ϕ_m.
(7) Compute the internal moment M_{mi} for the given axial load P_n using the $P-M-\phi$ relationship accounting for local buckling effects.
(8) Initialize three values of the curvature at the column ends $\phi_{e,1} = 10^{-10}$, $\phi_{e,3} = 10^{-6}$, $\phi_{e,2} = (\phi_{e,1} + \phi_{e,3})/2$ and calculate the corresponding $r_{pm,1}$, $r_{pm,2}$ and $r_{pm,3}$.
(9) Calculate a_2, b_2 and c_2 and adjust the curvature at the columns end φ_e using Eq. (25).
(10) Compute the moment M_e at the column ends and the internal bending moment M_{mi} using the $P-M-\phi$ relationship accounting for local buckling effects.
(11) Calculate r_{pm} using Eq. (29) and repeat steps (9)–(10) until $|r_{pm}| < \varepsilon_k$.
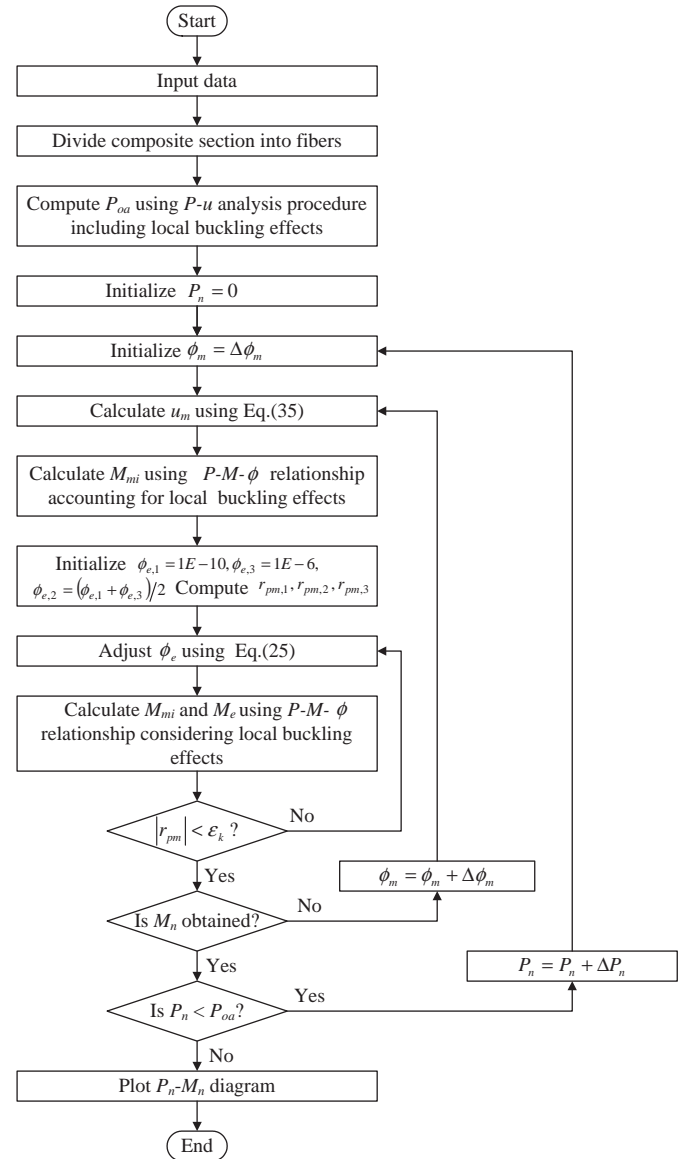(12) Increase the curvature at the mid-height of the beam-column by $\phi_m = \phi_m + \Delta\phi_m$.

Fig. 7. Flowchart for determining the axial load–moment interaction diagram for rectangular thin-walled CFST slender beam-columns.

(13) Repeat steps (6)–(12) until the ultimate bending strength $M_n(= M_{e\,max})$ at the column ends is obtained.
(14) Increase the axial load by $P_n = P_n + \Delta P_n$, where $\Delta P_n = P_{oa}/10$.
(15) Repeat steps (5)–(14) until the maximum load increment is reached.
(16) Plot the axial load–moment interaction diagram.

Numerical analysis shows that the proposed Muller algorithms are very efficient for obtaining converged solutions. The ultimate pure axial load P_{oa} is calculated by specifying the eccentricity of the applied to zero in the axial load–deflection analysis. Similarly, the ultimate pure bending strength of a slender beam-column is obtained by specifying the axial load to zero in the axial load–moment interaction strength analysis.

7. Conclusions

This paper has presented a new numerical model for simulating the behavior of high strength thin-walled rectangular CFST slender beam-columns under axial load and uniaxial bending. The effects of

local buckling, column slenderness, eccentricity of loading, high strength materials, initial geometric imperfections and material and geometric nonlinearities are considered in the numerical model developed. The numerical model for pin-ended CFST slender beam-columns with equal end eccentricities and single curvature bending was developed based on fiber element formulations. New Müller's method algorithms were developed to iterate the neutral axis depth in the composite cross-section and to adjust the curvature at the column ends in the slender beam-column to satisfy equilibrium conditions. The new numerical model is shown to be efficient for predicting the complete axial load–deflection and axial load–moment interaction curves for high strength thin-walled rectangular CFST slender beam-columns with local buckling effects. The comparison with corresponding experimental results and parametric studies is given in a companion paper.

References

[1] Bridge RQ. Concrete filled steel tubular columns. School of Civil Engineering, University of Sydney, Sydney, Australia, Research Report No. R283; 1976.
[2] Shakir-Khalil H, Zeghiche J. Experimental behaviour of concrete-filled rolled rectangular hollow-section columns. The Structural Engineer 1989;67(19):346–53.
[3] Matsui C, Tsuda K, Ishibashi Y. Slender concrete filled steel tubular columns under combined compression and bending. The 4th Pacific Structural Steel Conference Singapore, Pergamon 3(10): 1995. p. 29–36.
[4] Schneider SP. Axially loaded concrete-filled steel tubes. J Struct Eng ASCE 1998;124(10):1125–38.
[5] Han LH. Tests on stub columns of concrete-filled RHS sections. J Constr Steel Res 2002;58(3):353–72.
[6] Ellobody E, Young B, Lam D. Behaviour of normal and high strength concrete-filled compact steel tube circular stub columns. J Constr Steel Res 2006;62(7):706–15.
[7] Ge H, Usami T. Strength of concrete-filled thin-walled steel box columns: experiment. J Struct Eng ASCE 1992;118(11):3036–54.
[8] Bridge RQ, O'Shea MD. Behaviour of thin-walled steel box sections with or without internal restraint. J Constr Steel Res 1998;47(1–2):73–91.
[9] Uy B. Strength of concrete filled steel box columns incorporating local buckling. J Struct Eng ASCE 2000;126(3):341–52.
[10] Liang QQ, Uy B. Theoretical study on the post-local buckling of steel plates in concrete-filled box columns. Computers and Structures 2000;75(5): 479–90.
[11] Liang QQ, Uy B, Liew JYR. Local buckling of steel plates in concrete-filled thin-walled steel tubular beam-columns. J Constr Steel Res 2007;63(3):396–405.
[12] Chung J, Tsuda K, Matsui C. High-strength concrete filled square tube columns subjected to axial loading. The Seventh East Asia-Pacific Conference on Structural Engineering & Construction, Kochi, Japan, vol. 2; 1999. p. 955–60.
[13] Liu D. Behaviour of eccentrically loaded high-strength rectangular concrete-filled steel tubular columns. J Constr Steel Res 2006;62(8):839–46.
[14] Lue DM, Liu JL, Yen T. Experimental study on rectangular CFT columns with high-strength concrete. J Constr Steel Res 2007;63(1):37–44.
[15] Lakshmi B, Shanmugam NE. Nonlinear analysis of in-filled steel-concrete composite columns. J Struct Eng ASCE 2002;128(7):922–33.
[16] Vrcelj Z, Uy B. Strength of slender concrete-filled steel box columns incorporating local buckling. J Constr Steel Res 2002;58(2):275–300.
[17] Liang QQ. Performance-based analysis of concrete-filled steel tubular beam-columns, Part I: theory and algorithms. J Constr Steel Res 2009;65(2):363–72.
[18] Liang QQ. Strength and ductility of high strength concrete-filled steel tubular beam-columns. J Constr Steel Res 2009;65(3):687–98.
[19] Liang QQ. High strength circular concrete-filled steel tubular slender beam-columns, Part I: numerical analysis. J Constr Steel Res 2011;67(2):164–71.
[20] Liang QQ. High strength circular concrete-filled steel tubular slender beam-columns, Part II: fundamental behavior. J Constr Steel Res 2011;67(2): 172–80.
[21] Patel VI, Liang QQ, Hadi MNS. High strength thin-walled rectangular concrete-filled steel tubular slender beam-columns, Part II: behavior. Journal of Constructional Steel Research 2012;70(C):368–76.
[22] Mander JB, Priestly MNJ, Park R. Theoretical stress–strain model for confined concrete. J Struct Eng ASCE 1988;114(8):1804–26.
[23] ACI-318. Building code requirements for reinforced concrete. Detroit, MI: ACI; 2002.
[24] Tomii M, Sakino K. Elastic–plastic behavior of concrete filled square steel tubular beam-columns. Trans Architec Inst Jpn 1979;280:111–20.
[25] Müller DE. A method for solving algebraic equations using an automatic computer. MTAC 1956;10:208–15.

High strength thin-walled rectangular concrete-filled steel tubular slender beam-columns, Part II: Behavior

Vipulkumar Ishvarbhai Patel [a], Qing Quan Liang [a,*], Muhammad N.S. Hadi [b]

[a] School of Engineering and Science, Victoria University, PO Box 14428, Melbourne, VIC 8001, Australia
[b] School of Civil, Mining and Environmental Engineering, University of Wollongong, Wollongong, NSW 2522, Australia

ARTICLE INFO

ABSTRACT

Experimental and numerical research on full-scale high strength thin-walled rectangular steel slender tubes filled with high strength concrete has not been reported in the literature. In a companion paper, a new numerical model was presented that simulates the nonlinear inelastic behavior of uniaxially loaded high strength thin-walled rectangular concrete-filled steel tubular (CFST) slender beam-columns with local buckling effects. The progressive local and post-local buckling of thin steel tube walls under stress gradients was incorporated in the numerical model. This paper presents the verification of the numerical model developed and its applications to the investigation into the fundamental behavior of high strength thin-walled CFST slender beam-columns. Experimental ultimate strengths and load-deflection responses of CFST slender beam-columns tested by independent researchers are used to verify the accuracy of the numerical model. The verified numerical model is then utilized to investigate the effects of local buckling, column slenderness ratio, depth-to-thickness ratio, loading eccentricity ratio, concrete compressive strengths and steel yield strengths on the behavior of high strength thin-walled CFST slender beam-columns. It is demonstrated that the numerical model is accurate and efficient for determining the behavior of high strength thin-walled CFST slender beam-columns with local buckling effects. Numerical results presented in this study are useful for the development of composite design codes for high strength thin-walled rectangular CFST slender beam-columns.

© 2011 Elsevier Ltd. All rights reserved.

1. Introduction

The behavior of high strength thin-walled rectangular concrete-filled steel tubular (CFST) slender beam-columns under axial load and bending is influenced by many parameters such as the depth-to-thickness ratio, loading eccentricity, column slenderness, concrete compressive strength, steel yield strength, initial geometric imperfections and second order effects. Thin-walled CFST slender beam-columns under eccentric loading may fail by local and overall buckling. Researches on the interaction local and overall buckling behavior of high strength CFST slender beam-columns have been comparatively very limited. No design specifications on the design of high strength thin-walled CFST slender beam-columns are given in current design codes such as Eurocode 4 [1], LRFD [2] and ACI 318-05 [3]. Apparently, the fundamental behavior of high strength thin-walled CFST slender beam-columns with large depth-to-thickness ratios has not been fully understood and effective design methods have not been developed and incorporated in current composite design codes. In this paper, a numerical model developed is validated and

employed to investigate the behavior of high strength thin-walled CFST slender beam-columns with local buckling effects.

The local instability problem of CFST slender beam-columns was not identified in early experimental researches undertaken by Bridge [4] and Shakir-Khalil and Zeghiche [5]. Their test results indicated that all tested normal strength CFST slender columns with a depth-to-thickness ratio (D/t) of 20 or 24 failed by overall buckling without the occurring of local buckling. Local buckling of the steel tubes was expected in CFST columns with a D/t ratio greater than 35 as those tested by Matsui et al. [6]. Chung et al. [7] and Zhang et al. [8] tested high strength CFST slender beam-columns with D/t ratios ranging from 31 to 52 and compressive concrete cube strength of 94.1 MPa. Han [9] carried out tests on the flexural behavior of normal strength CFST members with D/t ratios ranging from 20 to 51. Further tests on CFST columns were conducted by Vrcelj and Uy [10], Varma et al. [11] and Giakoumelis and Lam [12]. However, the behavior of high strength rectangular steel tubular slender beam-columns filled with high strength concrete has not been investigated.

In design practice, the axial load–moment interaction diagrams need to be developed and are used to check for the strength adequacy of CFST slender beam-columns under axial load and bending. Most of the experiments conducted were to measure the load–deflection responses of CFST slender columns. It is highly expensive and time

consuming to obtain complete axial load–moment interaction curves for CFST slender beam-columns by experimental methods. Although the load–deflection analysis procedures such as those presented by Vrcelj and Uy [10] and Lakshmi and Shanmugam [13] can be used to develop strength envelopes by varying the loading eccentricity, they are not efficient when the loading eccentricity is large. Despite of this, the axial load–moment interaction diagrams of high strength rectangular CFST slender beam-columns have not been studied by Vrcelj and Uy [10] and Lakshmi and Shanmugam [13]. Ellobody and Young [14] used the finite element program ABAQUS to study the axial load–strain behavior of CFST short columns. Liang [15,16] utilized his numerical models to investigate the effects of various important parameters on the axial load–moment interaction curves for thin-walled CFST short beam-columns under axial load and biaxial bending. Moreover, Liang [17,18] studied concrete confinement effects on column curves and axial load–moment interaction curves for high strength circular CFST slender beam-columns.

Presented in this paper is the verification of the numerical model developed in a companion paper [19] and the behavior of high strength thin-walled CFST slender beam-columns with local buckling effects. Firstly, the numerical model is verified against existing experimental results. An extensive parametric study is then undertaken to investigate the effects of various important parameters on the ultimate strengths, load–deflection responses and axial load–moment interaction diagrams of high strength thin-walled CFST slender beam-columns. Benchmark numerical results obtained from the parametric study are presented and discussed.

2. Verification of the numerical model

The efficiency and accuracy of the developed numerical model are demonstrated through comparisons between the numerical and existing experimental results for a large number of slender beam-columns with different parameters. The ultimate axial and bending strengths and load–deflection curves of CFST slender beam-columns are considered in the verification of the numerical model developed.

2.1. Ultimate axial strengths of normal strength CFST columns

The geometry, material properties and experimental results of normal strength CFST slender columns tested by various researchers are given in Table 1. Specimens SCH-1, SCH-2 and SCH-7 were tested by Bridge [4]. The width (B) of the steel tubes varied between

152.5 mm and 204.0 mm while the depth (D) of the steel tubes ranged from 152.3 to 203.9 mm. The depth-to-thickness ratios (D/t) ranged from 20 to 24 while the length of the columns was either 2130 mm or 3050 mm. Specimen SCH-2 was tested under a concentric axial load. Initial geometric imperfections (u_o) at the mid-height of the specimens were measured as shown in Table 1. The axial load was applied at an eccentricity (e) of either 38 mm or 64 mm. The slender beam-columns were constructed by steel tubes filled with normal strength concrete of either 29.9 or 31.1 MPa. The steel yield strengths (f_{sy}) varied between 254 MPa and 291 MPa. The ultimate tensile strength (f_{su}) of steel tubes was assumed to be 410 MPa. The Young's modulus (E_s) of the steel material was 205 GPa.

Specimens R1, R2 and R5 shown in Table 1 were tested by Shakir-Khalil and Zeghiche [5]. These slender beam-columns with a cross-section of 80×120 mm were constructed by cold-formed steel tubes filled with normal strength concrete. The yield strength of the steel tubes ranged from 343.3 MPa to 386.3 MPa while the compressive strength of concrete varied between 34 MPa and 37.4 MPa. Specimens were fabricated from 5 mm thick steel tubes so that their depth-to-thickness ratio (D/t) was 24. The effective buckling lengths of the beam-columns were 3210 mm and 2940 mm about the major and minor axes respectively. The ultimate tensile strength of these steel tubes was assumed to be 430 MPa. Specimen R1 was tested under a concentric axial load while other specimens were tested under eccentric loads about either the major or minor axis. The loading eccentricity ratios (e/D) were in the range of 0.0 to 0.5. The initial geometric imperfections of specimens were not measured. Shakir-Khalil and Zeghiche [5] realized that the tested columns had initial geometric imperfections that should be recorded before testing. Therefore, the initial geometric imperfections of $L/1000$ at the mid-height of the columns were taken into account in the present study.

Slender columns tested by Matsui et al. [6] were also considered in this study. Test parameters of specimens designated by series S1 to S12 are presented in Table 1. The columns had a square cross-section of 149.8 mm wide and 4.27 mm thick. Steel tubes with yield strength of 445 MPa were filled with normal strength concrete of 31.9 MPa. The eccentricity of the applied axial load varied from zero to a maximum of 125 mm. The length of the columns varied from 600 mm to 4500 mm covering a wide range of column slenderness. However, only slender columns were considered in this paper. Specimens S1, S5 and S9 were tested under concentric axial loads. Experimental and analytical studies conducted by Matsui et al. [6] indicated that these specimens had significant geometric imperfections that were not recorded. The initial geometric

Table 1
Ultimate axial strengths of normal strength CFST slender beam-columns.

Specimens	$B \times D \times t$ (mm)	D/t	L (mm)	e_x (mm)	e_y (mm)	u_o (mm)	f'_c (MP)	f_{sy} (MPa)	f_{su} (MPa)	E_s (GPa)	$P_{u.exp}$ (kN)	$P_{u.num}$ (kN)	$\frac{P_{u.num}}{P_{u.exp}}$	Ref.
SCH-1	203.7×203.9×9.96	20	2130	0	38	1.19	29.9	291	410	205	1956	1995.73	1.02	[4]
SCH-2	204.0×203.3×10.01	20	3050	0	0	1.40	31.1	290	410	205	2869	2907.4	1.01	
SCH-7	152.5×152.3×6.48	24	3050	0	38	0.51	31.1	254	410	205	680	734.0	1.08	
R1	80×120×5	24	3210	0	0		37.4	386.3	430	205	600	600.41	1.00	[5]
R2	80×120×5	24	3210	0	24		34.0	386.3	430	205	393	383.61	0.98	
R5	80×120×5	24	2940	40	0		36.6	343.3	430	205	210	216.24	1.03	
S1	149.8×149.8×4.27	35	2700	0	0		31.9	445	498	200	1355	1356.99	1.00	[6]
S2	149.8×149.8×4.27	35	2700	0	25		31.9	445	498	200	847	868.80	1.03	
S3	149.8×149.8×4.27	35	2700	0	75		31.9	445	498	200	552	542.20	0.98	
S4	149.8×149.8×4.27	35	2700	0	125		31.9	445	498	200	383	393.13	1.03	
S5	149.8×149.8×4.27	35	3600	0	0		31.9	445	498	200	1143	1140.86	1.00	
S6	149.8×149.8×4.27	35	3600	0	25		31.9	445	498	200	706	734.41	1.04	
S7	149.8×149.8×4.27	35	3600	0	75		31.9	445	498	200	440	464.39	1.06	
S8	149.8×149.8×4.27	35	3600	0	125		31.9	445	498	200	325	346.85	1.07	
S9	149.8×149.8×4.27	35	4500	0	0		31.9	445	498	200	909	895.88	0.99	
S10	149.8×149.8×4.27	35	4500	0	25		31.9	445	498	200	588	602.78	1.03	
S11	149.8×149.8×4.27	35	4500	0	75		31.9	445	498	200	374	394.64	1.06	
S12	149.8×149.8×4.27	35	4500	0	125		31.9	445	498	200	278	302.98	1.09	
Mean													1.03	
Standard deviation (SD)													0.03	
Coefficient of variation (COV)													0.03	

imperfections of $L/1000$ at the mid-height of the tested specimens were considered in the present numerical analysis of these specimens.

The load–deflection analysis procedure developed by Patel et al. [19] was used to predict the ultimate strengths of these tested specimens. Test results indicated that specimen R1 did not attain its ultimate strength so that the measured maximum compressive concrete strain was used in the numerical analysis to determine the maximum load. The computational and experimental ultimate axial strengths of normal strength CFST slender beam-columns are given in Table 1, where $P_{u.\exp}$ represents the experimental ultimate axial strength and $P_{u.\text{num}}$ denotes the ultimate axial strength predicted by the numerical model. It can be seen from Table 1 that the predicted ultimate axial strengths of tested specimens are in good agreement with experimental results. The mean ultimate axial strength predicted by the numerical model is 1.03 times the experimental value with a standard deviation of 0.03 and a coefficient of variation of 0.03.

2.2. Ultimate axial strengths of high strength CFST columns

Table 2 presents the geometries, material properties and experimental results of high strength CFST slender columns tested by independent researchers. Chung et al. [7] tested a number of high strength CFST slender beam-columns subjected to axial load and uniaxial bending. The specimens were designated by series C18, C24 and C30. The lengths of specimens C18, C24 and C30 were 2250, 3000 and 3750 mm respectively. All specimens had a square cross-section of 125×125 mm. The steel tubes with yield strength of 450 MPa were filled with high strength concrete of 94.1 MPa. The tensile strength of the steel tubes was measured as 528 MPa. The depth-to-thickness ratio (D/t) of these specimens was 39. Specimens C30-0 was tested under a concentric axial load while other columns were subjected to axial loads at an eccentricity of either 20.5 mm or 61.5 mm.

Specimens CCH1, CCH2, CCM1 and CCM2 shown in Table 2 were tested by Vrcelj and Uy [10]. These columns were made of hot-rolled steel tubes which were cut into 1770 mm length. In order to simulate pinned-end support conditions, the specimen was provided with special knife-edge supports secured at their ends. The loading eccentricity ratio (e/D) was approximately equal to 0.05. The concrete compressive strength was either 52 MPa or 79 MPa while the steel yield strength was either 400 MPa or 450 MPa.

The load–deflection analysis procedure [19] was used to determine the ultimate axial strengths of these high strength specimens tested. The initial geometric imperfections of these high strength CFST slender beam-columns were not measured. However, real CFST slender beam-columns particularly small-scale ones usually have initial geometric imperfections. Therefore, the initial geometric imperfections of $L/1000$ at the mid-height of the columns were taken into account in the present numerical analysis of these columns. The

ultimate axial strengths of these specimens obtained from the numerical analysis and experiments are given in Table 2. It is seen that the numerical model predicts very well the ultimate axial strengths of high strength CFST slender beam-columns. The ratio of the mean ultimate axial strength computed by the numerical model to the experimental value is 1.01. The standard deviation of $P_{u.\text{num}}/P_{u.\exp}$ is 0.07 and the coefficient of variation is 0.07.

2.3. Ultimate bending strengths

Experimental results presented by Bridge [4], Shakir-Khalil and Zeghiche [5], Matsui et al. [6] and Chung et al. [7] were used to examine the accuracy of the axial–load moment interaction strength analysis program [19]. The initial geometric imperfections of $L/1000$ at the mid-height of the columns were taken into account in the analysis of the specimens tested by Shakir-Khalil and Zeghiche [5], Matsui et al. [6] and Chung et al. [7]. The ultimate axial loads obtained from experiments were applied in the numerical analysis to determine the ultimate bending strengths. The experimental and numerical ultimate bending strengths are presented in Table 3. The experimental ultimate bending strength $M_{n.\exp}$ was calculated as $M_{n.\exp} = P_{n.\exp} \times e$. It appears from Table 3 that the numerical model yields accurate predictions of the ultimate bending strengths of high strength CFST slender beam-columns. The ratio of the mean ultimate bending strength computed by the numerical model to the experimental value is 1.03 with the standard deviation of 0.05 and the coefficient of variation of 0.05.

2.4. Load–deflection curves

The load–deflection curves for CFST slender beam-columns predicted by the numerical model are compared with experimental results provided by Bridge [4], Shakir-Khalil and Zeghiche [5] and Matsui et al. [6]. Fig. 1 shows the load–deflection curves for specimen SCH2 predicted by the numerical model developed by Patel et al. [19] and obtained from the experiments conducted by Bridge [4]. It can be observed that the load–deflection curve predicted by the numerical model agrees reasonably well with the experimental results. The initial stiffness of the load–deflection curve predicted by the model is slightly higher than that of the experimental one. This is likely attributed to the uncertainty of the actual concrete stiffness and strength as the average concrete compressive strength was used in the numerical analysis. However, it can be seen from Fig. 1 that the numerical load–deflection curve is in excellent agreement with experimental results in the ultimate load range. The predicted and experimental axial load–deflection curves for specimen R5 tested by Shakir-Khalil and Zeghiche [5] are depicted in Fig. 2. The figure shows that the initial stiffness of the specimen predicted by the numerical model is almost the same as that of the experimental one up to loading level about

Table 2
Ultimate axial strengths of high strength CFST slender beam-columns.

Specimens	$B \times D \times t$ (mm)	D/t	L (mm)	e_x (mm)	e_y (mm)	f'_c (MP)	f_{sy} (MPa)	f_{su} (MPa)	E_s (GPa)	$P_{u.\exp}$ (kN)	$P_{u.\text{num}}$ (kN)	$\frac{P_{u.\text{num}}}{P_{u.\exp}}$	Ref.
C18-1	$125 \times 125 \times 3.2$	39	2250	0	20.5	94.1	450	528	200	830	874.28	1.05	[7]
C18-3	$12 \times 125 \times 3.2$	39	2250	0	61.5	94.1	450	528	200	457	490.57	1.07	
C24-0	$125 \times 125 \times 3.2$	39	3000	0	0	94.1	450	528	200	1079	1108.18	1.03	
C24-1	$125 \times 125 \times 3.2$	39	3000	0	20.5	94.1	450	528	200	664	676.12	1.02	
C24-3	$125 \times 125 \times 3.2$	39	3000	0	61.5	94.1	450	528	200	375	399.06	1.06	
C30-0	$125 \times 125 \times 3.2$	39	3750	0	0	94.1	450	528	200	747	814.05	1.09	
CCH1	$75 \times 75 \times 3$	25	1770	0	3.75	79	450	530	193.7	414	393.61	0.95	[10]
CCH2	$65 \times 65 \times 3$	22	1770	0	3.25	79	400	530	189.3	294	263.12	0.89	
CCM1	$75 \times 75 \times 3$	25	1770	0	3.75	52	450	530	193.7	343	355.98	1.04	
CCM2	$65 \times 65 \times 3$	22	1770	0	3.25	52	400	530	189.3	269	242.59	0.90	
Mean												1.01	
Standard deviation (SD)												0.07	
Coefficient of variation(COV)												0.07	

Table 3
Ultimate bending strengths of rectangular CFST slender beam-columns under eccentric loading.

Specimens	$B \times D \times t$ (mm)	D/t	L (mm)	e_x (mm)	e_y (mm)	u_o (mm)	f_c (MP)	f_{sy} (MPa)	f_{su} (MPa)	E_s (GPa)	$M_{n.\exp}$ (kNm)	$M_{n.\text{num}}$ (kNm)	$\frac{M_{n.\text{num}}}{M_{n.\exp}}$	Ref.
SCH-1	203.7×203.9×9.96	20	2130	0	38	1.19	29.9	291	410	205	74.33	79.12	1.06	[4]
R2	80×120×5	24	3210	0	24		34.0	386.3	430	205	9.43	8.76	0.93	[5]
R5	80×120×5	24	2940	40	0		36.6	343.3	430	205	8.4	8.82	1.05	
S2	149.8×149.8×4.27	35	2700	0	25		31.9	445	498	200	21.18	22.85	1.08	[6]
S3	149.8×149.8×4.27	35	2700	0	75		31.9	445	498	200	41.4	39.99	0.97	
S4	149.8×149.8×4.27	35	2700	0	125		31.9	445	498	200	47.88	49.57	1.04	
S10	149.8×149.8×4.27	35	4500	0	25		31.9	445	498	200	14.7	15.89	1.08	
C24-1	125×125×3.2	39	3000	0	20.5		94.1	450	528	200	13.61	14.29	1.05	[7]
Mean													1.03	
Standard deviation (SD)													0.05	
Coefficient of variation (COV)													0.05	

100 kN. After this loading, the stiffness of the specimen obtained from tests slightly differs from numerical predictions. This is likely attributed to the uncertainty of the concrete stiffness and strength. The numerical model was able to predict the post-peak behavior of the tested specimen R5.

Fig. 3 presents a comparison between numerical and experimental axial load–deflection curves for specimen S3. It is seen that the stiffness of the column predicted by the numerical model is in excellent agreement with experimental data for loading up to the ultimate load. In the post-peak range, the numerical model also predicts well the stiffness of the tested specimen but the predicted load capacity is lower than the test data. The verification shows that the numerical model yields good predictions of the ultimate axial and bending strengths and axial load–deflection curves for normal and high strength CFST slender beam-columns.

3. Parametric study

An extensive parametric study was performed to investigate the influences of local buckling of the steel tube, column slenderness ratio, depth-to-thickness ratio, eccentricity ratio, concrete compressive strengths and steel yield strengths on the fundamental behavior of full-scale high strength thin-walled rectangular CFST slender beam-columns under axial load and uniaxial bending. Only one variable was considered at a time to assess its individual effect.

3.1. Influences of local buckling

The numerical model was employed to study the effects of local buckling on the behavior of high strength rectangular CFST slender beam-columns. A thin-walled CFST beam-column with a cross-section of 700×700 mm was considered. The thickness of the steel tube was 7 mm so that its depth-to-thickness ratio (D/t) was 100. The yield and tensile strengths of the steel tube were 690 MPa and 790 MPa respectively while its Young's modulus was 200 GPa. High strength concrete with compressive strength of 70 MPa was filled into the steel tube. The column slenderness ratio (L/r) was 40. The axial load was applied at an eccentricity 70 mm so that the loading eccentricity ratio (e/D) was 0.1. The initial geometric imperfection at the mid-height of the beam-column was assumed to be $L/1500$. The slender beam-column was analyzed by considering and ignoring local buckling effects respectively.

Fig. 4 shows the influences of local buckling on the axial load–deflection curves for thin-walled CFST slender beam-columns and highlights the importance of considering local buckling in the analysis. It can be seen from Fig. 4 that local buckling remarkably reduces the stiffness and ultimate axial strength of the slender beam-column under eccentric loading. When the applied axial load is higher than about 10,000 kN, the stiffness of the slender beam-column is found to gradually reduce by progressive post-local buckling as illustrated in Fig. 4. The steel tube walls with a D/t ratio of 100 undergone elastic local and post-local buckling before yielding. Because the beam-column was subjected to axial load and bending, the two webs of the section were subjected to bending stresses under which local buckling was not considered in the effective width formulas given by Liang et al. [20]. After steel yielded, strain hardening occurred so that the two webs and the tension flange of the steel tube could carry the higher load than the yield load. This resulted in an increase in the load carrying capacity as shown on the load–deflection curve depicted in Fig. 4. However, thin-walled CFST slender beam-columns with a D/t ratio less than 80 exhibit smooth load–deflection
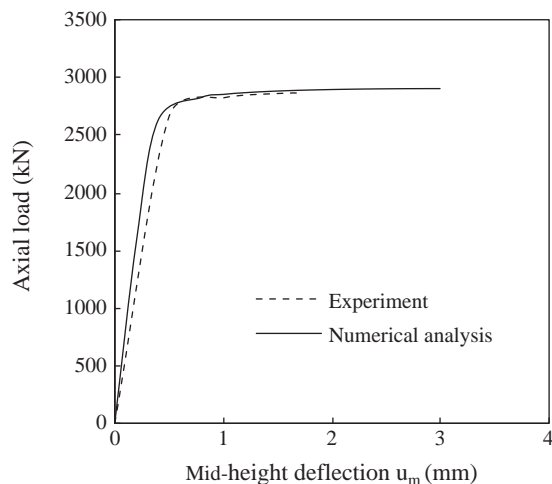

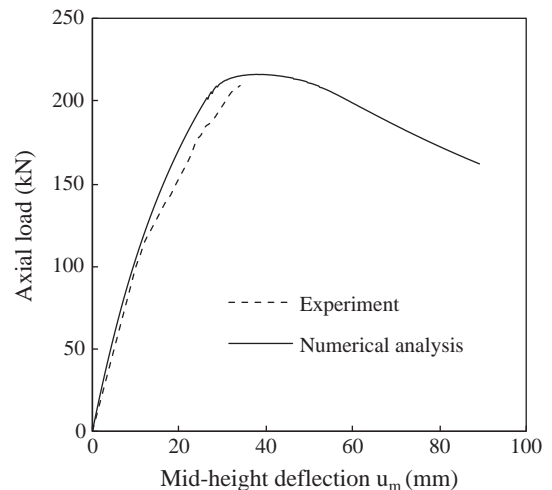**Fig. 1.** Comparison of predicted and experimental axial load–deflection curves for specimen SCH-2.

Fig. 2. Comparison of predicted and experimental axial load–deflection curves for specimen R5.
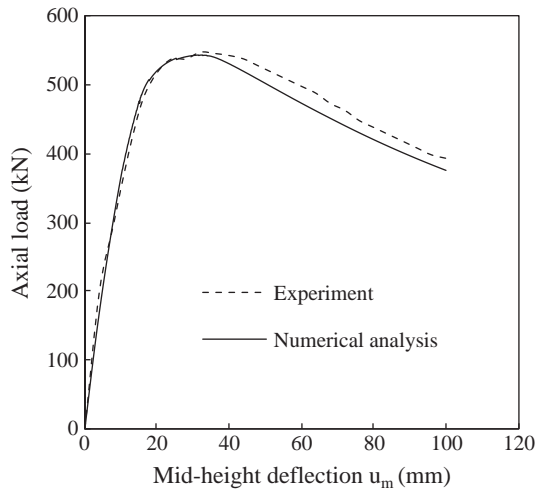
Fig. 3. Comparison of predicted and experimental axial load–deflection curves for specimen S3.

Fig. 5. Influence of local buckling on the axial load–moment interaction diagrams for thin-walled CFST slender beam-columns.

curves as shown in Fig. 9. The ultimate axial load of the slender beam-column is overestimated by 8.32% if local buckling was not considered.

Fig. 5 demonstrates the influences of local buckling on the axial load–moment interaction diagram for the CFST slender beam-column. As shown in Fig. 5, the ultimate axial strength was normalized by the ultimate axial load (P_{oa}) of the axially loaded slender column including local buckling effects, while the ultimate moment was normalized by the ultimate pure bending moment (M_o) of the slender beam-column with local buckling effects. It can be observed from Fig. 5 that local buckling considerably reduces the ultimate strength of the slender beam-column. If local buckling was not considered in the numerical analysis, the ultimate axial strength of the slender beam-column is overestimated by 5.02% while the maximum ultimate bending strength of the slender beam-column is overestimated by 7.49%.

3.2. Influences of column slenderness ratio

The numerical model developed was used to examine the effects of the column slenderness ratio (L/r) which is an important parameter that influences the behavior of CFST beam-columns. High strength thin-walled CFST slender beam-columns with a cross-section of 600×600 mm were considered. The depth-to-thickness ratio of the
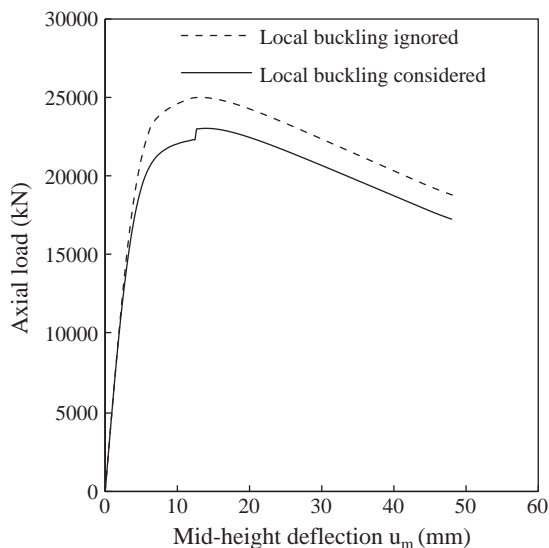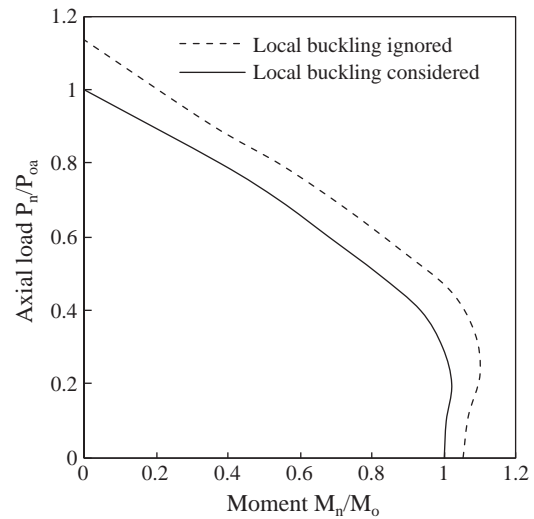
section was 50. Column slenderness ratios (L/r) of 22, 50, 65 and 80 were considered in the parametric study. The loading eccentricity ratio (e/D) of 0.1 was specified in the analysis of slender beam-columns with various L/r ratios. The initial geometric imperfection of $L/1500$ at the mid-height of the beam-columns was incorporated in the model. The beam-columns were made of high strength steel tubes with the yield and tensile strengths of 690 MPa and 790 MPa respectively. The Young's modulus of the steel tubes was 200 GPa. The steel tubes were filled with high strength concrete of 80 MPa.

Fig. 6 presents the axial load–deflection curves for the beam-columns with various slenderness ratios. It appears that the ultimate axial load is strongly affected by the column slenderness ratio. Increasing the column slenderness ratio significantly reduces its ultimate axial load. Columns with a smaller slenderness ratio are shown to be less ductile than the ones with a larger slenderness ratio. The mid-height deflection at the ultimate axial strength of the beam-columns increases with increasing the column slenderness ratio. Fig. 7 shows the ratio of the ultimate axial load (P_n) to the ultimate axial strength (P_{oa}) of the column's section under eccentric loading as a function of the column slenderness ratio. As

Fig. 4. Influence of local buckling on the axial load–deflection curves for thin-walled CFST slender beam-columns.
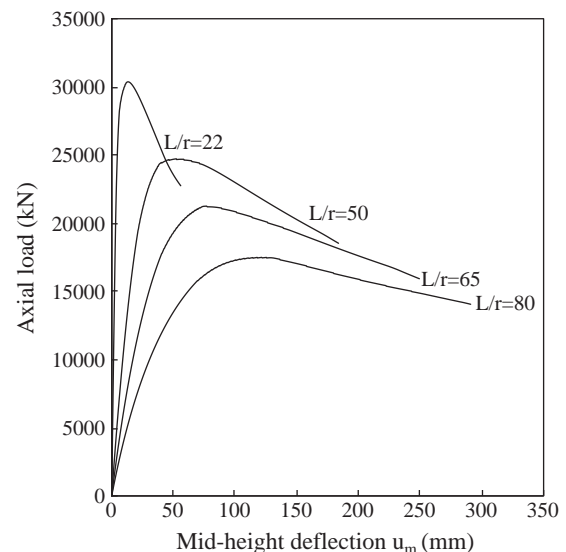

Fig. 6. Influence of column slenderness ratio on the axial load–deflection curves for thin-walled CFST slender beam-columns.

demonstrated in Fig. 7, the ultimate axial strength of the beam-column with a L/r ratio of 22 is 99% of the section's strength.

Fig. 8 demonstrates the effects of the column slenderness ratio on the axial load–moment strength interaction curves for CFST beam-columns. In Fig. 8, the ultimate axial strength (P_n) was normalized to the ultimate axial load (P_o) of the axially loaded beam-column section while the ultimate moment (M_n) was normalized to the ultimate pure bending moment (M_o) of the beam-column. The column slenderness ratio $L/r = 0$ was used in the axial load–moment interaction analysis to determine the ultimate strengths of the composite section. It can be seen from Fig. 8 that reducing the column L/r ratio enlarges the axial load–moment interaction diagram. The ultimate bending strength of the beam-column is shown to decrease as the column slenderness ratio increases.

3.3. Influences of depth-to-thickness ratio

Local buckling of a thin-walled steel tubes depends on its depth-to-thickness ratio (D/t). The numerical model was utilized to examine the effects of D/t ratio on the load–deflection and axial load–moment interaction curves for high strength CFST slender beam-columns. A square cross-section of 650×650 mm was considered in the analysis. The D/t ratios of the column sections were calculated as 40, 60, 80 and 100 by changing the thickness of the steel tubes. The column slenderness ratio (L/r) was 35. The loading eccentricity ratio (e/D) was taken as 0.1 in the analysis. The initial geometric imperfection of the beam-columns at mid-height was specified as $L/1500$. The yield and tensile strengths of the steel tubes were 690 MPa and 790 MPa respectively while the Young's modulus of the steel tubes was 200 GPa. The compressive strength of the in-filled concrete was 60 MPa.

The influences of D/t ratio on the axial load–deflection curves for high strength thin-walled CFST slender beam-columns are illustrated in Fig. 9. The figure shows that increasing the D/t ratio of the slender beam-columns slightly reduces their initial stiffness. However, increasing the D/t ratio significantly reduces the ultimate axial strength of eccentrically loaded CFST slender beam-columns. This is attributed to the fact that a column section with a larger D/t ratio has a lesser steel area and it may undergone local buckling which reduces the ultimate strength of the column.

Fig. 10 demonstrates the influence of D/t ratio on the axial load–moment interaction diagrams for high strength thin-walled CFST slender beam-columns. In each interaction curve, the axial load (P_n) was divided by the ultimate axial strength (P_{oa}) of the axially loaded slender beam-column, while the moment (M_n) was divided by the ultimate pure bending moment (M_o) of the beam-column. It can be
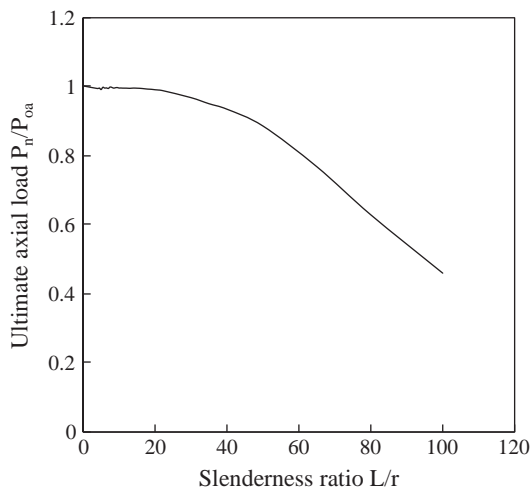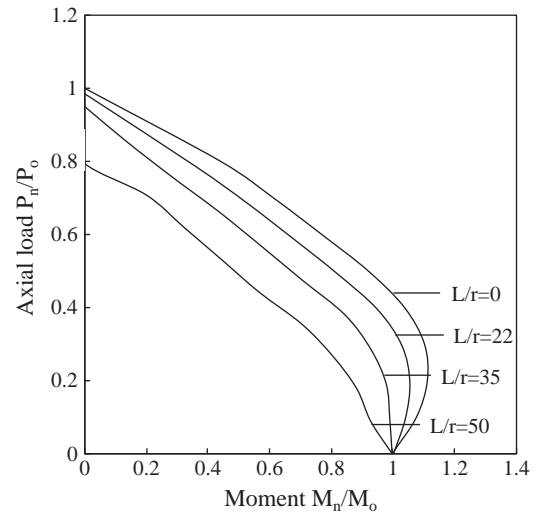

Fig. 8. Influence of column slenderness ratio on the axial load–moment interaction diagrams for thin-walled CFST slender beam-columns.

seen from Fig. 10 that decreasing the D/t ratio of the slender beam-column narrows the axial load–moment interaction diagram for the slender beam-column. In addition, the flexural strength at the maximum moment point is shown to increase remarkably with increasing the D/t ratio.

3.4. Influences of loading eccentricity ratio

The fundamental behavior of a rectangular CFST slender beam-column under axial load and uniaxial bending is influenced by the loading eccentricity ratio (e/D). To investigate this effect, a beam-column with a cross-section of 600×700 mm and loading eccentricity ranged from 0.1 to 0.2, 0.4 and 0.6 were analyzed using the numerical model. The depth-to-thickness ratio of the section was 60. The slenderness ratio (L/r) of the beam-column was 30. The initial geometric imperfection of the beam-column at the mid-height was assumed to be $L/1500$. The yield and tensile strengths of the steel tubes were 690 MPa and 790 MPa respectively. The beam-column was filled
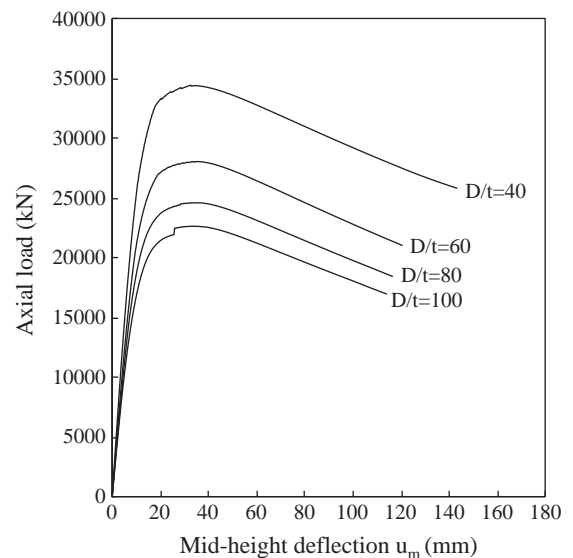

Fig. 7. Influence of column slenderness ratio on the ultimate axial loads of thin-walled CFST slender beam-columns.

Fig. 9. Influence of D/t ratio on the axial load–deflection curves for thin-walled CFST slender beam-columns.
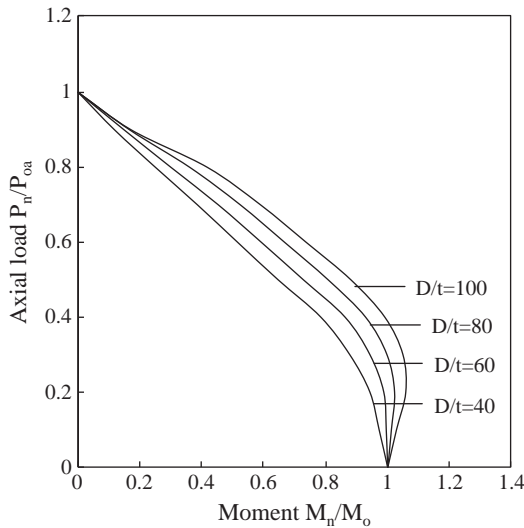
Fig. 10. Influence of D/t ratio on the axial load–moment interaction diagrams for thin-walled CFST slender beam-columns.

with high strength concrete of 90 MPa. The Young's modulus of 200 GPa was specified for the steel tubes in the analysis.

The computed axial load–deflection curves for high strength rectangular CFST slender beam-columns with different loading eccentricity ratios are presented in Fig. 11. It can be seen that the initial stiffness of the slender beam-columns decreases with an increase in the e/D ratio. In addition, increasing the e/D ratio significantly reduces the ultimate loads of the beam-columns. This is attributed to the fact that increasing the e/D ratio increases the bending moments at the column ends which significantly reduce the ultimate axial load of the slender beam-columns. Furthermore, the mid-height deflections at the maximum axial load of the slender beam-column increase with an increase in the eccentricity ratio. The displacement ductility of a slender beam-column is shown to be improved when increasing the eccentricity ratio. Fig. 12 shows that the ultimate axial load is a function of the loading eccentric ratio. The figure clearly shows that the effect of the loading eccentricity ratio on the ultimate axial strengths of CFST slender bean-columns is significant.
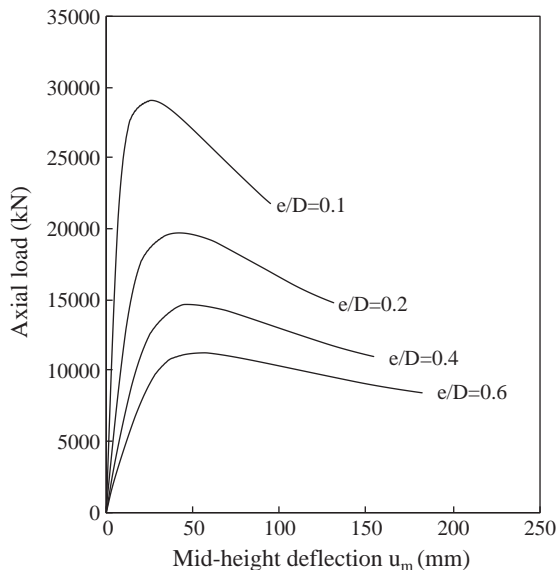
3.5. Influences of concrete compressive strengths

The effects of concrete compressive strengths on the strengths and behavior of high strength CFST slender beam-columns with local buckling effects were studied by the numerical model. In the parametric study, the concrete compressive strength was varied from 60 MPa to 100 MPa. The width and depth of the steel tube were 600 mm and 800 mm respectively. The steel tube wall was 10 mm thick so that its depth-to-thickness ratio (D/t) was 80. The slenderness ratio (L/r) of the beam-column was 32. The initial geometric imperfection of the beam-column at the mid-height was taken as $L/1500$. The loading eccentricity ratio (e/D) was 0.1. The steel yield and ultimate tensile strengths were 690 MPa and 790 MPa respectively and the Young's modulus of the steel tubes was 200 GPa.

The axial load–deflection curves for high strength rectangular CFST slender beam-columns with different concrete strengths are depicted in Fig. 13. It would appear from Fig. 13 that the ultimate axial strengths of rectangular CFST slender beam-columns increase significantly with an increase in the concrete compressive strength. Increasing the concrete compressive strength from 60 MPa to 80 MPa and 100 MPa increases the ultimate axial strength by18.13% and 35.84%, respectively. It can be seen from Fig. 13 that increasing the concrete compressive strength results in a slight increase in the initial stiffness of the slender beam-columns.

The normalized axial load–moment interaction diagrams for rectangular CFST slender beam-columns are given in Fig. 14. It can be observed that increasing the concrete compressive strength enlarges the P–M interaction curves. The ultimate bending moment of the slender beam-columns is found to increase considerably with increasing concrete compressive strength. By increasing the concrete compressive strength from 60 MPa to 80 MPa and 100 MPa, the ultimate bending moment of the column is increased by 7.23% and 13.87%, respectively. The ultimate pure bending strengths of rectangular CFST beam-columns are also found to increase with an increase in the compressive strength of the in-filled concrete.

3.6. Influences of steel yield strengths

Rectangular thin-walled CFST slender beam-columns with different steel yield strengths and a cross-section of 700×800 mm were analyzed using the numerical model. The depth-to-thickness (D/t) ratio of the section was 70. The yield strengths of the steel tubes were 500 MPa, 600 MPa and 690 MPa and the corresponding tensile strengths were 590 MPa, 690 MPa and 790 MPa, respectively. The

Fig. 11. Influence of loading eccentricity ratio on the axial load–deflection curves for thin-walled CFST slender beam-columns.
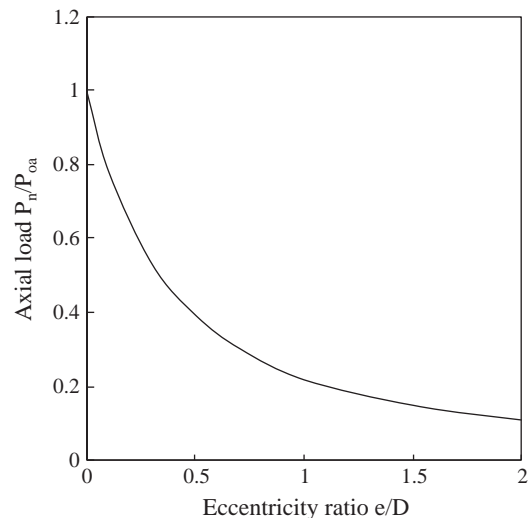

Fig. 12. Influence of loading eccentricity ratio on the ultimate axial loads of thin-walled CFST slender beam-columns.

Fig. 13. Influence of concrete compressive strengths on the axial load–deflection curves for thin-walled CFST slender beam-columns.

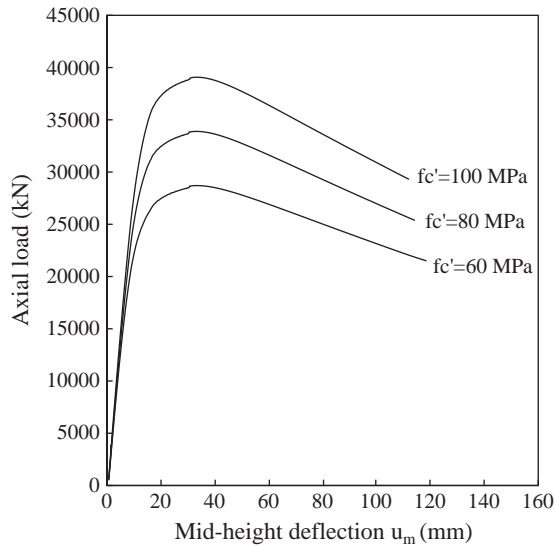**Fig. 15.** Influence of steel yield strengths on the axial load–deflection curves for thin-walled CFST slender beam-columns.

column slenderness ratio (L/r) of 45 was used in the parametric study with a loading eccentricity ratio (e/D) of 0.1. The initial geometric imperfection of the beam-column at the mid-height was taken as $L/1500$. The Young's modulus of steel was 200 GPa. The steel tubes were filled with 100 MPa concrete.

Fig. 15 illustrates the influences of steel yield strengths on the axial load–deflection curves for high strength rectangular CFST slender beam-columns. It can be observed from Fig. 15 that the steel yield strength does not have an effect on the initial stiffness of the beam-columns. However, the ultimate axial strength of slender beam-columns is found to increase significantly with an increase in the steel yield strength. By increasing the steel yield strength from 500 MPa to 600 MPa and 690 MPa, the ultimate axial load of the slender beam-column is found to increase by 4.92% and 8.95% respectively.

The normalized axial load–moment interaction diagrams for rectangular CFST beam-columns made of different strength steel tubes are presented in Fig. 16. The figure shows that the normalized axial load–moment interaction curve is enlarged by reducing the steel yield strength. In addition, the ultimate pure bending strength of the slender beam-column increases by 13.61% and 28.07%, when
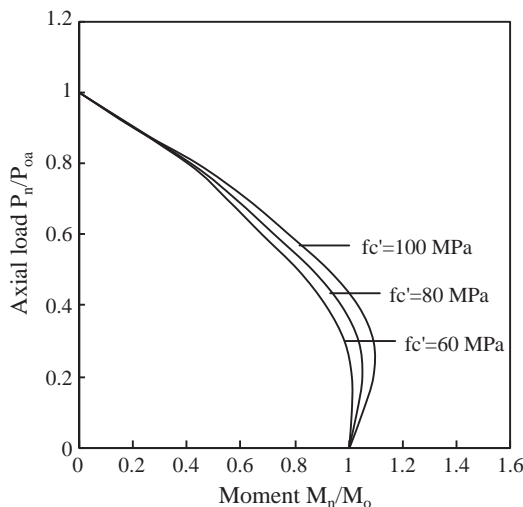
increasing the steel yield strength from 500 MPa to 600 MPa and 690 MPa, respectively. The ultimate pure bending strength of the slender beam-columns increases significantly with increasing the steel yield strength. When increasing the steel yield strength from 500 MPa to 600 MPa and 690 MPa, the maximum ultimate bending moment of the slender beam-columns is increased by 13.15% and 28.35% respectively.

4. Conclusions

The verification and applications of a numerical model developed for the nonlinear analysis of high strength thin-walled rectangular CFST slender beam-columns with local buckling effects have been presented in this paper. The numerical model was verified by comparisons of computational solutions with experimental results of normal and high strength CFST slender beam-columns presented by independent researchers. The numerical model can accurately predict the axial load–deflection responses and strength envelopes of thin-walled CFST slender beam-columns. This paper has provided new benchmark numerical results on the behavior of full-scale high strength thin-walled steel slender tubes filled with high strength concrete with various parameters including the effects of local buckling,

Fig. 14. Influence of concrete compressive strengths on the axial load–moment interaction diagrams for thin-walled CFST slender beam-columns.
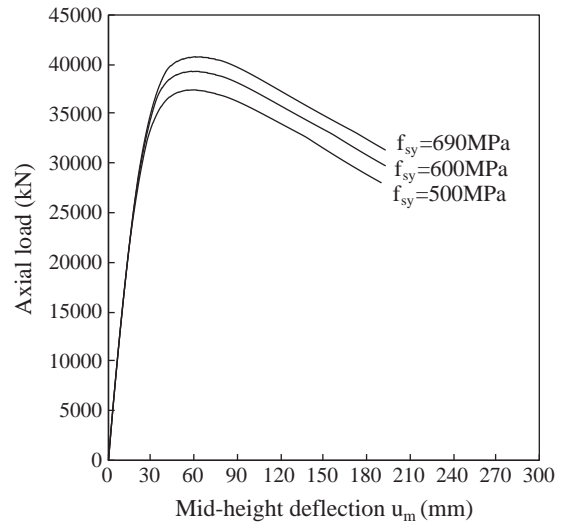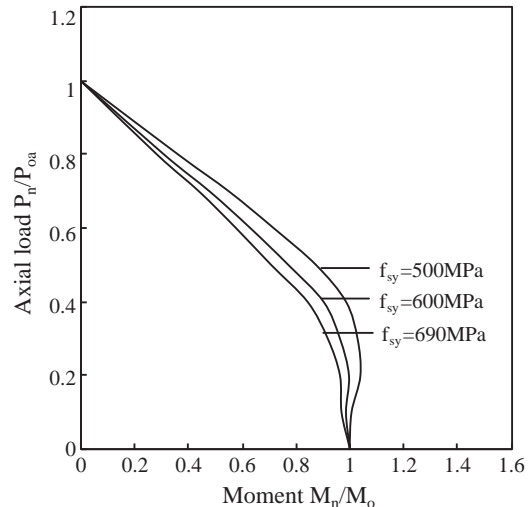

Fig. 16. Influence of steel yield strengths on the axial load–moment interaction diagrams for thin-walled CFST slender beam-columns.

column slenderness ratio, depth-to-thickness ratio, loading eccentricity ratio, concrete compressive strengths and steel yield strengths. The numerical results presented can be used to validate other non-linear analysis techniques and to develop composite design codes for high strength thin-walled rectangular CFST slender beam-columns. The numerical model can be used to analyze and design thin-walled CFST slender columns in practice.

References

[1] EN 1994-1-1. Eurocode 4: design of composite steel and concrete structures. Part 1-1, general rules and rules for buildings. CEN; 2004.

[2] LRFD. Load and resistance factor design specification for steel buildings. American Institution of Steel Construction; 1999.

[3] ACI-318. Building Code Requirements for Reinforced Concrete. Detroit (MI): ACI; 2005.

[4] Bridge RQ. Concrete filled steel tubular columns. School of Civil Engineering, The University of Sydney, Sydney, Australia; 1976. Research Report No. R 283.

[5] Shakir-Khalil H, Zeghiche J. Experimental behaviour of concrete-filled rolled rectangular hollow-section columns. The Structural Engineer 1989;67(3):346–53.

[6] Matsui C, Tsuda K, Ishibashi Y. Slender concrete filled steel tubular columns under combined compression and bending. Proceedings of the 4th Pacific Structural Steel Conference, Singapore, Pergamon, 3(10); 1995. p. 29–36.

[7] Chung J, Tsuda K, Matsui C. High-strength concrete filled square tube columns subjected to axial loading. The Seventh East Asia-Pacific Conference on Structural Engineering & Construction, Kochi, Japan, Vol. 2; 1999. p. 955–60.

[8] Zhang S, Guo L, Tian H. Eccentrically loaded high strength concrete-filled square steel tubes. Proceedings of the International Conference on Advances in Structures, Sydney, Australia, Vol. 2; 2003. p. 987–93.

[9] Han LH. Flexural behaviour of concrete-filled steel tubes. J Constr Steel Res 2004;60(2):313–37.

[10] Vrcelj Z, Uy B. Behaviour and design of steel square hollow sections filled with high strength concrete. Aust J Struct Eng 2002;3(3):153–70.

[11] Varma AH, Ricles JM, Sause R, Lu LW. Seismic behavior and modeling of high-strength composite concrete-filled steel tube (CFT) beam-columns. J Constr Steel Res 2002;58: 725–58.

[12] Giakoumelis G, Lam D. Axial capacity of circular concrete-filled tube columns. J Constr Steel Res 2004;60(7):1049–68.

[13] Lakshmi B, Shanmugam NE. Nonlinear analysis of in-filled steel-concrete composite columns. J Struct Eng, ASCE 2002;128(7):922–33.

[14] Ellobody E, Young B. Nonlinear analysis of concrete-filled steel SHS and RHS columns. Thin Walled Struct 2006;44(6):919–30.

[15] Liang QQ. Performance-based analysis of concrete-filled steel tubular beam-columns, part I: theory and algorithms. J Constr Steel Res 2009;65(2):363–72.

[16] Liang QQ. Performance-based analysis of concrete-filled steel tubular beam-columns, part II: verification and applications. J Constr Steel Res 2009;65(2):351–62.

[17] Liang QQ. High strength circular concrete-filled steel tubular slender beam-columns, part I: numerical analysis. J Constr Steel Res 2011;67(2):164–71.

[18] Liang QQ. High strength circular concrete-filled steel tubular slender beam-columns, part II: fundamental behavior. J Constr Steel Res 2011;67(2):172–80.

[19] Patel VI, Liang QQ, Hadi MNS. High strength thin-walled rectangular concrete-filled steel tubular slender beam-columns, part I: modeling. J Constr Steel Res 2012;70(C):377–84.

[20] Liang QQ, Uy B, Liew JYR. Local buckling of steel plates in concrete-filled thin-walled steel tubular beam-columns. J Constr Steel Res 2007;63(3):396–405.

3.6 CONCLUDING REMARKS

This chapter has presented a numerical model for thin-walled high strength rectangular CFST slender beam-columns under axial load and uniaxial bending. The effects of local buckling of steel tube walls under stress gradients, initial geometric imperfection and second order were considered in the numerical model. Performance indices have been proposed for evaluating the performance of thin-walled CFST slender beam-columns. Efficient Müller's method algorithms were developed and implemented in the computer program. These algorithms were used to iterate the neutral axis depth in the composite cross-section and to adjust the curvature at the column ends in the slender beam-column to satisfy equilibrium conditions. The analysis procedures have been presented.

It has been shown that the proposed numerical model can accurately predict the structural performance of CFST slender beam-columns. The numerical model developed was employed to investigate the effects of local buckling, depth-to-thickness ratios, loading eccentricity ratios, column slenderness ratios, concrete compressive strengths and steel yield strengths on the axial load-deflection curves and axial load-moment interaction diagrams for CFST beam-columns. Parametric studies indicated that increasing depth-to-thickness ratios reduces the ultimate axial strength of thin-walled CFST beam-columns but enlarges the normalized axial load-moment interaction diagrams. Increasing the concrete compressive strengths increases the ultimate axial strength of thin-walled CFST beam-columns and enlarges the normalized axial load-moment interaction diagrams but reduces steel contribution ratio and strength reduction factor.

Chapter 4

RECTANGULAR CFST SLENDER BEAM-COLUMNS UNDER AXIAL LOAD AND BIAXIAL BENDING

4.1 INTRODUCTION

This chapter presents a multiscale numerical model for simulating the structural behavior of high strength thin-walled rectangular CFST slender beam-columns under axial load and biaxial bending. The numerical model incorporates progressive local buckling, initial geometric imperfections, high strength materials and second order effects. The numerical model is validated against the test results available in the published literature. Steel and concrete contribution ratios and strength reduction factor are used to evaluate the performance of CFST slender beam-columns. Parametric studies using the numerical model are performed to investigate the effects of depth-to-

thickness ratios, loading eccentricity ratios, column slenderness ratios, concrete compressive strengths and steel yield strengths on the performance of thin-walled CFST slender beam-columns.

This chapter includes the following papers:

[1] Liang, Q. Q., Patel, V. I. and Hadi, M. N. S., "Biaxially loaded high-strength concrete-filled steel tubular slender beam-columns, Part I: Multiscale simulation", *Journal of Constructional Steel Research*, 2012, 75, 64-71.

[2] Patel, V. I., Liang, Q. Q. and Hadi, M. N. S., "Biaxially loaded high-strength concrete-filled steel tubular slender beam-columns, Part II: Parametric study", *Journal of Constructional Steel Research*, 2011 (submitted).

VICTORIA UNIVERSITY
MELBOURNE AUSTRALIA

PART B:

DECLARATION OF CO-AUTHORSHIP AND CO-CONTRIBUTION: PAPERS INCORPORATED IN THESIS BY PUBLICATION

This declaration is to be completed for each conjointly authored publication and placed at the beginning of the thesis chapter in which the publication appears.

Declaration by [candidate name]:	Signature:	Date:
VIPULKUMAR ISHVARBHAI PATEL	███████	11/01/2013

Paper Title:

Biaxially loaded high-strength concrete-filled steel tubular slender beam-columns, Part I: Multiscale simulation

In the case of the above publication, the following authors contributed to the work as follows:

Name	Contribution%	Nature of contribution
Vipulkumar Ishvarbhai Patel	55	Literature review Developed the numerical model Provided revision of the article Final approval of the manuscript
Qing Quan Liang	35	Initial concept Writing of the manuscript Manuscript submission
Muhammad N.S.Hadi	10	Provided critical revision of the article Final approval of the manuscript

VICTORIA UNIVERSITY
MELBOURNE AUSTRALIA

DECLARATION BY CO-AUTHORS

The undersigned certify that:

1. They meet criteria for authorship in that they have participated in the conception, execution or interpretation of at least that part of the publication in their field of expertise;

2. They take public responsibility for their part of the publication, except for the responsible author who accepts overall responsibility for the publication;

3. There are no other authors of the publication according to these criteria;

4. Potential conflicts of interest have been disclosed to **a)** granting bodies, **b)** the editor or publisher of journals or other publications, and **c)** the head of the responsible academic unit; and

5. The original data is stored at the following location(s):

Location(s): College of Engineering and Science, Victoria University, Melbourne, Victoria, Australia.

and will be held for at least five years from the date indicated below:

		Date
Signature 1		11/01/2013
Signature 2		11/01/2013
Signature 3		11/01/2013
Signature 4		

VICTORIA UNIVERSITY
M E L B O U R N E   A U S T R A L I A

PART B:

DECLARATION OF CO-AUTHORSHIP AND CO-CONTRIBUTION: PAPERS INCORPORATED IN THESIS BY PUBLICATION

This declaration is to be completed for each conjointly authored publication and placed at the beginning of the thesis chapter in which the publication appears.

| **Declaration by [candidate name]:** | **Signature:** | **Date:** |
| VIPULKUMAR ISHVARBHAI PATEL | | 11/01/2013 |

Paper Title:

Biaxially loaded high-strength concrete-filled steel tubular slender beam-columns, Part II: Parametric study

In the case of the above publication, the following authors contributed to the work as follows:

Name	Contribution%	Nature of contribution
Vipulkumar Ishvarbhai Patel	60	Literature review Verified the numerical model Carried out the parametric study Wrote the manuscript
Qing Quan Liang	30	Initial concept Provided critical revision of the article Manuscript submission
Muhammad N.S.Hadi	10	Provided critical revision of the article Final approval of the manuscript

VICTORIA UNIVERSITY
MELBOURNE AUSTRALIA

DECLARATION BY CO-AUTHORS

The undersigned certify that:

1. They meet criteria for authorship in that they have participated in the conception, execution or interpretation of at least that part of the publication in their field of expertise;

2. They take public responsibility for their part of the publication, except for the responsible author who accepts overall responsibility for the publication;

3. There are no other authors of the publication according to these criteria;

4. Potential conflicts of interest have been disclosed to **a)** granting bodies, **b)** the editor or publisher of journals or other publications, and **c)** the head of the responsible academic unit; and

5. The original data is stored at the following location(s):

Location(s): College of Engineering and Science, Victoria University, Melbourne, Victoria, Australia.

and will be held for at least five years from the date indicated below:

		Date
Signature 1		11/01/2013
Signature 2		11/01/2013
Signature 3		11/01/2013
Signature 4		

Biaxially loaded high-strength concrete-filled steel tubular slender beam-columns, Part I: Multiscale simulation

Qing Quan Liang [a],[*], Vipulkumar Ishvarbhai Patel [a], Muhammad N.S. Hadi [b]

[a] School of Engineering and Science, Victoria University, PO Box 14428, Melbourne, VIC 8001, Australia
[b] School of Civil, Mining and Environmental Engineering, University of Wollongong, Wollongong, NSW 2522, Australia

ABSTRACT

The steel tube walls of a biaxially loaded thin-walled rectangular concrete-filled steel tubular (CFST) slender beam-column may be subjected to compressive stress gradients. Local buckling of the steel tube walls under stress gradients, which significantly reduces the stiffness and strength of a CFST beam-column, needs to be considered in the inelastic analysis of the slender beam-column. Existing numerical models that do not consider local buckling effects may overestimate the ultimate strengths of thin-walled CFST slender beam-columns under biaxial loads. This paper presents a new multiscale numerical model for simulating the structural performance of biaxially loaded high-strength rectangular CFST slender beam-columns accounting for progressive local buckling, initial geometric imperfections, high strength materials and second order effects. The inelastic behavior of column cross-sections is modeled at the mesoscale level using the accurate fiber element method. Macroscale models are developed to simulate the load-deflection responses and strength envelopes of thin-walled CFST slender beam-columns. New computational algorithms based on the Müller's method are developed to iteratively adjust the depth and orientation of the neutral axis and the curvature at the column's ends to obtain nonlinear solutions. Steel and concrete contribution ratios and strength reduction factor are proposed for evaluating the performance of CFST slender beam-columns. Computational algorithms developed are shown to be an accurate and efficient computer simulation and design tool for biaxially loaded high-strength thin-walled CFST slender beam-columns. The verification of the multiscale numerical model and parametric study are presented in a companion paper.

© 2012 Elsevier Ltd. All rights reserved.

1. Introduction

High strength thin-walled rectangular concrete-filled steel tubular (CFST) slender beam-columns in composite frames may be subjected to axial load and biaxial bending. Biaxially loaded thin-walled CFST slender beam-columns with large depth-to-thickness ratios are vulnerable to local and global buckling. No numerical models have been developed for the multiscale inelastic stability analysis of biaxially loaded high strength thin-walled CFST slender beam-columns accounting for the effects of progressive local buckling of the steel tube walls under stress gradients. The difficulty is caused by the interaction between local and global buckling and biaxial bending. However, it is important to accurately predict the ultimate strength of a thin-walled CFST slender beam-column under biaxial loads because this strength is needed in the practical design. This paper addresses the important issue of multiscale simulation of high strength thin-walled rectangular CFST slender beam-columns under combined axial load and biaxial bending.

Extensive experimental investigations have been undertaken to determine the ultimate strengths of short and slender CFST columns under axial load or combined axial load and uniaxial bending [1–9]. Test results indicated that the confinement provided by the rectangular steel tube had little effect on the compressive strength of the concrete core but considerably improved its ductility. In addition, local buckling of the steel tubes was found to remarkably reduce the ultimate strength and stiffness of thin-walled CFST short columns as reported by Ge and Usami [10], Bridge and O'Shea [11], Uy [12] and Han [13]. As a result, the ultimate strengths of rectangular CFST short columns can be determined by summation of the capacities of the steel tube and concrete core, providing that local buckling effects are taken into account as shown by Liang et al. [14]. Moreover, experimental results demonstrated that the confinement effect significantly increased the compressive strength and ductility of the concrete core in circular CFST short columns. However, this confinement effect was found to reduce with increasing the column slenderness as illustrated by Knowles and Park [2] and Liang [15]. In comparisons with researches on CFST columns under axial load and uniaxial bending, experimental investigations on biaxially loaded rectangular thin-walled CFST slender beam-columns have received little attention [16–18].

Although the performance of CFST columns could be determined by experiments, they are highly expensive and time consuming. To overcome this limitation, nonlinear analysis techniques have been developed by researchers for composite columns under axial load or combined axial load and uniaxial bending [19–23]. However, only a few numerical models have been developed to predict the nonlinear inelastic behavior of slender composite columns under biaxial bending. El-Tawil et al. [24] and El-Tawil and Deierlein [25] proposed a fiber element model for determining the inelastic moment-curvature responses and strength envelopes of concrete-encased composite columns under biaxial bending. The fiber model, which accounted for concrete conferment effects and initial stresses caused by preloads, was used to investigate the strength and ductility of concrete-encased composite columns. A fiber element model was also developed by Muñoz and Hsu [26] that was capable of simulating the behavior of biaxially loaded concrete-encased slender composite columns. The relationship between the curvature and deflection was established by using the finite different method. The incremental deflection approach was employed to capture the post-peak behavior of slender concrete-encased composite columns.

Lakshmi and Shanmugam [27] presented a semi-analytical model for predicting the ultimate strengths of CFST slender beam-columns under biaxial bending. An incremental-iterative numerical scheme based on the generalized displacement control method was employed in the model to solve nonlinear equilibrium equations. Extensive comparisons of computer solutions with test results were made to examine the accuracy of the semi-analytical model. However, the effects of local buckling and concrete tensile strength were not taken into account in the semi-analytical model that may overestimate the ultimate strengths of thin-walled rectangular CFST columns with large depth-to-thickness ratios. Recently, Liang [28,29] developed a numerical model based on the fiber element method for simulating the inelastic load-strain and moment-curvature responses and strength envelopes of thin-walled CFST short beam-columns under axial load and biaxial bending. The effects of local buckling were taken into account in the numerical model by using effective width formulas proposed by Liang et al. [14]. Secant method algorithms were developed to obtain nonlinear solutions. Liang [29] reported that the numerical model was shown to be an accurate and efficient computer simulation tool for biaxially loaded thin-walled normal and high strength CFST short columns with large depth-to-thickness ratios.

This paper extends the numerical models developed by Liang [21,28] and Patel et al. [22,23] to biaxially loaded high-strength rectangular CFST slender beam-columns with large depth-to-thickness ratios. The mesoscale model is described that determines the inelastic behavior of column cross-sections incorporating progressive local buckling. Macroscale models are established for simulating the load-deflection responses and strength envelopes of slender beam-columns under biaxial bending. New computational algorithms based on the Müller's method are developed to obtain nonlinear solutions. Steel and concrete contribution ratios and strength reduction factor are proposed for CFST slender beam-columns. The verification of the numerical model developed and its applications are given in a companion paper [30].

2. Mesoscale simulation

2.1. Fiber element model

The mesoscale model is developed by utilizing the accurate fiber element method [28] to simulate the inelastic behavior of composite cross-sections under combined axial load and biaxial bending. The rectangular CFST beam-column section is discretized into fine fiber elements as depicted in Fig. 1. Each fiber element can be assigned either steel or concrete material properties. Fiber stresses are calculated from fiber strains using the material uniaxial stress–strain relationships.
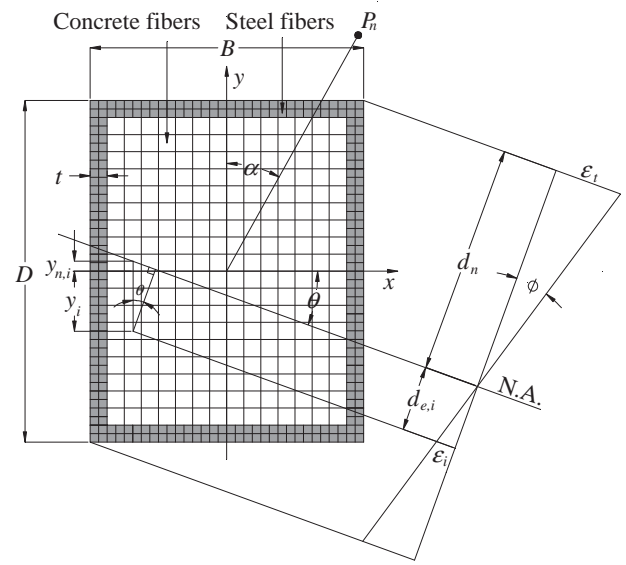

Fig. 1. Fiber element discretization and strain distribution of CFST beam-column section.

2.2. Fiber strains in biaxial bending

It is assumed that plane section remains plane under deformation. This results in a linear strain distribution throughout the depth of the section. In the numerical model, the compressive strain is taken as positive while the tensile strain is taken as negative. Fiber strains in biaxial bending depend on the depth (d_n) and orientation (θ) of the neutral axis of the section as illustrated in Fig. 1. For $0°\leq\theta<90°$, concrete and steel fiber strains can be calculated by the following equations proposed by Laing [28]:

$$y_{n,i} = \left|x_i - \frac{B}{2}\right|\tan\theta + \left(\frac{D}{2} - \frac{d_n}{\cos\theta}\right) \tag{1}$$

$$\varepsilon_i = \begin{cases} \phi|y_i - y_{n,i}|\cos\theta & \text{for } y_i \geq y_{n,i} \\ -\phi|y_i - y_{n,i}|\cos\theta & \text{for } y_i < y_{n,i} \end{cases} \tag{2}$$

in which B and D are the width and depth of the rectangular column section respectively, x_i and y_i are the coordinates of fiber i and ε_i is the strain at the ith fiber element and $y_{n,i}$ is the distance from the centroid of each fiber to the neutral axis.

When $\theta = 90°$, the beam-column is subjected to uniaxial bending and fiber strains can be calculated by the following equations given by Liang [28]:

$$\varepsilon_i = \begin{cases} \phi\left|x_i - \left(\frac{B}{2} - d_n\right)\right| & \text{for } x_i \geq x_{n,i} \\ -\phi\left|x_i - \left(\frac{B}{2} - d_n\right)\right| & \text{for } x_i < x_{n,i} \end{cases} \tag{3}$$

where $x_{n,i}$ is the distance from the centroid of each fiber element to the neutral axis.

2.3. Stresses in concrete fibers

Stresses in concrete fibers are calculated from the uniaxial stress–strain relationship of concrete. A general stress–strain curve for concrete in rectangular CFST columns is shown in Fig. 2. The stress–strain curve accounts for the effect of confinement provided by the steel tube, which improves the ductility of the concrete core in a rectangular
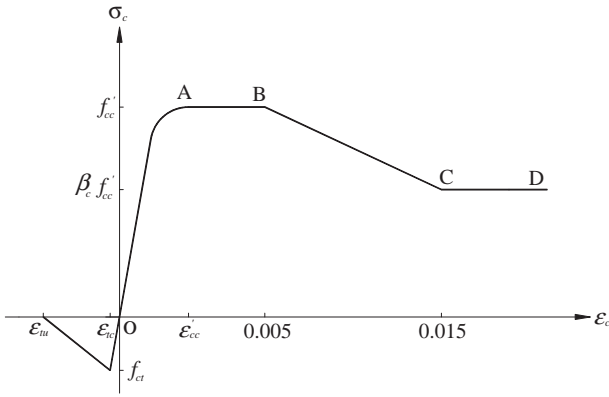
Fig. 2. Stress–strain curve for confined concrete in rectangular CFST columns.

CFST column. The concrete stress from O to A in the stress–strain curve is calculated based on the equations given by Mander et al. [31] as:

$$\sigma_c = \frac{f'_{cc}\lambda\left(\frac{\varepsilon_c}{\varepsilon'_{cc}}\right)}{\lambda-1+\left(\frac{\varepsilon_c}{\varepsilon'_{cc}}\right)^{\lambda}} \tag{4}$$

$$\lambda = \frac{E_c}{E_c - \left(\frac{f'_{cc}}{\varepsilon'_{cc}}\right)} \tag{5}$$

$$E_c = 3320\sqrt{f'_c} + 6900 \text{(MPa)} \tag{6}$$

in which σ_c stands for the compressive concrete stress, f'_{cc} represents the effective compressive strength of concrete, ε_c denotes the compressive concrete strain, ε'_{cc} is the strain at f'_{cc} and is between 0.002 and 0.003 depending on the effective compressive strength of concrete [28]. The Young's modulus of concrete E_c was given by ACI [32]. The effective compressive strength of concrete f'_{cc} is taken as $\gamma_c f'_c$, where γ_c is the strength reduction factor proposed by Liang [28] to account for the column size effect and is expressed by

$$\gamma_c = 1.85 D_c^{-0.135} \quad (0.85 \le \gamma_c \le 1.0) \tag{7}$$

where D_c is taken as the larger of $(B-2t)$ and $(D-2t)$ for a rectangular cross-section, and t is the thickness of the steel tube wall as shown in Fig. 1.

The parts AB, BC and CD of the stress–strain curve for concrete shown in Fig. 2 are defined by the following equations proposed by Liang [28]:

$$\sigma_c = \begin{cases} f'_{cc} & \text{for } \varepsilon'_{cc} < \varepsilon_c \le 0.005 \\ \beta_c f'_{cc} + 100(0.015-\varepsilon_c)(f'_{cc}-\beta_c f'_{cc}) & \text{for } 0.005 < \varepsilon_c \le 0.015 \\ \beta_c f'_{cc} & \text{for } \varepsilon_c > 0.015 \end{cases} \tag{8}$$

where β_c was proposed by Liang [28] based on experimental results provided by Tomii and Sakino [33] to account for confinement effects on the post-peak behavior and is given by

$$\beta_c = \begin{cases} 1.0 & \text{for } \frac{B_s}{t} \le 24 \\ 1.5 - \frac{1}{48}\frac{B_s}{t} & \text{for } 24 < \frac{B_s}{t} \le 48 \\ 0.5 & \text{for } \frac{B_s}{t} > 48 \end{cases} \tag{9}$$

where B_s is taken as the larger of B and D for a rectangular cross-section.

The stress–strain curve for concrete in tension is shown in Fig. 2. The constitutive model assumes that the concrete tensile stress increases linearly with the tensile strain up to concrete cracking. After

concrete cracking, the tensile stress of concrete decreases linearly to zero as the concrete softens. The concrete tensile stress is considered to be zero at the ultimate tensile strain which is taken as 10 times of the strain at concrete cracking. The tensile strength of concrete is taken as $0.6\sqrt{f'_{cc}}$.

2.4. Stresses in steel fibers

Stresses in steel fibers are calculated from uniaxial stress–strain relationship of steel material. Steel tubes used in CFST cross-sections are normally made from three types of structural steels such as high strength structural steels, cold-formed steels and mild structural steels, which are considered in the numerical model. Fig. 3 shows the stress–strain relationship for three types of steels. The steel material generally follows the same stress–strain relationship under the compression and tension. The rounded part of the stress–strain curve can be defined by the equation proposed by Liang [28]. The hardening strain ε_{st} is assumed to be 0.005 for high strength and cold-formed steels and $10\varepsilon_{sy}$ for mild structure steels in the numerical model. The ultimate strain ε_{su} is taken as 0.2 for steels.

2.5. Initial local buckling

Local buckling significantly reduces the strength and stiffness of thin-walled CFST beam-columns with large depth-to-thickness ratios. Therefore, it is important to account for local buckling effects in the inelastic analysis of high strength CFST slender beam-columns. However, most of existing numerical models for thin-walled CFST beam-columns have not considered local buckling effects. This may be attributed to the complexity of the local instability problem as addressed by Liang et al. [14]. The steel tube walls of a CFST column under axial load and biaxial bending may be subjected to compressive stress gradients as depicted in Fig. 4. Due to the presence of initial geometric imperfections, no bifurcation point can be observed on the load-deflection curves for real thin steel plates. The classical elastic local buckling theory [34] cannot be used to determine the initial local buckling stress of real steel plates with imperfections. Liang et al. [14] proposed formulas for estimating the initial local buckling stresses of thin steel plates under stress gradients by considering the effects of geometric imperfections and residual stresses. Their formulas are incorporated in the numerical model to account for initial local buckling of biaxially loaded CFST beam-columns with large depth-to-thickness ratios.

2.6. Post-local buckling

The effective width concept is commonly used to describe the post-local buckling behavior of a thin steel plate as illustrated in
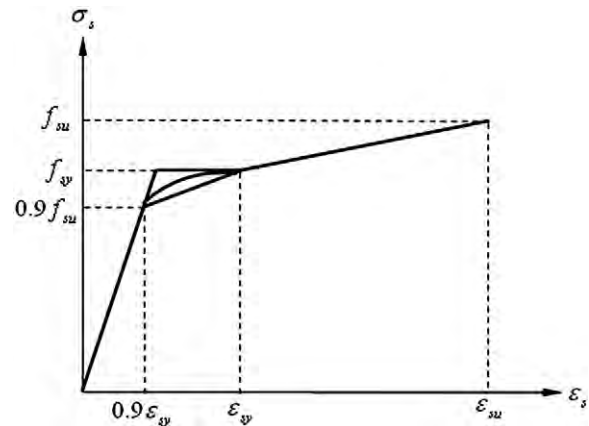

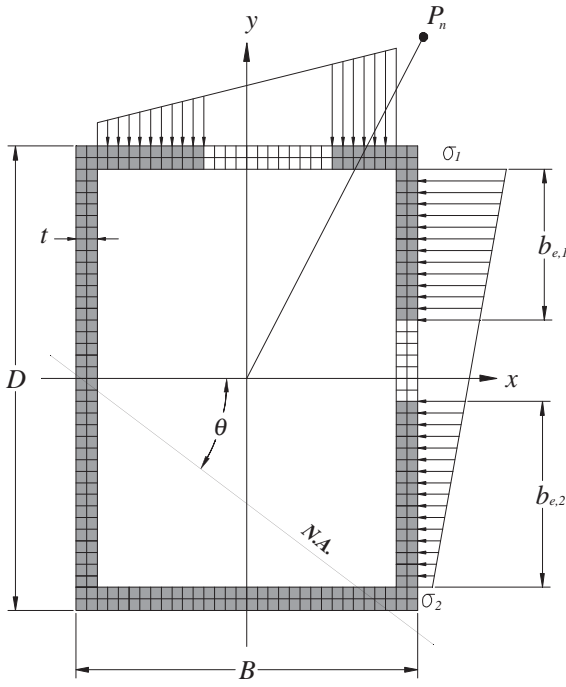**Fig. 3.** Stress–strain curves for structural steels.

113

Fig. 4. Effective and ineffective areas of steel tubular cross-section under axial load and biaxial bending.

Fig. 4. Liang et al. [14] proposed effective width and strength formulas for determining the post-local buckling strengths of the steel tube walls of thin-walled CFST beam-columns under axial load and biaxial bending. Their formulas are incorporated in the numerical model to account for the post-local buckling effects of the steel tube walls under compressive stress gradients. The effective widths b_{e1} and b_{e2} of a steel plate under stress gradients as shown in Fig. 4 are given by Liang et al. [14] as

$$\frac{b_{e1}}{b} = \begin{cases} 0.2777 + 0.01019\left(\frac{b}{t}\right) - 1.972\times10^{-4}\left(\frac{b}{t}\right)^2 + 9.605\times10^{-7}\left(\frac{b}{t}\right)^3 & \text{for } \alpha_s > 0.0 \\ 0.4186 - 0.002047\left(\frac{b}{t}\right) + 5.355\times10^{-5}\left(\frac{b}{t}\right)^2 - 4.685\times10^{-7}\left(\frac{b}{t}\right)^3 & \text{for } \alpha_s = 0.0 \end{cases}$$

(10)

$$\frac{b_{e2}}{b} = (2-\alpha_s)\frac{b_{e1}}{b}$$

(11)

in which b is the clear width of a steel flange or web of a CFST column section, and the stress gradient coefficient $\alpha_s = \sigma_2/\sigma_1$, where σ_2 is the minimum edge stress acting on the plate and σ_1 is the maximum edge stress acting on the plate.

Liang et al. [14] suggested that the effective width of a steel plate in the nonlinear analysis can be calculated based on the maximum stress level within the steel plate using the linear interpolation method. The effective width concept implies that a steel plate attains its ultimate strength when the maximum edge stress acting on the plate reaches its yield strength. Stresses in steel fiber elements within the ineffective areas as shown in Fig. 4 are taken as zero after the maximum edge stress σ_1 reaches the initial local buckling stress σ_{1c} for a steel plate with a b/t ratio greater than 30. If the total effective width of a plate ($b_{e1} + b_{e2}$) is greater than its width (b), the effective strength formulas proposed by Liang et al. [14] are employed in the numerical model to determine the ultimate strength of the tube walls.

2.7. Stress resultants

The internal axial force and bending moments acting on a CFST beam-column section under axial load and biaxial bending are determined as stress resultants in the section as follows:

$$P = \sum_{i=1}^{ns} \sigma_{s,i} A_{s,i} + \sum_{j=1}^{nc} \sigma_{c,j} A_{c,j}$$

(12)

$$M_x = \sum_{i=1}^{ns} \sigma_{s,i} A_{s,i} y_i + \sum_{j=1}^{nc} \sigma_{c,j} A_{c,j} y_j$$

(13)

$$M_y = \sum_{i=1}^{ns} \sigma_{s,i} A_{s,i} x_i + \sum_{j=1}^{nc} \sigma_{c,j} A_{c,j} x_j$$

(14)

in which P stands for the axial force, M_x and M_y are the bending moments about the x and y axes, $\sigma_{s,i}$ denotes the stress of steel fiber i, $A_{s,i}$ represents the area of steel fiber i, $\sigma_{c,j}$ is the stress of concrete fiber j, $A_{c,j}$ is the area of concrete fiber j, x_i and y_i are the coordinates of steel element i, x_j and y_j stand for the coordinates of concrete element j, ns is the total number of steel fiber elements and nc is the total number of concrete fiber elements.

2.8. Inelastic moment-curvature responses

The inelastic moment-curvature responses of a CFST beam-column section can be obtained by incrementally increasing the curvature and solving for the corresponding moment value for a given axial load (P_n) applied at a fixed load angle (α). For each curvature increment, the depth of the neutral axis is iteratively adjusted for an initial orientation of the neutral axis (θ) until the force equilibrium condition is satisfied. The moments of M_x and M_y are then computed and the equilibrium condition of $\tan \alpha = M_y/M_x$ is checked. If this condition is not satisfied, the orientation of the neutral axis is adjusted and the above process is repeated until both equilibrium conditions are met. The effects of local buckling are taken into account in the calculation of the stress resultants. The depth and orientation of the neutral axis of the section can be adjusted by using the secant method algorithms developed by Liang [28] or the Müller's method [35] algorithms which are discussed in Section 4. A detailed computational procedure for predicting the inelastic moment-curvature responses of composite sections was given by Liang [28].

3. Macroscale simulation

3.1. Macroscale model for simulating load-deflection responses

The pin-ended beam-column model is schematically depicted in Fig. 5. It is assumed that the deflected shape of the slender beam-column is part of a sine wave. The lateral deflection of the beam-column can be described by the following displacement function:

$$u = u_m \sin\left(\frac{\pi z}{L}\right)$$

(15)

where L stands for the effective length of the beam-column and u_m is the lateral deflection at the mid-height of the beam-column.

The curvature at the mid-height of the beam-column can be obtained as

$$\phi_m = \left(\frac{\pi}{L}\right)^2 u_m$$

(16)

For a beam-column subjected to an axial load at an eccentricity of e as depicted in Fig. 5 and an initial geometric imperfection u_o at the
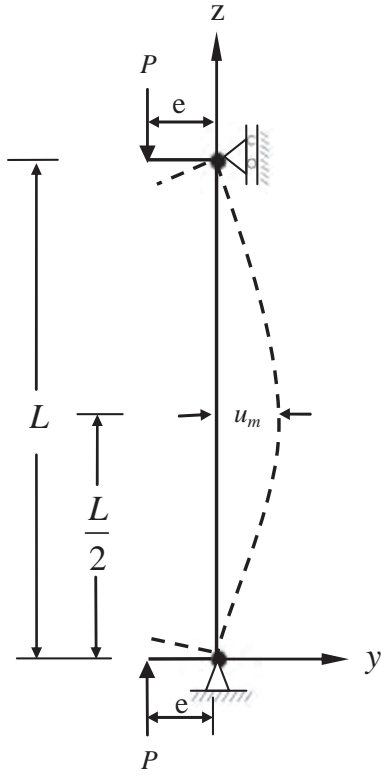
Fig. 5. Pin-ended beam-column model.

mid-height of the beam-column, the external moment at the mid-height of the beam-column can be calculated by

$$M_{me} = P(e + u_m + u_o) \tag{17}$$

To capture the complete load-deflection curve for a CFST slender beam-column under biaxial loads, the deflection control method is used in the numerical model. In the analysis, the deflection at the mid-height u_m of the slender beam-column is gradually increased. The curvature ϕ_m at the mid-height of the beam-column can be calculated from the deflection u_m. For this curvature, the neutral axis depth and orientation are adjusted to achieve the moment equilibrium at the mid-height of the beam-column. The equilibrium state for biaxial bending requires that the following equations must be satisfied:

$$P(e + u_m + u_o) - M_{mi} = 0 \tag{18}$$

$$\tan\alpha - \frac{M_y}{M_x} = 0 \tag{19}$$

in which M_{mi} is the resultant internal moment which is calculated as $M_{mi} = \sqrt{M_x^2 + M_y^2}$.

The macroscale model incorporating the mesoscale model is implemented by a computational procedure. A computer flowchart is shown in Fig. 6 to implicitly demonstrate the computational procedure for load-deflection responses. The main steps of the computational procedure are described as follows:

(1) Input data.
(2) Discretize the composite section into fine fiber elements.
(3) Initialize the mid-height deflection of the beam-column $u_m = \Delta u_m$.
(4) Calculate the curvature ϕ_m at the mid-height of the beam-column.
(5) Adjust the depth of the neutral axis (d_n) using the Müller's method.
(6) Compute stress resultants P and M_{mi} considering local buckling.
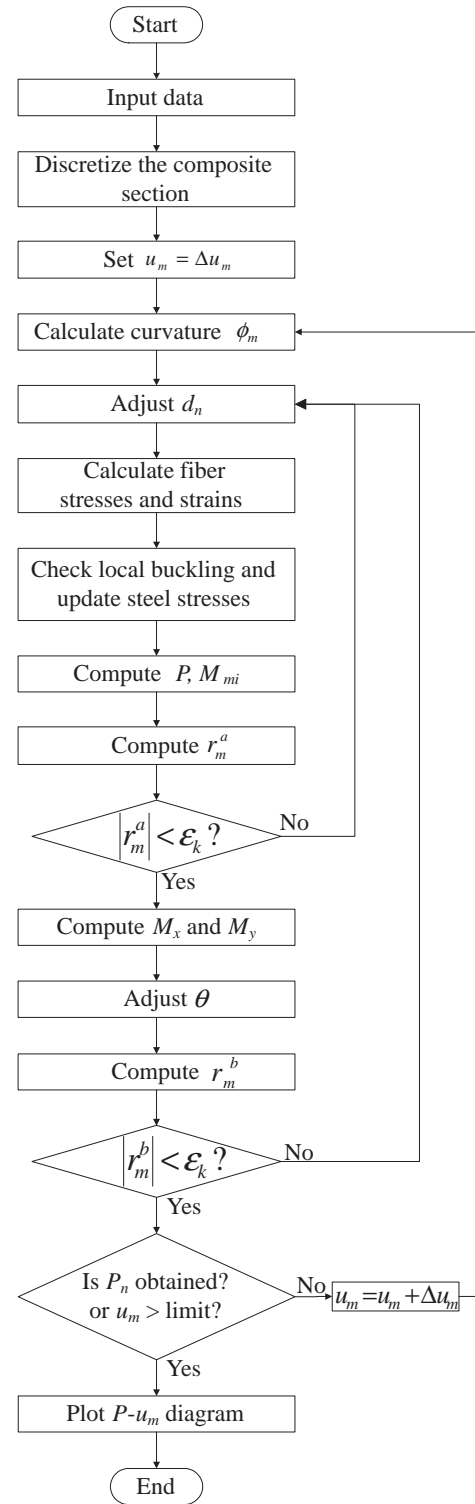
Fig. 6. Computer flowchart for predicting the axial load-deflection responses of thin-walled CFST slender beam-columns under biaxial loads.

(7) Compute the residual moment $r_m^a = M_{me} - M_{mi}$.
(8) Repeat Steps (5)–(7) until $|r_m^a| < \varepsilon_k$.
(9) Compute bending moments M_x and M_y.
(10) Adjust the orientation of the neutral axis (θ) using the Müller's method.
(11) Calculate the residual moment $r_m^b = \tan\alpha - \frac{M_y}{M_x}$.
(12) Repeat Steps (5)–(11) until $|r_m^b| < \varepsilon_k$.

(13) Increase the deflection at the mid-height of the beam-column by $u_m = u_m + \Delta u_m$.

(14) Repeat Steps (4)–(13) until the ultimate axial load P_n is obtained or the deflection limit is reached.

(15) Plot the load-deflection curve.

In the above procedure, ε_k is the convergence tolerance and taken as 10^{-4} in the numerical analysis.

3.2. Macroscale model for simulating strength envelopes

In design practice, it is required to check for the design capacities of CFST slender beam-columns under design actions such as the design axial force and bending moments, which have been determined from structural analysis. For this design purpose, the axial load-moment strength interaction curves (strength envelopes) need to be developed for the beam-columns. For a given axial load applied (P_n) at a fixed load angle (α), the ultimate bending strength of a slender beam-column is determined as the maximum moment that can be applied to the column ends. The moment equilibrium is maintained at the mid-height of the beam-column. The external moment at the mid-height of the slender beam-column is given by

$$M_{me} = M_e + P_n (u_m + u_o) \tag{20}$$

in which M_e is the moment at the column ends. The deflection at the mid-height of the slender beam-column can be calculated from the curvature as

$$u_m = \left(\frac{L}{\pi}\right)^2 \phi_m \tag{21}$$

To generate the strength envelope, the curvature (ϕ_m) at the mid-height of the beam-column is gradually increased. For each curvature increment, the corresponding internal moment capacity (M_{mi}) is computed by the inelastic moment-curvature responses discussed in Section 2.8. The curvature at the column ends (ϕ_e) is adjusted and the corresponding moment at the column ends is calculated until the maximum moment at the column ends is obtained. The axial load is increased and the strength envelope can be generated by repeating the above process. For a CFST slender beam-column under combined axial load and bending, the following equilibrium equations must be satisfied:

$$P_n - P = 0 \tag{22}$$

$$\tan \alpha - \frac{M_y}{M_x} = 0 \tag{23}$$

$$M_e + P_n (u_m + u_o) - M_{mi} = 0 \tag{24}$$

Fig. 7 shows a computer flowchart that implicitly illustrates the computational procedure for developing the strength envelope. The main steps of the computational procedure are described as follows:

(1) Input data.

(2) Discretize the composite section into fine fiber elements.

(3) The load-deflection analysis procedure is used to compute the ultimate axial load P_{oa} of the axially loaded slender beam-column with local buckling effects.

(4) Initialize the applied axial load $P_n = 0$.

(5) Initialize the curvature at the mid-height of the beam-column $\phi_m = \Delta \phi_m$.

(6) Compute the mid-height deflection u_m from the curvature ϕ_m.

(7) Adjust the depth of the neutral axis (d_n) using the Müller's method.

(8) Calculate resultant force P considering local buckling.

(9) Compute the residual force $r_m^c = P_n - P$.
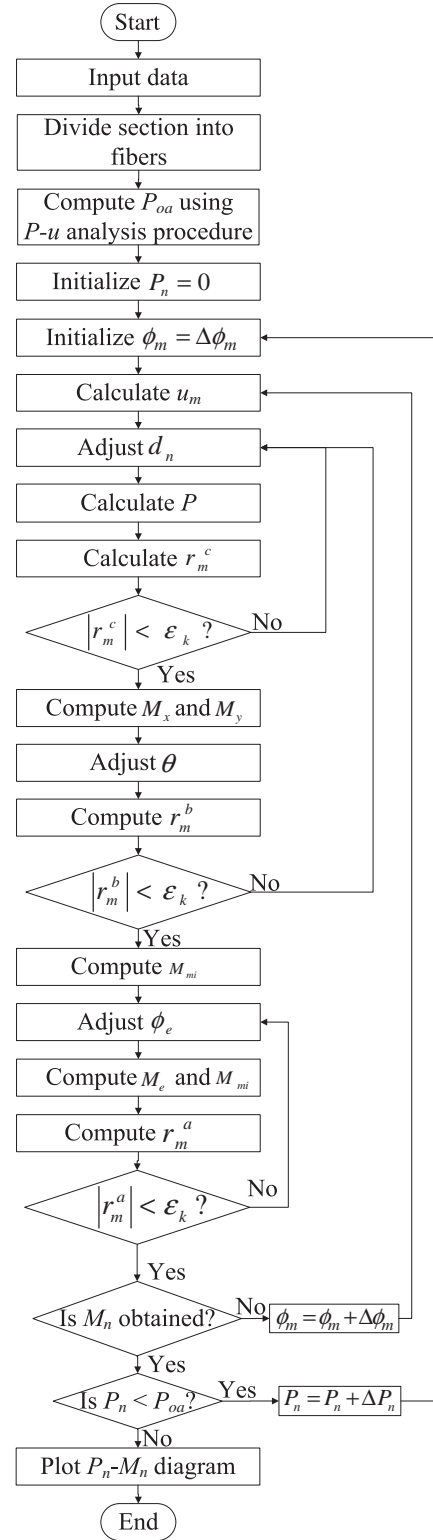
Fig. 7. Computer flowchart for simulating the strength envelops of thin-walled CFST slender beam-columns under biaxial loads.

(10) Repeat Steps (7)–(9) until $|r_m^c| < \varepsilon_k$.

(11) Compute bending moment M_x and M_y.

(12) Adjust the orientation of the neutral axis (θ) using the Müller's method.

(13) Calculate the residual moment $r_m^b = \tan \alpha - \frac{M_y}{M_x}$.

(14) Repeat Steps (7)–(13) until $|r_m^b| < \varepsilon_k$.

(15) Compute the internal resultant moment M_{mi}.

(16) Adjust the curvature at the column end ϕ_e using the Müller's method.
(17) Compute the moment M_e at the column ends accounting for local buckling effects.
(18) Compute $r_m^a = M_{me} - M_{mi}$.
(19) Repeat Steps (16)–(18) until $|r_m^a| < \varepsilon_k$.
(20) Increase the curvature at the mid-height of the beam-column by $\phi_m = \phi_m + \Delta\phi_m$.
(21) Repeat Steps (6)–(20) until the ultimate bending strength $M_n (= M_{e\,max})$ at the column ends is obtained.
(22) Increase the axial load by $P_n = P_n + \Delta P_n$, where $\Delta P_n = P_{oa}/10$.
(23) Repeat Steps (5)–(22) until the maximum load increment is reached.
(24) Plot the axial load-moment interaction diagram.

4. Numerical solution scheme

4.1. General

As discussed in the preceding sections, the depth and orientation of the neutral axis and the curvature at the column ends need to be iteratively adjusted to satisfy the force and moment equilibrium conditions in the inelastic analysis of a slender beam-column. For this purpose, computational algorithms based on the secant method have been developed by Liang [21,28]. Although the secant method algorithms are shown to be efficient and reliable for obtaining converged solutions, computational algorithms based on the Müller's method [35], which is a generalization of the secant method, are developed in the present study to determine the true depth and orientation of the neutral axis and the curvature at the column ends.

4.2. The Müller's method

In general, the depth (d_n) and orientation (θ) of the neutral axis and the curvature (ϕ_e) at the column ends of a slender beam-column are design variables which are denoted herein by ω. The Müller's method requires three starting values of the design variables ω_1, ω_2, and ω_3. The corresponding force or moment functions $r_{m,1}$, $r_{m,2}$ and $r_{m,3}$ are calculated based on the three initial design variables. The new design variable ω_4 that approaches the true value is determined by the following equations:

$$\omega_4 = \omega_3 + \frac{-2c_m}{b_m \pm \sqrt{b_m^2 - 4a_m c_m}} \tag{25}$$

$$a_m = \frac{(\omega_2 - \omega_3)\left(r_{m,1} - r_{m,3}\right) - (\omega_1 - \omega_3)\left(r_{m,2} - r_{m,3}\right)}{(\omega_1 - \omega_2)(\omega_1 - \omega_3)(\omega_2 - \omega_3)} \tag{26}$$

$$b_m = \frac{(\omega_1 - \omega_3)^2\left(r_{m,2} - r_{m,3}\right) - (\omega_2 - \omega_3)^2\left(r_{m,1} - r_{m,3}\right)}{(\omega_1 - \omega_2)(\omega_1 - \omega_3)(\omega_2 - \omega_3)} \tag{27}$$

$$c_m = r_{m,3} \tag{28}$$

When adjusting the neutral axis depth and orientation, the sign of the square root term in the denominator of Eq. (25) is taken to be the same as that of b_m. However, this sign is taken as positive when adjusting the curvature at the column ends. In order to obtain converged solutions, the values of ω_1, ω_2 and ω_3 and corresponding residual forces or moments $r_{m,1}$, $r_{m,2}$ and $r_{m,3}$ need to be exchanged as discussed by Patel et al. [22]. Eq. (25) and the exchange of design variables and force or moment functions are executed iteratively until the convergence criterion of $|r_m| < \varepsilon_k$ is satisfied.

In the numerical model, three initial values of the neutral axis depth $d_{n,1}$, $d_{n,3}$ and $d_{n,2}$ are taken as $D/4$, D and $(d_{n,1} + d_{n,3})/2$ respectively;

the orientations of the neutral axis θ_1, θ_3 and θ_2 are initialized to $\alpha/4$, α and $(\theta_1 + \theta_3)/2$ respectively; and the curvature at the column ends $\phi_{e,1}$, $\phi_{e,3}$ and $\phi_{e,2}$ are initialized to 10^{-10}, 10^{-6} and $(\phi_{e,1} + \phi_{e,3})/2$ respectively.

5. Performance indices for CFST slender beam-columns

Performance indices are used to evaluate the contributions of the concrete and steel components to the ultimate strengths of CFST slender beam-columns and to quantify the strength reduction caused by the section and column slenderness, loading eccentricity and initial geometric imperfections. These performance indices can be used to investigate the cost effective designs of CFST slender beam-columns under biaxial loads.

5.1. Steel contribution ratio (ξ_s)

The steel contribution ratio is used to determine the contribution of the hollow steel tubular beam-column to the ultimate strength of the CFST slender beam-column under axial load and biaxial bending, which is given by

$$\xi_s = \frac{P_s}{P_n} \tag{29}$$

where P_n is the ultimate axial strength of the CFST slender beam-column and P_s is the ultimate axial strength of the hollow steel tubular beam-column, which is calculated by setting the concrete compressive strength f'_c to zero in the numerical analysis while other conditions of the hollow steel tubular beam-column remain the same as those of the CFST beam-column. The effects of local buckling are taken into account in the determination of both P_n and P_s.

5.2. Concrete contribution ratio (ξ_c)

The concrete contribution ratio quantifies the contribution of the concrete component to the ultimate axial strength of a CFST slender beam-column. The slender concrete core beam-column without reinforcement carries very low loading and does not represents the concrete core in a CFST slender beam-column. Portolés et al. [9] used the capacity of the hollow steel tubular beam-column to define the concrete contribution ratio (CCR), which is given by

$$CCR = \frac{P_n}{P_s} \tag{30}$$

Eq. (30) is an inverse of the steel contribution ratio and may not accurately quantify the concrete contribution. To evaluate the contribution of the concrete component to the ultimate axial strength of a CFST slender beam-column, a new concrete contribution ratio is proposed as

$$\xi_c = \frac{P_n - P_s}{P_n} \tag{31}$$

It can be seen from Eq. (31) that the concrete contribution to the ultimate axial strength of a CFST slender beam-column is the difference between the ultimate axial strength of the CFST column and that of the hollow steel column.

5.3. Strength reduction factor (α_c)

The ultimate axial strength of a CFST short column under axial loading is reduced by increasing the section and column slenderness, loading eccentricity, and initial geometric imperfections. To reflect on these effects, the strength reduction factor is defined as

$$\alpha_c = \frac{P_n}{P_o} \tag{32}$$

117

where P_o is the ultimate axial strength of the column cross-section under axial compression. The ultimate axial strengths of P_n and P_o are determined by considering the effects of local buckling of the steel tubes.

6. Conclusions

This paper has presented a new multiscale numerical model for the nonlinear inelastic analysis of high strength thin-walled rectangular CFST slender beam-columns under combined axial load and biaxial bending. At the mesoscale level, the inelastic axial load-strain and moment-curvature responses of column cross-sections subjected to bi-axial loads are modeled using the accurate fiber element method, which accounts for the effects of progressive local buckling of the steel tube walls under stress gradients. Macroscale models together with computational procedures have been described that simulate the axial load-deflection responses and strength envelopes of CFST slender beam-columns under biaxial bending. Initial geometric imperfections and second order effects between axial load and deformations are taken into account in the macroscale models. New solution algorithms based on the Müller's method have been developed and implemented in the numerical model to obtain converged solutions.

The computer program that implements the multiscale numerical model developed is an efficient and powerful computer simulation and design tool that can be used to determine the structural performance of biaxially loaded high strength rectangular CFST slender beam-columns made of compact, non-compact or slender steel sections. This overcomes the limitations of experiments which are extremely expensive and time consuming. Moreover, the multiscale numerical model can be implemented in frame analysis programs for the nonlinear analysis of composite frames. Steel and concrete contribution ratios and strength reduction factor proposed can be used to study the optimal designs of high strength CFST beam-columns. The verification of the numerical model and parametric study are given in a companion paper [30].

References

[1] Furlong RW. Strength of steel-encased concrete beam-columns. J Struct Div ASCE 1967;93(5):113–24.
[2] Knowles RB, Park R. Strength of concrete-filled steel tubular columns. J Struct Div ASCE 1969;95(12):2565–87.
[3] Schneider SP. Axially loaded concrete-filled steel tubes. J Struct Eng ASCE 1998;124(10):1125–38.
[4] Varma AH, Ricles JM, Sause R, Lu LW. Seismic behavior and modeling of high-strength composite concrete-filled steel tube (CFT) beam-columns. J Constr Steel Res 2002;58: 725–58.
[5] Sakino K, Nakahara H, Morino S, Nishiyama I. Behavior of centrally loaded concrete-filled steel-tube short columns. J Struct Eng ASCE 2004;130(2):180–8.
[6] Fujimoto T, Mukai A, Nishiyama I, Sakino K. Behavior of eccentrically loaded concrete-filled steel tubular columns. J Struct Eng ASCE 2004;130(2):203–12.
[7] Ellobody E, Young B, Lam D. Behaviour of normal and high strength concrete-filled compact steel tube circular stub columns. J Constr Steel Res 2006;62(7):706–15.
[8] Liu D. Behaviour of eccentrically loaded high-strength rectangular concrete-filled steel tubular columns. J Constr Steel Res 2006;62(8):839–46.
[9] Portolés JM, Romero ML, Bonet JL, Filippou FC. Experimental study on high strength concrete-filled circular tubular columns under eccentric loading. J Constr Steel Res 2011;67(4):623–33.
[10] Ge HB, Usami T. Strength of concrete-filled thin-walled steel box columns: experiment. J Struct Eng ASCE 1992;118(11):3036–54.
[11] Bridge RQ, O'Shea MD. Behaviour of thin-walled steel box sections with or without internal restraint. J Constr Steel Res 1998;47(1–2):73–91.
[12] Uy B. Strength of concrete filled steel box columns incorporating local buckling. J Struct Eng ASCE 2000;126(3):341–52.
[13] Han LH. Tests on stub columns of concrete-filled RHS sections. J Constr Steel Res 2002;58(3):353–72.
[14] Liang QQ, Uy B, Liew JYR. Local buckling of steel plates in concrete-filled thin-walled steel tubular beam-columns. J Constr Steel Res 2007;63(3):396–405.
[15] Liang QQ. High strength circular concrete-filled steel tubular slender beam-columns, part II: fundamental behavior. J Constr Steel Res 2011;67(2):172–80.
[16] Bridge RQ. Concrete filled steel tubular columns. School of Civil Engineering, The University of Sydney, Sydney, Australia, Research Report No. R283; 1976.
[17] Shakir-Khalil H, Zeghiche J. Experimental behaviour of concrete-filled rolled rectangular hollow-section columns. Struct Eng 1989;67(19):346–53.
[18] Shakir-Khalil H, Mouli M. Further tests on concrete-filled rectangular hollow-section columns. Struct Eng 1990;68(20):405–13.
[19] Vrcelj Z, Uy B. Strength of slender concrete-filled steel box columns incorporating local buckling. J Constr Steel Res 2002;58(2):275–300.
[20] Hu HT, Huang CS, Wu MH, Wu YM. Nonlinear analysis of axially loaded concrete-filled tube columns with confinement effect. J Struct Eng ASCE 2003;129(10): 1322–9.
[21] Liang QQ. High strength circular concrete-filled steel tubular slender beam-columns, part I: numerical analysis. J Constr Steel Res 2011;67(2):164–71.
[22] Patel VI, Liang QQ, Hadi MNS. High strength thin-walled rectangular concrete-filled steel tubular slender beam-columns, part I: modeling. J Constr Steel Res 2012;70: 377–84.
[23] Patel VI, Liang QQ, Hadi MNS. High strength thin-walled rectangular concrete-filled steel tubular slender beam-columns, part II: behavior. J Constr Steel Res 2012;70:368–76.
[24] El-Tawil S, Sanz-Picon CF, Deierlein GG. Evaluation of ACI 318 and AISC (LRFD) strength provisions for composite beam-columns. J Constr Steel Res 1995;34(1): 103–23.
[25] El-Tawil S, Deierlein GG. Strength and ductility of concrete encased composite column. J Struct Eng 1999;125(9):1009–19.
[26] Muñoz PR, Hsu CTT. Behavior of biaxially loaded concrete-encased composite columns. J Struct Eng ASCE 1997;123(9):1163–71.
[27] Lakshmi B, Shanmugam NE. Nonlinear analysis of in-filled steel-concrete composite columns. J Struct Eng ASCE 2002;128(7):922–33.
[28] Liang QQ. Performance-based analysis of concrete-filled steel tubular beam-columns, part I: theory and algorithms. J Constr Steel Res 2009;65(2):363–72.
[29] Liang QQ. Performance-based analysis of concrete-filled steel tubular beam-columns, part II: verification and applications. J Constr Steel Res 2009;65(2):351–62.
[30] Patel VI, Liang QQ, Hadi MNS. Biaxially loaded high-strength concrete-filled steel tubular slender beam-columns, part II: parametric study. J Constr Steel Res submitted for publication.
[31] Mander JB, Priestley MJN, Park R. Theoretical stress–strain model for confined concrete. J Struct Eng ASCE 1988;114(8):1804–26.
[32] ACI-318. Building code requirements for reinforced concrete. Detroit, MI: ACI; 2002.
[33] Tomii M, Sakino K. Elastic–plastic behavior of concrete filled square steel tubular beam-columns. Trans Archit Inst Japn 1979;280:111–20.
[34] Bulson PS. The stability of flat plates. London: Chatto and Windus; 1970.
[35] Müller DE. A method for solving algebraic equations using an automatic computer. MTAC 1956;10:208–15.

Revised manuscript prepared for

Journal of Constructional Steel Research

January 2012

Biaxially Loaded High-Strength Concrete-Filled Steel Tubular Slender Beam-Columns, Part II: Parametric Study

Vipulkumar Ishvarbhai Patel[a], Qing Quan Liang[a],*, Muhammad N. S. Hadi[b]

[a]School of Engineering and Science, Victoria University, PO Box 14428, Melbourne, VIC 8001, Australia

[b]School of Civil, Mining and Environmental Engineering, University of Wollongong, Wollongong, NSW 2522, Australia

Corresponding author:

Dr. Qing Quan Liang
School of Engineering and Science
Victoria University
PO Box 14428
Melbourne VIC 8001
Australia
Phone: +61 3 9919 4134
Fax: +61 3 9919 4139
E-mail: Qing.Liang@vu.edu

Biaxially loaded high-strength concrete-filled steel tubular slender beam-columns, Part II: Parametric study

Vipulkumar Ishvarbhai Patel[a], Qing Quan Liang[a],*, Muhammad N. S. Hadi[b]

[a] *School of Engineering and Science, Victoria University, PO Box 14428, Melbourne, VIC 8001, Australia*
[b] *School of Civil, Mining and Environmental Engineering, University of Wollongong, Wollongong, NSW 2522, Australia*

ABSTRACT

Biaxially loaded high strength rectangular concrete-filled steel tubular (CFST) slender beam-columns with large depth-to-thickness ratios, which may undergo local and global interaction buckling, have received very little attention. This paper presents the verification of a multiscale numerical model described in a companion paper and an extensive parametric study on the performance of high strength thin-walled rectangular CFST slender beam-columns under biaxial loads. Comparisons of computer solutions with existing experimental results are made to examine the accuracy of the multiscale numerical model developed. The effects of the concrete compressive strength, loading eccentricity, depth-to-thickness ratio and columns slenderness on the ultimate axial strength, steel contribution ratio, concrete contribution ratio and strength reduction factor of CFST slender beam-columns under biaxial bending are investigated by using the numerical model. Comparative results demonstrate that the multiscale numerical model is capable of accurately predicting the ultimate strength and deflection behavior

---

of CFST slender beam-columns under biaxial loads. Benchmark numerical results presented in this paper provide a better understanding of the local and global interaction buckling behavior of high strength thin-walled CFST slender beam-columns and are useful for the development of composite design codes.

Keywords: Biaxial bending; Concrete-filled steel tubes; High strength materials; Local and post-local buckling; Nonlinear analysis; Slender beam-columns.

1. Introduction

High strength thin-walled rectangular concrete-filled steel tubular (CFST) slender columns with large depth-to-thickness ratios are increasingly used in lateral load resisting systems in high-rise composite buildings to resist heavy axial loads as well as biaxial bending moments. These composite beam-columns are characterized by high strength, large depth-to-thickness ratio, slenderness and biaxial bending. The failure mode of thin-walled CFST slender beam-columns may involve interaction local and global buckling, which significantly complicates their analysis and design procedures. There has been a lack of experimental and numerical studies on this type of composite columns so that their fundamental behavior has not been adequately understood. Therefore, researches on the structural performance of high strength thin-walled CFST slender beam-columns under biaxial bending are much needed. This paper is concerned with numerical studies on the structural performance of biaxial loaded high strength thin-walled CFST slender beam-columns incorporating the effects of local buckling of the steel tube walls under stress gradients.

The performance of CFST short and slender columns under axial load or combined axial load and uniaxial bending has been investigated experimentally by researchers [1-7]. However, there have been relatively few experimental studies on the behavior of biaxially loaded rectangular CFST slender beam-columns with large depth-to-thickness ratios. Bridge [8] performed experiments on biaxially loaded normal strength square CFST slender beam-columns. The main variables examined in the test program were the loading eccentricity, column slenderness and biaxial bending. Test results showed that the ultimate axial strength of CFST slender beam-columns decreased with increasing the loading eccentricity or the column slenderness. Local buckling was not observed because compact steel sections with a depth-to-thickness ratio of 20 were used. Experimental studies were carried out by Shakir-Khalil and Zeghiche [9] and Shakir-Khalil and Mouli [10] to determine the ultimate axial loads of normal strength rectangular CFST slender beam-columns under axial load and biaxial bending. Tests parameters examined included the section size, steel yield strength, concrete compressive strength, column length and eccentricity of loading. The authors reported that the relative load carrying capacity of the composite to steel columns increased when the size of the steel section or the concrete compressive strength was increased. However, they observed reversed influence for the loading eccentricity and column length. The typical failure mode of these tested specimens was overall column buckling. Recently, Guo et al. [11] undertook tests on normal strength rectangular CFST slender beam-columns with rib stiffeners and under biaxial bending. Test results showed that local buckling of the steel tube walls between the rib stiffeners occurred after specimens attained their ultimate strengths.

Numerical analysis techniques have been used to study the nonlinear inelastic behavior of short and slender composite columns under axial load and uniaxial bending [12-19]. Lakshmi and Shanmugam [20] used a semi-analytical model to determine the ultimate axial strengths, load-deflection responses and strength envelopes of CFST columns under axial load and biaxial bending. Their analytical results demonstrated that increasing the loading eccentricity significantly reduced the ultimate axial strength and stiffness of CFST slender columns. The semi-analytical model was used to develop the strength envelopes of CFST cross-sections under uniaxial bending. However, the strength envelopes of thin-walled CFST slender beam-columns under biaxial bending have not been investigated by Lakshmi and Shanmugam [20]. In addition, the effects of local buckling were not taken into account in their model and numerical studies. Liang [21, 22] employed a performance-based analysis technique accounting for progressive local buckling of the steel tube walls [23] to investigate the effects of the depth-to-thickness ratio, concrete compressive strength, steel yield strength and axial load level on the ultimate axial strengths, load-strain behavior, moment-curvature responses and strength envelopes of thin-walled CFST short columns under axial load and biaxial bending. However, numerical studies on the behavior of biaxially loaded high strength CFST slender beam-columns with local buckling effects have not been reported in the literature.

The purpose of this paper is to validate the multiscale numerical model presented in a companion paper [24] and to study the structural performance of high strength CFST slender beam-columns made of slender steel sections. Verification studies involve thorough and comprehensive comparisons of the predicted ultimate axial loads, ultimate

bending strengths and complete load-deflection responses of CFST slender beam-columns to existing experimental results. The parametric study focuses on the ultimate axial strength, steel contribution ratio, concrete contribution ratio, strength reduction factor and strength envelopes of high strength thin-walled CFST slender beam-columns under biaxial loads. The paper is organized as follows. In section 2, the verification of the numerical model is presented. This is followed by an extensive parametric study on the fundamental behavior of high strength thin-walled CFST slender beam-columns. Finally, important conclusions are given.

2. Verification of the multiscale numerical model

To verify the accuracy of the multiscale numerical model developed, the predicted ultimate strengths and axial load-deflection responses of biaxially loaded CFST slender beam-columns are compared with existing experimental results in this section.

2.1 Ultimate axial strengths of CFST slender beam-columns

The geometry and material properties of biaxially loaded CFST slender beam-columns tested by independent researchers are given in Table 1. Experiments on specimens SCH-3, SCH-4, SCH-5 and SCH-6 were conducted by Bridge [8]. These column sections with a depth-to-thickness ratio (D/t) of 20 were considered to be compact. The ultimate tensile strength (f_{su}) of steel tubes was assumed to be 430 MPa. Experimental results on specimen R6 in Table 1 were given by Shakir-Khalil and Zeghiche [9]. The axial load was applied at eccentricities of 16 mm and 24 mm about the major and minor

axis respectively. Specimens M2-M9 shown in Table 1 were tested by Shakir-Khalil and Mouli [10]. The concrete cylinder compressive strength $\left(f_c'\right)$ shown in Table 1 was taken as 0.85 times the concrete cube strength. Initial geometric imperfections $\left(u_o\right)$ at the mid-height of specimens R6 and M2-M9 were not measured. To consider this effect, the initial geometric imperfection of $L/600$ at the mid-height of the columns as suggested by Portolés et al. [17] was taken into account in the present numerical analysis.

Ultimate axial strengths obtained from experiments $\left(P_{n.\exp}\right)$ and numerical analyses $\left(P_{n.\text{num}}\right)$ are compared in Table 1. It can be seen from Table 1 that there is a good agreement between computational solutions and experimental results. The mean value of $P_{n.\text{num}}/P_{n.\exp}$ ratio is 1.01 with a standard deviation (SD) of 0.05 and a coefficient of variation (COV) of 0.05. This comparative study demonstrates that the macroscale model for simulating the load-deflection responses can accurately predict the ultimate axial strengths of CFST slender beam-columns under biaxial loads. It should be noted that the numerical model for high strength CFST slender beam-columns under axial load and uniaxial bending has been validated by Liang [21] and Patel et al. [18].

2.2 Ultimate bending strengths of CFST slender beam-columns

The ultimate bending strengths of CFST slender beam-columns were determined using the macroscale model for simulating strength envelopes and compared with experimental results presented by Bridge [8], Shakir-Khalil and Zeghiche [9] and

Shakir-Khalil and Mouli [10]. The initial geometric imperfection of $L/600$ at the mid-height of the columns was taken into account in the numerical analysis if it was not measured in the tests. The experimental ultimate axial loads were used in numerical analyses to determine the corresponding ultimate bending strengths. Computational and experimental ultimate bending strengths obtained are given in Table 2, where the experimental ultimate bending strength $M_{n.\exp}$ was calculated as $M_{n.\exp} = P_{u.\exp} \times e$. It can be seen from Table 2 that numerical predictions are in good agreement with experimental results. The ratio of the mean ultimate bending strength computed by the numerical model to the experimental value is 1.0. The standard deviation (SD) of the ratio is 0.08 while the coefficient of variation (COV) is 0.07. This comparison shows that the macroscale model for strength envelopes can yield accurate predictions of the ultimate bending strengths of biaixally loaded CFST slender beam-columns.

2.3 Load-deflection responses

The numerical model was used to predict the load-deflection responses of specimens tested by by Bridge [8]. Fig. 1 shows a comparison of experimental and computational load-deflection curves for specimen SCH-3. The figure demonstrates that numerical results are in excellent agreement with experimentally observed behaviors. It is noted that the initial stiffness of the tested specimen slightly differs from that predicted by the numerical model. This is likely attributed to the uncertainty of the actual concrete stiffness and strength as the average concrete compressive strength was used in the numerical analysis. It can be seen from Fig. 2 that the numerical model predicts well the load-deflection curve for the tested specimen SCH-6 up to the ultimate axial load. The

predicted initial stiffness of the column is almost identical to that of the experimentally observed value. However, the experimental load-deflection curve slightly differs from the computed one at the axial load higher than 600 kN. This is likely caused by the uncertainty of the actual concrete stiffness and strength of the specimen.

3. Parametric study

Parametric studies were carried out to examine the effects of concrete compressive strength, loading eccentricity, depth-to-thickness ratio and column slenderness on the ultimate axial strength, steel contribution ratio, concrete contribution ratio and strength reduction factor of full-scale high strength CFST slender beam-columns under axial load and biaxial bending. In the present study, the initial geometric imperfection at the mid-height of the beam-column was taken as $L/1000$. The yield and tensile strengths of the steel were 690 MPa and 790 MPa respectively while the Young's modulus of steel material was 200 GPa. The effects of local and post-local buckling were considered in all analyses.

3.1 Ultimate axial strengths

The ultimate axial strengths of high strength CFST slender beam-columns under axial load and biaxial bending were determined by performing load-deflection analyses. The beam-columns with a cross-section of 700 × 700 mm and under the eccentric load applied at an angle of 60°with respect to the y-axis were analyzed. The following basic parameters were specified in the parametric study. The loading eccentricity ratio $\left(e/D\right)$

was 0.4. The concrete compressive strength was 80 MPa. The column slenderness ratio (L/r) of 60 and depth-to-thickness ratio (D/t) of 70 were used in parametric study. Each parameter was varied to examine its individual effects on the ultimate axial strengths.

Fig. 3 shows the effects of concrete compressive strengths ranging from 25 to 120 MPa on the ultimate axial strengths of high strength thin-walled CFST slender beam-columns. It can be seen from Fig. 3 that increasing the concrete compressive strength significantly increases the ultimate axial strengths of biaxially loaded slender beam-columns. When increasing the concrete compressive strength from 30 MPa to 70 MPa and 120 MPa, the ultimate axial strength is found to increase by 32.2% and 59.6%, respectively. The ultimate axial load ratio is described in Fig. 4 as a function of the loading eccentricity ratio ranging from zero to 2.0. As shown in Fig. 4, the ultimate axial strength of the slender beam-column under eccentric loading (P_n) was normalized by the ultimate axial load of the slender column under axial compression (P_{oa}). It can be observed from Fig. 4 that the ultimate axial strength of a CFST slender beam-column is significantly reduced by increasing the loading eccentricity ratio. For the end eccentricity ratios of zero and 2.0, the axial load ratios are 1.0 and 0.103 respectively.

The effects of D/t ratio ranging from 20 to 100 on the ultimate axial loads of CFST slender beam-columns are demonstrated in Fig. 5. The figure illustrates that increasing the D/t ratio remarkably reduces the ultimate axial loads of CFST slender beam-columns under biaxial loads. When the D/t ratio increases from 20 to 60 and 100, the reduction in the ultimate axial strength of the slender beam-columns is 50% and 64.1%,

respectively. The relationship between the ultimate axial strength and the column slenderness ratio ranging from zero to 100 is demonstrated in Fig. 6, where P_{os} is the ultimate axial strength of the cross-section under eccentric loading. It would appear from Fig. 6 that increasing the column slenderness ratio causes a significant reduction in the ultimate axial load of the beam-column. The ultimate axial load ratio is 0.93, 0.71 and 0.39 for the columns with a L/r ratio of 20, 50 and 100 respectively.

3.2 Steel contribution ratio

The numerical model was employed to study the effects of various parameters on the steel contribution ratio which is defined as the calculated ultimate axial strength of the slender hollow steel tube to the ultimate axial strength of the CFST slender beam-column [24]. A thin-walled CFST beam-column with a cross-section of 700 × 800 mm was considered. The axial load was applied at an angle of 45° for biaxial bending. For this case, the basic parameters were the depth-to-thickness ratio of 50, loading eccentricity ratio of 0.4, slenderness ratio of 35 and the concrete compressive strength of 90 MPa. Each of these parameters was varied to quantify its individual effects on the steel contribution ratio.

The relationship between the steel contribution ratio and the concrete compressive strength ranging from 25 to 120 MPa obtained by the numerical model is demonstrated in Fig. 7. The figure shows that the use of higher strength concrete in CFST slender beam-columns results in a remarkable decrease in the steel contribution ratio. This is because increasing the concrete compressive strength significantly increases the

ultimate axial strength of the CFST beam-column but has not effect on the strength of the hollow steel tube. The steel contribution ratio of a CFST slender beam-column with concrete compressive strength of 35 MPa is 0.70, while it is only 0.48 for a CFST slender beam-column with the concrete compressive strength of 120 MPa. Fig. 8 illustrates that the steel contribution ratio is a function of the loading eccentricity ratio ranging from zero to 2.0. It can be observed from Fig. 8 that the larger the loading eccentricity, the higher the steel contribution ratio. This is attributed to the fact that the ultimate axial strengths of both the hollow steel tube and the CFST column are reduced by increasing the loading eccentricity, but the CFST column has a greater reduction in its ultimate axial strength than the hollow steel tube. For loading eccentricity ratio of 0.0 and 2.0, the steel contribution ratio of a slender CFST beam-column is 0.41 and 0.75 respectively.

Fig. 9 presents the steel contribution ratio of CFST columns with D/t ratios ranging from 20 to 100. It can be seen from the figure that the steel contribution ratio decreases with an increase in the depth-to-thickness ratio. This means that the reduction in the ultimate axial strength of the hollow steel tube is greater than that in the one filled with concrete due to the same increase in the D/t ratio. In other words, the D/t ratio has a lesser effect on the capacity of CFST columns than on the hollow steel tubes. For depth-to-thickness ratio of 20, 40 and 100, the steel contribution ratio is 0.76, 0.59 and 0.30 respectively. The relationship between the steel contribution ratio and the column slenderness ratio ranging from 5 to 100 is shown in Fig. 10. The figure shows that the more slender of the CFST beam-column, the more contribution of the steel tube to the capacity of the CFST beam-column. It is noted that increasing the column slenderness

significantly reduces the ultimate axial strengths of both the hollow steel tube and CFST column, but the reduction in the CFST column is greater than that in the hollow steel tube. The steel contribution ratio is 0.5, 0.57 and 0.65 for the column with the column slenderness ratio L/r of 20, 50 and 100 respectively.

3.3 Concrete contribution ratio

The concrete contribution ratio, which is defined as $(P_n - P_s)/P_n$ [24], was studied using the numerical model. Numerical analyses were undertaken on thin-walled CFST slender beam-columns with a cross-section of 600×600 mm and under the axial load applied at an angle of 30° with respect to the y-axis. The basic parameters examined in the study included the depth-to-thickness ratio of 60, loading eccentricity ratio of 0.4 and the slenderness ratio of 40 and the concrete compressive strength of 100 MPa.

The concrete contribution ratios of thin-walled CFST slender beam-columns with concrete compressive strengths ranging from 25 to 120 MPa are given in Fig. 11. The figure demonstrates that increasing the concrete compressive strength significantly increases the concrete contribution ratio. This implies that the axial strength performance of a CFST slender beam-column can be improved significantly by using high strength concrete as infill. The calculated concrete contribution ratio for the concrete compressive strength of 25 MPa, 75 MPa and 120 MPa is 0.29, 0.51 and 0.60 respectively. The concrete contribution curve is described in Fig. 12 as a function of the loading eccentricity ratio ranging from zero to 2.0. It appears from Fig. 12 that the concrete component has a lesser contribution to the ultimate axial strength of a CFST

slender beam-column when subjected to a larger loading eccentricity. To increase the axial load capacity of CFST slender beam-columns with a large loading eccentricity, the steel area and strength should be increased rather than the concrete. The concrete contribution ratio of the rectangular CFST slender beam-column with a zero eccentricity is 0.68, while it is only 0.36 with a e/D ratio of 2.0.

The effects of the D/t ratio ranging from 20 to 100 on the concrete contribution ratio of biaxially loaded CFST slender beam-columns are shown in Fig. 13. The concrete contribution ratio is found to increase significantly with an increase in the D/t ratio. This may be explained by the fact that increasing the D/t ratio reduces the axial load capacity of the steel tube and increases the cross-sectional area of the concrete core, thereby increasing the contribution of the concrete component. The concrete contribution ratio of the CFST slender beam-column with a D/t ratio of 20 is 0.28, while it is 0.73 for the column with a D/t ratio of 100. Fig. 14 presents the results of the concrete contribution ratios calculated by varying the column slenderness ratios ranging from zero to 100. It appears that the concrete contribution to the ultimate axial strength of CFST slender beam-columns decreases when increasing the column slenderness ratio.

3.4 Strength reduction factor

In Eurocode 4 [25], the strength reduction factor is used to account for the effect of column slenderness in the calculation of the ultimate axial load of a slender composite column under axial compression. In this section, the strength reduction factor [24] was

studied by varying the concrete compressive strengths, loading eccentricity, depth-to-thickness ratio and column slenderness. Biaxially loaded CFST slender beam-columns with the cross-section of 600 × 700 mm were considered. The angle of the applied axial load was 45°. The basic parameters studied were the depth-to-thickness ratio of 70, loading eccentricity ratio of 0.4, the column slenderness ratio of 100 and concrete compressive strength of 110 MPa. Each parameter was varied to examine its effects on the strength reduction factor.

Fig. 15 presents a strength reduction factor curve as a function of the concrete compressive strength ranging from 25 to 120 MPa. The figure indicates that increasing the concrete compressive strength considerably reduces the strength reduction factor of CFST slender beam-columns. It should be noted that the concrete compressive strength has a pronounced effect on the axial strength of a CFST column section but has a lesser effect on slender columns. When the concrete compressive strength is increased from 30 MPa to 60 MPa, 90MPa and 120 MPa, the strength reduction factor is found to be reduced from 0.25 to 0.20, 0.17 and 0.15 respectively. The strength reduction factors were obtained by varying the loading eccentricity ratio from zero to 2.0. Fig. 16 clearly shows that a large loading eccentricity leads to a significant reduction in the ultimate axial strength of a CFST slender beam-column.

Fig. 17 demonstrates the effects of the D/t ratio ranging from 20 to 100 on the strength reduction factor of slender beam-columns. It can be observed from the figure that the strength reduction factor decreases considerably with an increase in the D/t ratio of the same size cross-section. It is known that increasing the D/t ratio causes a reduction in

the ultimate axial strengths of both the section and the CFST slender beam-column. However, the *D/t* ratio has a lesser effect on the strength of a slender beam-column than on its cross-section. The strength reduction factor is 0.19, 0.17 and 0.14 for the column with D/t ratio of 20, 50 and 100 respectively. The strength reduction factor of the slender beam-columns was determined by varying the column slenderness ratio ranging from zero to 100 and the results are presented in Fig. 18. The figure indicates that the column slenderness has a pronounced effect on the ultimate axial strengths of CFST beam-columns. The strength reduction factor is significantly reduced by increasing the column slenderness ratio. The strength reduction factor of CFST columns under biaxial bending with the column slenderness ratio of 10, 50 and 100 is 0.41, 0.29 and 0.15 respectively.

3.5 Strength envelopes

The inelastic stability analyses of high strength thin-walled CFST slender beam-columns were undertaken to examine the effects of the column slenderness ratio on the strength envelopes. The cross-section of 500 × 500 mm was considered. The D/t ratio of the high strength steel tube was 50. The beam-column was filled with high strength concrete of 120 MPa. The angle of the axial load was fixed at 60° with respect to the y-axis. The eccentricity ratio e/D of 0.4 was considered.

The strength envelopes of rectangular CFST beam-columns with the column slenderness ratios of 0.0, 22 and 30 are presented in Fig. 19. The ultimate axial strength was normalized to the ultimate axial load of the axially loaded column $\left(P_{\mathrm{oa}}\right)$ while the

ultimate moment was normalized to the ultimate pure bending moment of the beam-column (M_o). The curve for $L/r = 0$ represents the strength envelope of the composite section which is not affected by the global stability analysis. It appears from Fig. 19 that reducing the L/r ratio of the beam-column enlarges the normalized the strength envelope of the beam-column. For beam-columns under the same axial load level, increasing the column slenderness ratio L/r reduces the ultimate bending strengths.

4. Conclusions

The verification of a multiscale numerical model and an extensive parametric study on the behavior of high strength thin-walled rectangular CFST slender beam-columns under axial load and biaxial bending and with local buckling effects have been presented in this paper. Verification studies were undertaken by comparing computational ultimate axial loads, ultimate bending strengths and complete load-deflection responses of CFST slender beam-columns to experimentally observed behavior reported by other researchers. Good agreement between computer solutions and experimental results was obtained. The fundamental behavior of high strength thin-walled CFST slender beam-columns under biaxial loads was described, including the ultimate axial strength, steel contribution ratio, concrete contribution ratio, strength reduction factor and strength envelope. It has been demonstrated that the ultimate strength and behavior of high strength thin-walled CFST slender beam-columns under biaxial bending are affected by many parameters including the concrete strength, loading eccentricity, depth-to-thickness ratio and column slenderness. The design methods given current composite design codes may yield very conservative designs of

biaxially loaded high strength thin-walled CFST slender beam-columns with local buckling effects. Benchmark numerical results presented in this paper overcome the limitations of current composite design codes and are useful not only for the design of CFST slender beam-columns but also for validating other numerical models.

References

[1] Ge HB, Usami T. Strength of concrete-filled thin-walled steel box columns: Experiment. Journal of Structural Engineering, ASCE 1992; 118(11):3036-54.

[2] Schneider SP. Axially loaded concrete-filled steel tubes. Journal of Structural Engineering, ASCE 1998; 124(10):1125-38.

[3] Liu D, Gho WM, Yuan J. Ultimate capacity of high-strength rectangular concrete-filled steel hollow section stub columns. Journal of Constructional Steel Research 2003; 59(12): 1499-1515.

[4] Varma AH, Ricles JM, Sause R, Lu LW. Seismic behavior and design of high-strength square concrete-filled steel tube beam–columns. Journal of Structural Engineering, ASCE 2004; 130(2):169-179.

[5] Sakino K, Nakahara H, Morino S, Nishiyama I. Behavior of centrally loaded concrete-filled steel-tube short columns. Journal of Structural Engineering, ASCE 2004; 130(2):180-88.

[6] Young B, Ellobody E. Experimental investigation of concrete-filled cold-formed high strength stainless steel tube columns. Journal of Constructional Steel research 2006; 62(5):484-492.

[7]   Han LH, Liu W, Yang YF. Behaviour of concrete-filled steel tubular stub columns subjected to axially local compression. Journal of Constructional Steel Research 2008; 64(4):377-387.

[8]   Bridge RQ. Concrete filled steel tubular columns. School of Civil Engineering, The University of Sydney, Sydney, Australia, 1976, Research Report No. R 283.

[9]   Shakir-Khalil H, Zeghiche J. Experimental behaviour of concrete-filled rolled rectangular hollow-section columns. The structural Engineer 1989; 67(19): 346-53.

[10]   Shakir-Khalil H, Mouli M. Further tests on concrete-filled rectangular hollow-section columns. The structural Engineer 1990; 68(20): 405-13.

[11]   Guo L, Zhang S, Xu Z. Behaviour of filled rectangular steel HSS composite columns under bi-axial bending. Advances in Structural Engineering 2011; 14(2): 295-306.

[12]   El-Tawil S, Sanz-Picón CF, Deierlein GG. Evaluation of ACI 318 and AISC (LRFD) strength provisions for composite beam-columns. Journal of Constructional Steel Research 1995; 34(1):103-23.

[13]   Hu HT, Huang CS, Chen ZL. Finite element analysis of CFT columns subjected to an axial compressive force and bending moment in combination. Journal of Constructional Steel Research 2005; 61(12):1692-1712.

[14]   Dai X, Lam D. Numerical modeling of the axial compressive behaviour of short concrete-filled elliptical steel columns. Journal of Constructional Steel research 2010; 66(7):931-942.

[15] Liang QQ. High strength circular concrete-filled steel tubular slender beam-columns, Part I: Numerical analysis. Journal of Constructional Steel Research 2011; 67(2): 164-171.

[16] Liang QQ. High strength circular concrete-filled steel tubular slender beam-columns, Part II: Fundamental behavior. Journal of Constructional Steel Research 2011; 67(2): 172-180.

[17] Portolés JM, Romero ML, Filippou FC, Bonet JL. Simulation and design recommendations of eccentrically loaded slender concrete-filled tubular columns. Engineering Structures 2011; 33(5): 1576-93.

[18] Patel VI, Liang QQ, Hadi MNS. High strength thin-walled rectangular concrete-filled steel tubular slender beam-columns, Part I: Modeling. Journal of Constructional Steel Research 2012; 70:377-384.

[19] Patel VI, Liang QQ, Hadi MNS. High strength thin-walled rectangular concrete-filled steel tubular slender beam-columns, Part II: Behavior. Journal of Constructional Steel Research 2012; 70:368-376.

[20] Lakshmi B, Shanmugam NE. Nonlinear analysis of in-filled steel-concrete composite columns. Journal of Structural Engineering, ASCE 2002; 128(7): 922-33.

[21] Liang QQ. Performance-based analysis of concrete-filled steel tubular beam-columns, Part I: Theory and algorithms. Journal of Constructional Steel research 2009; 65(2): 363-72.

[22] Liang QQ. Performance-based analysis of concrete-filled steel tubular beam-columns, Part II: Verification and applications. Journal of Constructional Steel research 2009; 65(2): 351-62.

[23] Liang QQ, Uy B, Liew JYR. Local buckling of steel plates in concrete-filled thin-walled steel tubular beam-columns. Journal of Constructional Steel Research 2007; 63(3):396-405.

[24] Liang QQ, Patel VI, Hadi MNS. Biaxially loaded high-strength concrete-filled steel tubular slender beam-columns, Part I: Multiscale simulation. Journal of Constructional Steel Research 2011 (submitted).

[25] EN 1994-1-1, Eurocode 4: design of composite steel and concrete structures. Part 1-1, General rules and rules for buildings, CEN 2004.

Figures and tables

Table 1. Ultimate axial strengths of biaxially loaded CFST slender beam-columns.

Specimens	$B \times D \times t$ (mm)	D/t	L (mm)	e_x (mm)	e_y (mm)	e (mm)	α (°)	u_o (mm)	f'_c (MPa)	f_{sy} (MPa)	f_{su} (MPa)	E_s (GPa)	$P_{u.\exp}$ (kN)	$P_{u.num}$ (kN)	$\dfrac{P_{u.num}}{P_{u.\exp}}$	Ref.
SCH-3	200× 200 × 10.03	20	2130			38	60	0.79	37.2	313	430	205	2180	2201.1	1.01	[8]
SCH-4	200× 200 × 9.88	20	2130			38	45	0.56	39.2	317	430	205	2162	2259.2	1.04	
SCH-5	200× 200 × 10.01	20	3050			38	60	0.28	44.3	319	430	205	2037	2135.2	1.05	
SCH-6	200× 200 × 9.78	20	3050			64	45	1.12	36.1	317	430	205	1623	1601.2	0.99	
R6	80×120 × 5	24	3210	16	24	28.84	33.69		38.25	343.3	430	205	268	271.5	1.01	[9]
M2	80×120 × 5	24	3210	8	12	14.42	33.69		36.21	341	430	205	348	331.5	0.95	[10]
M3	80×120 × 5	24	3210	28	42	50.48	33.69		39.27	341	430	205	198.5	212.9	1.07	
M4	80×120 × 5	24	3210	40	24	46.65	59.03		36.04	362.5	430	205	206.8	197.1	0.95	
M5	80×120 × 5	24	3210	16	60	62.10	14.93		34.68	362.5	430	205	209.8	228.6	1.09	
M7	100×150 × 5	30	3210	10	15	18.03	33.69		39.27	346.7	430	209.6	596.2	569.9	0.96	
M9	100×150 × 5	30	3210	50	75	90.14	33.69		40.12	340	430	208.6	254.6	270.9	1.06	
Mean															1.01	
Standard deviation (SD)															0.05	
Coefficient of variation (COV)															0.05	

Table 2. Ultimate bending strengths of biaxially loaded CFST slender beam-columns.

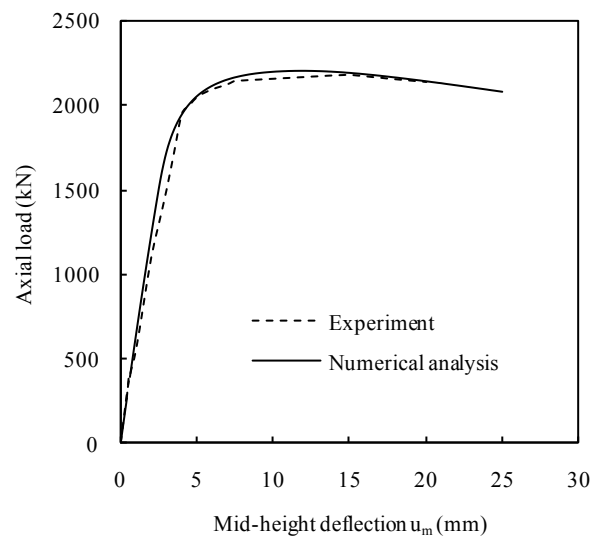| pecimens	$B \times D \times t$ (mm)	D/t	L (mm)	e_x (mm)	e_y (mm)	e (mm)	α (°)	u_o (mm)	f'_c (MPa)	f_{sy} (MPa)	f_{su} (MPa)	E_s (GPa)	$M_{n.\exp}$ (kNm)	$M_{n.num}$ (kNm)	$\dfrac{M_{n.num}}{M_{n.\exp}}$	Ref.
SCH-3	200× 200 × 10.03	20	2130			38	60	0.79	37.2	313	430	205	82.84	85.32	1.03	[8]
SCH-6	200× 200 × 9.78	20	3050			64	45	1.12	36.1	317	430	205	103.87	101.03	0.97	
R6	80×120 × 5	24	3210	16	24	28.84	33.69		38.25	343.3	430	205	7.73	8.00	1.03	[9]
M4	80×120 × 5	24	3210	40	24	46.65	59.03		36.04	362.5	430	205	9.65	8.66	0.90	[10]
M9	100×150 × 5	30	3210	50	75	90.14	33.69		40.12	340	430	208.6	22.95	25.15	1.10	
Mean															1.00	
Standard deviation (SD)															0.08	
Coefficient of variation (COV)															0.07	

Fig. 1. Comparison of computational and experimental axial load-deflection curves for specimen SCH-3.
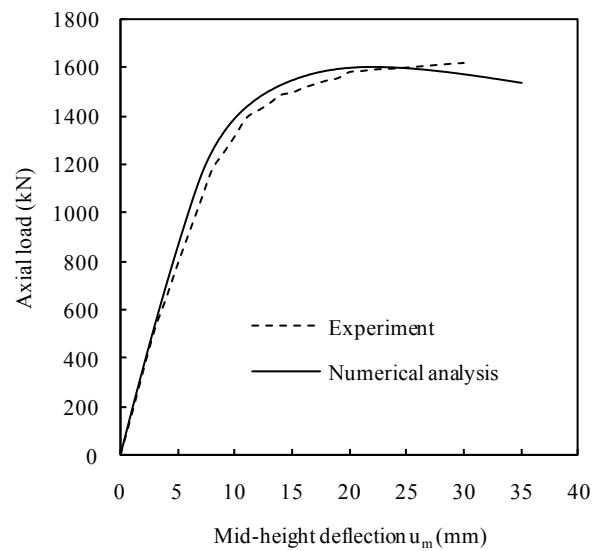
Fig. 2. Comparison of predicted and experimental axial load-deflection curves for specimen SCH-6.
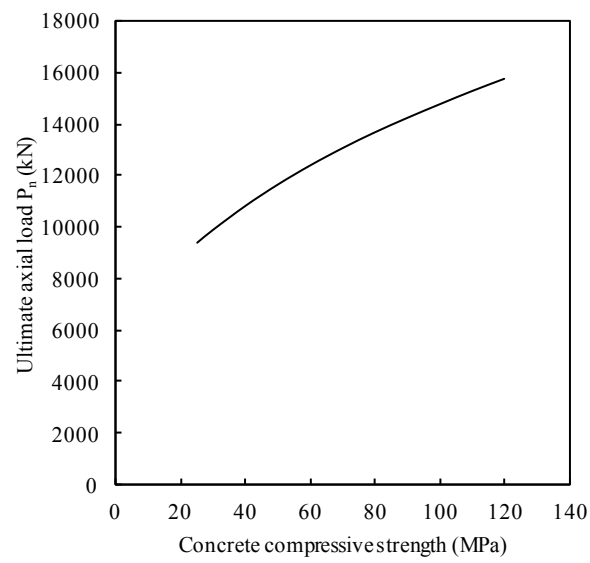
Fig. 3. Effects of concrete compressive strengths on the ultimate axial loads.
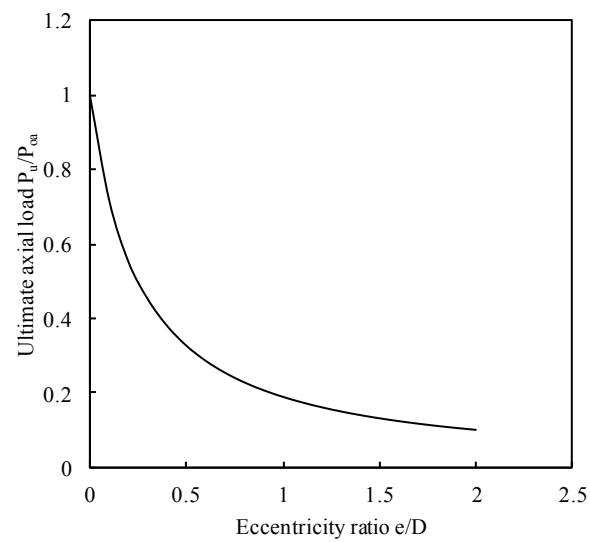
Fig. 4. Effects of e/D ratio on the ultimate axial loads.
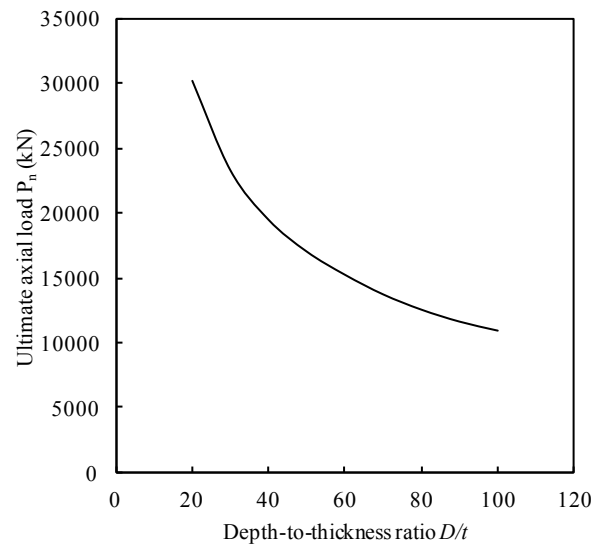
Fig. 5. Effects of D/t ratio on the ultimate axial loads.
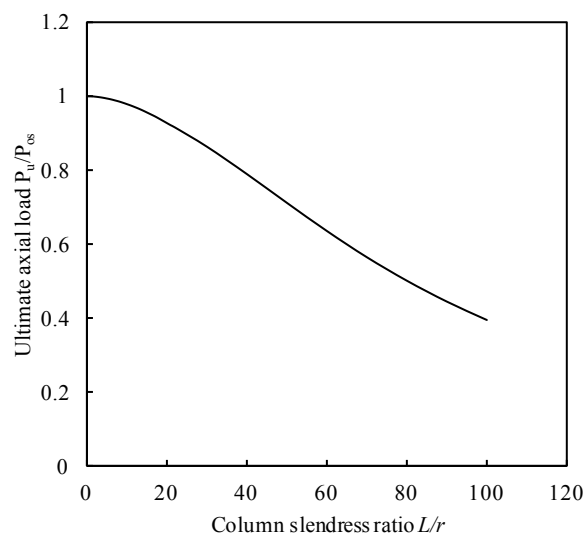
Fig. 6. Effects of column slenderness ratio on the ultimate axial loads.
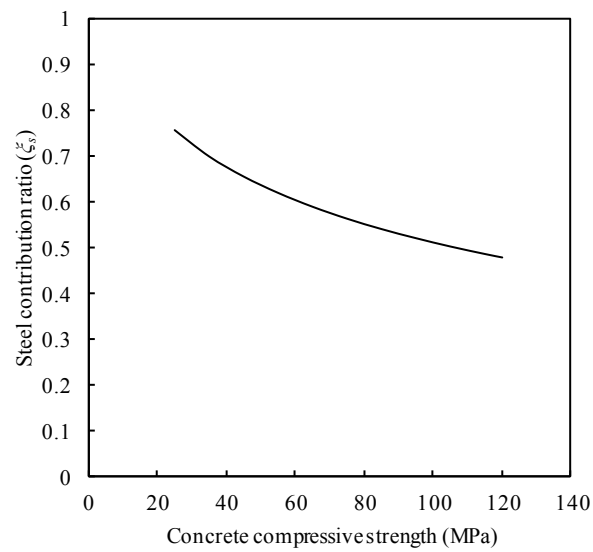
Fig. 7. Effects of concrete compressive strengths on the steel contribution ratio.
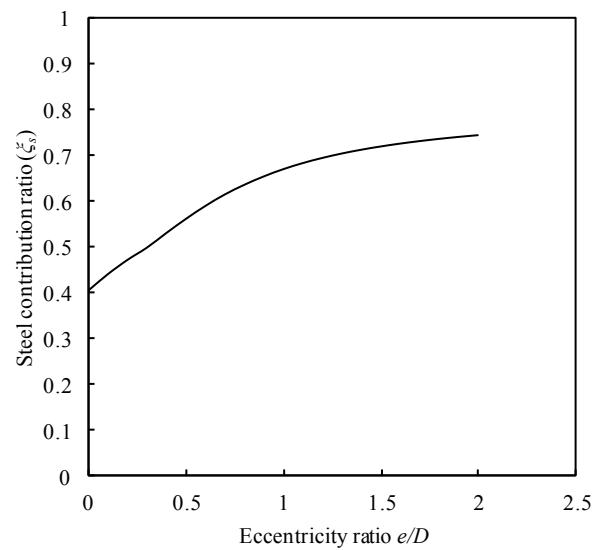
Fig. 8. Effects of e/D ratio on the steel contribution ratio.
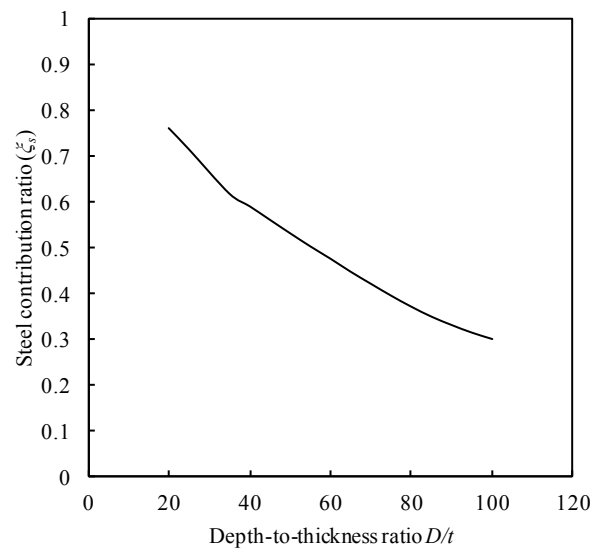
Fig. 9. Effects of D/t ratio on the steel contribution ratio.
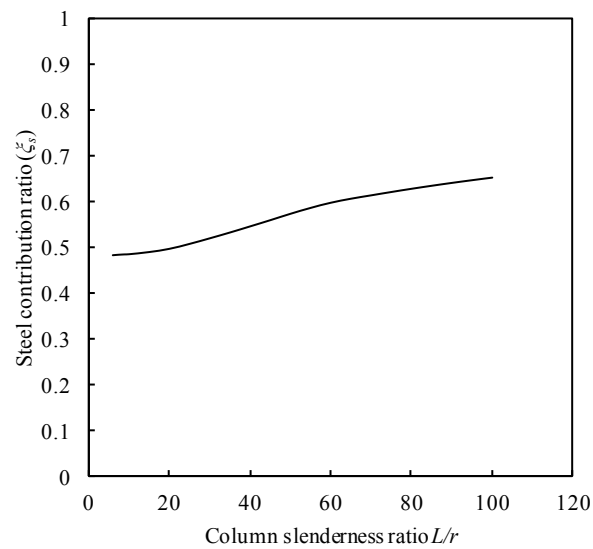
Fig. 10. Effects of column slenderness ratio on the steel contribution ratio.
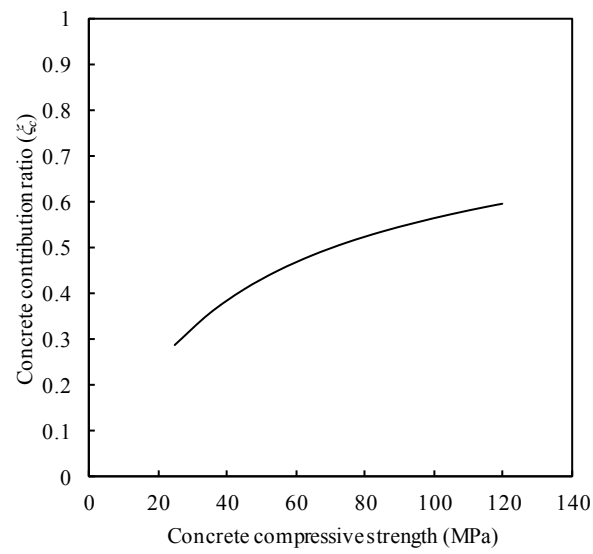
Fig. 11. Effects of concrete compressive strengths on the concrete contribution ratio.
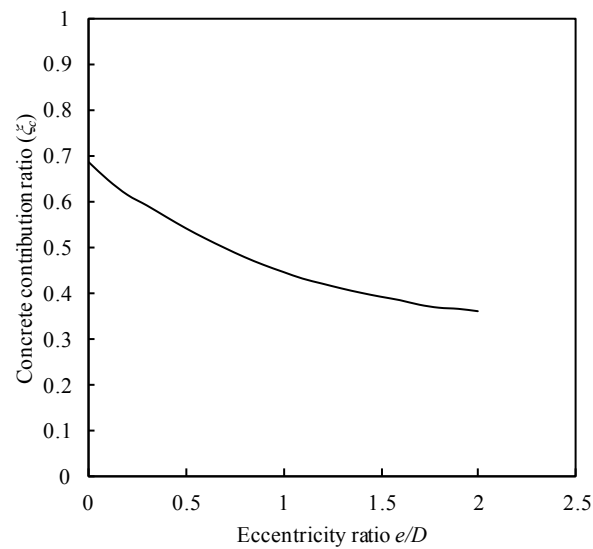
Fig. 12. Effects of e/D ratio on the concrete contribution ratio.
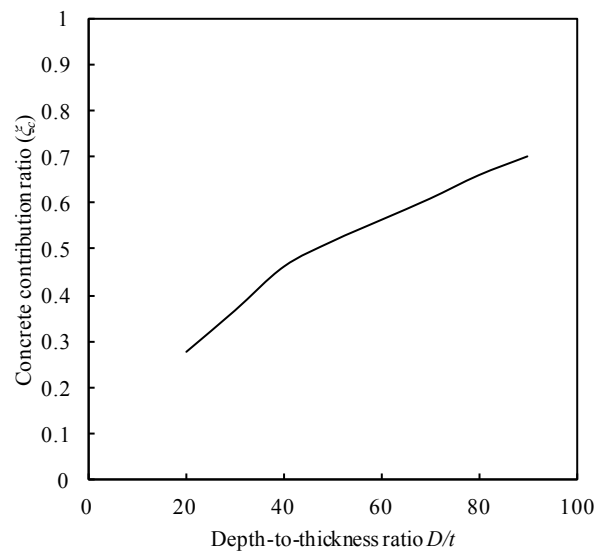
Fig. 13. Effects of D/t ratio on the concrete contribution ratio.
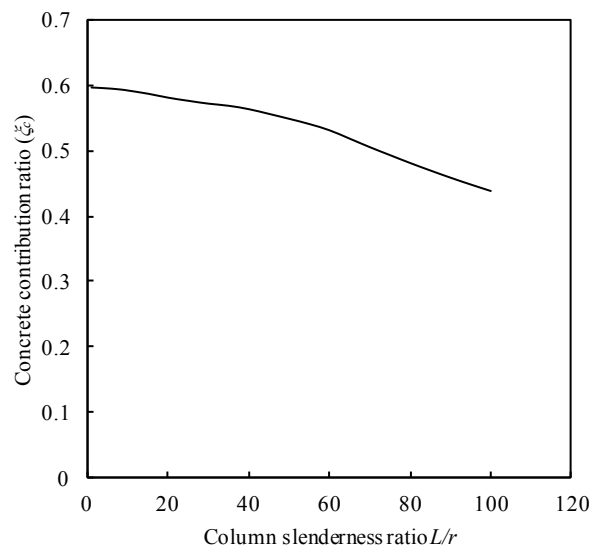
Fig. 14. Effects of column slenderness ratio on the concrete contribution ratio.
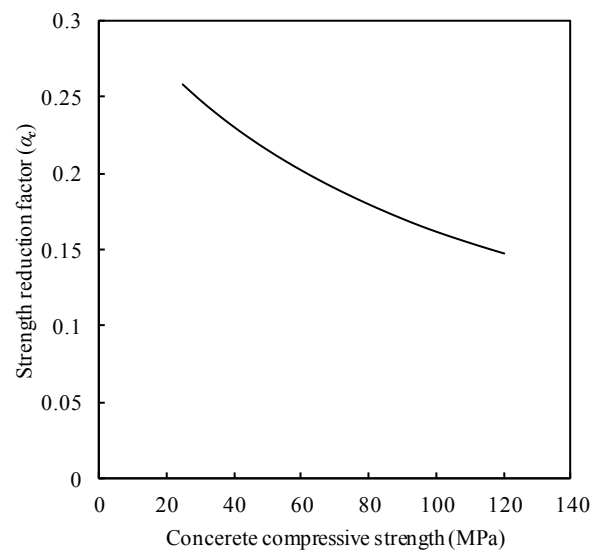
Fig. 15. Effects of concrete compressive strengths on the strength reduction factor.
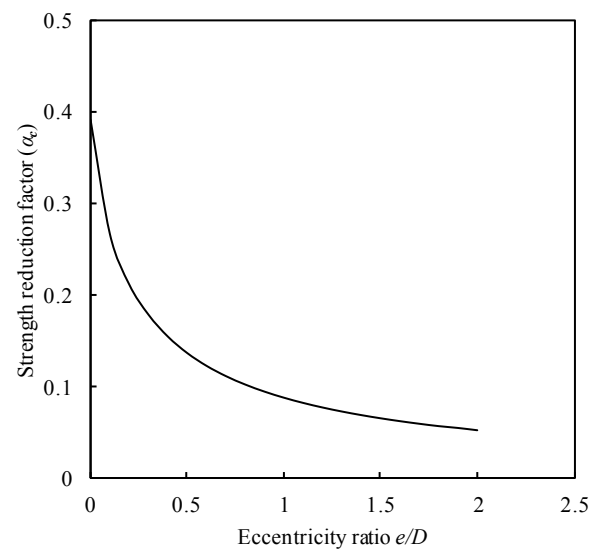
Fig. 16. Effects of e/D ratio on the strength reduction factor.
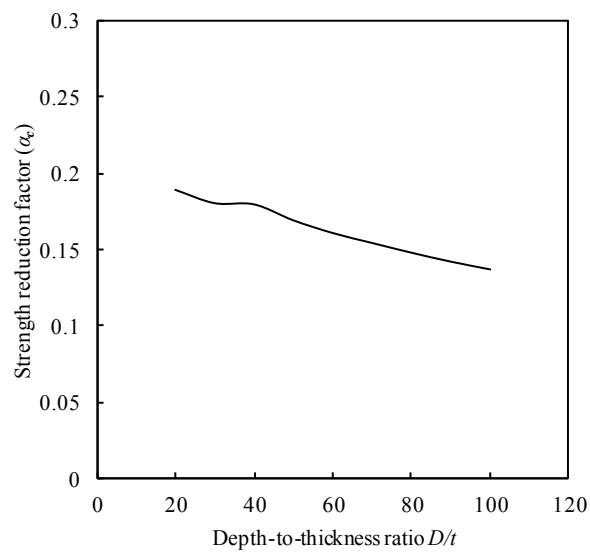
Fig. 17. Effects of D/t ratio on the strength reduction factor.
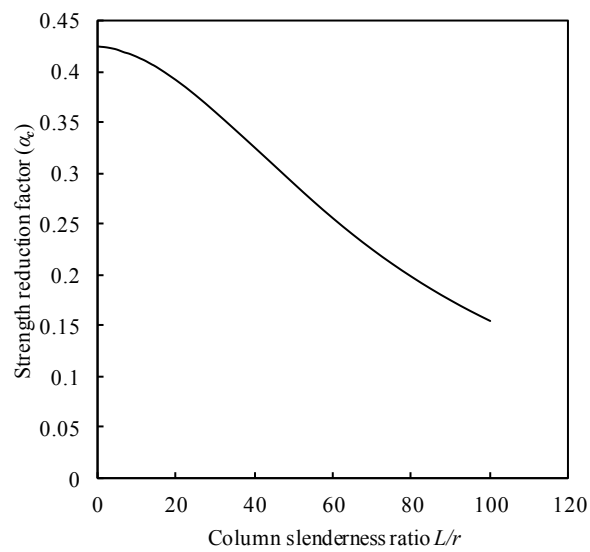
Fig. 18. Effects of column slenderness ratio on the strength reduction factor.
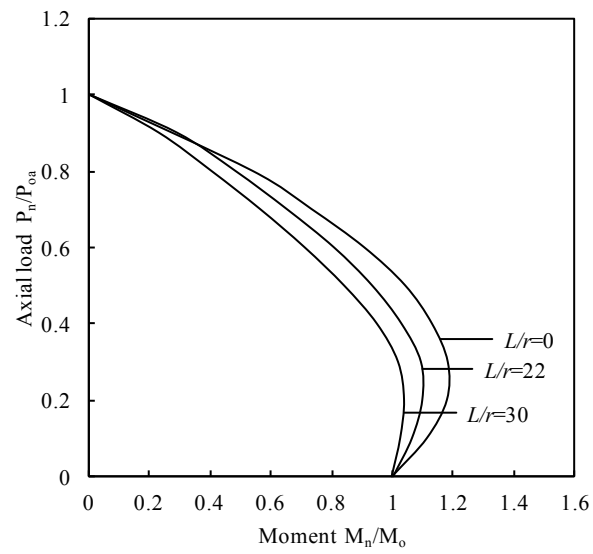
Fig. 19. Effects of column slenderness ratio on the strength envelopes.

4.5 CONCLUDING REMARKS

A multiscale numerical model has been presented in this chapter for the design and nonlinear analysis of high strength thin-walled rectangular CFST slender beam-columns under axial load and biaxial bending. The multiscale numerical model was formulated based on the fiber element method. Müller's method algorithms were developed. These algorithms were implemented in the numerical model and used to iterate the neutral axis depth in a composite cross-section and adjust the curvature at the column ends in a slender beam-column. Axial load-deflection and axial load-moment interaction analysis procedures have been presented. Steel contribution ratio, concrete contribution ratio and strength reduction factor were proposed to quantify the performance of thin-walled rectangular CFST slender beam-columns. The effects of concrete compressive strengths, steel yield strengths, loading eccentricity ratios, column slenderness ratios and depth-to-thickness ratio on the ultimate axial load, concrete contribution ratio, steel contribution ratio and strength reduction factor were investigated.

The multiscale numerical model can predict the complete axial load-deflection responses and axial load-moment interaction diagrams. The ultimate axial load of CFST beam-columns is found to increase with an increase in concrete compressive strength but decreases with increasing the loading eccentricity ratio, depth-to-thickness ratio and column slenderness ratio. The results indicate that increasing concrete compressive strength and depth-to-thickness ratio decreases the steel contribution ratio. However, the steel contribution ratio of CFST beam-columns increases with an increase in the loading eccentricity ratio and column slenderness ratio.

Chapter 5

CIRCULAR AND RECTANGULAR CFST SLENDER BEAM-COLUMNS WITH PRELOAD EFFECTS

5.1 INTRODUCTION

In the construction of a composite building, hollow steel tubes are erected first. These hollow steel tubes are subjected to preloads from upper floors before infilling of the wet concrete. These preloads induce initial stresses and deformations which have a significant effect on the performance of CFST slender beam-columns. The nonlinear inelastic behavior of preloaded high strength CFST slender beam-columns is discussed in this chapter. Fiber element models are developed for the nonlinear analysis of circular and rectangular CFST slender beam-columns with preload effects. Material models for confined concrete and structural steels are incorporated in the numerical model. The effects of local buckling and concrete confinement are also considered in the fiber element model. In addition, initial geometric imperfection of the slender beam-columns is incorporated in the numerical model. The fiber element model is validated against

tests conducted by independent researchers on circular and rectangular CFST slender beam-columns. Furthermore, important parameters that influence the structural performance of CFST slender beam-columns are investigated in a parametric study.

This chapter includes the following papers:

[1]   Patel, V. I., Liang, Q. Q. and Hadi, M. N. S., "Numerical analysis of circular concrete-filled steel tubular slender beam-columns with preload effects", *International Journal of Structural Stability and Dynamics*, 2013, 13(3), 1250065 (23 pages).

[2]   Patel, V. I., Liang, Q. Q. and Hadi, M. N. S., "Nonlinear analysis of rectangular concrete-filled steel tubular slender beam-columns with preload effects", *Journal of Constructional Steel Research* (submitted on 16 August 2012).

VICTORIA UNIVERSITY
MELBOURNE AUSTRALIA

PART B:

DECLARATION OF CO-AUTHORSHIP AND CO-CONTRIBUTION: PAPERS INCORPORATED IN THESIS BY PUBLICATION

This declaration is to be completed for each conjointly authored publication and placed at the beginning of the thesis chapter in which the publication appears.

Declaration by [candidate name]:	Signature:	Date:
VIPULKUMAR ISHVARBHAI PATEL	███████	11/01/2013

Paper Title:

Numerical analysis of circular high strength concrete-filled steel tubular slender beam-columns with preload effects

In the case of the above publication, the following authors contributed to the work as follows:

Name	Contribution%	Nature of contribution
Vipulkumar Ishvarbhai Patel	60	Literature review Developed a numerical model Verified the numerical model Carried out the parametric study Wrote the manuscript
Qing Quan Liang	30	Initial concept Provided critical revision of the article Manuscript submission
Muhammad N.S.Hadi	10	Provided critical revision of the article Final approval of the manuscript

VICTORIA UNIVERSITY
MELBOURNE AUSTRALIA

DECLARATION BY CO-AUTHORS

The undersigned certify that:

1. They meet criteria for authorship in that they have participated in the conception, execution or interpretation of at least that part of the publication in their field of expertise;

2. They take public responsibility for their part of the publication, except for the responsible author who accepts overall responsibility for the publication;

3. There are no other authors of the publication according to these criteria;

4. Potential conflicts of interest have been disclosed to **a)** granting bodies, **b)** the editor or publisher of journals or other publications, and **c)** the head of the responsible academic unit; and

5. The original data is stored at the following location(s):

Location(s): College of Engineering and Science, Victoria University, Melbourne, Victoria, Australia.

and will be held for at least five years from the date indicated below:

		Date
Signature 1		11/01/2013
Signature 2		11/01/2013
Signature 3		11/01/2013
Signature 4		

VICTORIA UNIVERSITY
MELBOURNE AUSTRALIA

PART B:

DECLARATION OF CO-AUTHORSHIP AND CO-CONTRIBUTION: PAPERS INCORPORATED IN THESIS BY PUBLICATION

This declaration is to be completed for each conjointly authored publication and placed at the beginning of the thesis chapter in which the publication appears.

Declaration by [candidate name]:	Signature:	Date:
VIPULKUMAR ISHVARBHAI PATEL		11/01/2013

Paper Title:

Numerical analysis of rectangular high strength concrete-filled steel tubular slender beam-columns with preload effects

In the case of the above publication, the following authors contributed to the work as follows:

Name	Contribution%	Nature of contribution
Vipulkumar Ishvarbhai Patel	60	Literature review Developed a numerical model Verified the numerical model Carried out the parametric study Wrote the manuscript
Qing Quan Liang	30	Initial concept Provided critical revision of the article Manuscript submission
Muhammad N.S.Hadi	10	Provided critical revision of the article Final approval of the manuscript

VICTORIA UNIVERSITY
MELBOURNE AUSTRALIA

DECLARATION BY CO-AUTHORS

The undersigned certify that:

1. They meet criteria for authorship in that they have participated in the conception, execution or interpretation of at least that part of the publication in their field of expertise;

2. They take public responsibility for their part of the publication, except for the responsible author who accepts overall responsibility for the publication;

3. There are no other authors of the publication according to these criteria;

4. Potential conflicts of interest have been disclosed to **a)** granting bodies, **b)** the editor or publisher of journals or other publications, and **c)** the head of the responsible academic unit; and

5. The original data is stored at the following location(s):

Location(s): College of Engineering and Science, Victoria University, Melbourne, Victoria, Australia.

and will be held for at least five years from the date indicated below:

		Date
Signature 1		11|01|2013
Signature 2		11/01/2013
Signature 3		11/01/2013
Signature 4		

Numerical analysis of circular concrete-filled steel tubular slender beam-columns with preload effects by *Vipulkumar Ishavarbhai Patel, Qing Quan Liang and Muhammad N.S. Hadi authors* was published in the peer review journal, *International Journal of Structural Stability and Dynamics, 13/3, 2013.*

The published article is available from: https://doi.org/10.1142/S0219455412500654

Nonlinear Analysis of Rectangular Concrete-Filled Steel Tubular Slender Beam-Columns with Preload Effects

Vipulkumar Ishvarbhai Patel[a], Qing Quan Liang[a,]*, Muhammad N. S. Hadi[b]

[a]School of Engineering and Science, Victoria University, PO Box 14428, Melbourne, VIC 8001, Australia

[b]School of Civil, Mining and Environmental Engineering, University of Wollongong, Wollongong, NSW 2522, Australia

Corresponding author:

Dr. Qing Quan Liang
School of Engineering and Science
Victoria University
PO Box 14428
Melbourne VIC 8001
Australia
Phone: +61 3 9919 4134
Fax: +61 3 9919 4139
E-mail: Qing.Liang@vu.edu.au

Nonlinear analysis of rectangular concrete-filled steel tubular slender beam-columns with preload effects

Vipulkumar Ishvarbhai Patel[a], Qing Quan Liang[a,*], Muhammad N. S. Hadi[b]

[a] School of Engineering and Science, Victoria University, PO Box 14428, Melbourne, VIC 8001, Australia
[b] School of Civil, Mining and Environmental Engineering, University of Wollongong, Wollongong, NSW 2522, Australia

ABSTRACT

This paper is concerned with the nonlinear analysis and behavior of biaxially loaded thin-walled rectangular concrete-filled steel tubular (CFST) slender beam-columns with preload effects. An effective theoretical model is developed for the nonlinear analysis of biaxially loaded CFST slender beam-columns that considers the effects of preloads, local buckling, initial geometric imperfections and second order. Deflections caused by preloads are treated as initial geometric imperfections in the global stability analysis of CFST slender beam-columns. Analysis procedures are proposed that computes the complete load-deflection responses and strength envelopes of thin-walled CFST slender beam-columns considering preload effects. The theoretical model is validated by comparisons with existing experimental results. The behavior of thin-walled CFST slender beam-column under combined axial load and biaxial bending is studied by using the computer program developed based on the proposed theoretical model. Parameters examined include local buckling, preload ratio, depth-to-thickness ratio, column

* Corresponding author. Tel.: 61 3 9919 4134; fax: +61 3 9919 4139.
  E-mail address: Qing.Liang@vu.edu.au (Q. Q. Liang)

slenderness, loading eccentricity and steel yield strength. The results obtained indicate that the preloads on the steel tubes significantly reduce the stiffness and strength of CFST slender beam-columns with a maximum strength reduction of more than 15.8%. The theoretical model proposed allows for the structural designer to analyze and design biaxially loaded CFST slender beam-columns made of compact, non-compact or slender steel sections subjected to preloads from the upper floors of a high-rise composite building during construction.

Keywords: Concrete-filled steel tubes; Biaxial bending; Local buckling; Nonlinear analysis; Slender beam-columns.

1. Introduction

Rectangular concrete-filled steel tubular (CFST) slender beam-columns have been widely used in the construction of modern high-rise composite buildings because of their high strength and stiffness performance. During the construction of a high-rise composite building, hollow steel tubes are subjected to preloads arising from construction loads and permanent loads of the upper floors before infilling of the wet concrete. The stresses and deformations in the hollow steel tubes induced by the preloads might significantly reduce the ultimate strengths of CFST slender beam-columns. Experimental and theoretical studies on biaxially loaded thin-walled rectangular CFST slender beam-columns with preload effects have not been reported in the literature. Therefore, an effective theoretical model for the nonlinear analysis and design of biaxially loaded thin-walled CFST slender beam-columns incorporating preload effects is much needed.

Extensive experimental studies on the behavior of CFST columns without preload effects have been conducted [1-11]. Test results demonstrated that the confinement effect provided by the rectangular steel tube did not increase the compressive strength of the concrete core but considerably improved its ductility [1]. In addition, local buckling of the steel tubes was found to remarkably reduce the ultimate strength and stiffness of thin-walled CFST columns [12-17]. Moreover, Liang et al. [16, 17] utilized the finite element method to investigate the local and post-local buckling behavior of steel plates in double skin composite panels and thin-walled CFST columns under axial load and biaxial bending. They proposed a set of formulas for determining the initial local buckling stresses and post-local buckling strengths of steel plates in CFST columns under stress gradients. These formulas can be incorporated in numerical models to account for local buckling effects in the nonlinear analysis of thin-walled CFST columns under biaxial bending.

There have been very limited experimental investigations on CFST columns with preload effects. The effects of preload on the ultimate axial strengths of eccentrically loaded circular CFST slender beam-columns were studied experimentally by Zha [18] and Zhang et al. [19]. Han and Yao [20] described experimental investigations on eccentrically loaded normal strength rectangular CFST columns including preload effects. The constant preload was applied to the steel tube by pre-stressing bars before filling the wet concrete. Test parameters included the preload ratio, column slenderness and loading eccentricity. Test results indicated that the preload on the steel tube caused initial deflections which reduced the ultimate axial strengths of CFST beam-columns.

Liew and Xiong [21] undertook tests on axially loaded circular CFST short and slender columns with preloads on the steel tubes. Their study showed that the preload on the steel tube might reduce the ultimate axial strength of the circular CFST slender beam-column by 15%, provided that it was greater than 60% of the ultimate axial strength of the hollow steel tube. The strength and behavior of short circular CFST columns were not affected by preloads.

Analytical and numerical models have been developed for simulating the nonlinear inelastic behavior of CFST columns without preload effects [22-24]. A semi-analytical model was presented by Lakshmi and Shanmugam [25] that simulates the behavior of CFST slender columns under axial load and biaxial bending. A generalized displacement control method was employed in the model to solve nonlinear equilibrium equations. Liang [26, 27] developed a performance-based analysis (PBA) technique for predicting the ultimate strength and ductility of biaxially loaded thin-walled CFST short beam-columns without preload effects. The PBA technique incorporated effective width formulas proposed by Liang et al. [17] to account for the effects of progressive local buckling. Moreover, numerical models that do not consider preload effects were developed by Patel et al. [28, 29] and Liang et al. [30] that simulate the load-deflection responses and load-moment interaction diagrams of high strength thin-wall rectangular CFST slender beam-columns under combined axial load and bending.

Xiong and Zha [31] utilized the finite element analysis ABAQUS program to study the behavior of eccentrically loaded circular CFST slender beam-columns considering preload effects. It was observed that the ultimate axial strengths of CFST columns

decreased with increasing the preloads on the steel tubes. They proposed a simplified formula for calculating the ultimate strength of CFST beam-columns subjected to axial or eccentric loading. However, their model and formula are applicable only to circular CFST slender beam-columns. Liew and Xiong [21] proposed a design method for determining the strength of axially loaded circular CFST slender columns incorporating preload effects. A numerical model was proposed by Patel et al. [32] for predicting the load-deflection behavior of eccentrically loaded circular CFST slender beam-columns accounting for the effects of preloads, initial geometric imperfections, concrete confinement and second order.

This paper has two aims. It presents firstly a theoretical model for the nonlinear inelastic analysis of biaxially loaded rectangular CFST slender beam-columns incorporating preload effects. Theoretical analyses of cross-sections and slender beam-columns accounting for the effects of preloads and local buckling are described together with analysis procedures and numerical solution algorithms. The second aim of this paper is to investigate the fundamental behavior of biaxially loaded thin-walled CFST slender beam-columns with various preload ratios, depth-to-thickness ratios, columns slenderness ratios, loading eccentricities and steel yield strengths.

2. Nonlinear analysis of cross-sections

2.1. Fiber element method

The inelastic behavior of CFST cross-sections is modeled by the fiber element method [26]. The column cross-section is divided into fine fiber elements as shown in Fig. 1. Each fiber element can be assigned either steel or concrete material properties. Fiber stresses are calculated from fiber strains using material uniaxial stress-strain relationships. It is assumed that there is no slippage between the steel tube and the concrete so that the plane section remains plane after deformation. This results in a linear strain distribution throughout the depth of the section as depicted in Fig. 1. Note that the fiber strain is a function of the curvature (ϕ), and orientation (θ) and depth (d_n) of the neutral axis in the section under axial load and biaxial bending.

For $0^o \leq \theta < 90^o$, the beam-column is subjected to biaxial bending and the strains in concrete and steel fibers can be calculated by the following equations given by Liang [26]:

$$y_{n,i} = \left| x_i - \frac{B}{2} \right| \tan\theta + \left(\frac{D}{2} - \frac{d_n}{\cos\theta} \right) \tag{1}$$

$$\varepsilon_i = \begin{cases} \phi \left| y_i - y_{n,i} \right| \cos\theta & \text{for } y_i \geq y_{n,i} \\ -\phi \left| y_i - y_{n,i} \right| \cos\theta & \text{for } y_i < y_{n,i} \end{cases} \tag{2}$$

where $y_{n,i}$ is the distance from the centroid of each fiber to the neutral axis, x_i and y_i are the coordinates of the fiber i, B and D are the width and depth of the cross-section and ε_i is the strain at the ith fiber element. For $\theta = 90^o$, the beam-column is subjected to uniaxial bending and fiber strain calculation is given by Liang [26]. In the strain calculation, compressive strains are taken as positive while tensile strains are taken as

negative. The strain at the extreme fiber $\left(\varepsilon_t\right)$ is the product of the neutral axis depth and the curvature.

2.2. Constitutive models for concrete and steel

The general stress-strain curve for concrete in rectangular CFST columns suggested by Liang [26] is shown in Fig. 2. The confinement effect which increases the ductility of concrete in rectangular CFST columns is included in the stress-strain curve for concrete. The concrete stress from O to A on the stress-strain curve is calculated based on the equations given by Mander et al. [33] as:

$$\sigma_c = \frac{f_{cc}'\lambda\left(\dfrac{\varepsilon_c}{\varepsilon_{cc}'}\right)}{\lambda - 1 + \left(\dfrac{\varepsilon_c}{\varepsilon_{cc}'}\right)^{\lambda}} \tag{3}$$

$$\lambda = \frac{E_c}{E_c - \left(\dfrac{f_{cc}'}{\varepsilon_{cc}'}\right)} \tag{4}$$

$$E_c = 3320\sqrt{\gamma_c f_c'} + 6900 \quad \text{(MPa)} \tag{5}$$

where σ_c is the compressive concrete stress, f_{cc}' is the effective compressive strength of concrete, f_c' is the compressive strength of concrete cylinder, ε_c is the compressive concrete strain, ε_{cc}' is the strain at f_{cc}'. The Young's modulus of concrete E_c is given by ACI 318-11 [34]. The effective compressive strength f_{cc}' in Eq. (3) is taken as $\gamma_c f_c'$,

where γ_c is the strength reduction factor proposed by Liang [26] to account for the column section size effects and is expressed by

$$\gamma_c = 1.85 D_c^{-0.135} \qquad\qquad (0.85 \le \gamma_c \le 1.0) \qquad\qquad (6)$$

where D_c is taken as the larger of $(B - 2t)$ and $(D - 2t)$ for a rectangular cross-section and t is the thickness of the steel tube wall.

The strain ε_{cc}' corresponding to f_{cc}' is taken as 0.002 when the effective compressive strength of concrete is under 28 MPa while it is taken as 0.003 for concrete strength over 82 MPa. The strain ε_{cc}' is determined by the linear interpolation for the effective compressive strength of concrete between 28 and 82 MPa.

The concrete stress from A to D on the stress-strain curve is calculated using on the following equations given by Liang [26]:

$$\sigma_c = \begin{cases} f_{cc}' & \text{for } \varepsilon_{cc}' < \varepsilon_c \le 0.005 \\ \beta_c f_{cc}' + 100\left(0.015 - \varepsilon_c\right)\left(f_{cc}' - \beta_c f_{cc}'\right) & \text{for } 0.005 < \varepsilon_c \le 0.015 \\ \beta_c f_{cc}' & \text{for } \varepsilon_c > 0.015 \end{cases} \qquad (7)$$

where β_c was proposed by Liang [26] based on experimental results presented by Tomii and Sakino [35] to account for the confinement effect on the post-peak behavior and is given by

$$
\beta_c = \begin{cases} 1.0 & \text{for } \dfrac{B_s}{t} \leq 24 \\[2ex] 1.5 - \dfrac{1}{48}\dfrac{B_s}{t} & \text{for } 24 < \dfrac{B_s}{t} \leq 48 \\[2ex] 0.5 & \text{for } \dfrac{B_s}{t} > 48 \end{cases}
\tag{8}
$$

where B_s is taken as the larger of B and D for a rectangular cross-section.

The stress-strain curve for concrete in tension is shown in Fig. 2. In the theoretical model, the tensile strength of concrete is taken as $0.6\sqrt{f'_{cc}}$ while the ultimate tensile strain is taken as 10 times of the strain at concrete cracking.

Fig. 3 shows the stress-strain curves for structural steels. The steel generally follows the same stress-strain relationship under the tension and compression. For mild structural steels, an idealized tri-linear stress-strain curve is assumed as shown in Fig. 3. A linear-rounded-linear stress-strain curve is used for cold-formed steels but the rounded part is replaced by a straight line for high strength steels. The rounded part for cold-formed steels as shown in Fig. 3 can be modeled by the formula given by Liang [26]. For high strength and cold-formed steels, the hardening strain ε_{st} is taken as 0.005 while it is considered to be $10\varepsilon_{sy}$ for mild structural steels in the theoretical model. The ultimate strain ε_{su} of steels is assumed to be 0.2.

2.3. Local and post-local buckling

Thin steel plates in contact with concrete are constrained to buckle locally outward when subjected to compressive stress gradients as depicted in Fig. 4. Local buckling significantly reduces the strength and stiffness of CFST beam-columns with large depth-to-thickness ratios. Liang et al. [17] proposed formulas that consider the effects of geometric imperfections and residual stresses for estimating the initial local buckling stresses of thin steel plates under stress gradients. Their formulas have been implemented in the theoretical model and are expressed by

$$\frac{\sigma_{1c}}{f_{sy}} = a_1 + a_2 \left(\frac{b}{t} \right) + a_3 \left(\frac{b}{t} \right)^2 + a_4 \left(\frac{b}{t} \right)^3 \tag{9}$$

where σ_{1c} is the maximum edge stress in a steel tube wall when initial local buckling occurs, f_{sy} is the yield strength of the steel tube, b is the clear width of a steel flange or web in a CFST column section and the constants a_1, a_2, a_3 and a_4 are given by Liang et al. [17].

The effective width concept is commonly used to describe the post-local buckling behavior of thin steel plates under uniform compression or stress gradients as illustrated in Fig. 4. The effective widths b_{e1} and b_{e2} of the steel plate under stress gradients as shown in Fig. 4 are given by Liang et al. [17] as

$$\frac{b_{e1}}{b} = \begin{cases} 0.2777 + 0.01019 \left(\frac{b}{t}\right) - 1.972 \times 10^{-4} \left(\frac{b}{t}\right)^2 + 9.605 \times 10^{-7} \left(\frac{b}{t}\right)^3 & \text{for } \alpha_s > 0.0 \\ 0.4186 - 0.002047 \left(\frac{b}{t}\right) + 5.355 \times 10^{-5} \left(\frac{b}{t}\right)^2 - 4.685 \times 10^{-7} \left(\frac{b}{t}\right)^3 & \text{for } \alpha_s = 0.0 \end{cases} \tag{10}$$

$$\frac{b_{e2}}{b} = \left(1 + \phi_s\right) \frac{b_{e1}}{b} \tag{11}$$

where $\phi_s = 1 - \alpha_s$ and α_s is the stress gradient coefficient which is the ratio of the minimum edge stress σ_2 to the maximum edge stress σ_1 acting on the plate.

The post-local buckling behavior of thin steel plates can also be described by the effective strength concept. Liang et al. [17] proposed effective strength formulas for determining the post-local buckling strengths of steel plates in thin-walled CFST beam-columns under axial load and biaxial bending. The ultimate strength of steel plates under a stress gradient greater than zero can be calculated approximately by

$$\frac{\sigma_{1u}}{f_{sy}} = \left(1 + 0.5\phi_s\right) \frac{\sigma_u}{f_{sy}} \qquad \left(0 \le \phi < 1.0\right) \tag{12}$$

where σ_{1u} is the ultimate stress that corresponds to the maximum edge stress σ_1 at the ultimate state and σ_u is the ultimate stress of the steel plate under uniform compression. For intermediate stress gradients, the ultimate stress σ_{1u} is calculated by linear interpolations.

The progressive post-local buckling is modeled by gradually redistributing the normal stresses within the steel tube walls under increasing compression load based on the stress levels as suggested by Liang [26]. After initial local buckling, steel fiber stresses are updated to account for post-local buckling effects.

2.4. Stress resultants

The internal axial force and bending moments of the CFST column section can be determined by the following equations:

$$P = \sum_{i=1}^{ns} \sigma_{s,i} A_{s,i} + \sum_{j=1}^{nc} \sigma_{c,j} A_{c,j} \tag{13}$$

$$M_x = \sum_{i=1}^{ns} \sigma_{s,i} A_{s,i} y_i + \sum_{j=1}^{nc} \sigma_{c,j} A_{c,j} y_j \tag{14}$$

$$M_y = \sum_{i=1}^{ns} \sigma_{s,i} A_{s,i} x_i + \sum_{j=1}^{nc} \sigma_{c,j} A_{c,j} x_j \tag{15}$$

where P is the axial force, $\sigma_{s,i}$ is the stress of steel fiber i, $A_{s,i}$ is the area of steel fiber i, $\sigma_{c,j}$ is the stress of concrete fiber j, $A_{c,j}$ is the area of concrete fiber j, M_x is the bending moment about the x-axis, M_y is the bending moment about the y-axis, x_i and y_i are the coordinates of steel element i, x_j and y_j are the coordinates of concrete element j, ns is the total number of steel fiber elements and nc is the total number of concrete fiber elements.

3. Nonlinear analysis of slender beam-columns

3.1. Theory

The load control analysis procedure proposed by Patel et al. [32] is used to determine the mid-height deflection u_{mo} of the hollow steel tube subjected to preload. In the analysis, the internal moment M_{mi} at the mid-height of the hollow steel tube is determined from the load-moment-curvature relationship. The curvature ϕ_{mo} at the mid-height of the steel tube is adjusted until the moment equilibrium is obtained at its mid-height. The deflection u_{mo} at the mid-height of the hollow steel tube can be calculated from the curvature ϕ_{mo}. It is assumed that the hollow steel tube does not buckle under the given preload. The preload ratio is defined as

$$\beta_a = \frac{P_{pre}}{P_{us}} \tag{16}$$

where P_{pre} is the preload applied to the hollow steel tube and P_{us} is the ultimate axial strength of the hollow steel tube including local buckling effects.

The curvature at the mid-height of the CFST beam-column can be obtained as

$$\phi_m = \left(\frac{\pi}{L}\right)^2 u_m \tag{17}$$

where L is the effective length of the CFST beam-column and u_m is the mid-height deflection of the CFST beam-column.

The mid-height deflection u_{mo} of the steel tube caused by preloads is treated as the initial geometric imperfection in the CFST beam-column. The external moment at the mid-height of the CFST beam-column with preload effects can be determined as

$$M_{me} = P\left(e + u_o + u_{mo} + u_m\right) \tag{18}$$

where P is the applied load, e is the eccentricity of the applied load, u_o is the initial geometric imperfection at the mid-height of the hollow steel tube and u_{mo} is the mid-height deflection of the hollow steel tube under the preload.

In the nonlinear analysis of CFST slender beam-column, the mid-height deflection u_m of the CFST slender beam-column under axial load and biaxial bending is gradually increased until the ultimate axial strength is obtained or deflection limit is reached. The curvature ϕ_m at the mid-height of the CFST beam-column can be calculated from the deflection u_m. For this curvature, the applied axial load P is determined by solving for the internal force that satisfies the equilibrium condition in which the external moment M_{me} is equal to the internal moment M_{mi} at the mid-height of the CFST beam-column. The Müller's method [36] is used to adjust the depth and orientation of the neutral axis in order to maintain the moment equilibrium at the mid-height of the CFST slender beam-column. The equilibrium equations for beam-columns under biaxial loads are:

$$M_{me} - M_{mi} = 0 \tag{19}$$

$$\tan\alpha - \frac{M_y}{M_x} = 0 \tag{20}$$

where M_{mi} is the resultant internal moment which is calculated as $M_{mi} = \sqrt{M_x^2 - M_y^2}$

and α is the angle of the applied load with respect to y-axis as depicted in Fig. 1.

3.2. Analysis procedure

Computational algorithms are shown in Fig. 5 that compute the load-deflection responses of rectangular CFST slender beam-columns with preload and local buckling effects. The main steps of the analysis procedure are given as follows:

(1) Input data.

(2) Discretize the composite section into fine fiber elements.

(3) Calculate the mid-height deflection u_{mo} of the hollow steel tube using the load control procedure.

(4) Set $u_o = u_o + u_{mo}$.

(5) Initialize the mid-height deflection of the CFST beam-column: $u_m = \Delta u_m$.

(6) Calculate the curvature ϕ_m at the mid-height of the CFST beam-column.

(7) Adjust the neutral axis depth d_n using the Müller's method.

(8) Compute stress resultants P and M_{mi} considering local buckling.

(9) Calculate the residual moment $r_m^a = M_{me} - M_{mi}$.

(10) Repeat Steps (7)-(9) until $\left| r_m^a \right| < \varepsilon_k$.

(11) Compute bending moments M_x and M_y.

(12) Adjust the orientation (θ) of the neutral axis using the Müller's method.

(13) Calculate the residual moment $r_m^b = \tan\alpha - \dfrac{M_y}{M_x}$.

(14) Repeat Steps (7)-(13) until $\left| r_m^b \right| < \varepsilon_k$.

(15) Increase the deflection at mid-height of the CFST beam-column by $u_m = u_m + \Delta u_m$.

(16) Repeat Steps (6)-(15) until the ultimate axial load P_n is obtained or the deflection

limit is reached.

(18) Plot the load-deflection curve.

In the above analysis procedure, the convergence tolerance ε_k is set to 10^{-4}. The computational procedure proposed can predict the complete load-deflection responses of biaxially loaded rectangular CFST slender beam-columns with preload and local buckling effects.

3.3. Development of strength envelopes

The load-deflection analysis procedure can be used to generate strength envelopes by varying the loading eccentricity. The ultimate axial strength P_n is calculated by specifying the eccentricity e of the applied load in the load-deflection analysis. The ultimate bending strength M_n for a given loading eccentricity e and ultimate axial load

P_n is calculated as $M_n = P_n \times e$. A pair of the ultimate bending strength M_n and the ultimate axial load P_n is used to plot the strength envelope. Note that the pure axial load P_{oa} is calculated by specifying the eccentricity of the applied load to zero in the load-deflection analysis procedure. However, the load-deflection procedure is not efficient for determining the pure bending strength. Therefore, the pure bending strength of a slender beam-column is obtained by specifying the axial load to zero in the load-moment interaction analysis procedure proposed by Liang et al. [30].

4. Solution algorithms

Computational algorithms based on the Müller's method [36] are developed to iterate the neutral axis depth (d_n) and orientation (θ) in the cross-sectional analysis. The Müller's method requires three initial values of the d_n and θ to start the iterative process. In the theoretical model, three initial values of the neutral axis depth $d_{n,1}$, $d_{n,3}$ and $d_{n,2}$ are taken as $D/4$, D and $(d_{n,1} + d_{n,3})/2$ respectively while the initial values for the orientation of the neutral axis θ_1, θ_3 and θ_2 are assigned to $\alpha/4$, α and $(\theta_1 + \theta_3)/2$ respectively. For these three initial values, the moment residuals $r_{m,1}$, $r_{m,2}$ and $r_{m,3}$ are calculated. The depth and orientation of the neutral axis are adjusted by the following equations:

$$\omega_4 = \omega_3 - \frac{2c_m}{b_m \pm \sqrt{b_m^2 - 4a_m c_m}} \tag{21}$$

$$a_m = \frac{(\omega_2 - \omega_3)(r_{m,1} - r_{m,3}) - (\omega_1 - \omega_3)(r_{m,2} - r_{m,3})}{(\omega_1 - \omega_2)(\omega_2 - \omega_3)(\omega_1 - \omega_3)} \qquad (22)$$

$$b_m = \frac{(\omega_1 - \omega_3)^2 (r_{m,2} - r_{m,3}) - (\omega_2 - \omega_3)^2 (r_{m,1} - r_{m,3})}{(\omega_1 - \omega_2)(\omega_2 - \omega_3)(\omega_1 - \omega_3)} \qquad (23)$$

$$c_m = r_{m,3} \qquad (24)$$

where ω_1, ω_2 and ω_3 are the design variables which represent d_n and θ. The sign in the denominator of Eq. (21) is taken as the same as that of b_m. Patel et al. [28] reported that the values of ω_1, ω_2 and ω_3 and the corresponding residuals $r_{m,1}$, $r_{m,2}$ and $r_{m,3}$ need to switch in order to obtain converged solutions. Eq. (21) and the exchange of design parameters and moment residuals are executed repetitively until the convergence criterion of $|r_m| < \varepsilon_k$ is satisfied.

5. Comparisons of computer solutions with experimental results

Experimental results of uniaxially or concentrically loaded square CFST slender columns with or without preload effects given by Han and Yao [20] were used to verify the accuracy of the theoretical model developed. In the present study, an initial geometric imperfection of $L/1000$ at the mid-height of the beam-columns was taken into account in the analyses of Specimens L-2 to LP-6. It was assumed that the eccentricity of the preload on the hollow steel tube was the same as that of the applied compressive load on the CFST beam-column. The compressive strength of concrete cylinder was taken as 0.85 times the concrete cube strength. As shown in Table 1, good agreement between computational results and test data is obtained. The mean value of

the predicted to the experimental ultimate axial strength $\left(P_{u,num}/P_{u,exp}\right)$ is 0.93 with a standard deviation of 0.04 and a coefficient of variation of 0.04. The theoretical model yields conservative predictions of the ultimate axial strengths of rectangular CFST slender beam-columns considering preload effects.

The load-deflection responses of specimens tested by Han and Yao [20] were simulated by the theoretical model. Fig. 6 shows a comparison of predicted and experimental axial load-deflection curves for Specimen LP-1. The figure demonstrates that the theoretical model predict well the initial stiffness of the specimen. However, after the loading level of about 170 kN, the experimental curve slightly departs from the computational one. In addition, the theoretical model also predicts well the stiffness of the tested specimen in the post-peak range. The discrepancy between predicted and experimental results is likely attributed to the uncertainty of the actual concrete compressive strength and stiffness as the average concrete compressive strength was used in the analysis. The predicted and experimental axial load-deflection curves for Specimen LP-6 are depicted in Fig. 7. As indicated in this figure, the results obtained by the model are generally in good agreement with test data. In the post-peak range, the theoretical model also yields good predictions of the stiffness of the tested specimen. However, it is noted that the initial stiffness of the specimen predicted by the theoretical model is slightly higher than that of the experimental one. This is likely caused by the uncertainty of the actual concrete stiffness and strength of the specimen.

6. Fundamental behavior with preload effects

The theoretical model developed was used to investigate the effects of local buckling, preload ratio, depth-to-thickness ratio (D/t), column slenderness ratio (L/r), loading eccentricity ratio (e/D) and steel yield strength (f_{sy}) on the behavior of biaxially loaded normal and high strength thin-walled CFST slender beam-columns. It was assumed that the eccentricity of the preload on the steel tube was the same as that of the applied axial load on the CFST beam-column. In addition to this, local buckling of the steel tubes under preloads is prevented in the study as it would not be expected in the real construction of CFST columns. The initial geometric imperfection at the mid-height of the hollow steel tube was considered to be $L/1000$. The Young's modulus of the steel tubes was 200 GPa.

6.1. Effects of local buckling

The theoretical model developed was utilized to study the effects of local buckling on the behavior of normal strength rectangular CFST slender beam-columns. The beam-column with a cross-section of 600×600 mm and under the eccentric load applied at an angle of 45º with respect to the y-axis was analyzed. The D/t ratio of the section was 90 while the L/r ratio was 40. The e/D ratio of 0.2 was specified in the analysis. Normal strength concrete with compressive strength of 50 MPa was filled into the steel tube. The yield and tensile strengths of the steel tube were 300 MPa and 430 MPa respectively. The preload ratio of 0.3 was considered. The CFST slender beam-column was analyzed by considering and ignoring local buckling effects respectively.

Fig. 8 depicts the predicted load-deflection curves for the CFST slender beam-column. The figure indicates that local buckling remarkably reduces the stiffness and ultimate axial strength of the CFST slender beam-column with the same preload ratio. The ultimate axial load of the slender beam-column is overestimated by 8.7% if local buckling was not considered. Fig. 9 illustrates the effects of local buckling on the strength envelope of the CFST slender beam-column. In each interaction curve shown in Fig. 9, the ultimate axial strength was normalized to the ultimate axial load (P_{oa}) of the axially loaded slender column including local buckling effects, while the ultimate moment was normalized to the pure bending moment (M_o) of the slender beam-column with local buckling effects. It can be observed that for the same preload ratio, the ultimate bending strength is reduced by local buckling when the axial load is greater than 30% of the ultimate axial strength P_{oa}.

6.2. Effects of preloads

The effects of the preload ratio on the behavior of a normal strength steel tube filled with high strength concrete were investigated herein. A CFST beam-column with a cross-section of 700 × 700 mm was considered. The D/t ratio of the column cross-section was 30. The angle of the applied load was 30º for biaxial bending. The steel yield strength of the welded mild steel tube was 300 MPa and its tensile strength was 430 MPa. The compressive strength of infill concrete was 60 MPa. The L/r ratio of 40 and the e/D ratio of 0.2 were specified in the analysis. The preload ratios of 0.0, 0.4 and 0.8 were considered in the investigations.

Load-deflection curves for the CFST slender beam-column with various preload ratios are presented in Fig. 10. The figure shows that the ultimate axial strength and flexural stiffness of the CFST slender beam-column decrease with increasing the preload ratio. In addition, it is seen that the higher the preload ratio, the larger the mid-height deflection in the CFST beam-column at the ultimate load. Increasing the preload ratio from 0.0 to 0.4 reduces the ultimate axial strength of the CFST beam-column by 6%. However, this strength reduction could be up to 14.1% when the preload ratio is increased from 0.0 to 0.8. The strength envelopes of the CFST slender beam-column with preload ratios of 0.0 and 0.4 are given in Fig. 11, where P_{op} is the ultimate axial load of the axially loaded slender column including preload effects. It can be seen from Fig. 11 that considering preload effects narrows the strength envelope of the slender beam-column. It should be noted that pure bending strength of the slender beam-column is not affect by the preload on the hollow steel tube.

6.3. *Effects of preloads and depth-to-thickness ratio*

The fundamental behavior of a rectangular CFST slender beam-column is influenced by the D/t ratio. The CFST slender beam-columns with a square cross-section of 800 ×800 mm were considered in the analysis. The D/t ratio of the steel section was varied from 20 to 50 by changing the thickness of the section. The L/r ratio was 80 while the e/D ratio was taken as 0.2 in the analysis. The axial load was applied at an angle of 60° for biaxial bending. The yield and tensile strengths of the steel tubes were 690 MPa and

790 MPa respectively. The concrete compressive strength of 40 MPa was considered. The preload ratios of 0.0, 0.3 and 0.6 were used in the analysis.

The effects of D/t ratio on the ultimate axial strengths of CFST slender beam-columns with various preload ratios are demonstrated in Fig.12. It can be seen from the figure that the ultimate axial strengths of rectangular CFST slender beam-columns decrease considerably with increasing the D/t ratio under the same preload ratio. This may be attributed to the fact that the cross-sectional area of steel and the post-local buckling strength of the steel tube decrease with an increase in the D/t ratio. Fig. 13 shows the reduction in the ultimate axial strength caused by preloads. The corresponding strength reduction with the D/t ratio of 20 and the preload ratio of 0.3 is 5.3% while for a CFST slender beam-column with the D/t ratio of 50, the preload with a ratio of 0.6 causes a 12% reduction in its ultimate axial strength.

6.4. Effects of preloads on column strength curves

The effects of preloads on the column strength curves for high strength steel tubes filled with high strength concrete were examined. The width and depth of the rectangular steel tube were 600 mm and 800 mm respectively. The L/r ratio varied from 0 to 100 while the dimension of the section was not changed. The e/D ratio of 0.2 was specified in the analysis of the CFST beam-columns with various L/r ratios. The angle of the applied axial load was 30º while the D/t ratio of 50 was specified in the analysis. The CFST beam-columns were made of high strength steel tubes with the yield and tensile

strengths of 690 and 790 MPa respectively filled with high strength concrete of 70 MPa. The preload with a ratio of 0.0, 0.3 and 0.6 was applied to the steel tube respectively.

The normalized column strength curves for biaxially loaded CFST beam-columns with various preload ratios are presented in Fig. 14, in which P_n is the ultimate axial load of the biaxially loaded CFST beam-column and P_o is the ultimate axial strength (P_o) of the column section under axial compression. It appears from Fig. 14 that the ultimate axial strength of CFST slender beam-columns under the same preload ratio is strongly affected by the columns slenderness. Increasing the column slenderness ratio significantly reduce the ultimate axial load of CFST beam-columns regardless of the preload ratios. The strength reduction-column slenderness curves with preload ratios of 0.3 and 0.6 are illustrated in Fig. 15. The figure shows that the strength reduction increases with increasing the column slenderness ratio as well as the preload ratio. As presented in Fig. 15, the preload having a ratio of 0.6 reduces the ultimate axial strength of the CFST column with an L/r ratio of 100 by 15.8%. However, for the short beam-column with an L/r ratio of 22, the preload with a ratio of 0.3 reduces the ultimate axial strength of the CFST column by only 0.7%. This means that the preload effect can be ignored in the design of CFST short beam-columns with an L/r ratio less than 22.

6.5. Effects of preloads and loading eccentricity ratio

The behavior of normal strength slender steel tubes filled with normal strength concrete and with various *e/D* ratios were studied. A CFST slender beam-column with a cross-section of 700 × 800 mm and loading eccentricities ranged from 0 to 2 were analyzed using the computer program developed. The angle of the axial load was fixed at 45°

with respect to the y-axis. The depth-to-thickness ratio of the section was 50 while the L/r ratio of the beam-column was 80. The yield and tensile strengths of the steel tubes were 300 MPa and 430 MPa respectively. The concrete compressive strength was 40 MPa. The preload ratios were taken as 0.0, 0.3 and 0.6 in the analyses.

Fig. 16 shows the ultimate axial load ratio as a function of the e/D ratio. The ultimate axial strengths of CFST slender beam-columns are shown to decrease with an increase in the loading eccentricity ratio regardless of preload ratios. The strength reduction-loading eccentricity curves for CFST slender beam-columns with preload ratios of 0.3 and 0.6 are given in Fig. 17. The figure illustrates that the strength reduction increases with increasing the loading eccentricity ratio from 0 to 0.4. After reaching the maximum value, the reduction in the ultimate axial load decreases with an increase in the loading eccentricity ratio. It is interesting to note that the preload on the hollow steel tube causes a maximum reduction in the ultimate axial strength of a CFST beam-column when the e/D ratio is equal to 0.4. For the axially loaded CFST slender column with preload ratios of 0.3 and 0.6, the strength reduction caused by the preload is 1.2% and 2.7% respectively. However, the preload having a ratio of 0.6 leads to a reduction of 8.2% in the ultimate axial load of the CFST slender beam-column with an e/D ratio of 0.4.

6.6. Effects of preloads and steel yield strengths

In this section, the effects of steel yield strengths on the strength and behavior of square steel tubes with various yield strength filled with high strength concrete of 80 MPa were studied. A column cross-section of 650 × 650 mm was considered in the parametric study. The depth-to-thickness ratio of 65, the column slenderness ratio of 80 and the

loading eccentricity ratio of 0.2 were used to examine the effects of preloads and steel yield strengths. The steel yield strength was varied from 250 MPa to 690 MPa. The applied axial load angle was fixed at 60° with respect to the y-axis. The preload ratios were taken as 0.0, 0.3 and 0.6 in the analysis.

Fig. 18 gives the normalized ultimate axial strengths of CFST slender beam-columns with various preload ratios and steel yield strengths. It can be seen from Fig. 18 that regardless of the preload ratio, the ultimate axial strength ratio of CFST slender beam-columns increases as the steel yield strength increases from 250 MPa to 450 MPa. However, the strength ratio tends to decrease when the steel yield strength increases from 450 MPa to 690 MPa. This is attributed to the fact that the ultimate axial strengths of both the CFST column section and the CFST column are increased by increasing the steel yield strength, but CFST column section has a greater increment in its ultimate axial strength than the CFST column. The percentage reduction in the ultimate axial strength caused by preloads is shown in Fig. 19. It can be observed from this figure that for a CFST slender beam-column with the steel yield strength of 250 MPa, the preload with a ratio of 0.3 causes a 3.6% reduction in its ultimate axial strength. However, when increasing the steel yield strength from 250 MPa to 690 MPa and the preload ratio from 0.3 to 0.6, the strength reduction could be as much as 13.2%.

7. Conclusions

This paper has presented an effective theoretical model for the nonlinear analysis and design of biaxially loaded thin-walled rectangular CFST slender beam-columns with

preload effects. The method of nonlinear analysis and computational algorithms together with solution schemes have been developed for simulating the load-deflection responses and strength envelopes of thin-walled CFST slender beam-columns, incorporating the important effects of preloads on the steel tubes and of progressive local buckling of the steel tube walls under stress gradients. The theoretical model developed was verified by existing experimental results with a good agreement and utilized to study the fundamental behavior of biaxially loaded thin-walled CFST slender beam-columns by varying various important parameters.

Based on the results obtained from the present study, the following important conclusions are drawn:

(1) Local buckling of the steel tubes considerably reduces the stiffness and strength of rectangular thin-walled CFST slender beam-columns and thus must be taken into account in the nonlinear analysis and design.

(2) Preloads on the steel tubes increase the lateral deflections of CFST slender beam-columns and remarkably reduce the ultimate strengths of CFST slender beam-columns.

(3) The ultimate axial strengths of thin-walled CFST slender beam-columns are found to decrease with increasing the D/t ratio regardless of the preload ratio. For a slender beam-column with a D/t ratio of 50, the preload having a ratio of 0.6 may cause a strength reduction of 12%.

(4) The effect of preloads on the ultimate axial strength of the CFST beam-columns increases with increasing the column slenderness ratio. The preload might reduce

the ultimate axial strength of CFST slender beam-columns by more than 15.8%, providing that the column slenderness ratio is greater than 100 and the preload ratio is 0.6. However, the preload effect on CFST short beam-columns with an L/r ratio less than 22 can be ignored in design.

(5) The strength reduction due to the preload effects increases with an increase in the e/D ratio up to 0.4. When the e/D ratio is greater than 0.4, however, the strength reduction tends to decrease with increasing the e/D ratio. The preload has the most pronounced effect on CFST slender beam-columns with an e/D ratio of 0.4.

(6) The strength ratio of CFST beam-columns increases with increasing the steel yield strength up to 450 MPa. However, the strength ratio is found to decrease with increasing the steel yield strength which is higher than 450 MPa.

References

[1] Furlong RW. Strength of steel-encased concrete beam columns. J Struct Div ASCE 1967;93(5):113-24.

[2] Knowles RB, Park R. Strength of concrete-filled steel tubular columns. J Struct Div ASCE 1969;95(12):2565-87.

[3] Shakir-Khalil H, Zeghiche J. Experimental behaviour of concrete-filled rolled rectangular hollow-section columns. Struct Eng 1989;67(19):346-53.

[4] Shakir-Khalil H, Mouli M. Further tests on concrete-filled rectangular hollow-section columns. Struct Eng 1990;68(20):405-13.

[5] Schneider SP. Axially loaded concrete-filled steel tubes. J Struct Eng ASCE 1998;124(10):1125-38.

[6]   Varma AH, Ricles JM, Sause R, Lu LW. Seismic behavior and modeling of high-strength composite concrete-filled steel tube (CFT) beam-columns. J Constr Steel Res 2002;58(5-8):725-58.

[7]   Sakino K, Nakahara H, Morino S, Nishiyama I. Behavior of centrally loaded concrete-filled steel-tube short columns. J Struct Eng ASCE 2004;130(2):180-88.

[8]   Fujimoto T, Mukai A, Nishiyama I, Sakino K. Behavior of eccentrically loaded concrete-filled steel tubular columns. J Struct Eng ASCE 2004;130(2):203-12.

[9]   Ellobody E, Young B, Lam D. Behaviour of normal and high strength concrete-filled compact steel tube circular stub columns. J Constr Steel Res 2006;62(7):706-15.

[10]   Liu D. Behaviour of eccentrically loaded high-strength rectangular concrete-filled steel tubular columns. J Constr Steel Res 2006;62(8):839-46.

[11]   Lue DM, Liu JL, Yen T. Experimental study on rectangular CFT columns with high-strength concrete. J Constr Steel Res 2007;63(1):37-44.

[12]   Ge HB, Usami T. Strength of concrete-filled thin-walled steel box columns: experiment. J Struct Eng ASCE 1992;118(11):3036-54.

[13]   Bridge RQ, O'Shea MD. Behaviour of thin-walled steel box sections with or without internal restraint. J Constr Steel Res 1998;47(1-2):73-91.

[14]   Uy B. Strength of concrete filled steel box columns incorporating local buckling. J Struct Eng ASCE 2000;126(3):341-52.

[15]   Han LH. Tests on stub columns of concrete-filled RHS sections. J Constr Steel Res 2002;58(3):353-72.

[16] Liang QQ, Uy B, Wright HD, Bradford MA. Local buckling of steel plates in double skin composite panels under biaxial compression and shear. J Struct Eng ASCE 2004;130(3):443-451.

[17] Liang QQ, Uy B, Liew JYR. Local buckling of steel plates in concrete-filled thin-walled steel tubular beam-columns. J Constr Steel Res 2007;63(3):396-405.

[18] Zha XX. The theoretical and experimental study on the behaviour of concrete filled steel tubular members subjected to compression-bending-torsion and initial stresses on the steel tubes. Ph.D. Dissertation, Harbin University of Civil Engineering and Architecture, Harbin, China, 1996 (in Chinese).

[19] Zhang XQ, Zhong ST, Yan SZ, Lin W, Cao HL. Experimental study about the effect of initial stress on bearing capacity of concrete-filled steel tubular members under eccentric compression. Journal of Harbin University of Civil Engineering and Architecture 1997;30(1):50-6 (in Chinese).

[20] Han LH, Yao GH. Behaviour of concrete-filled hollow structural steel (HSS) columns with pre-load on the steel tubes. J Constr Steel Res 2003;59(12):1455-75.

[21] Liew JYR, Xiong DX. Effect of preload on the axial capacity of concrete-filled composite columns. J Constr Steel Res 2009;65(3):709-22.

[22] Hu HT, Huang CS, Wu MH, Wu YM. Nonlinear analysis of axially loaded concrete-filled tube columns with confinement effect. J Struct Eng ASCE 2003;129(10):1322-29.

[23] Choi KK, Xiao Y. Analytical studies of concrete-filled circular steel tubes under axial compression. J Struct Eng ASCE 2010;136(5):565-73.

[24] Portolés JM, Romero ML, Filippou FC, Bonet JL. Simulation and design recommendations of eccentrically loaded slender concrete-filled tubular columns. Eng Struct 2011;33(5):1576-93.

[25] Lakshmi B, Shanmugam NE. Nonlinear analysis of in-filled steel-concrete composite columns. J Struct Eng ASCE 2002;128(7):922-33.

[26] Liang QQ. Performance-based analysis of concrete-filled steel tubular beam-columns, Part I: Theory and algorithms. J Constr Steel Res 2009;65(2):363-72.

[27] Liang QQ. Performance-based analysis of concrete-filled steel tubular beam-columns, Part II: Verification and applications. J Constr Steel Res 2009;65(2):351-62.

[28] Patel VI, Liang QQ, Hadi MNS. High strength thin-walled rectangular concrete-filled steel tubular slender beam-columns, Part I: Modeling. J Constr Steel Res 2012;70:377-84.

[29] Patel VI, Liang QQ, Hadi MNS. High strength thin-walled rectangular concrete-filled steel tubular slender beam-columns, Part II: Behavior. J Constr Steel Res 2012;70:368-76.

[30] Liang QQ, Patel VI, Hadi MNS. Biaxially loaded high-strength concrete-filled steel tubular slender beam-columns, Part I: Multiscale simulation. J Constr Steel Res 2012;75:64-71.

[31] Xiong DX, Zha XX. A numerical investigation on the behaviour of concrete-filled steel tubular columns under initial stresses. J Constr Steel Res 2007;63(5):599-611.

[32] Patel VI, Liang QQ, Hadi MNS. Numerical analysis of circular concrete-filled steel tubular slender beam-columns with preload effects. Int J of Struct Stability and Dny 2013, 13(3) (accepted for publication).

[33] Mander JB, Priestley MJN, Park R. Theoretical stress-strain model for confined concrete. J Struct Eng ASCE 1988;114(8):1804-26.

[34] ACI-318. Building Code Requirements for Structural Concrete and Commentary. Detroit (MI): ACI; 2011.

[35] Tomii M, Sakino K. Elastic-plastic behavior of concrete filled square steel tubular beam-columns. Trans Architec Inst Jpn 1979;280:111-20.

[36] Müller DE. A method for solving algebraic equations using an automatic computer. Mathematical Tables and Other Aids to Computation 1956;10(56):208-15.

Figures and tables

Table 1. Ulatimate axial strengths of square CFST beam-columns with preload effects.

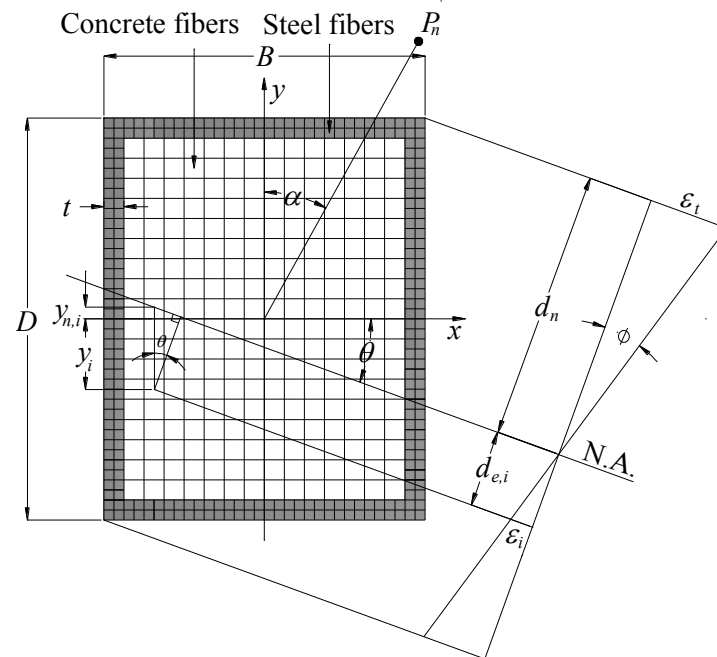| Specimens	$B \times D \times t$ (mm)	D/t	L (mm)	u_o (mm)	e (mm)	$f_c^{'}$ (MPa)	f_{sy} (MPa)	f_{su} (MPa)	E_s (GPa)	$P_{preload}$ (kN)	$P_{u.\exp}$ (kN)	$P_{u.num}$ (kN)	$\frac{P_{u.num}}{p_{u.exp}}$	Ref.
S-1	120 × 120 ×2.65	45.2	360	0	0	17.09	340	439.6	207	0	640	579.07	0.90	
SP-1	120 × 120 ×2.65	45.2	360	0	0	17.09	340	439.6	207	211	664	580.31	0.87	
S-2	120 × 120 ×2.65	45.2	360	0	14	17.09	340	439.6	207	0	533	478.67	0.90	
SP-2	120 × 120 ×2.65	45.2	360	0	14	17.09	340	439.6	207	211	538	480.85	0.89	
S-3	120 × 120 ×2.65	45.2	360	0	0	30.6	340	439.6	207	0	816	754.39	0.92	
SP-3	120 × 120 ×2.65	45.2	360	0	0	30.6	340	439.6	207	211	812	753.41	0.93	
S-4	120 × 120 ×2.65	45.2	360	0	14	30.6	340	439.6	207	0	600	610.29	1.02	
SP-4	120 × 120 ×2.65	45.2	360	0	14	30.6	340	439.6	207	211	622	613.28	0.99	
SP-5	120 × 120 ×2.65	45.2	360	0	14	30.6	340	439.6	207	127	650	613.54	0.94	
SP-6	120 × 120 ×2.65	45.2	360	0	31	30.6	340	439.6	207	198	500	481.38	0.96	[20]
L-2	120 × 120 ×2.65	45.2	1400	L/1000	0	30.6	340	439.6	207	0	769	716.93	0.93	
LP-2	120 × 120 ×2.65	45.2	1400	L/1000	0	30.6	340	439.6	207	194	730	715.31	0.98	
L-1	120 × 120 ×2.65	45.2	1400	L/1000	14	30.6	340	439.6	207	0	590	536.83	0.91	
LP-1	120 × 120 ×2.65	45.2	1400	L/1000	14	30.6	340	439.6	207	194	560	527.24	0.94	
LP-3	120 × 120 ×2.65	45.2	1400	L/1000	14	30.6	340	439.6	207	272	552	522.52	0.95	
LP-4	120 × 120 ×2.65	45.2	1400	L/1000	31	30.6	340	439.6	207	194	452	403.89	0.89	
L-5	120 × 120 ×2.65	45.2	1400	L/1000	31	25.5	340	439.6	207	0	412	385.47	0.94	
LP-6	120 × 120 ×2.65	45.2	1400	L/1000	31	25.5	340	439.6	207	117	397	378.81	0.95	
Mean													0.93	
Standard deviation (SD)													0.04	
Coefficient of variation (COV)													0.04	

Fig. 1. Fiber strain distribution in CFST beam-column section under axial load and biaxial bending.
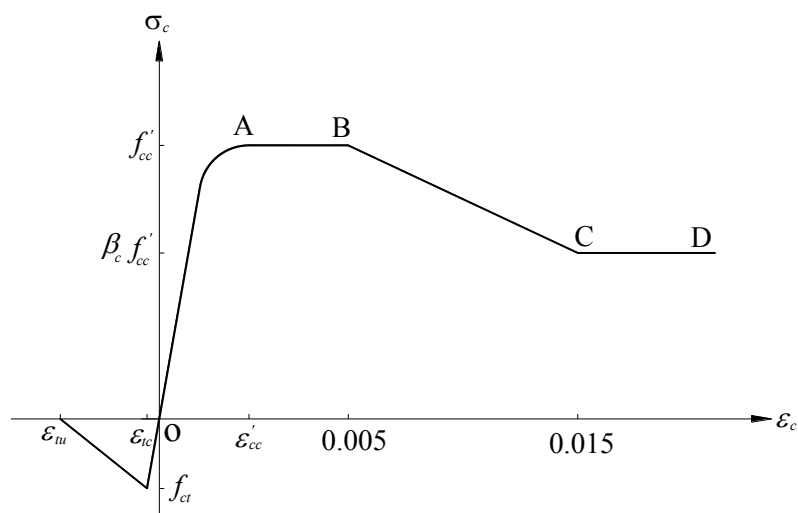

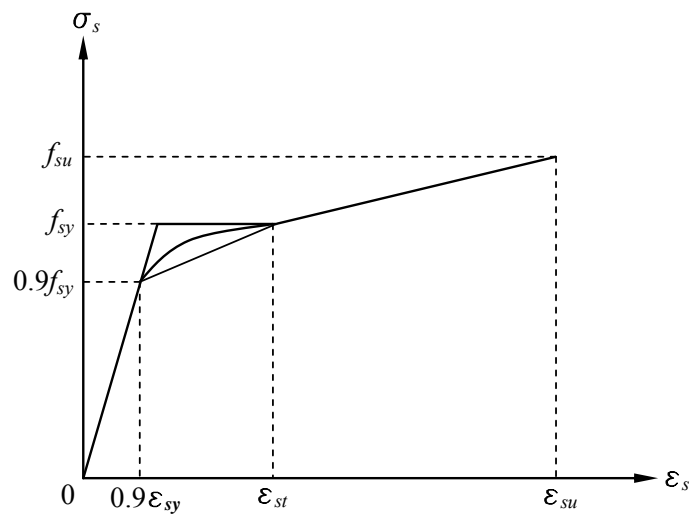**Fig. 2.** Stress-strain curve for concrete in rectangular CFST columns.

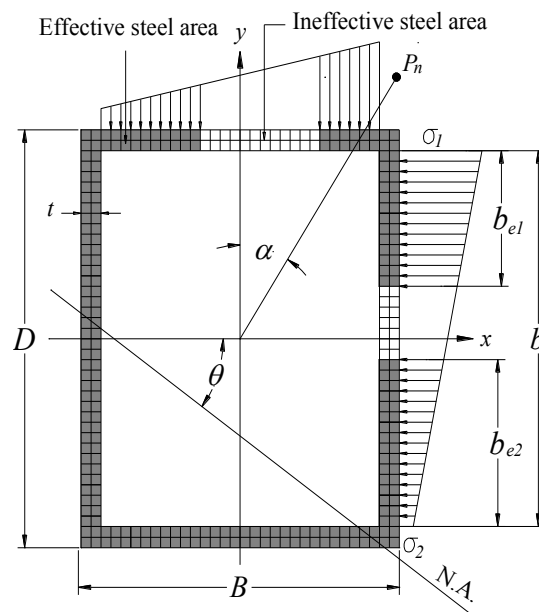**Fig. 3.** Stress-strain curves for structural steels.

Fig. 4. Effective and ineffective areas of steel tubular cross-section under axial load and biaxial bending.
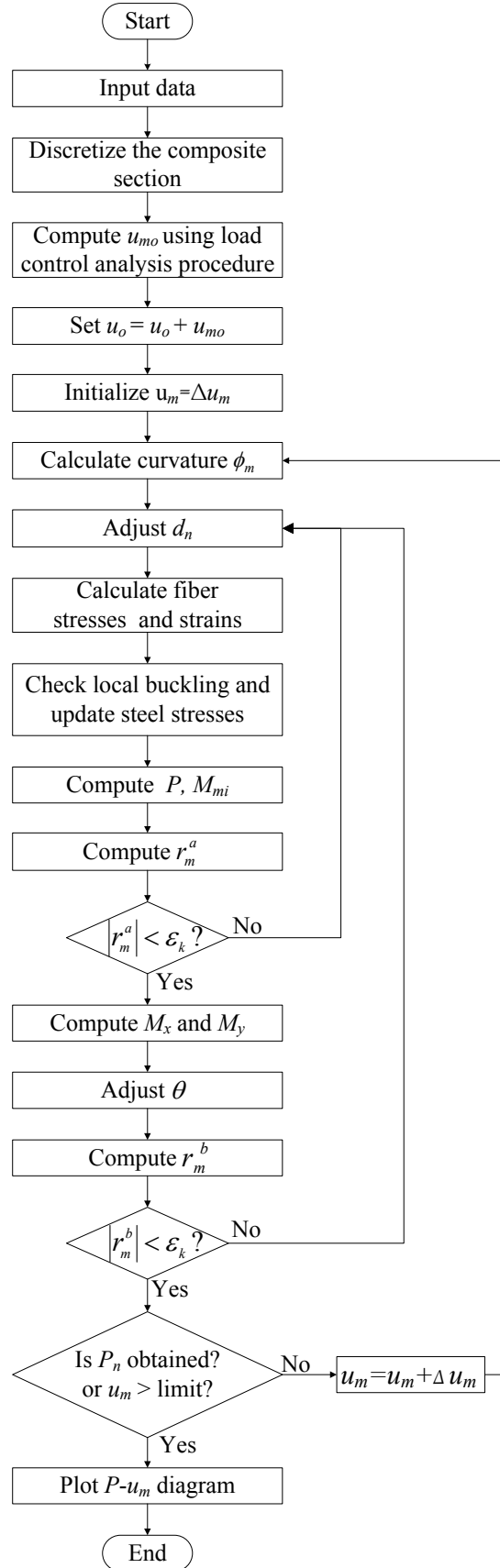
```
                          ( Start )
                              │
                    ┌─────────────────┐
                    │   Input data    │
                    └─────────────────┘
                              │
                    ┌─────────────────┐
                    │ Discretize the composite │
                    │      section    │
                    └─────────────────┘
                              │
                    ┌─────────────────┐
                    │ Compute u_mo using load │
                    │ control analysis procedure │
                    └─────────────────┘
                              │
                    ┌─────────────────┐
                    │ Set u_o = u_o + u_mo │
                    └─────────────────┘
                              │
                    ┌─────────────────┐
                    │ Initialize u_m=Δu_m │
                    └─────────────────┘
                              │
                    ┌─────────────────┐◄──────────────────┐
                    │ Calculate curvature φ_m │             │
                    └─────────────────┘                    │
                              │                            │
                    ┌─────────────────┐◄──────────┐        │
                    │   Adjust d_n    │           │        │
                    └─────────────────┘           │        │
                              │                   │        │
                    ┌─────────────────┐           │        │
                    │ Calculate fiber │           │        │
                    │ stresses and strains │      │        │
                    └─────────────────┘           │        │
                              │                   │        │
                    ┌─────────────────┐           │        │
                    │ Check local buckling and │  │        │
                    │ update steel stresses │    │        │
                    └─────────────────┘           │        │
                              │                   │        │
                    ┌─────────────────┐           │        │
                    │ Compute  P, M_mi │          │        │
                    └─────────────────┘           │        │
                              │                   │        │
                    ┌─────────────────┐           │        │
                    │ Compute r_m^a   │           │        │
                    └─────────────────┘           │        │
                              │                   │        │
                        ╱ |r_m^a| < ε_k ? ╲  No    │        │
                        ╲               ╱─────────┘        │
                              │ Yes                         │
                    ┌─────────────────┐                    │
                    │ Compute M_x and M_y │                 │
                    └─────────────────┘                    │
                              │                            │
                    ┌─────────────────┐                    │
                    │   Adjust θ      │                    │
                    └─────────────────┘                    │
                              │                            │
                    ┌─────────────────┐                    │
                    │ Compute r_m^b   │                    │
                    └─────────────────┘                    │
                              │                            │
                        ╱ |r_m^b| < ε_k ? ╲  No             │
                        ╲               ╱──────────────────┘
                              │ Yes
                        ╱ Is P_n obtained? ╲  No   ┌──────────────────┐
                        ╲ or u_m > limit?  ╱──────►│ u_m=u_m+Δ u_m    │──┐
                              │ Yes               └──────────────────┘  │
                    ┌─────────────────┐
                    │ Plot P-u_m diagram │
                    └─────────────────┘
                              │
                          ( End )
```

Fig. 5. Computer flowchart for predicting the axial load-deflection responses of CFST beam-columns with prleoad effect
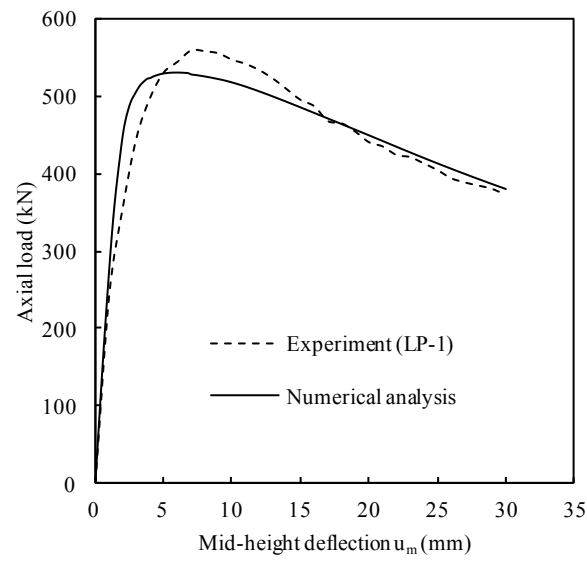
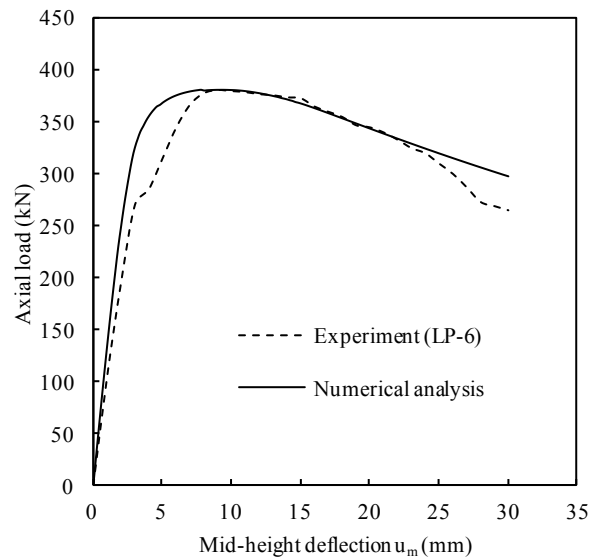**Fig. 6.** Comparison of computational and experimental axial load-deflection curves for specimen LP-1.

Fig. 7. Comparison of predicted and experimental axial load-deflection curves for specimen LP-6.
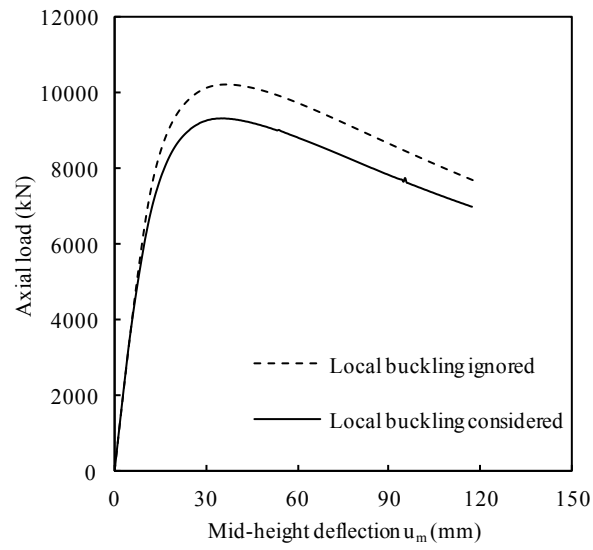
Fig. 8. Effects of local buckling on the axial load-deflection curves for CFST slender beam-column $\left(\beta_a = 0.3\right)$.
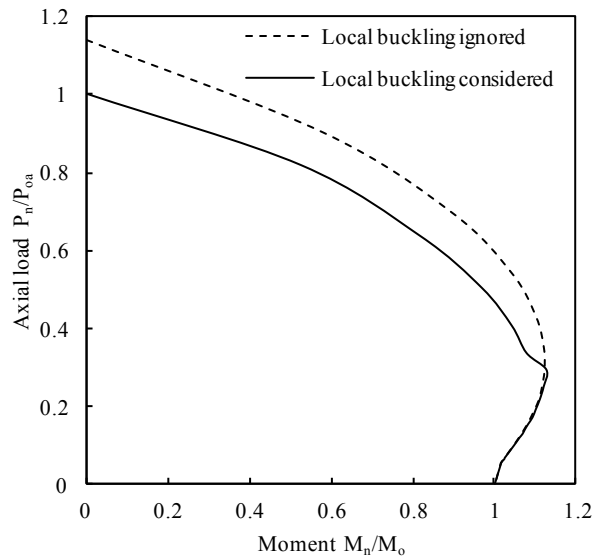

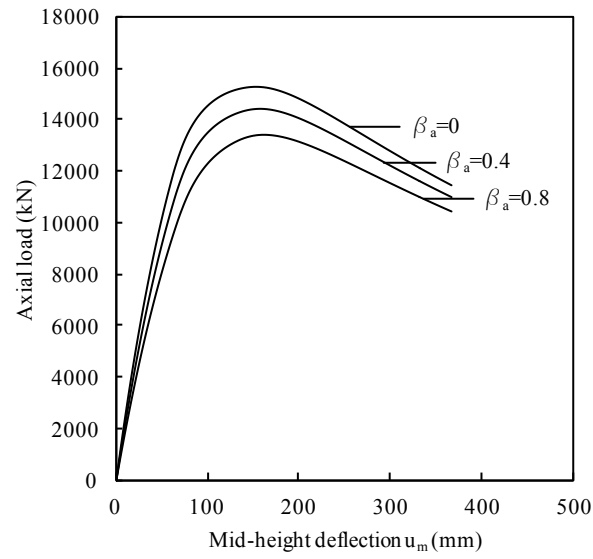**Fig. 9.** Effects of local buckling on the strength envelopes for CFST slender beam-column $\left(\beta_a = 0.3\right)$.

Fig. 10. Effects of preloads on the axial load-deflection curves for CFST beam-columns.
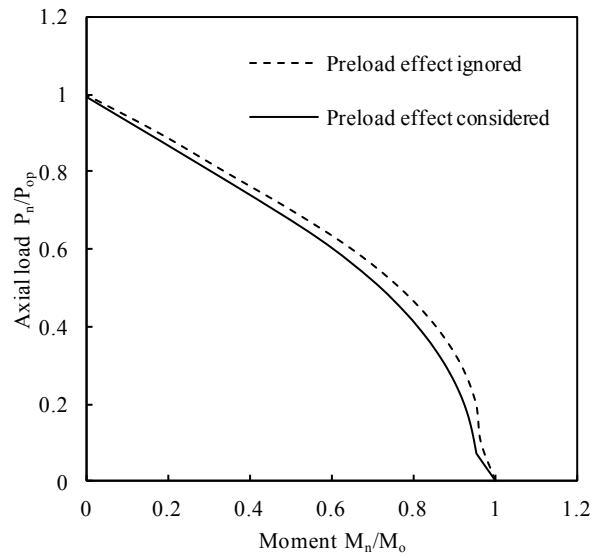
Fig. 11. Effects of preloads on the strength envelopes for CFST slender beam-column.
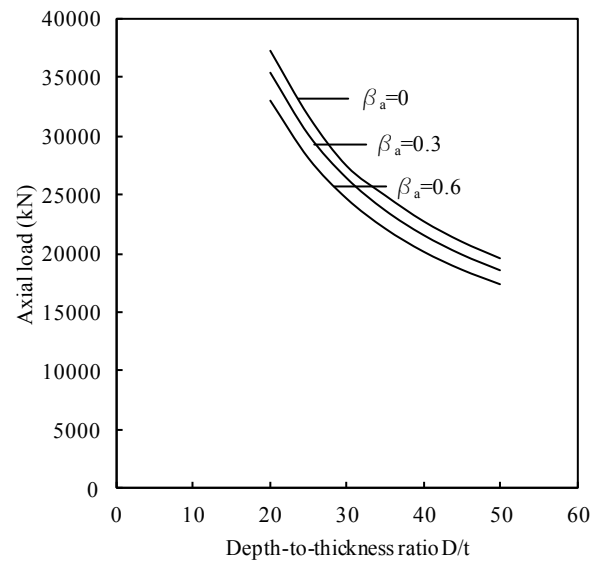
Fig. 12. Effects of preloads and diameter-to-thickness ratio on the ultimate axial strengths.
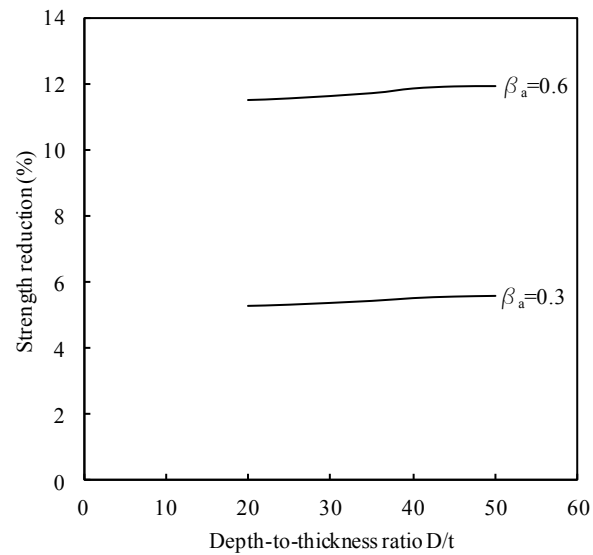
Fig. 13. Strength reduction caused by preloads in CFST beam-column with various depth-to-thickness ratios.
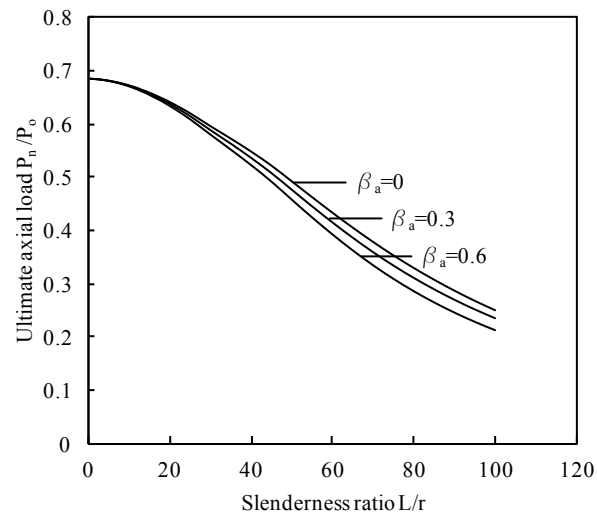
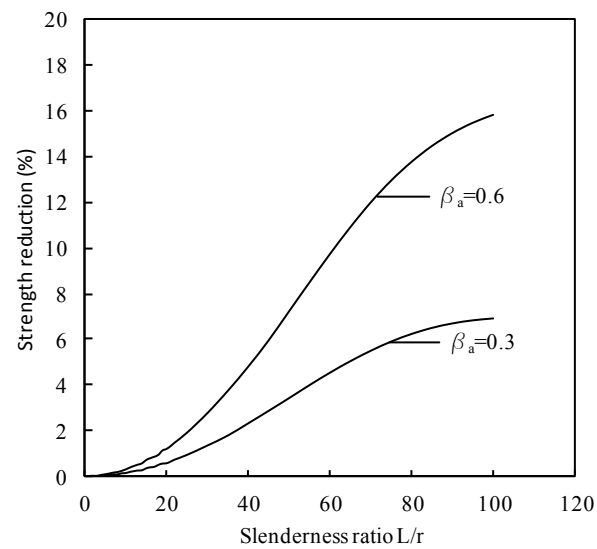**Fig. 14.** Effects of preloads on the column strength curves.

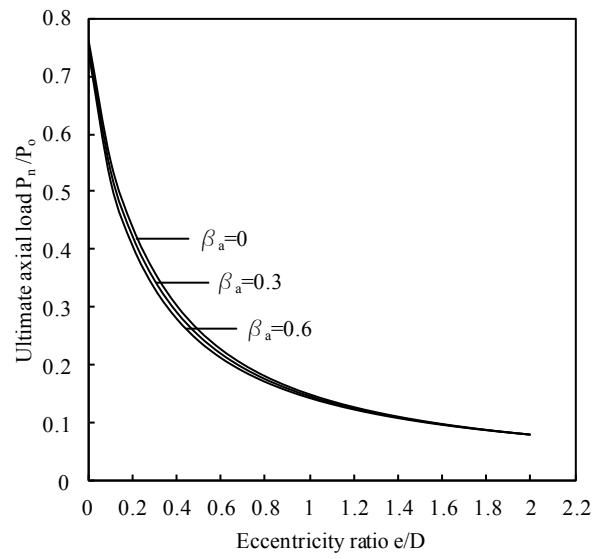**Fig. 15.** Strength reduction caused by preloads in CFST beam-columns with various slenderness ratios.

Fig. 16. Effects of preloads and loading eccentricity ratio on the ultimate axial strength.
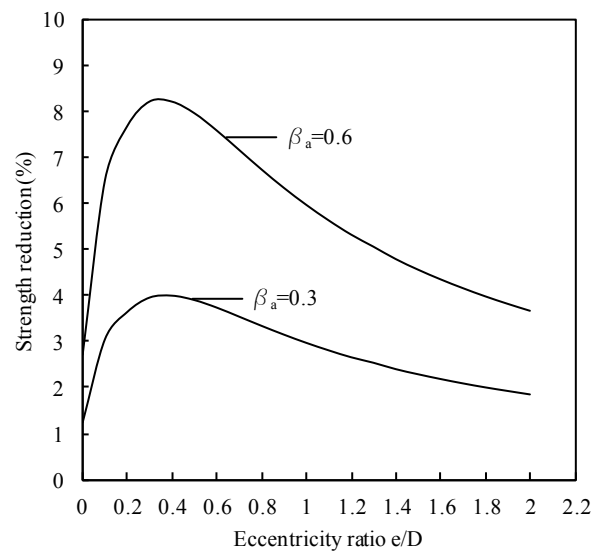

Fig. 17. Strength reduction caused by preloads in CFST beam-columns with various loading eccentricity ratios.
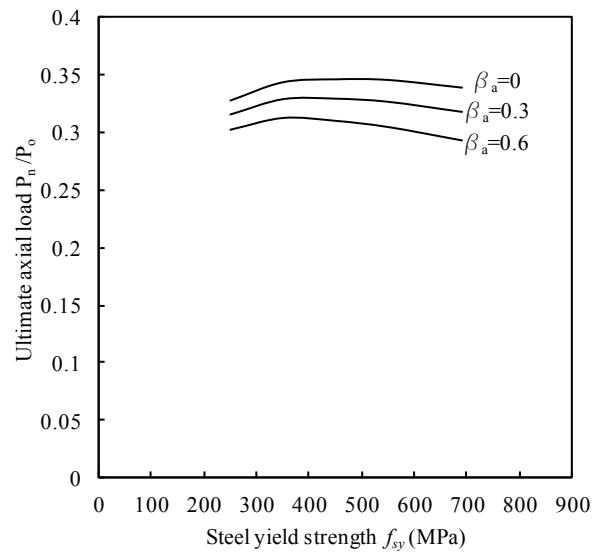
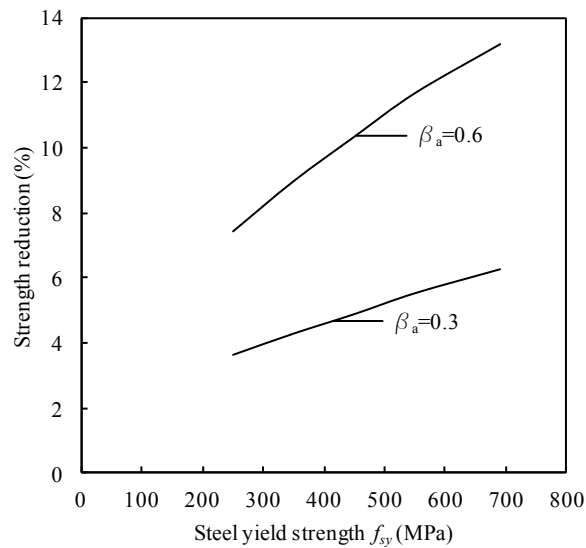**Fig. 18.** Effects of preloads and steel yield strengths on the ultimate axial strength.

Fig. 19. Strength reduction caused by preloads in CFST beam-columns with various steel yield strengths.

5.5 CONCLUDING REMARKS

Numerical models for simulating the behavior of eccentrically loaded circular and rectangular CFST slender beam-columns with preload effects have been developed in this chapter. The effects of preloads, local buckling, concrete confinement, initial geometric imperfections and second order have been considered in the numerical models. The inelastic behavior of composite cross-sections with local buckling effects is modeled using the accurate fiber element method. Deflections caused by preloads on the steel tubes are incorporated in the inelastic stability analysis of CFST slender beam-columns as additional geometric imperfections. Computational procedures have been developed for simulating the load-deflection responses of CFST slender beam-columns under axial load and bending. The accuracy of the numerical models developed has been established by comparisons of computer solutions with existing experimental results. The numerical models were used to investigate the effects of the preload ratio, depth-to-thickness ratio, column slenderness and loading eccentricity on the behavior of thin-walled CFST slender beam-column under axial load and bending.

Chapter 6

RECTANGULAR CFST SLENDER BEAM-COLUMNS UNDER CYCLIC LOADING

6.1 INTRODUCTION

This chapter presents a numerical model for simulating the cyclic behavior of high strength thin-walled rectangular CFST slender beam-columns with cyclic local buckling effects. Uniaxial cyclic stress-strain relationships for the concrete core and structural steels are incorporated in the numerical model. The effects of initial geometric imperfections, high strength materials and second order are also taken into account in the numerical model for CFST slender beam-columns under constant axial load and cyclically varying lateral loading. Müller's method algorithms are developed and implemented in the numerical model to iterate the neutral axis depth in a thin-walled CFST beam-column section. The ultimate lateral loads and cyclic load-deflection curves for thin-walled CFST beam-columns predicted by the numerical model are verified by

experimental data. The numerical model is then utilized to investigate the effects of cyclic local buckling, column slenderness ratio, depth-to-thickness ratio, concrete compressive strengths and steel yield strengths on the cyclic load-deflection responses of CFST slender beam-columns.

This chapter includes the following paper:

[1]   Patel, V. I., Liang, Q. Q. and Hadi, M. N. S., "Numerical analysis of high-strength concrete-filled steel tubular slender beam-columns under cyclic loading", Journal of Constructional Steel Research, 2013 (submitted).

VICTORIA UNIVERSITY
MELBOURNE AUSTRALIA

PART B:

DECLARATION OF CO-AUTHORSHIP AND CO-CONTRIBUTION: PAPERS INCORPORATED IN THESIS BY PUBLICATION

This declaration is to be completed for each conjointly authored publication and placed at the beginning of the thesis chapter in which the publication appears.

Declaration by [candidate name]:	Signature:	Date:
VIPULKUMAR ISHVARBHAI PATEL		11 01 2013

Paper Title:

Numerical analysis of high-strength concrete-filled steel tubular slender beam-columns under cyclic loading

In the case of the above publication, the following authors contributed to the work as follows:

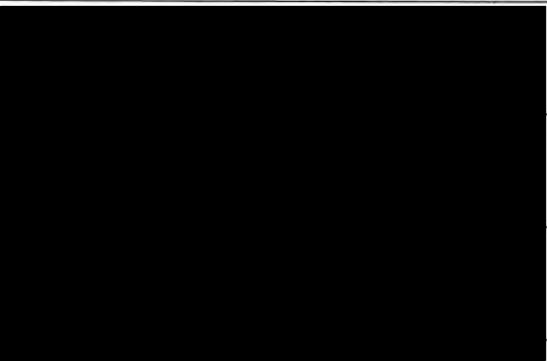| Name	Contribution%	Nature of contribution
Vipulkumar Ishvarbhai Patel	60	Literature search Developed a numerical model Verified the numerical model Carried out the parametric study Wrote the manuscript
Qing Quan Liang	30	Initial concept Provided critical revision of the article Manuscript submission
Muhammad N.S.Hadi	10	Provided critical revision of the article Final approval of the manuscript

VICTORIA UNIVERSITY
MELBOURNE AUSTRALIA

DECLARATION BY CO-AUTHORS

The undersigned certify that:

1. They meet criteria for authorship in that they have participated in the conception, execution or interpretation of at least that part of the publication in their field of expertise;

2. They take public responsibility for their part of the publication, except for the responsible author who accepts overall responsibility for the publication;

3. There are no other authors of the publication according to these criteria;

4. Potential conflicts of interest have been disclosed to **a)** granting bodies, **b)** the editor or publisher of journals or other publications, and **c)** the head of the responsible academic unit; and

5. The original data is stored at the following location(s):

Location(s): College of Engineering and Science, Victoria University, Melbourne, Victoria, Australia.

and will be held for at least five years from the date indicated below:

		Date
Signature 1		11|01|2013
Signature 2		11/01/2013
Signature 3		11/01/2013
Signature 4		

Manuscript prepared for

Journal of Constructional Steel Research

January 2013

Numerical Analysis of High-Strength Concrete-Filled Steel Tubular Slender Beam-Columns under Cyclic Loading

Vipulkumar Ishvarbhai Patel[a], Qing Quan Liang[a,*], Muhammad N. S. Hadi[b]

[a]College of Engineering and Science, Victoria University, PO Box 14428, Melbourne, VIC 8001, Australia

[b]School of Civil, Mining and Environmental Engineering, University of Wollongong, Wollongong, NSW 2522, Australia

Corresponding author:

Associate Professor Qing Quan Liang
College of Engineering and Science
Victoria University
PO Box 14428
Melbourne VIC 8001
Australia
Phone: +61 3 9919 4134
E-mail: Qing.Liang@vu.edu.au

Numerical analysis of high-strength concrete-filled steel tubular slender beam-columns under cyclic loading

Vipulkumar Ishvarbhai Patel[a], Qing Quan Liang[a,*], Muhammad N. S. Hadi[b]

[a] College of Engineering and Science, Victoria University, PO Box 14428, Melbourne, VIC 8001, Australia
[b] School of Civil, Mining and Environmental Engineering, University of Wollongong, Wollongong, NSW 2522, Australia

ABSTRACT

The effects of cyclic local buckling on the cyclic behavior of concrete-filled steel tubular (CFST) slender beam-columns were approximately considered in existing analytical models by modifying the stress-strain curve for the steel tube in compression. This modified stress-strain curve method, however, cannot simulate the progressive cyclic local and post-local buckling of the steel tubes. This paper presents a new numerical model for predicting the cyclic performance of high strength thin-walled rectangular CFST slender beam-columns accounting for the effects of progressive cyclic local and post-local buckling of steel tube walls under stress gradients. Uniaxial cyclic constitutive laws for the concrete core and steel tubes are incorporated in the fiber element formulation of the model. The effects of initial geometric imperfections, high strength materials and second order are also included in the nonlinear analysis of CFST slender beam-columns under constant axial load and cyclically varying lateral loading.

---

* Corresponding author. Tel.: 61 3 9919 4134.
  E-mail address: Qing.Liang@vu.edu.au (Q. Q. Liang)

The Müller's method is adopted to solve nonlinear equilibrium equations. The accuracy of the numerical model is examined by comparisons of computer solutions with experimental results. A parametric study is conducted to investigate the effects of cyclic local buckling, column slenderness ratio, depth-to-thickness ratio, concrete compressive strength and steel yield strength on the cyclic responses of CFST slender beam-columns. It is shown that the numerical model predicts well the experimentally observed cyclic lateral load-deflection characteristics of CFST slender beam-columns. The numerical results presented reflect the cyclic local and global buckling behavior of high strength rectangular CFST slender beam-columns, which have not been reported in the literature.

Keywords: *Concrete-filled steel tubes; Cyclic loading; High strength; Local and post-local buckling; Nonlinear analysis; Slender beam-columns.*

1. Introduction

High strength thin-walled rectangular CFST slender beam-columns have increasingly been used in composite buildings and bridges in seismic regions due to their high structural performance such as high strength, high stiffness, high ductility and large energy absorption capacity. In seismic regions, thin-walled CFST slender beam-columns may be subjected to a constant axial load from upper floors and cyclically varying lateral loading due to the earthquake. These cyclically loaded beam-columns may undergo cyclic local and global interaction buckling, which makes the predictions of their cyclic performance highly complicated. Cyclic local buckling reduces the

strength and ductility of thin-walled CFST slender beam-columns. It is therefore important to incorporate cyclic local buckling effects in nonlinear analysis techniques so that the cyclic performance of thin-walled CFST slender beam-columns under cyclic loading can be accurately predicted.

Experimental studies on the ultimate strengths of CFST columns under monotonic axial load or combined monotonic axial load and bending have been very extensive in the past [1-12]. However, only limited tests have been conducted on CFST beam-columns under cyclic loading. Experiments on square CFST beam-columns under axial load and cyclic lateral loading were performed by Varma et al. [13,14]. These test specimens were made of high strength concrete of 110 MPa and steel tube with yield stress ranging from 269 MPa to 660 MPa. Their studies indicated that the cracking of the infilled concrete and local buckling of the steel tubes reduced the flexural stiffness of CFST beam-columns. Han et al. [15] investigated experimentally the effects of the depth-to-thickness ratio, concrete compressive strength and axial load level on the cyclic behavior of square and rectangular CFST beam-columns. They reported that local buckling of CFST beam-columns occurred after the steel yielded. Tests on normal strength square CFST beam-columns under cyclic loading were undertaken by Wu et al. [16]. It was observed that the steel tube walls buckled outward after the concrete was damaged.

Various nonlinear analysis techniques for predicting the cyclic responses of CFST beam-columns have been reported in the literature. Varma et al. [13] developed a fiber element model for rectangular CFST beam-columns under cyclic loading. The uniaxial

cyclic stress-strain relationships for steel and concrete were derived from the nonlinear finite element analyses of CFST beam-columns. The stress-strain curve for steel in compression was modified to approximately account for the effects of local buckling. Gayathri et al. [17,18] proposed an efficient fiber element technique for the nonlinear analysis of CFST short and slender beam-columns under monotonic and cyclic loading. Their technique was formulated for normal strength CFST beam-columns where local buckling effects were not included. Chung et al. [19] presented a fiber element model for the analysis of cyclically loaded square CFST beam-columns. The effect of local buckling was approximately taken into account in the model by modifying the stress-strain curve for steel in compression. However, their model did not consider concrete tensile strength and high strength materials. Zubydan and ElSabbagh [20] proposed a mathematical model for the nonlinear analysis of normal strength rectangular CFST beam-columns where local buckling was approximately considered by modifying the stress-strain curve for steel in compression. The fiber element model presented by Wu et al. [16] could be used to analyze normal strength square CFST beam-columns, providing that the steel sections are compact. It should be noted that the modified stress-strain curve method used in the above mentioned models might overestimate or underestimate the cyclic local buckling strengths of steel tubes under stress gradients. This is because they cannot model the progressive cyclic local buckling of the steel tube from the onset to the post-local buckling, which is characterized by stress redistributions within the buckled tube wall.

The local buckling problem of thin-walled CFST columns has been studied experimentally by various researchers [21-24]. Liang et al. [25] proposed a fiber

element model for the nonlinear analysis of thin-walled CFST short columns under axial compression, accounting for progressive local buckling effects by using effective width formulas. Liang [26,27] developed a numerical model for simulating the axial load-strain responses, moment-curvature relationships and axial load-moment interaction diagrams of high strength rectangular CFST short beam-columns under axial load and biaxial bending. The effects of local buckling of steel tube walls under stress gradients were incorporated in the model by using initial local buckling equations and effective width formulas proposed by Liang et al [28]. Patel et al.[29,30] and Liang et al. [31] extended the numerical models developed by Liang et al. [25] and Liang [26,27] to the nonlinear analysis of eccentrically loaded high strength thin-walled rectangular CFST slender beam-columns considering the effects of local buckling, geometric imperfections, second order and high strength materials.

The above literature review indicates that there is relatively little numerical study on the fundamental behavior of cyclically loaded high strength rectangular CFST slender beam-columns with large depth-to-thickness ratios. In this paper, a numerical model is developed to simulate the cyclic performance of high strength thin-walled rectangular CFST slender beam-columns incorporating cyclic local buckling effects. Comparative study is undertaken to verify the numerical model. The fundamental cyclic behavior of CFST slender beam-columns under constant axial load and cyclically varying lateral loading is investigated using the computer program developed and the results obtained are discussed.

2. Material constitutive models

2.1 Cyclic constitutive models for concrete

The confinement provided by the steel tube increases only the ductility of the concrete core in a rectangular CFST column but not its strength. This confinement effect is considered in the cyclic stress-strain curves schematically depicted in Fig. 1. The cyclic stress-strain relationships account for the effects of stiffness degradation and crack opening and closing characteristics of concrete under cyclic loading. The envelope curve for the concrete under cyclic axial compression can be characterized by the monotonic stress-strain curve of the concrete, which is divided into ascending, constant, linearly descending and constant parts as shown in Fig. 1. The longitudinal compressive concrete stress for the ascending part from O to A is calculated based on the equation given by Mander et al. [32] as:

$$\sigma_c = \frac{f_{cc}' \lambda \left(\dfrac{\varepsilon_c}{\varepsilon_{cc}'} \right)}{\lambda - 1 + \left(\dfrac{\varepsilon_c}{\varepsilon_{cc}'} \right)^{\lambda}} \tag{1}$$

$$\lambda = \frac{E_c}{E_c - \left(\dfrac{f_{cc}'}{\varepsilon_{cc}'} \right)} \tag{2}$$

where f_{cc}' is the effective compressive strength of concrete, ε_c is the longitudinal compressive strain of concrete, ε_{cc}' is the strain at f_{cc}' and E_c is the Young's modulus of concrete which is given by ACI 318-11 [33] as

$$E_c = 3320\sqrt{f_{cc}'} + 6900 \qquad \text{(MPa)} \tag{3}$$

The effective compressive strengths of concrete $\left(f_{cc}'\right)$ is taken as $\lambda_c f_c'$, where λ_c is the strength reduction factor proposed by Liang [26] to account for the column size effects and expressed as

$$\lambda_c = 1.85 D_c^{-0.135} \qquad \left(0.85 \le \lambda_c \le 1.0\right) \tag{4}$$

in which D_c is taken as the larger of $\left(B - 2t\right)$ and $\left(D - 2t\right)$ for a rectangular cross-section, where B is the width of the cross-section, D is the depth of the cross-section, and t is the thickness of the steel tube wall.

In the numerical model, the strain ε_{cc}' corresponding to f_{cc}' is taken as 0.002 for the effective compressive strength less than or equal to 28 MPa and 0.003 for $f_{cc}' > 82\,\text{MPa}$. For the effective compressive strength between 28 and 82 MPa, the strain ε_{cc}' is determined by the linear interpolation.

The parts AB, BC and CD of the stress-strain curve for concrete in CFST columns as shown in Fig. 1 are defined by the following equations given by Liang [26]:

$$\sigma_c = \begin{cases} f_{cc}' & \text{for } \varepsilon_{cc}' < \varepsilon_c \le 0.005 \\ \beta_c f_{cc}' + 100\left(0.015 - \varepsilon_c\right)\left(f_{cc}' - \beta_c f_{cc}'\right) & \text{for } 0.005 < \varepsilon_c \le 0.015 \\ \beta_c f_{cc}' & \text{for } \varepsilon_c > 0.015 \end{cases} \tag{5}$$

where β_c was proposed by Liang [26] based on experimental results presented by Tomii and Sakino [34] as follows:

$$
\beta_c = \begin{cases}
1.0 & \text{for } \dfrac{B_s}{t} \leq 24 \\[2ex]
1.5 - \dfrac{1}{48}\dfrac{B_s}{t} & \text{for } 24 < \dfrac{B_s}{t} \leq 48 \\[2ex]
0.5 & \text{for } \dfrac{B_s}{t} > 48
\end{cases}
\tag{6}
$$

in which B_s is taken as the larger of B and D for a rectangular cross-section.

The concrete under compression is initially loaded up to an unloading strain and then unloaded to a zero stress level. The reloading of the concrete from the zero stress up to the envelope curve is characterized by the linear stress-strain relationships. For the unloading of concrete, the parabolic curve of the concrete is defined by the following equations [32]:

$$
\sigma_c = f_{un} - \frac{f_{un}\lambda_u\left(\dfrac{\varepsilon_c - \varepsilon_{un}}{\varepsilon_{pl} - \varepsilon_{un}}\right)}{\lambda_u - 1 + \left(\dfrac{\varepsilon_c - \varepsilon_{un}}{\varepsilon_{pl} - \varepsilon_{un}}\right)^{\lambda_u}} \qquad \left(\varepsilon_{pl} < \varepsilon_c < \varepsilon_{un}\right)
\tag{7}
$$

$$
\lambda_u = \frac{E_u}{E_u - \left(\dfrac{f_{un}}{\varepsilon_{un} - \varepsilon_{pl}}\right)}
\tag{8}
$$

where f_{un} is the compressive stress of concrete at the unloading, ε_{un} is the strain at f_{un}, ε_{pl} is the plastic strain which is proposed by Mander et al. [32] as:

$$\varepsilon_{pl} = \varepsilon_{un} - \frac{f_{un}\varepsilon_{un} + f_{un}\varepsilon_a}{f_{un} + E_c\varepsilon_a} \tag{9}$$

in which ε_a is given as

$$\varepsilon_a = a\sqrt{\varepsilon_{un}\varepsilon_{cc}'} \tag{10}$$

where a is taken as the larger of $\varepsilon_{cc}'/(\varepsilon_{cc}' + \varepsilon_{un})$ and $0.09\varepsilon_{un}/\varepsilon_{cc}$ for a rectangular cross-section.

In Eq. (8), E_u is the initial modulus of elasticity at the unloading proposed by Mander et al. [32] and is expressed by:

$$E_u = \left(\frac{f_{un}}{f_{cc}'}\right)\left(\sqrt{\frac{\varepsilon_{cc}'}{\varepsilon_{un}}}\right)E_c \tag{11}$$

in which $(f_{un}/f_{cc}') \geq 1.0$, and $\sqrt{\varepsilon_{cc}'/\varepsilon_{un}} \leq 1.0$.

For the reloading of concrete, a linear stress-strain relationship is assumed as follows:

$$\sigma_c = E_r(\varepsilon_c - \varepsilon_{ro}) + f_{ro} \qquad (\varepsilon_{pl} < \varepsilon_c < \varepsilon_{ro}) \tag{12}$$

where E_r is given by

$$E_r = \frac{f_{ro} - f_{re}}{\varepsilon_{ro} - \varepsilon_{re}} \tag{13}$$

in which f_{ro} is the concrete stress at the reloading, ε_{ro} is the strain at f_{ro}, and ε_{re} and f_{re} are the return strain and stress on the monotonic curve as shown in Fig. 1.

The envelop stress-strain curve for concrete under tension is divided into the linear descending and ascending parts as shown in Fig. 1. The concrete tensile stress linearly increases with the tensile strain of concrete up to concrete cracking. After concrete cracking, the tensile stress of concrete is inversely proportional to the tensile strain of concrete up to the ultimate tensile strain. The tensile strength of concrete is taken as $0.6\sqrt{f_{cc}'}$. The concrete tensile stress is considered zero at the ultimate tensile strain. The ultimate tensile strain is taken as 10 times of the strain at cracking.

For unloading from a compressive envelope curve, the stress in the concrete fiber under tension can be given by:

$$\sigma_t = \begin{cases} \dfrac{f_{ct}' \left(\varepsilon_c - \varepsilon_{pl} \right)}{\left(\varepsilon_{ct}' - \varepsilon_{tu}' \right)} & \text{for } \varepsilon_{tu}' < \varepsilon_c \leq \varepsilon_{ct}' \\[4mm] \dfrac{f_{ct}' \left(\varepsilon_c - \varepsilon_{pl} \right)}{\varepsilon_{ct}'} & \text{for } \varepsilon_{ct}' < \varepsilon_c < \varepsilon_{pl} \end{cases} \tag{14}$$

in which

$$f_{ct}^{'} = f_{ct}\left(1 - \frac{\varepsilon_{pl}}{\varepsilon_{cc}^{'}}\right) \tag{15}$$

$$\varepsilon_{ct}^{'} = \varepsilon_{ct} + \varepsilon_{pl} \tag{16}$$

For unloading from a tensile envelope curve, the reloading the concrete cannot carry the load up to the tensile strength so that the reloading branch follows the unloading branch.

2.2. Cyclic constitutive models for structural steels

The cyclic stress-strain relationship for the structural steels is shown in Fig. 2. The mild structural steels have a linear stress-strain relationship up to $0.9 f_{sy}$, where f_{sy} is the steel yield strength. The parabolic curve for cold-formed structural steels can be defined by the equation proposed by Liang [26]. The parabolic curve is replaced by the straight line for high strength steels. The hardening strain ε_{st} is assumed to be 0.005 for high strength and cold-formed steels and $10\,\varepsilon_{sy}$ for mild structural steels in the numerical model. The ultimate strain of steels is taken as 0.2.

For the cyclic stress-strain curve, the unloading follows a straight line with the same slope as the initial stiffness as shown in Fig. 2. The unloading part of the structural steels can be defined by the following equation:

$$\sigma_s = E_s\left(\varepsilon_s - \varepsilon_{mo}\right) \qquad \left(\varepsilon_o < \varepsilon_s \le \varepsilon_{mo}\right) \tag{17}$$

where σ_s is the stress in a steel fiber, E_s is the Young's modulus of steel, ε_s is the strain in the steel fiber and ε_{mo} is given by:

$$\varepsilon_{mo} = \varepsilon_o - \frac{f_o}{E_s} \tag{18}$$

in which ε_o is the strain at the unloading, f_o is the stress at the unloading.

The reloading curve for steels is described by the equations given by Shi et al. [35] as:

$$\sigma_s = E_s\left(\varepsilon_s - \varepsilon_{mo}\right) - \eta\left(E_s - E_k\right)\left(\varepsilon_s - \varepsilon_o\right) \qquad \left(\varepsilon_{mo} < \varepsilon_s \le \varepsilon_b\right) \tag{19}$$

$$E_k = \frac{\sigma_b}{\varepsilon_b - \varepsilon_{mo}} \tag{20}$$

where η is proposed by Shi et al. [35] as:

$$\eta = \begin{cases} 1.048 - \dfrac{0.05}{\dfrac{\varepsilon_s - \varepsilon_o}{\varepsilon_b - \varepsilon_o} + 0.05} & \text{for} \left|\varepsilon_b - \varepsilon_o\right| \ge 0.04 \\[4ex] 1.074 - \dfrac{0.08}{\dfrac{\varepsilon_s - \varepsilon_o}{\varepsilon_b - \varepsilon_o} + 0.08} & \text{for} \left|\varepsilon_b - \varepsilon_o\right| < 0.04 \end{cases} \tag{21}$$

For the reloading, the initial value of the strain ε_b is taken as $0.9\varepsilon_{sy}$. The stress f_b at the strain ε_b can be determined from the monotonic stress-strain curves. For the strain

greater than the strain ε_b, the cyclic skeleton curve is used to predict the stress in the steel fiber. After initial reloading, the reloading is directed toward the previous unloading.

3. Modeling of cross-sectional strengths

3.1. Strain calculations

The behavior of composite cross-sections is modeled using the accurate fiber element method. The cross-section is divided into fiber elements as shown in Fig. 3. Each fiber element can be assigned with either steel or concrete material properties. Fiber element stresses are calculated from fiber strains using cyclic stress-strain relationships. The strain ε_t at the top fiber of the cross-section can be determined by multiplication of the curvature ϕ and the neutral axis depth d_n. For bending about the x-axis, strains in concrete and steel fibers can be calculated by the following equations proposed by Liang [26]:

$$y_{n,i} = \frac{D}{2} - d_n \tag{22}$$

$$d_{e,i} = \left| y_i - y_{n,i} \right| \tag{23}$$

$$\varepsilon_i = \begin{cases} \phi d_{e,i} & \text{for } y_i \geq y_{n,i} \\ -\phi d_{e,i} & \text{for } y_i < y_{n,i} \end{cases} \tag{24}$$

in which d_n is the neutral axis depth, $d_{e,i}$ is the orthogonal distance from the centroid of each fiber element to the neutral axis, y_i is the coordinates of the fiber i and ε_i is the strain at the ith fiber element.

3.2. Initial local buckling of steel tube walls under stress gradients

The steel tube walls of a CFST column are restrained by the concrete core so that they can only buckle outward. The edges of the tube wall can be assumed as clamped. Liang et al. [28] developed nonlinear finite element models to study the local and post-local buckling behavior of clamped steel plates that form a CFST column under stress gradients. The models accounted for geometric imperfection of $0.1t$ at the plate centre and compressive residual stresses of $0.25 f_{sy}$, which were balanced by the tensile residual stresses locked in the same plate. Based on the finite element results, Liang et al. [28] proposed a set of formulas for determining the initial local buckling stress of steel tube walls subjected to compressive stress gradients. These formulas are incorporated in the numerical model to determine the onset of cyclic local buckling of thin-walled CFST slender beam-columns.

3.3. Post-local buckling of steel tube walls under stress gradients

The effective width concept is usually used to determine the post-local buckling strengths of thin steel plates. Liang et al. [28] proposed a set of effective width formulas for steel tube walls of CFST columns under compressive stress gradients. The effective width is a function of the width-to-thickness ratio (b/t) and compressive stress gradient

(α_s). Their formulas are incorporated in the numerical model to determine the ultimate strengths of steel tube walls subjected to stress gradients. Fig. 3 shows the effective and ineffective areas of a steel cross-section under axial load and uniaxial bending. The effective widths b_{e1} and b_{e2} of a steel tube wall under stress gradients are given by Liang et al. [28] as

$$\frac{b_{e1}}{b} = \begin{cases} 0.2777 + 0.01019\left(\frac{b}{t}\right) - 1.972 \times 10^{-4}\left(\frac{b}{t}\right)^2 + 9.605 \times 10^{-7}\left(\frac{b}{t}\right)^3 & \text{for } \alpha_s > 0.0 \\ 0.4186 - 0.002047\left(\frac{b}{t}\right) + 5.355 \times 10^{-5}\left(\frac{b}{t}\right)^2 - 4.685 \times 10^{-7}\left(\frac{b}{t}\right)^3 & \text{for } \alpha_s = 0 \end{cases} \tag{25}$$

$$\frac{b_{e2}}{b} = (2 - \alpha_s)\frac{b_{e1}}{b} \tag{26}$$

where b is the clear width of a steel flange or web in the section, and $\alpha_s = \sigma_2/\sigma_1$, σ_1 is the maximum edge stress acting on the steel tube wall and σ_2 is the minimum edge stress acting on the same steel tube wall. It is noted that the effective width formulas were proposed for clamped steel plates with b/t ratio ranging from 30 to 100. For a plate with a b/t ratio less than 30, the plate is treated as compact.

The post-local buckling of a thin steel plate is characterized by the gradual redistribution of stresses within the buckled plate. After the onset of local buckling, the ineffective width of the plate increases with increasing the compressive load until the plate attains its ultimate strength, which is governed by the effective widths given by Eqs. (25) and (26). In the present study, the progressive post-local buckling of steel tube walls under stress gradients is modeled by gradually redistributing the normal stresses

within the steel tube wall. This can be done by assigning the steel fiber elements located in the ineffective areas to zero stress (Liang 26).

3.4. Stress resultants

The internal axial force and bending moment carried by a composite cross-section under axial load and uniaxial bending are determined as the stress resultants, which are expressed by:

$$P_n = \sum_{i=1}^{ns} \sigma_{s,i} A_{s,i} + \sum_{j=1}^{nc} \sigma_{c,j} A_{c,j} \qquad (27)$$

$$M_x = \sum_{i=1}^{ns} \sigma_{s,i} A_{s,i} y_i + \sum_{j=1}^{nc} \sigma_{c,j} A_{c,j} y_j \qquad (28)$$

where P_n is the internal axial force, M_x is the internal bending moment about the x-axis, $\sigma_{s,i}$ is the longitudinal stress at the centroid of steel fiber i, $A_{s,i}$ is the area of steel fiber i, $\sigma_{c,j}$ is the longitudinal stress at the centroid of concrete fiber j, $A_{c,j}$ is the area of concrete fiber j, y_i is the coordinates of steel element i, y_j is the coordinates of concrete element j, ns is the total number of steel fiber elements and nc is the total number of concrete fiber elements.

3.5. The Müller's method

The Müller's method [36] is an efficient numerical technique for solving nonlinear equilibrium equations. It is a generalization of the secant method, which has been used to obtain nonlinear solutions to CFST short beam-columns under axial load and biaxial bending by Liang [26]. Computational algorithms based on the Müller's method are developed to iterate the neutral axis depth in a rectangular CFST cross-section. The Müller's method requires three initial values of the neutral axis depth $d_{n,1}$, $d_{n,2}$ and $d_{n,3}$. The corresponding residual forces $r_{p,1}$, $r_{p,2}$ and $r_{p,3}$ are calculated based on the three initial values of the neutral axis depth. The new neutral axis depth $d_{n,4}$ is determined by the following equations:

$$d_{n,4} = d_{n,3} - \frac{2c_m}{b_m \pm \sqrt{b_m^2 - 4a_m c_m}} \tag{29}$$

$$a_m = \frac{(d_{n,2} - d_{n,3})(r_{p,1} - r_{p,3}) - (d_{n,1} - d_{n,3})(r_{p,2} - r_{p,3})}{(d_{n,1} - d_{n,2})(d_{n,2} - d_{n,3})(d_{n,1} - d_{n,3})} \tag{30}$$

$$b_m = \frac{(d_{n,1} - d_{n,3})^2 (r_{p,2} - r_{p,3}) - (d_{n,2} - d_{n,3})^2 (r_{p,1} - r_{p,3})}{(d_{n,1} - d_{n,2})(d_{n,2} - d_{n,3})(d_{n,1} - d_{n,3})} \tag{31}$$

$$c_m = r_{p,3} \tag{32}$$

The values of the neutral axis depth $d_{n,1}$, $d_{n,2}$ and $d_{n,3}$ and corresponding residual forces $r_{p,1}$, $r_{p,2}$ and $r_{p,3}$ need to be exchanged as discussed by Patel et al. [29]. Eq. (29) and the exchange of the neutral axis depths and residual forces are iteratively executed until the convergence criteria of $|r_p| < \varepsilon_k$ is satisfied. The sign of the square toot term in the denominator of Eq. (29) is taken as the same sign of b_m.

4. Modeling of cyclic load-deflection responses

4.1. Formulation

A cantilever column under a constant axial load (P) and cyclically varying lateral loading (F) is considered in the numerical model. The deflected shape and coordinate system for the cantilever column are depicted in Fig. 4, where L represents the actual length of the column and u_l demotes the lateral deflection at the tip of the column. The effective length of the cantilever column is taken as $2L$. The deflected shape of the cantilever column is assumed to be part of a sine wave which is described by the following displacement function:

$$u = u_l \sin\left(\frac{\pi z}{2L}\right) \tag{33}$$

The curvature along the length of the cantilever column can be derived from Eq. (33) as

$$\phi = \frac{\partial^2 u}{\partial z^2} = \left(\frac{\pi}{2L}\right)^2 u_l \sin\left(\frac{\pi z}{2L}\right) \tag{34}$$

The curvature at the base of the cantilever column is given by

$$\phi_b = \left(\frac{\pi}{2L}\right)^2 u_l \tag{35}$$

The external moment at the base of the cantilever column can be determined as

$$M_{me} = FL + P(e + u_l + u_{lo})$$ (36)

in which e is the eccentricity of the axial load and it is taken as zero for the pure axial load in the present study, u_{lo} is the initial geometric imperfection at the tip of the cantilever columns.

The column must satisfy the force and moment equilibrium conditions at its base as follows:

$$P_n - P = 0$$ (37)

$$FL + P(e + u_l + u_{lo}) - M_x = 0$$ (38)

where M_x is the internal bending moment of the cross-section at the column base.

The lateral load can be determined as:

$$F = \frac{M_x - P(e + u_l + u_{lo})}{L}$$ (39)

4.2. Computational procedure

An incremental-iterative numerical scheme based on the displacement control method was employed in the computational procedure to predict the cyclic load-deflection responses of slender beam-columns. The lateral deflection at the tip of the beam-column is initialized. The curvature ϕ_b at the column base is calculated from the given lateral deflection u_l using Eq. (35). The neutral axis depth of the composite cross-section is iteratively adjusted using the Müller's method. The force and moment equilibriums are maintained at the base of the cantilever column. The internal bending moment M_x is determined from axial force and curvature relationship. The cyclic lateral load F at the tip of the cantilever column is calculated using Eq. (39). The lateral deflection at the tip of the cantilever column is gradually increased up to the predefined unloading deflection. After the unloading deflection, the lateral deflection is gradually decreased up to the reloading level. Note that the stresses of the steel and concrete fiber elements depend not only on the strain of the element, but also on the complete stress-strain history. The stresses and strains of the fiber elements for each lateral deflection are recorded in the numerical analysis. The process is repeated until the ultimate cyclic lateral load is obtained or the deflection limit is reached. The main steps of the computational procedure are given as follows:

(1) Input data.

(2) Discretize the composite cross-section into fiber elements.

(3) Initialize the first unloading deflection u_{ul}

(4) Initialize the lateral deflection at the tip of the cantilever column $u_l = \Delta u_l$.

(5) Calculate the curvature ϕ_b at the base of the cantilever column.

(6) Set $\Delta u_l = -\Delta u_l$ if $u_l > (u_{ul} - \Delta u_l)$ or $u_l < (-u_{ul} - \Delta u_l)$.

(7) Define the next unloading deflection u_{ul} if $(u_l - u_{llast})(u_{llast} - u_{lold}) < 0$ and $u_l > u_{llast}$.

(8) Recall the unloading strains and stresses at the unloading deflection.

(9) Adjust the neutral axis depth (d_n) using the Müller's method.

(10) Calculate fiber strains and stresses using cyclic stress-strain relationships.

(11) Check cyclic local buckling and update steel fiber stresses.

(12) Calculate resultant force P considering local buckling effects.

(13) Compute the residual force $r_p = P_n - P$.

(14) Repeat Steps (9)-(13) until $|r_p| < \varepsilon_k$.

(15) Compute the internal bending moment M_x.

(16) Calculate the cyclic lateral force F using Eq. (39).

(17) Record the deflection $u_{lold} = u_{llast}$ and $u_{llast} = u_l$

(18) Store the fiber strains and fiber stresses under the current deflection.

(19) Increase the deflection at the tip of the cantilever column by $u_l = u_l + \Delta u_l$.

(20) Repeat Steps (5)-(19) until the ultimate cyclic lateral load F_u is obtained or the deflection limit is reached.

(21) Plot the cyclic load-deflection curve.

The convergence tolerance ε_k is taken as 10^{-4} in the numerical analysis.

5. Validation of the numerical model

The accuracy of the developed numerical model is evaluated by comparing the numerical solutions with experimental results given by Verma et al. [14]. The ultimate cyclic lateral loads and cyclic load-deflection curves for high strength thin-walled square CFST beam-columns are considered in the verification of the numerical model developed.

5.1. Ultimate cyclic lateral loads

The dimensions and material properties of high strength CFST beam-columns tested by Varma et al. [14] are given in Table 1. In the table, $F_{u.\exp}$ represents the experimental ultimate cyclic lateral load and $F_{u.\text{num}}$ denotes the ultimate cyclic lateral load predicted by the numerical model. Specimens were tested under rotating axial load and cyclic loading using special clevises-pins supports. All specimens had a square cross-section of 305 × 305 mm. The depth-to-thickness ratios (D/t) ranged from 34 to 52 while the length of the column was 1200 mm. The steel tube of the specimens was filled with high strength concrete of 110 MPa. It should be noted that the concrete compressive strength given in Table 1 is the cylinder compressive strength. The yield strengths (f_{sy}) of the steel tube varied from 269 MPa to 660 MPa. The experimental axial load applied to each specimen was employed in the numerical analysis. It can be observed from Table 1 that the ultimate cyclic lateral loads predicted by the numerical model are in good agreement with experimental results. The mean ultimate cyclic lateral load predicted by the numerical model is 99% of the experimental value with a standard deviation of 0.11 and a coefficient of variation of 0.11.

5.2. Cyclic load-deflection curves

Cyclic load-deflection curves provide useful information on the initial stiffness, ultimate cyclic lateral load, unloading stiffness, reloading stiffness and post-peak behavior of thin-walled CFST beam-columns. To examine the accuracy of the proposed numerical model, cyclic load-deflection curves predicted by the numerical model are compared with experimental results reported by Varma et al. [14] in Figs. 5-7.

The D/t ratios of these columns ranged from 34 to 52. Therefore, the local buckling of the steel tube wall under stress gradients was considered in the numerical model. It can be seen from Figs. 5-7 that the numerical model predicts well the ultimate cyclic lateral loads when compared to test results. The predicted ultimate cyclic lateral load for specimen CBC-32-80-10 is 95% of the experimental value. Reasonable agreement between computed and experimental cyclic load-deflection curves is achieved for specimens CBC-48-80-10, CBC-48-80-20, CBC-32-46-20, CBC-48-46-10 and CBC-48-46-20. The ratios of computed ultimate cyclic lateral load to experimental value for specimens CBC-48-80-10, CBC-48-80-20, CBC-32-46-20, CBC-48-46-10 and CBC-48-46-20 are 1.14, 1.06, 0.86, 1.07 and 1.07, respectively. The predicted post-peak behavior of the cyclic load-deflection curves for specimens is in reasonable agreement with experimental data. The unloading and reloading stiffness of the cyclic load-deflection curves predicted by the numerical model slightly differ from experimental ones. This is likely due to the uncertainty of the actual concrete stiffness and strength.

6. Parametric study

In the parametric study, the axial load was taken as 10% of the ultimate axial strength of the column cross-section. The computer program developed by Liang et al. [25] was used to determine the ultimate axial strengths of column cross-sections under axial compression. In the present study, the initial geometric imperfection at the tip of the beam-column was taken as $L/1000$. The Young's modulus of steel material was 200 GPa. The yield stress of 690 MPa and the tensile strength of 790 MPa were assumed for steel tubes, except where specially indicated. The effects of cyclic local and post-local buckling were considered in all analyses. The typical cyclic loading pattern used in the parametric study is illustrated in Fig. 8.

6.1. Effects of local buckling

The numerical model was employed to investigate the effects of cyclic local buckling on the cyclic load-deflection curves for high strength CFST slender beam-columns under constant axial load and cyclically varying lateral loading. A thin-walled CFST beam-column with a cross-sectional dimension of 700×800 mm was considered. The thickness of the steel tube was 8 mm so that its depth-to-thickness ratio (D/t) was 100. The compressive cylinder strength of concrete was 80 MPa. The column slenderness ratio (L_e/r) was 22. The applied axial load was 4623.1 kN. Analyses of the beam-column were carried out by considering and ignoring cyclic local buckling effects respectively.

Fig. 9 shows the effects of cyclic local buckling on the cyclic load-deflection curves for thin-walled CFST beam-columns. It can be seen from Fig. 9 that cyclic local buckling considerably reduces the stiffness and ultimate cyclic lateral load of the slender beam-column with the same axial load level. The ultimate cyclic lateral load of the slender beam-column is overestimated by 4.3% if local buckling was not considered. More reduction in the ultimate cyclic lateral load would be expected if higher axial load was applied to the column. In addition, cyclic local buckling tends to reduce the ductility of the column under cyclic loading, which is important for seismic design of composite buildings. These highlight the importance of considering cyclic local buckling in the analysis and design.

6.2. Effects of column slenderness ratio

The numerical model developed was used to examine the important effects of the column slenderness ratio. High strength thin-walled CFST slender beam-columns with a cross-section of 700×700 mm were considered. The depth-to-thickness ratio of the section was 70. Column slenderness ratios (L_e/r) of 22 and 30 were considered in the parametric study. The steel tubes were filled with high strength concrete of 70 MPa. The axial load of 4131.2 kN was applied to the beam-column.

The cyclic load-deflection curves for high strength thin-walled CFST slender beam-columns with L_e/r ratios of 22 and 30 are presented respectively in Figs. 10(a) and 10(b). The ultimate lateral load of thin-walled CFST slender beam-columns tends to decrease when increasing the column slenderness ratio of the beam-columns under the

same axial load level. Columns with a smaller L_e/r ratio are shown to be less ductile than the ones with a larger L_e/r ratio. The lateral deflection at the ultimate cyclic lateral load of the beam-columns increases with increasing the column slenderness ratio. When increasing the column slenderness ratio from 22 to 30, the ultimate cyclic lateral load of the slender beam-column decreases by 28.7%. This demonstrates that the column slenderness has a significant effect on the cyclic lateral load capacities of CFST slender beam-columns.

6.3. Effects of depth-to-thickness ratio

Local buckling of thin-walled rectangular CFST slender beam-columns depends on its depth-to-thickness ratio (D/t). The numerical model was employed to investigate the effects of D/t ratio on the cyclic load-deflection curves for high strength CFST slender beam-columns with an L_e/r ratio of 30 and subjected to a constant axial load of 4450.9 kN and cyclically varying lateral loading. The dimensions of the composite section analyzed were 600 × 600 mm. The D/t ratios of the column sections were calculated as 50 and 80 by changing the thickness of the steel tubes. The compressive strength of the in-filled concrete was 100 MPa.

Fig. 11 illustrates the effects of the D/t ratio on the cyclic load-deflection curves for thin-walled CFST slender beam-columns. It can be seen from the figure that the ultimate cyclic lateral load and stiffness of the CFST slender beam-columns decrease with an increase in the D/t ratio for the same size composite section. This is because

the column section with a larger D/t ratio has a lesser steel area and it may undergo local buckling which reduces the ultimate strength of the column. When the D/t ratio is increased from 50 to 80, the ultimate cyclic lateral load of the beam-column is found to decrease by 31.1%. The results suggest that the cyclic lateral load capacity of a CFST slender beam-column can be significantly increased by using a smaller D/t ratio for the cross-section in the design.

6.4. Effects of concrete compressive strengths

The effects of concrete compressive strengths on the cyclic load-deflection responses of high strength CFST slender beam-columns with cyclic local buckling effects were studied by the numerical model. The compressive cylinder concrete strengths used in the parametric study were 60 MPa and 100 MPa. The dimensions of the cross-section were 700×800 mm with a D/t ratio of 80. The column slenderness ratio (L_e/r) of 30 was specified. The applied axial load was 4119.5 kN.

The computed cyclic load-deflection curves for high strength rectangular CFST slender beam-columns with different concrete compressive strengths are depicted in Fig. 12. The ultimate cyclic lateral loads of CFST slender beam-columns increase with an increase in the concrete compressive strength. Increasing the concrete compressive strength from 60 MPa to 100 MPa increases the ultimate cyclic lateral strength by 7.2%. However, the initial flexural stiffness of the slender beam-columns has a slight increase due to the use of higher strength concrete. The results indicate that the use of high

strength concrete will not lead to significant increase in the cyclic lateral load capacity and flexural stiffness.

6.5. Effects of steel yield strengths

Square thin-walled CFST slender beam-columns with different steel yield strengths and a cross-section of 650×650 mm were analyzed using the numerical model. The depth-to-thickness (D/t) ratio of the section was 65. The yield strengths of the steel tubes were 300 MPa and 690 MPa and the corresponding tensile strengths were 430 MPa and 790 MPa respectively. The column slenderness ratio (L/r) of 30 was used in the parametric study. The steel tube was filled with 60 MPa concrete. A constant axial load of 2606.9 kN was applied to the columns.

Fig. 13 gives the cyclic lateral load-deflection curves for CFST slender beam-columns with different steel yield strengths. It can be observed from figure that the steel yield strength does not have an effect on the initial flexural stiffness of the beam-columns. However, the ultimate cyclic lateral load of slender beam-columns is found to increase significantly with an increase in the steel yield strength. By increasing the steel yield strength from 300 MPa to 690 MPa, the ultimate cyclic lateral load of the slender beam-column is found to increase by 91.3%. This is because the moment capacity of the cantilever column is significantly increased by increasing the steel yield stress. Consequently, the use of high strength steel tubes leads to a significant increase in the cyclic lateral load capacities of CFST slender beam-columns.

7. Conclusions

This paper has presented a numerical model for the nonlinear inelastic analysis of high strength thin-walled rectangular CFST slender beam-columns under constant axial load and cyclically varying lateral loading. The model accounts for the important effects of progressive cyclic local buckling of steel tube walls under stress gradients by gradually redistributing the normal stresses within buckled steel tube walls. This method gives a more accurate simulation of the actual cyclic post-local buckling behavior of steel tubes than the modified stress-strain curve approach, which cannot model the progressive cyclic local and post-local buckling. Moreover, geometric and material nonlinearities are taken into account in the numerical model. The comparative study shows that the numerical model developed predicts well the cyclic load-deflection responses of thin-walled CFST slender beam-columns.

Based on the parametric study, the following important conclusions are drawn:

(1) The cyclic local buckling considerably reduces the ultimate cyclic lateral loads and ductility of CFST slender beam-columns.

(2) Increasing the column or section slenderness ratio significantly reduces the ultimate cyclic lateral loads of CFST slender beam-columns.

(3) The use of high strength concrete does not result in a significant increase in the ultimate cyclic lateral loads of CFST slender beam-columns.

(4) The use of high strength steel tubes leads to a significant increase in the cyclic lateral load capacities of CFST slender beam-columns.

References

[1]   Furlong RW. Strength of steel-encased concrete beam-columns. J Struct Eng ASCE 1997;93(5):113-24.

[2]   Knowles RB, Park R. Strength of concrete-filled steel tubular columns. J Struct Div ASCE 1969;95(12):2565-87.

[3]   Schneider SP. Axially loaded concrete-filled steel tubes. J Struct Eng ASCE 1998;124(10):1125-38.

[4]   Sakino K, Nakahara H, Morino S, Nishiyama I. Behavior of centrally loaded concrete- filled steel-tube short columns. J Struct Eng ASCE 2004;130(2):180-8.

[5]   Fujimoto T, Mukai A, Nishiyama I, Sakino K. Behavior of eccentrically loaded concrete-filled steel tubular columns. J Struct Eng ASCE 2004;130(2):203–12.

[6]   Ellobody E, Young B, Lam D. Behaviour of normal and high strength concrete-filled compact steel tube circular stub columns. J Constr Steel Res 2006;62(7):706-15.

[7]   Liu D. Behaviour of eccentrically loaded high-strength rectangular concrete-filled steel tubular columns. J Constr Steel Res 2006;62(8):839-46.

[8]   Portolés JM, Romero ML, Bonet JL, Filippou FC. Experimental study on high strength concrete-filled circular tubular columns under eccentric loading. J Constr Steel Res 2011;67(4):623-33.

[9]   Mursi M, Uy B. Behaviour and design of fabricated high strength steel columns subjected to biaxial bending part 1: experiments. Adv Steel Const 2006;2(4):286-313.

[10] Shakir-Khalil H, Zeghiche J. Experimental behaviour of concrete-filled rolled rectangular hollow-section columns. Struct Eng 1989;67(19):346-53.

[11] Vrcelj Z, Uy B. Strength of slender concrete-filled steel box columns incorporating local buckling. J Constr Steel Res 2002;58(2):275-300.

[12] Hu HT, Huang CS, Wu MH, Wu YM. Nonlinear analysis of axially loaded concrete-filled tube columns with confinement effect. J Struct Eng ASCE 2003;129(10):1322-9.

[13] Varma AH, Ricles JM, Sause R, Lu LW. Seismic behavior and modeling of high-strength composite concrete-filled steel tube (CFT) beam-columns. J Constr Steel Res 2002;58(5-8):725–58.

[14] Varma AH, Ricles JM, Sause R, Lu LW. Seismic behavior and design of high-strength square concrete-filled steel tube beam columns. J Struct Eng ASCE 2004;130(2):169-79.

[15] Han LH, Yang YF, Tao Z. Concrete-filled thin-walled steel SHS and RHS beam-columns subjected to cyclic loading. Thin-Walled Structure 2003;41(9):801-33.

[16] Wu B, Zhao XY, Zhang JS. Cyclic behavior of thin-walled square steel tubular columns filled with demolished concrete lumps and fresh concrete. J Constr Steel Res 2012;77:69-81.

[17] Gayathri V, Shanmugam NE, Choo YS. Concrete-filled tubular columns part 1-cross-section analysis. Int J Struct Stab Dyn 2004;4(4):459-78.

[18] Gayathri V, Shanmugam NE, Choo YS. Concrete-filled tubular columns part 2-column analysis. Int J Struct Stab Dyn 2004;4(4):479-95.
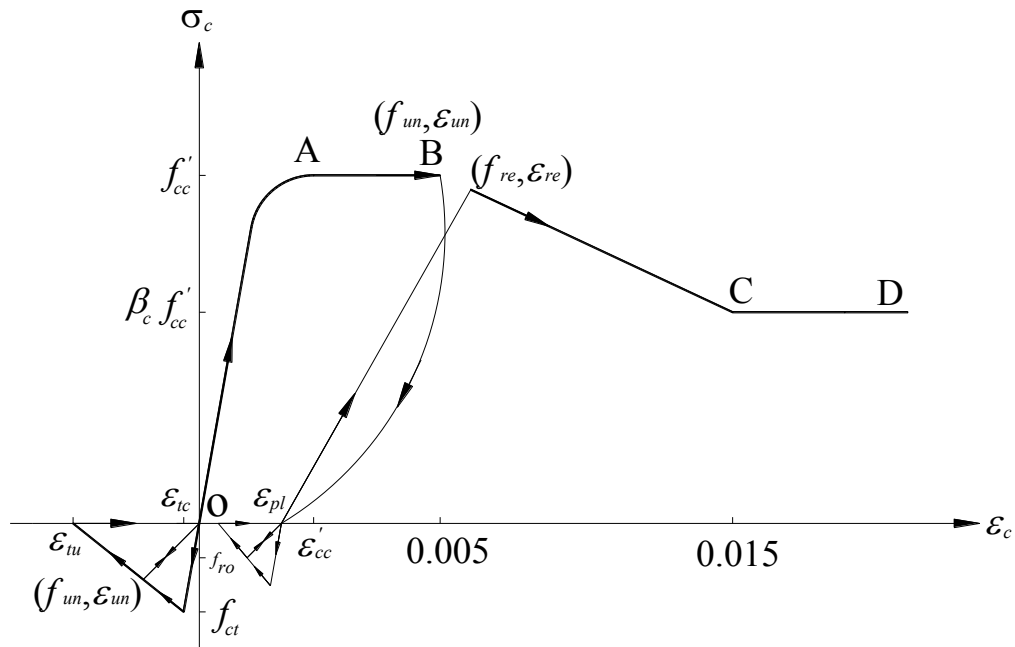
[19] Chung K, Chung J, Choi S. Prediction of pre- and post-peak behavior of concrete-filled square steel tube columns under cyclic loads using fiber element method. Thin-Walled Structure 2007;45(9):747-58.

[20] Zubydan AH, ElSabbagh AI. Monotonic and cyclic behavior of concrete-filled steel-tube beam-columns considering local buckling effect. Thin-Walled Structure 2011;49(4): 465-481.

[21] Ge HB, Usami T. Strength of concrete-filled thin-walled steel box columns: experiment. J Struct Eng ASCE 1992;118(11):3036-54.

[22] Bridge RQ, O'Shea MD. Behaviour of thin-walled steel box sections with or without internal restraint. J Constr Steel Res 1998;47(1-2):73-91.

[23] Uy B. Strength of concrete filled steel box columns incorporating local buckling. J Struct Eng ASCE 2000;126(3):341-52.

[24] Han LH. Tests on stub columns of concrete-filled RHS sections. J Constr Steel Res 2002;58(3):353-72.

[25] Liang QQ, Uy B, Liew JYR. Nonlinear analysis of concrete-filled thin-walled steel box columns with local buckling effects. J Constr Steel Res 2006;62(6):581-91.

[26] Liang QQ. Performance-based analysis of concrete-filled steel tubular beam-columns, part I: theory and algorithms. J Constr Steel Res 2009;65(2):363-72.

[27] Liang QQ. Performance-based analysis of concrete-filled steel tubular beam-columns, part II: verification and applications. J Constr Steel Res 2009;65(2):351-62.

[28] Liang QQ, Uy B, Liew JYR. Local buckling of steel plates in concrete-filled thin-walled steel tubular beam-columns. J Const Steel Res 2007;63(3):369-405.

[29] Patel VI, Liang QQ, Hadi MNS. High strength thin-walled rectangular concrete-filled steel tubular slender beam-columns, part I: modeling. J Constr Steel Res 2012;70:377-84.

[30] Patel VI, Liang QQ, Hadi MNS. High strength thin-walled rectangular concrete-filled steel tubular slender beam-columns, part II: behavior. J Constr Steel Res 2012;70:368-76.

[31] Liang QQ, Patel VI, Hadi MNS. Biaxially loaded high-strength concrete-filled steel tubular slender beam-columns, part I: multiscale simulation. J Constr Steel Res 2012;75:64-71.

[32] Mander JB, Priestley MJN, Park R. Theoretical stress-strain model for confined concrete. J Struct Eng ASCE 1988;114(8):1804-26.

[33] ACI Committee 318. ACI-318-11: Building code requirements for structural concrete and commentary. Detroit(MI):ACI;2011.

[34] Tomii M, Sakino K. Elastic-plastic behavior of concrete filled square steel tubular beam-columns. Trans Archit Inst Japn 1979;280:111-20.

[35] Shi G, Wang M, Bai Y, Wang F, Shi Y, Wang Y. Experimental and modeling study of high-strength structural steels under cyclic loading. Eng Struct 2012;37:1-13.

[36] Müller DE. A method for solving algebraic equations using an automatic computer. MTAC 1956;10:208-15.

Figures and tables

Table 1 Ultimate cyclic lateral loads of thin-walled CFST slender beam-columns.

Specimens	$B \times D \times t$ (mm)	D/t	L (mm)	f_c' (MPa)	f_{sy} (MPa)	f_{su} (MPa)	E_s (GPa)	P (kN)	$F_{u.exp}$ (kN)	$F_{u.num}$ (kN)	$\dfrac{F_{u.num}}{F_{u.exp}}$	Ref.
CBC-32-80-10	305 × 305 ×8.9	34.29	1200	110	600	674	200	1523	729.55	696.5	0.95	
CBC-32-80-20	305 × 305 ×8.9	34.29	1200	110	600	674	200	3050	743.18	698.2	0.94	
CBC-48-80-10	305 × 305 ×6.1	50.00	1200	110	660	737	200	1355	495	562.7	1.14	
CBC-48-80-20	305 × 305 ×6.1	50.00	1200	110	660	737	200	2715	545.45	578.4	1.06	[14]
CBC-32-46-10	305 × 305 ×8.6	35.29	1200	110	269	429	200	1255	429.55	370.1	0.86	
CBC-32-46-20	305 × 305 ×8.6	35.29	1200	110	269	429	200	2515	470.45	404.8	0.86	
CBC-48-46-10	305 × 305 ×5.8	52.17	1200	110	471	534	200	1178	388.66	415.7	1.07	
CBC-48-46-20	305 × 305 ×5.8	52.17	1200	110	471	534	200	2270	415.91	445.0	1.07	
Mean											0.99	
Standard deviation (SD)											0.11	
Coefficient of variation (COV)											0.11	

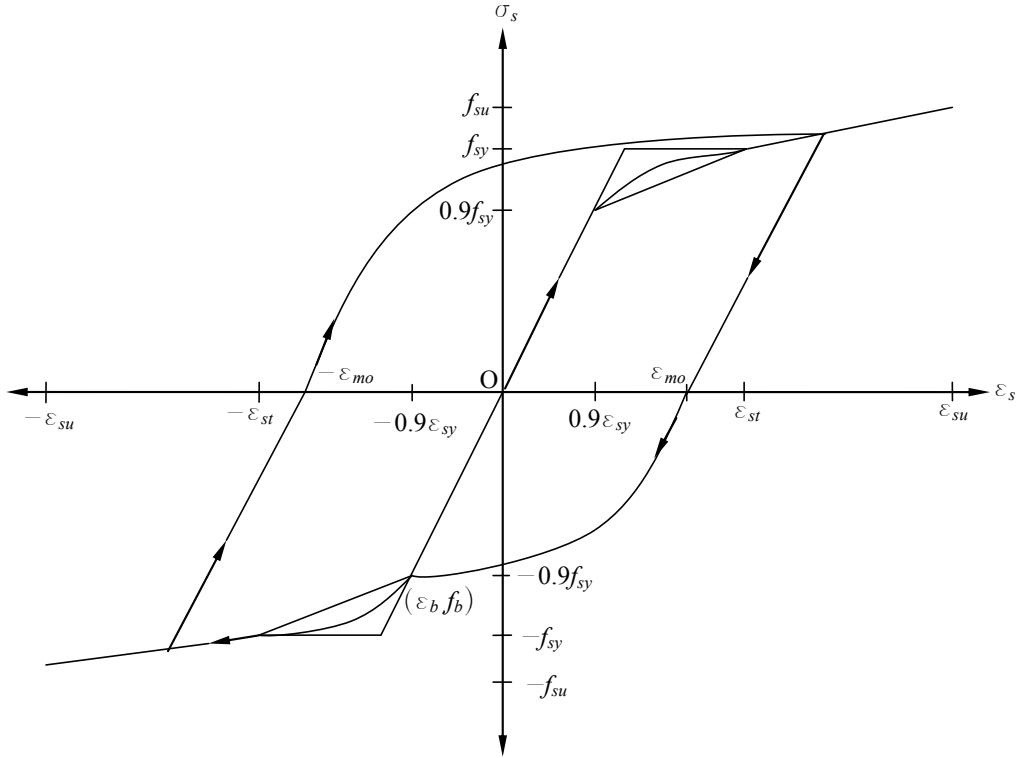**Fig. 1.** Cyclic stress-strain curves for concrete in rectangular CFST columns.

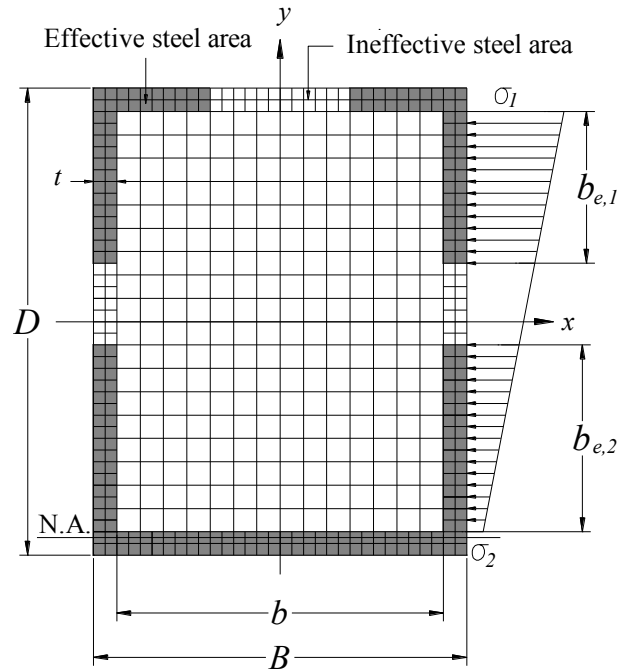**Fig. 2.** Cyclic stress-strain curves for structural steels.

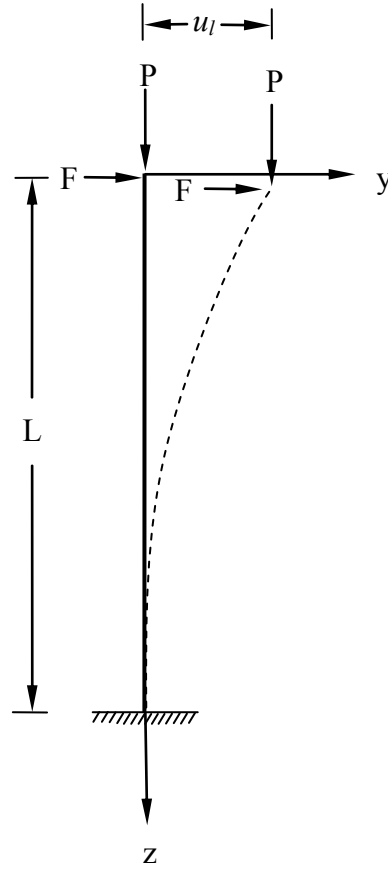**Fig. 3.** Effective area of steel tubular cross-section under axial load and uniaxial bending.
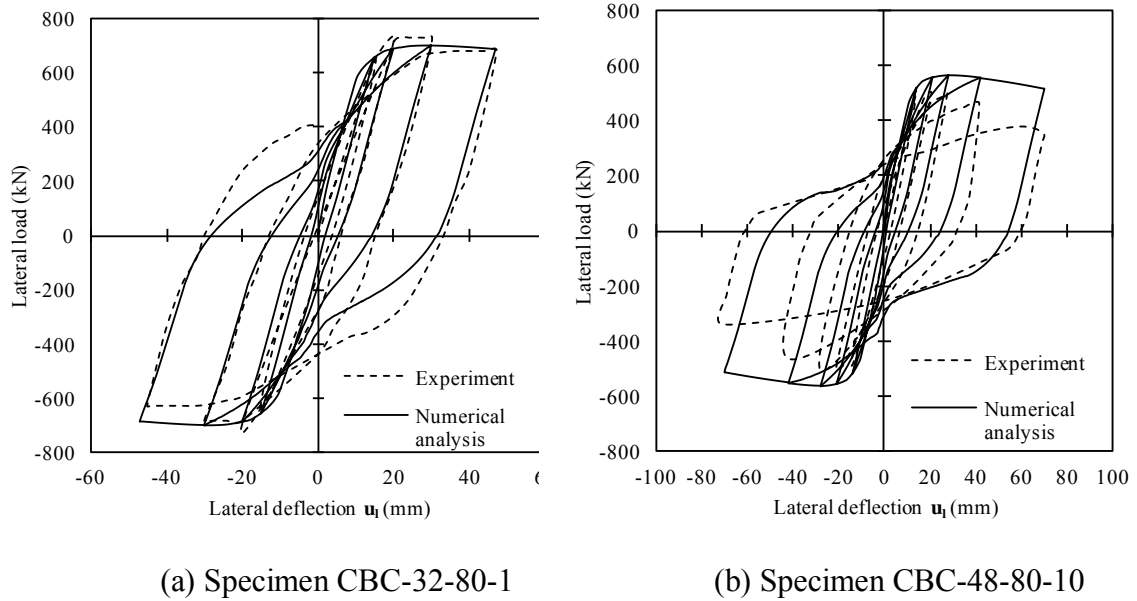
Fig. 4. Cantilever column model.

(a) Specimen CBC-32-80-1

(b) Specimen CBC-48-80-10

Fig. 5. Comparison of predicted and experimental cyclic load-deflection curves for specimens CBC-32-80-10 and CBC-48-80-10.
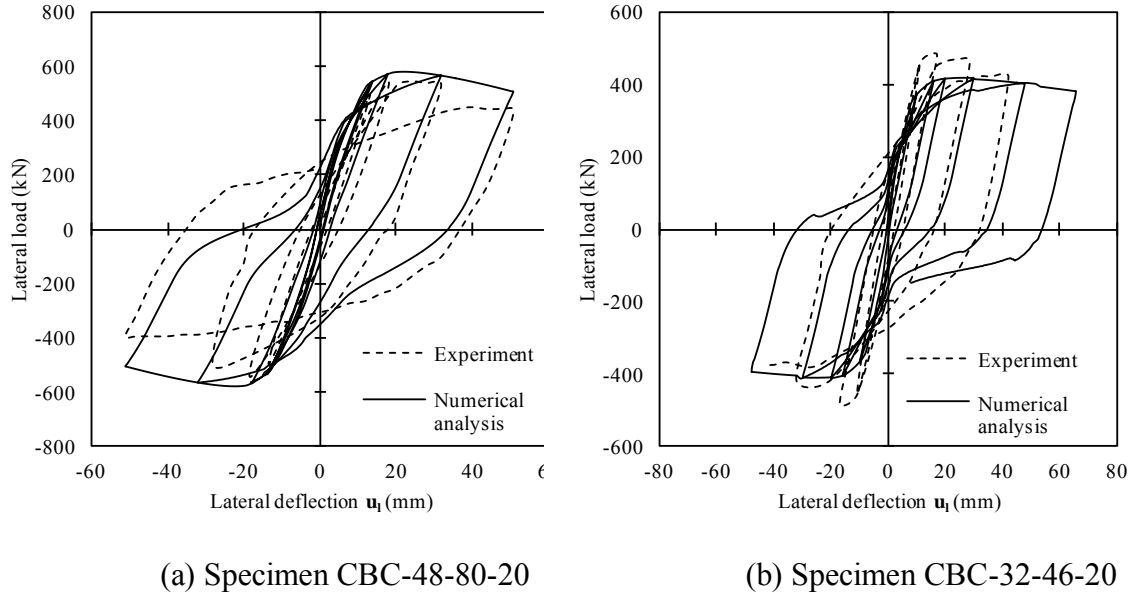
(a) Specimen CBC-48-80-20

(b) Specimen CBC-32-46-20

Fig. 6. Comparison of predicted and experimental cyclic load-deflection curves for specimens CBC-48-80-20 and CBC-32-46-20.

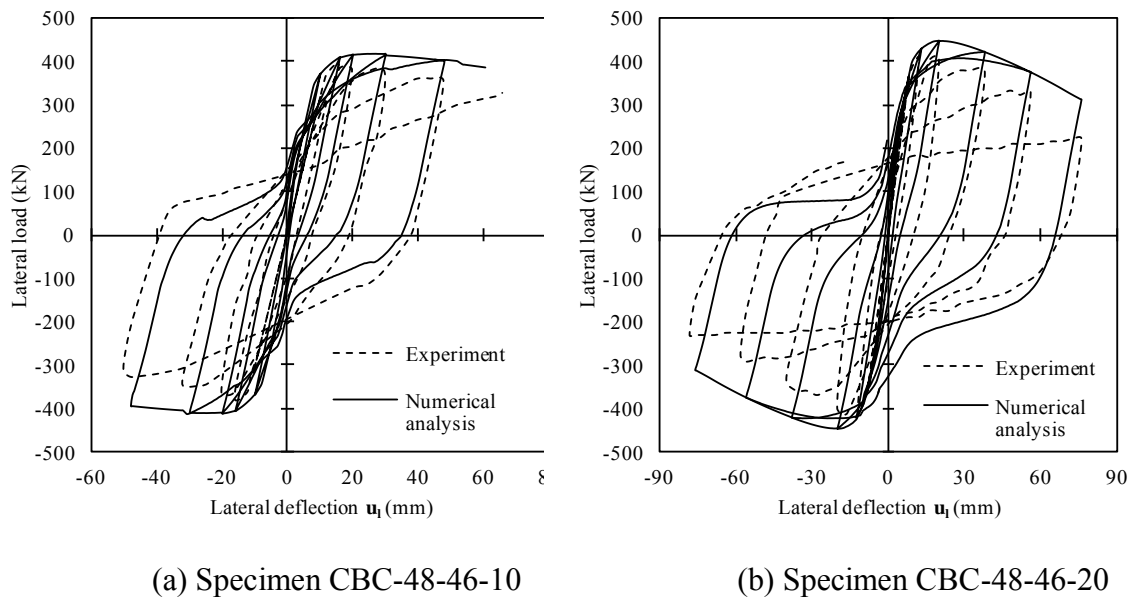(a) Specimen CBC-48-46-10

(b) Specimen CBC-48-46-20

Fig. 7. Comparison of predicted and experimental cyclic load-deflection curves for specimens CBC-48-46-10 and CBC-48-46-20.

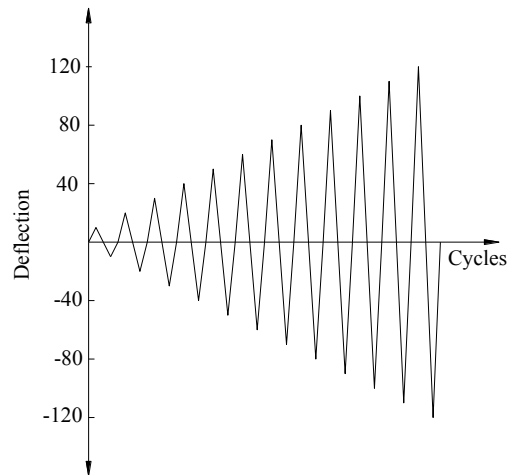**Fig. 8.** Typical cyclic loading pattern

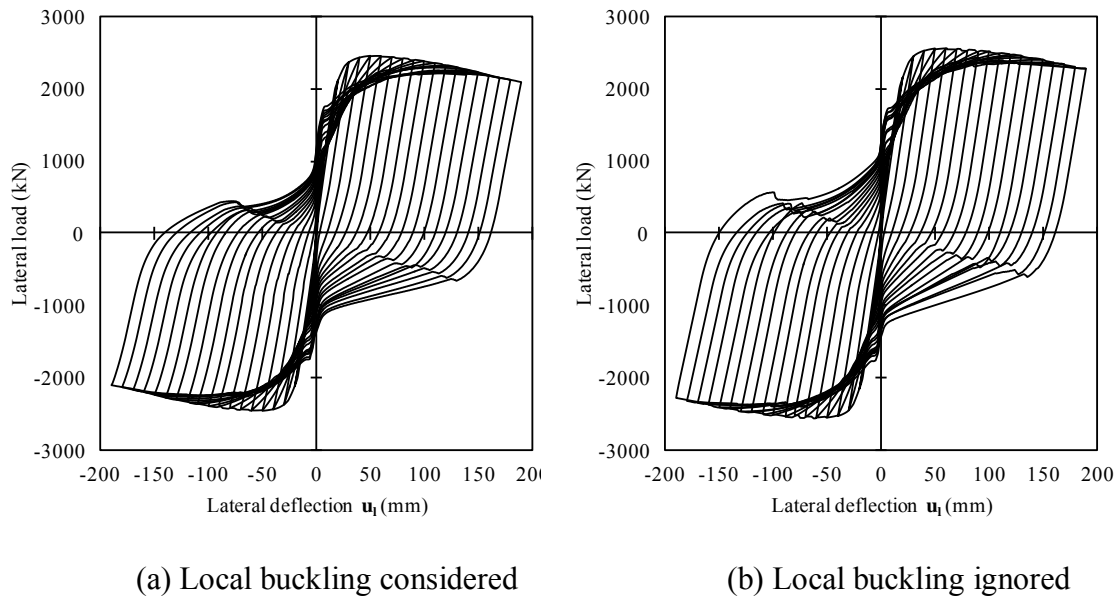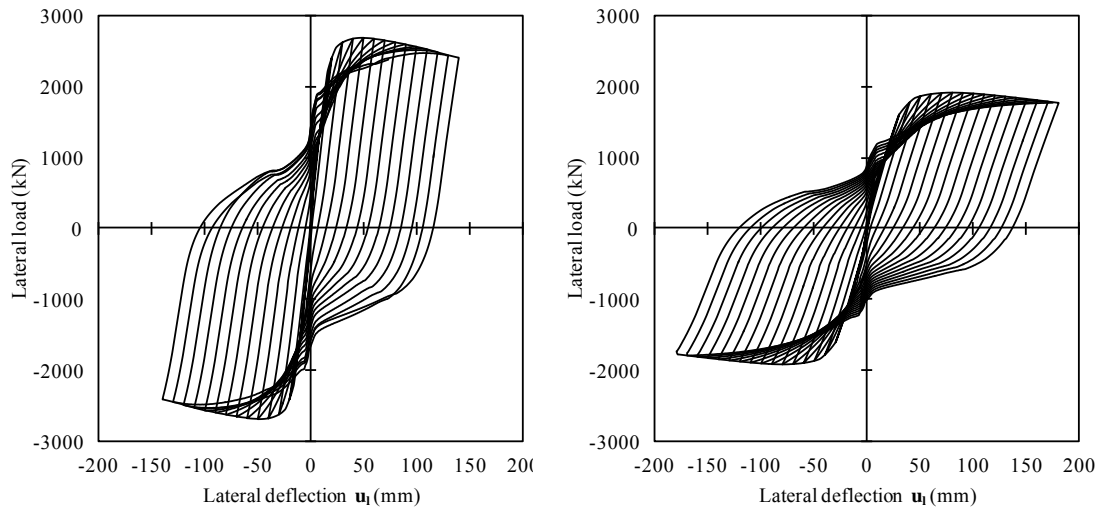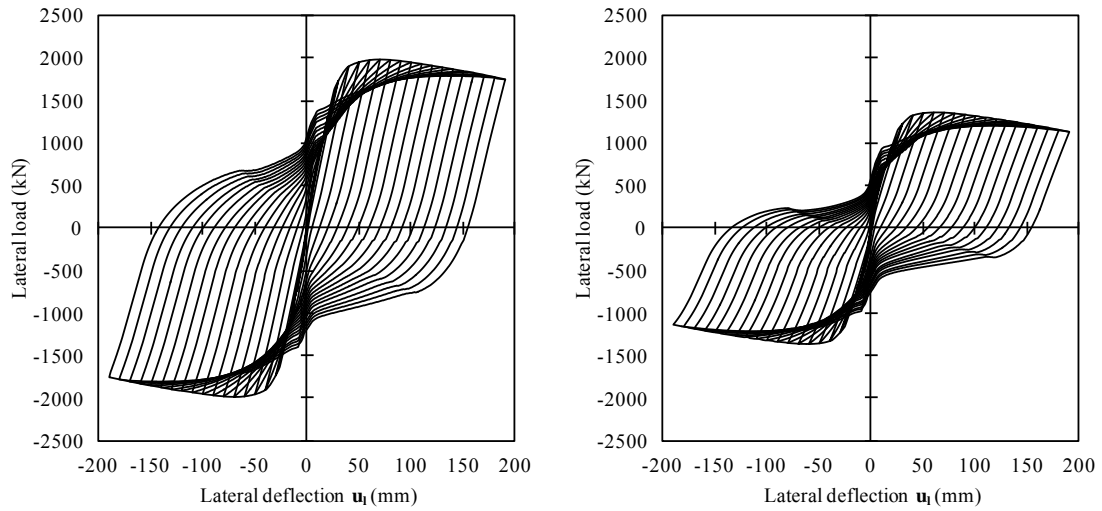(a) Local buckling considered (b) Local buckling ignored

Fig. 9. Effects of local buckling on the cyclic load-deflection curves for thin-walled CFST slender beam-columns.

(a) $L_e/r = 22$ (b) $L/r = 30$

Fig. 10. Effects of column slenderness ratio on the cyclic load-deflection curves for thin-walled CFST slender beam-columns.

(a) $D/t = 50$ (b) $D/t = 80$

Fig. 11. Effects of D/t ratio on the cyclic load-deflection curves for thin-walled CFST slender beam-columns.
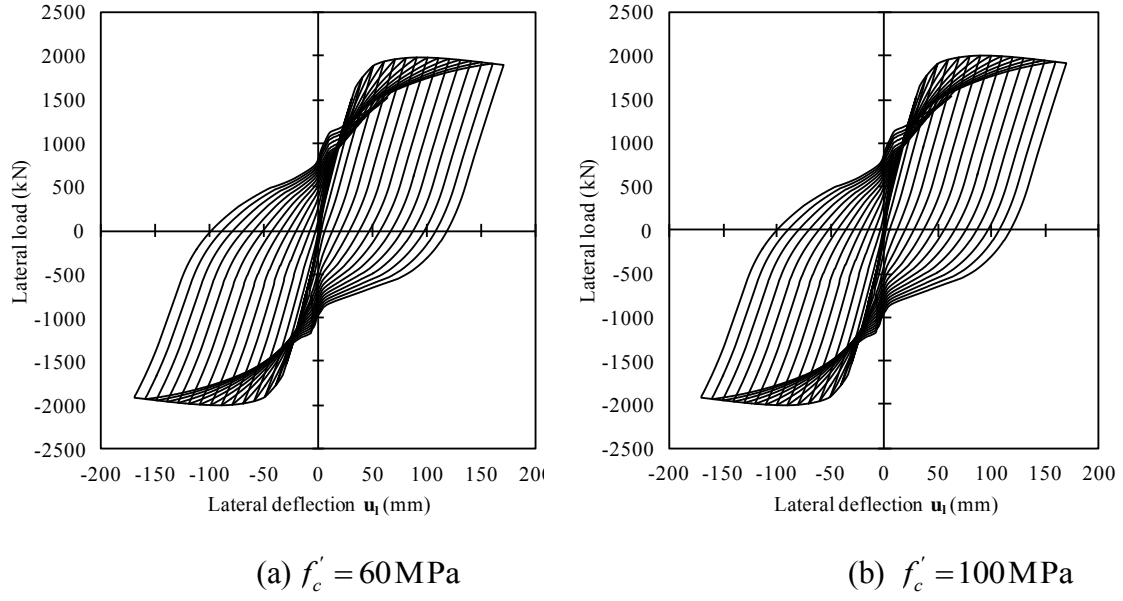
(a) $f_c' = 60\,\text{MPa}$ (b) $f_c' = 100\,\text{MPa}$

Fig. 12. Effects of concrete compressive strengths on the cyclic load-deflection curves for thin-walled CFST slender beam-columns.

(a) $f_{sy} = 300\,\text{MPa}$ (b) $f_{sy} = 690\,\text{MPa}$
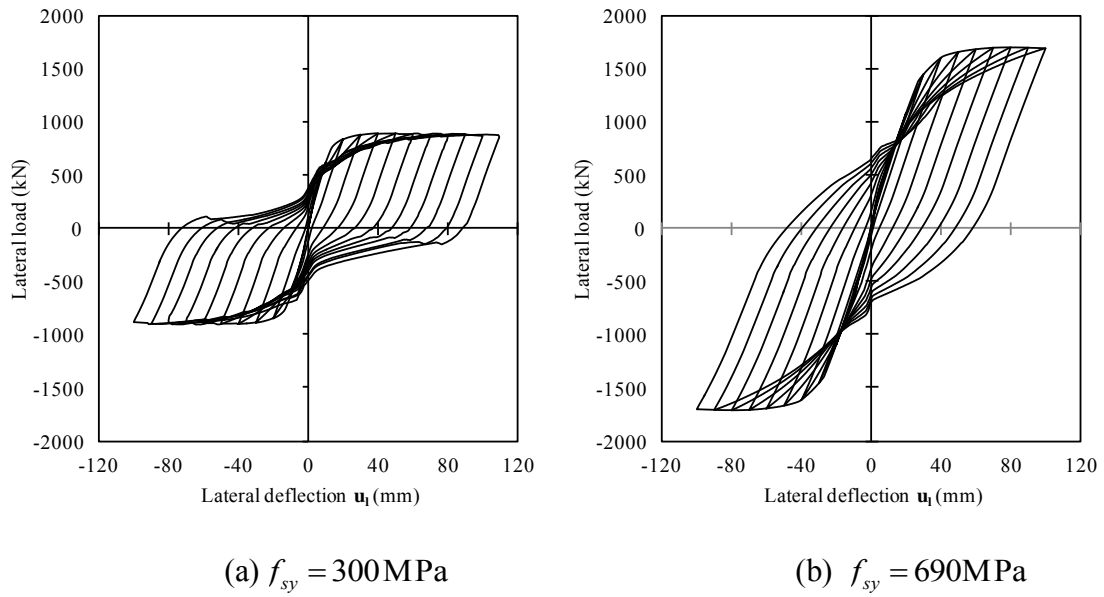
Fig. 13. Effects of steel yield strengths on the cyclic load-deflection curves for thin-walled CFST slender beam-columns.

6.4 CONCLUDING REMARKS

In this chapter, a numerical model has been extended to the nonlinear analysis of high strength thin-walled rectangular CFST slender beam-columns under constant axial load and cyclically varying lateral loading. The numerical model simulates the progressive local and post-local buckling by gradually redistributing the normal stresses within the steel tube walls. The ultimate lateral loads and cyclic load-deflection curves for thin-walled CFST beam-columns predicted by the numerical model were compared with experimental results reported in the literature. Good agreement between numerical and experimental results was achieved. The numerical model developed has been employed to investigate the effects of cyclic local buckling, column slenderness ratio, depth-to-thickness ratio, concrete compressive strengths and steel yield strengths on the ultimate lateral loads and cyclic load-deflection curves of thin-walled CFST beam-columns. The results obtained have been discussed.

Chapter 7

CONCLUSIONS

7.1 SUMMARY

New numerical models based on fiber element formulations for simulating the nonlinear inelastic behavior of CFST slender beam-columns under uniaxial loads, biaxial loads, preloads or cyclic loading have been presented. The effects of concrete confinement, initial geometric imperfections, second order and high strength materials were taken into account in the numerical models. Effective width formulas were incorporated into the numerical models to account for local buckling effects of the tube walls under stress gradients. The progressive local buckling of thin-walled steel tubes in CFST beam-columns was simulated by gradually redistributing the normal stresses within steel tube walls.

Axial load-moment-curvature relationships were computed from the cross-section analysis of CFST beam-columns. Müller's method algorithms were developed and implemented in the numerical models to obtain solutions. Deflections caused by preloads on the steel tubes were considered in the analysis of CFST slender beam-columns. Computational procedures for determining the axial load-deflection responses and axial load-moment interaction diagrams of thin-walled CFST slender beam-columns under various loading conditions have been presented.

The ultimate strengths, ultimate lateral loads, axial load-deflection curves and cyclic load-deflection responses were compared with experimental results reported in the literature. The numerical models can effectively generate complete axial load-deflection curves, axial load-moment strength interaction diagrams and cyclic load-deflection responses for thin-walled CFST slender beam-columns with local buckling effects. A set of performance indices was proposed and implemented in the numerical models to quantify the performance of CFST beam-columns. The verified numerical models were utilized to undertake parametric studies on the behavior of CFST slender beam-columns with a wide range of parameters.

7.2 ACHIEVEMENTS

This thesis has made significant contributions to the area of CFST slender beam-columns. Research achievements are summarized as follows:

(1) Developed a numerical model for high strength rectangular CFST slender beam-columns under axial load and uniaxial bending with local buckling effects.

(2) Developed a numerical model for biaxially loaded high strength rectangular CFST slender beam-columns with local buckling effects.

(3) Developed a numerical model for circular high strength CFST slender beam-columns with preload and confinment effects.

(4) Developed a numerical model for high strength thin-walled rectangular CFST slender beam-columns with preload and local buckling effects.

(5) Developed a numerical model for high strength thin-walled rectangular CFST slender beam-columns under axial load and cyclic loading with local buckling effects.

(6) The numerical models developed provide structural designers with advanced analysis and design tools that can be used to design safe and economical composite buildings.

(7) Performance indices proposed can be used to quantify the contribution of the concrete core and steel tube to the ultimate strengths of CFST slender beam-columns in order to achieve designs.

(8) The numerical models proposed overcome the limitations of traditional plastic analysis methods which are applicable to compact steel sections only. The proposed numerical models allow the designer to analyse and design CFST beam-columns made of the compact, non-compact or slender steel sections with any strength grades and high strength concrete.

7.3 FURTHER RESEARCH

The numerical models developed have been shown to be accurate computer simulation tools which can be used to investigate the fundamental behavior of CFST slender beam-columns. Further research is still needed to extend the numerical models developed to composite columns under other loading conditions. The recommendations for further research are summarized as follows:

(1)   The numerical models developed can be directly used in the design of high strength CFST beam-columns at room temperature. The effects of temperature dependent material properties on the behavior of CFST beam-columns have not been incorporated in the numerical models. Therefore, research on the development of efficient and accurate numerical techniques for simulating the nonlinear inelastic behavior of CFST slender beam–columns at elevated temperature is needed.

(2)   The numerical model presented in the thesis have been developed for high strength CFST slender beam-columns and are not applicable to concrete encased composite columns. Further research is needed to extend the numerical models to concrete encased composite columns at ambient and elevated temperatures.

(3)   The numerical models developed can be implemented in the advanced analysis programs for the nonlinear analysis of composite frames with short-term loading. The behavior of CFST beam-columns may change with time. The limitation of the proposed model is that it did not account for the effects of long-term loading on the behavior of CFST beam-columns. Therefore, the numerical models need to be extended for the nonlinear time-dependent analysis of slender steel-concrete composite beam-columns.

(4)   The proposed numerical models allow for the analysis and design of rectangular thin-walled CFST beam-columns with a depth-to-thickness ratio up to 100. Further research is needed to extend the numerical models developed to the nonlinear inelastic analysis of thin-walled CFST beam-columns with depth-to-thickness ratios greater than 100.

REFERENCES

Abed, F. Alhamaydeh, M. and Abdalla, S. (2013). "Experimental and numerical investigations of the compressive behavior of concrete filled steel tubes (CFSTs)." *Journal of Constructional Steel Research*, **80**, 429-439.

ACI Committee 209 (1992). Prediction of creep, shrinkage and temperature effects in concrete structures. Designing for effects of creep, shrinkage and temperature in concrete structures, ACI SP27-3, Detroit, MI, 51-93.

\

ACI-318. (2002). *Building code requirements for reinforced concrete*. Detroit (MI): ACI.

ACI (2011). *Building code requirements for structural concrete and commentary*. USA, American Concrete Institute (ACI).

AIJ (1997). *Recommendations for design and construction of concrete filled steel tubular structures*. Architectural Institutive of Japan, Tokyo, Japan.

AISC 360-05. (2005). *Specification for structural steel buildings*. Chicago (IL, USA), American Institute of Steel Construction.

AISC 360-10. (2010). *Specification for structural steel buildings*. Chicago. Chicago, Illinois: American Institute of Steel Construction.

References

AISC-LRFD (1993). *Load and resistance factor specification for structural steel buildings*. AISC, Chicago, IL.

AISC-LRFD (1999). *Load and resistance factor specification for structural steel buildings*. AISC, Chicago, IL.

AISC-LRFD (2005). *Load and resistance factor specification for structural steel buildings*. AISC, Chicago, IL.

AS 4100 (1998). Australian Standard, Steel Structures, Sydney, Australia.

AS 5100 (2004). *Bridge design, part 6: steel and composite construction*. Sydney, Australia.

AS 3600 (2009). Australian Standard, Cconcrete structures, Sydney, Australia.

Bridge, R. Q. (1976). "Concrete filled steel tubular columns." School of Civil Engineering, The University of Sydney, Sydney, Australia, Research Report No. R283.

Bridge, R. Q. and O'Shea, M. D. (1998). "Behaviour of thin-walled steel box sections with or without internal restraint." *Journal of Constructional Steel Research*, **47**(1-2), 73-91.

References

BS 5400 (1979). *Steel, concrete and composite bridges: Part: 5 Code of practice for design of composite bridges*, London, British Standards Institution.

CECS159 (2004). *Technical specification for structures with concrete-filled rectnagular steel tube members*. Beijing, China (in Chinese).

Chen, S. F., Teng, J. G. and Chan, S. L. (2001). "Design of biaxially loaded short composite columns of arbitrary section." *Journal of Structural Engineering*, ASCE, **127**(6), 678-685.

Choi, K. K. and Xiao, Y. (2010). "Analytical studies of concrete-filled circular steel tubes under axial compression." *Journal of Structural Engineering*, ASCE, **136**(5), 565-573.

Chung, J., Tsuda, K. and Matsui, C. (1999). "High-strength concrete filled square tube columns subjected to axial loading." *The Seventh East Asia-Pacific Conference on Structural Engineering & Construction*, Kochi, Japan, **2**, 955-960**.**

Chung, K. (2010). "Prediction of pre- and post-peak behavior of concrete-filled circular steel tube columns under cyclic loads using fiber element method." *Thin-Walled Structures*, **48**(2), 169-178.

Chung, K., Chung, J. and Choi, S. (2007). "Prediction of pre- and post-peak behavior of concrete-filled square tube columns under cyclic loads using fiber element method." *Thin-Walled Structures*, **45**(9), 747-758.

Chung, K. S., Kim, J. H. and Yoo, J. H. (2012). "Prediction of hysteretic behavior of high-strength square concrete-filled steel tubular columns subjected to eccentric loading." *International Journal of Steel Structures*, **12**(2), 243-252.

DBJ (2003). *Technical specification for concrete-filled steel tubular structures*. Fuzhou China, The Department of Housing and Urban–Rural Development of Fujian Province (in Chinese).

DBJ/T 13-51. (2010). *Technical specification for concrete-filled steel tubular structures*. Fuzhou, China, The Department of Housing and Urban–Rural Development of Fujian Province (in Chinese).

Ellobody, E., Young, B. and Lam, D. (2006). "Behaviour of normal and high strength concrete-filled compact steel tube circular stub columns." *Journal of Constructional Steel Research*, **62**(7), 706-715.

Ellobody, E. and Ghazy, M. F. (2012a). "Tests and design of stainless steel tubular columns filled with polypropylene fibre reinforced concrete." *Proceedings of the 10th international conference on advances in steel concrete composite and hybrid structures*, Singapore, 281-289.

Ellobody, E. and Ghazy, M. F. (2012b). "Experimental investigation of eccentrically loaded fibre reinforced concrete-filled stainless steel tubular columns." *Journal of Constructional Steel Research*, **76**, 167-176.

Ellobody, E. (2013). "Numerical modelling of fibre reinforced concrete-filled stainless steel tubular columns." *Thin-Walled Structures*, **63**, 1-12.

El-Heweity, M. M. (2012). "On the performance of circular concrete-filled high strength steel columns under axial loading." *Alexandria Engineering Journal*, **51**(2), 109-119.

EI-Tawil, S., Sanz-Picón, C. F. and Deierlein, G. G. (1995). "Evaluation of ACI 318 and AISC (LRFD) strength provisions for composite beam-columns." *Journal of Constructional Steel Research*, **34**(1), 103-123.

Eurocode 3 (1992). *Design of steel structuresm Part 1.1 General rules and rules for buildings*. London.

Eurocode 4 (1992). *Design of composite steel and concrete structures, Part 1.1 general rules and rules for buildings*. Commision of European Communities, Brussels, Belgium.

Eurocode 4 (1994). *Design of composite steel and concrete structures, Part 1.1 General rules and rules for buildings*. London.

Eurocode 4 (2004). *Design of composite steel and concrete structures. Part 1-1, General rules and rules for buildings*. CEN 2004.

Eurocode 4 (2005). *Design of composite steel and concrete structures, Part 1-1, General rules and rules for buildings*, CEN, 2005.

Fam, A., Qie, F. S. and Rizkalla, S. (2004). "Concrete-filled steel tubes subjected to axial compression and lateral cyclic loads." *Journal of Structural Engineering*, ASCE, **130**(4), 631-640.

Fujimoto, T., Mukai, A., Nishiyama, I. and Sakino, K. (2004). "Behavior of eccentrically loaded concrete-filled steel tubular columns." *Journal of Structural Engineering*, ASCE, **130**(2), 203-212.

Furlong, R. W. (1967). "Strength of steel-encased concrete beam columns." *Journal of the Structural Division*, ASCE, **93**(5), 113-124.

Gajalakshmi, P. and Helena, H. J. (2012). "Behaviour of concrete-filled steel columns subjected to lateral cyclic loading." *Journal of Constructional Steel Research*, **75**, 55-63.

Ge, H. and Usami, T. (1992). "Strength of concrete-filled thin-walled steel box columns: experiment." *Journal of Structural Engineering*, ASCE, **118**(11), 3036-3054.

References

Giakoumelis, G. and Lam, D. (2004). "Axial capacity of circular concrete-filled tube columns." *Journal of Constructional Steel Research*, **60**(7), 1049-1068.

Guo, L., Zhang, S. and Xu, Z. (2011). "Behaviour of filled rectangular steel HSS composite columns under bi-axial bending." *Advances in Structural Engineering*, **14**(2), 295-306.

Hajjar, J. F. and Gourley, B. C. (1996). "Representation of concrete-filled steel tube cross-section strength." *Journal of Structural Engineering*, **122**(11), 1327-1335.

Han, L. H. (2002). "Tests on stub columns of concrete-filled RHS sections." *Journal of Constructional Steel Research*, **58**(3), 353-372.

Han, L. H. (2007). *Theory and practice of concrete-filled steel tubular structure*. Beijing, China (in Chinese).

Han, L. H., Tao, Z. and Yao, G. H. (2008). "Behaviour of concrete-filled steel tubular members subjected to shear and constant axial compression." *Thin-Walled Structures*, **46**(7-9), 765-780.

Han, L. H. and Yang, Y. F. (2003). "Analysis of thin-walled steel RHS columns filled with concrete under long-term sustained loads." *Thin-Walled Structures*, **41**(9), 849-870.

References

Han, L. H., Yang, Y. F. and Tao, Z. (2003). "Concrete-filled thin-walled steel SHS and RHS beam-columns subjected to cyclic loading." *Thin-Walled Structures*, **41**(9), 801-833.

Han, L. H. and Yao, G. H. (2003). "Behaviour of concrete-filled hollow structural steel (HSS) columns with pre-load on the steel tubes." *Journal of Constructional Steel Research*, **59**(12), 1455-1475.

Hu, H. T., Huang, C. S., Wu, M. H. and Wu, Y. M. (2003). "Nonlinear analysis of axially loaded concrete-filled tube columns with confinement effect." *Journal of Structural Engineering*, ASCE, **129**(10), 1322-1329.

Klöppel, V. K., Goder, W. (1957). "An investigation of the load carrying capacity of concrete filled steel tubes and development of design formula." *Der Stahlbau*, **26**(2), 44-50.

Knowles, R. B. and Park, R. (1969). "Strength of concrete-filled steel tubular columns." *Journal of Structural Division*, ASCE, **95**(12), 2565-2587.

Lakshmi, B. and Shanmugam, N. E. (2002). "Nonlinear analysis of in-filled steel-concrete composite columns." *Journal of Structural Engineering*, ASCE, **128**(7), 922-933.

References

Lee, T. K. and Pan, A. D. E. (2001). "Analysis of composite beam-columns under lateral cyclic loading." *Journal of Structural Engineering*, ASCE, **127**(2), 186-193.

Lee, S. H., Uy, B., Kim, S. H., Choi, Y. H. and Choi, S. M. (2011). "Behavior of high-strength circular concrete-filled steel tubular (CFST) column under eccentric loading." *Journal of Constructional Steel Research*, **67**(1), 1-13.

Liang, Q. Q. (2009a). "Performance-based analysis of concrete-filled steel tubular beam–columns, Part II: verification and applications." *Journal of Constructional Steel Research*, **65**(2), 351-362.

Liang, Q. Q. (2009b). "Performance-based analysis of concrete-filled steel tubular beam–columns, part I: theory and algorithms." *Journal of Constructional Steel Research*, **65**(2), 363-372.

Liang, Q. Q. (2009c). "Strength and ductility of high strength concrete-filled steel tubular beam-columns." *Journal of Constructional Steel Research*, **65**(3), 687-698.

Liang, Q. Q. (2011a). "High strength circular concrete-filled steel tubular slender beam-columns, Part I: Numerical analysis." *Journal of Constructional Steel Research*, **67**(2), 164-171.

References

Liang, Q. Q. (2011b). "High strength circular concrete-filled steel tubular slender beamcolumns, Part II: Fundamental behavior." *Journal of Constructional Steel Research*, **67**(2), 172-180.

Liang, Q. Q. and Fragomeni, S. (2009). "Nonlinear analysis of circular concrete-filled steel tubular short columns under axial loading." *Journal of Constructional Steel Research*, **65**(12), 2186-2196.

Liang, Q. Q. and Fragomeni, S. (2010). "Nonlinear analysis of circular concrete-filled steel tubular short columns under eccentric loading." *Journal of Constructional Steel Research*, **66**(2), 159-169.

Liang, Q. Q. and Uy, B. (2000). "Theoretical study on the post-local buckling of steel plates in concrete-filled box columns." *Computers and Structures*, **75**(5), 479-490.

Liang, Q. Q., Uy, B., and Liew, J. Y. R. (2006). "Nonlinear analysis of concrete-filled thin-walled steel box columns with local buckling effects." *Journal of Constructional Steel Research*, **62**(6), 581-591.

Liang, Q. Q., Uy, B. and Liew, J. Y .R. (2007). "Local buckling of steel plates in concrete-filled thin-walled steel tubular beam-columns." *Journal of Constructional Steel Research*, **63**(3), 396-405.

References

Liew, J. Y. R. and Xiong, D. X. (2009). "Effect of preload on the axial capacity of concrete-filled composite columns." *Journal of Constructional Steel Research*, **65**(3), 709-722.

Liew, J. Y. R. and Xiong, D. X. (2012). "Ultra-high strength concrete filled composite columns for multi-storey building construction." *Advances in Structural Engineering*, **15**(9), 1487-1504.

LRFD. (1999). *Load and resistance factor design specification for steel buildings*. American Institution of Steel Construction.

Liu, D. (2006). "Behaviour of eccentrically loaded high-strength rectangular concrete-filled steel tubular columns." *Journal of Constructional Steel Research*, **62**(8), 839-846.

Lue, D. M., Liu, J. L. and Yen, T. (2007). "Experimental study on rectangular CFT columns with high-strength concrete." *Journal of Constructional Steel Research*, **63**(1), 37-44.

Matsui, C., Tsuda, K. and Ishibashi, Y. (1995). "Slender concrete filled steel tubular columns under combined compression and bending." *Proceedings of the 4th Pacific Structural Steel Conference*, Singapore, Pergamon, **3**(10), 29-36.

Mander, J. B. and Priestley, M. J. N. and Park, R. (1988). "Theoretical stress–strain model for confined concrete." *Journal of Structural Engineering*, ASCE, **114**(8), 1804-1826.

Mursi, M. and Uy, B. (2006a). "Behaviour and design of fabricated high strength steel columns subjected to biaxial bending part I: Experiments." *Advanced Steel Construction*, **2**(4), 286-313.

Mursi, M. and Uy, B. (2006b). "Behaviour and design of fabricated high strength steel columns subjected to biaxial bending part II: Analysis and design codes." *Advanced Steel Construction*, **2**(4), 314-354.

Nakahara, H., Sakino, K., and Inai, E. (1998). "Analytical model for axial compressive behavior of concrete filled square steel tubular columns." *Transaction of the Japan Concrete Institute*, **20**, 171-178 (in Japanese).

Neogi, P. K., Sen, H. K. and Chapman, J. C. (1969). "Concrete-filled tubular steel columns under eccentric loading." *The Structural Engineer*, **47**(5), 187-195.

O'Brien, A. D. and Rangan, B. V. (1993). "Tests on slender tubular steel columns filled with high strength concrete." *Australian Civil Engineering Transactions*, **35**(4), 287-292.

References

O'Shea, M. D. and Bridge, R. Q. (2000). "Design of circular thin-walled concrete filled steel tubes." *Journal of structural engineering*, ASCE, **126**(11), 1295-1303.

Portolés, J. M., Romero, M. L., Bonet, J. L. and Filippou, F. C. (2011). "Experimental study of high strength concrete-filled circular tubular columns under eccentric loading." *Journal of Constructional Steel Research*, **67**(4), 623-633.

Portolés, J. M., Romero, M. L., Filippou, F. C. and Bonet, J. L. (2011). "Simulation and design recommendations of eccentrically loaded slender concrete-filled tubular columns." *Engineering Structures*, **33**(5), 1576-1593.

Rangan, B. V. and Joyce, M. (1992). "Strength of eccentrically loaded slender steel tubular columns filled with high-strength concrete." *ACI Structural Journal*, **89**(6), 676-681.

Roderick, J. W. and Rogers, D. F. (1969). "Load carrying capacity of simple composite columns." *Proc. Am. Soc. Civ. Engrs., Journal of Structural Division*, **XCV**(ST2), 209-228.

Sakino, K., Nakahara, H., Morino, S. and Nishiyama, I. (2004). "Behavior of centrally loaded concrete-filled steel-tube short columns." *Journal of Structural Engineering*, ASCE, **130**(2), 180-188.

References

Sanz-Pic6n, C. F. (1992). *Behavior of composite column cross sections under biaxial bending*, MS thesis, School of Civil and Envionmental Engineering, Cornell University, Ithaca, N.Y.

Schneider, S. P. (1998). "Axially loaded concrete-filled steel tubes." *Journal of Structural Engineering*, ASCE, **124**(10), 1125-1138.

Shakir-Khalil, H. and Zeghiche, J. (1989). "Experimental Behaviour of concrete-filled rolled rectangular hollow-section columns." *The Structural Engineer*, **67**(19), 346-353.

Shakir-Khalil, H. and Mouli, M. (1990). "Further tests on concrete-filled rectangular hollow-section columns." *The structural Engineer*, **68**(20), 405-413.

Shams, M. and Saadeghvaziri, M. A. (1997). "State of the art of concrete-filled steel tubular columns." *ACI Structural Journal*, **94**(5), 558-571.

Shanmugam, N. E. and Lakshmi, B. (2001). "State of the art report on steel-concrete composite columns." *Journal of Constructional Steel Research*, **57**(10), 1041-1080.

Shanmugam, N. E., Lakshmi, B. and Uy, B. (2002). "An analytical model for thin-walled steel box columns with concrete in-fill." *Engineering Structures*, **24**(6), 825-838.

References

Gayathri, V., Shanmugam, N.E. and Choo, Y. S. (2004a). "Concrete-filled tubular columns part 1- cross-section analysis." *International Journal of Structural Stability and Dynamics*, **4**(4), 459-478.

Gayathri, V., Shanmugam, N.E. and Choo, Y. S. (2004b). "Concrete-filled tubular columns part 2- column analysis." International *Journal of Structural Stability and Dynamics*, **4**(4), 479-495.

Spacone, E. and El-Tawil, S. (2004). "Nonlinear analysis of steel-concrete composite structures: state of the art." *Journal of Structural Engineering*, ASCE, **130**(2), 159-168.

Susantha, K. A. S., Ge, H. and Usami, T. (2001). "Uniaxial stress-strain relationship of concrete confined by various shaped steel tubes." *Engineering Structures*, **23**(10), 1331-1347.

Tang, J., Hino, S., Kuroda, I. and Ohta, T. (1996). "Modeling of stressstrain relationships for steel and concrete in concrete filled circular steel tubular columns." *Steel Construction Engineering*, JSSC, **3**(11), 35-46.

Thai, H. T. and Kim, S. E. (2011). "Nonlinear inelastic analysis of concrete-filled steel tubular frames." *Journal of Constructional steel Research*, **67**(12), 1797-1805.

References

Tomii, M., Sakino, K. (1979). "Elastic–plastic behavior of concrete filled square steel tubular beam-columns." *Transactions of the Architectural Institute of Japan*, **280**, 111-120.

Uy, B., Tao, Z. and Han, L. H. (2011). "Behaviour of short and slender concrete-filled stainless steel tubular columns." *Journal of Constructional Steel Research*, **67**(3), 360-378.

Varma, A. H., Ricles, J. M., Sause, R. and Lu, L. W. (2002), "Seismic behavior and modeling of high strength composite concrete-filled steel tube (CFT) beam–columns." *Journal of Constructional Steel Research*, **58**(5-8), 725-758.

Varma, A. H., Ricles, J. M., Sause, R. and Lu, L. W. (2004). "Seismic behavior and design of high-strength square concrete-filled steel tube beam columns." *Journal of Structural Engineering* ASCE, **130**(2), 169-179.

Vrcelj, Z. and Uy, B. (2002). "Strength of slender concrete-filled steel box columns incorporating local buckling." *Journal of Constructional Steel Research*, **58**(2), 275-300.

Wei, L., Han, L. H. and Zhao, X. L. (2012). "Axial strength of concrete-filled double skin steel tubular (CFDST) columns with preload on steel tubes." *Thin-Walled Structures*, **56**, 9-20.

References

Wu, B., Zhao, X. Y. and Zhang, J. S. (2012). "Cyclic behavior of thin-walled square steel tubular columns filled with demolished concrete lumps and fresh concrete." *Journal of Constructional Steel Research*, **77**, 69-81.

Xiong, D. X. and Zha, X. X. (2007). "A numerical investigation on the behaviour of concrete-filled steel tubular columns under initial stresses." *Journal of Constructional Steel Research*, **63**(5), 599-611.

Zhang, X. Q., Zhong, S. T., Yan, S. Z., Lin, W. and Cao, H. L. (1997). "Experimental study about the effect of initial stress on bearing capacity of concrete-filled steel tubular members under eccentric compression." *Journal of Harbin University of Civil Engineering and Architecture*, **30**(1), 50-56 (in Chinese).

Zha, X. X. (1996). "The theoretical and experimental study on the behaviour of concrete-filled steel tubular members subjected to compression-bending-torsion and initial stresses on the steel tubes." Ph.D. Dissertation, Harbin University of Civil Engineering and Architecture, Harbin, China (in Chinese).

Zhang, S., Guo, L. and Tian, H.(2003). "Eccentrically loaded high strength concrete-filled square steel tubes." *Proceedings of the International Conference on Advances in Structures*, Sydney, Australia, **2**, 987-93.

Zhang, S. M., Guo, L. H., Ye, Z. L. and Wang, Y. Y. (2005). "Behavior of steel tube and confined high strength concrete for concrete-filled RHS tubes." *Advances in Strucutral Engineering*, **8**(2), 101-116.

Zubydan, A. H. and ElSabbagh, A. I. (2011). "Monotonic and cyclic behavior of concrete-filled steel-tube beam-columns considering local buckling effect." *Thin-Walled Structure*, **49**(4), 465-481.